Dissertation zur Erlangung des Doktorgrades
der Fakultät für Chemie und Pharmazie
der Ludwig-Maximilians-Universität München

Coordination Chemistry of Sugar-Phosphate Complexes with Palladium(II), Rhenium(V) and Zinc(II)

Christian Martin Steinborn

aus

Berlin

2013

Erklärung:

Diese Dissertation wurde im Sinne von § 7 der Promotionsordnung vom 28. November 2011 von Herrn Prof. Dr. Peter Klüfers betreut.

Eidesstattliche Versicherung:

Diese Dissertation wurde eigenständig und ohne unerlaubte Hilfe erarbeitet.

München, den 02. April 2013

Martin Steinborn

Dissertation eingereicht am 05. April 2013

1. Gutachter: Prof. Dr. Peter Klüfers

2. Gutachter: Prof. Dr. Hans-Christian Böttcher

Mündliche Prüfung am 21. Mai 2013

Diese Arbeit wurde in der Zeit von Oktober 2009 bis März 2013 am Department Chemie der Ludwig-Maximilians-Universität München am Lehrstuhl für Bioanorganische Chemie und Koordinationschemie unter Anleitung von Herrn Prof. Dr. Peter Klüfers durchgeführt.

Contents

1 Introduction 1

1.1 The biological importance of sugar phosphates 1

1.2 Coordination chemistry of sugar-phosphate complexes 2

1.3 Use of NMR spectroscopy and quantum-chemical calculations 4

1.4 Aims of this work 6

2 Results 7

2.1 Coordination of sugar phosphates to $Re^{V}ON_2$ fragments 7

2.1.1 Coordination of D-fructose 1,6-bisphosphate 7

2.1.2 Coordination of *rac*-glycerol 1-phosphate 9

2.1.3 Coordination of further sugar phosphates 13

2.2 Coordination of sugar phosphates to the Pd^{II}(tmen) fragment 14

2.2.1 Coordination of α-D-glucose 1-phosphate 15

2.2.2 Coordination of *rac*-glycerol 1-phosphate 20

2.2.3 Coordination of D-glucose 6-phosphate 22

2.2.3.1 Influence of the pH value and the stoichiometry 27

2.2.3.2 Influence of the palladium(II) fragment 28

2.2.3.3 Influence of the phosphate group 30

2.2.4 Coordination of D-mannose 6-phosphate 32

2.2.5 Coordination of D-fructose 1-phosphate 36

2.2.6 Coordination of D-fructose 6-phosphate 40

2.2.7 Coordination of D-fructose 1,6-bisphosphate 42

2.2.8 Coordination of D-ribose 5-phosphate 47

2.2.9 Preparation of crystalline compounds 50

2.3 Coordination of diolato compounds to the Zn^{II}(dien) fragment 51

2.3.1 Coordination of polyols 52

2.3.2 Coordination of methylated sugars 54

2.3.3 Coordination of reducing sugars 56

2.3.3.1 D-Lyxose 56

2.3.3.2 D-Arabinose 59

2.3.3.3 D-Xylose 62

2.3.3.4 D-Ribose 65

2.3.3.5 D-Galactose 67

2.3.3.6 D-Glucose 70

2.3.3.7 D-Mannose 73

2.3.3.8 D-Fructose 75

2.3.4 Coordination of sugar phosphates 78

2.3.4.1 D-Fructose 1-phosphate 78

2.3.4.2 D-Fructose 6-phosphate 81

2.3.4.3 D-Fructose 1,6-bisphosphate 82

2.3.4.4 D-Mannose 6-phosphate 84

2.3.4.5 D-Glucose 6-phosphate 87

2.3.4.6 α-D-Glucose 1-phosphate 89

2.3.4.7 *rac*-Glycerol 1-phosphate 91

2.3.4.8 D-Ribose 5-phosphate 92

2.3.5 Preparation of crystalline compounds 92

2.3.6 Experiments with further spectator ligands 93

3 Discussion 95

3.1 Coordination of sugar phosphates to $Re^{V}ON_2$ fragments 95

3.2 The pH dependence of sugar-phosphate complexes with the Pd^{II}(tmen) metal fragment 96

3.3 Chelation preferences of sugar phosphates in complexes with the Pd^{II}(tmen) metal fragment at alkaline pH values 98

3.4 Equilibration times in experiments with D-glucose and D-glucose 6-phosphate 101

3.5 Experiments with the Zn^{II}(dien) metal fragment 103

3.6 Chelation preferences of sugars and sugar phosphates in complexes with the Zn^{II}(dien) metal fragment 104

3.6.1 Pentoses 106

3.6.2 Hexoses 109

3.6.3 Sugar phosphates 110

3.7 Calculation of NMR chemical shifts 111

4 Summary 113

5 Experimental Section 119

5.1 Common working techniques 119

5.2 Reagents and solvents 119

5.3 NMR spectroscopy and species assignment 121

5.4 Crystal-structure determination and refinement 122

5.5 Preparation of the precursor compounds 124

5.5.1 *trans*-[$ReOCl_3(PPh_3)_2$] 124

5.5.2 [$Pd(en)Cl_2$] 124

5.5.3 [$Pd(en)(OH)_2$] (0.3 M) 124

5.5.4 [$Pd(tmen)Cl_2$] 124

5.5.5 [$Pd(tmen)(OH)_2$] (0.3 M) 125

5.5.6 Zinc(II) hydroxide 125

5.5.7 Disodium D-ribose 5-phosphate hydrate 125

5.6 Preparation of the crystalline complex compounds 126

5.6.1 [ReO(tmen)(*rac*-Glyc2,3H$_{-2}$1*P*H-$\kappa^3O^{2,3,P}$)] (2a) · 2 H_2O 126

5.6.2 [ReO(phen)(*rac*-Glyc2,3H$_{-2}$1*P*H-κ^3*O*^{2,3,P})] (2c) · MeOH 126

5.7 Preparation of the complex compounds in solution 126

5.7.1 [ReO(tmen)(β-D-Fru2,3H$_{-2}$1,6P_2H$_2$-κ^3*O*^{2,3,P1})]$^-$ (1a) 126

5.7.2 [ReO(en)(β-D-Fru2,3H$_{-2}$1,6P_2H$_2$-κ^3*O*^{2,3,P1})]$^-$ (1b) 127

5.7.3 [ReO{(*R*,*R*)-chxn}(β-D-Fru2,3H$_{-2}$1,6P_2H$_2$-κ^3*O*^{2,3,P1})]$^-$ (1c) 127

5.7.4 [ReO(en)(*rac*-Glyc2,3H$_{-2}$1*P*H-κ^3*O*^{2,3,P})] (2b) 128

5.7.5 Complexes of α-D-glucose 1-phosphate with the Pd^{II}(tmen) fragment 128

5.7.6 Complexes of *rac*-glycerol 1-phosphate with the Pd^{II}(tmen) fragment 129

5.7.7 Complexes of D-glucose 6-phosphate with the Pd^{II}(tmen) fragment 129

5.7.8 Complexes of D-glucose 6-phosphate with the Pd^{II}(en) fragment 131

5.7.9 Complexes of D-glucose with the Pd^{II}(tmen) fragment 132

5.7.10 Complexes of D-mannose 6-phosphate with the Pd^{II}(tmen) fragment 133

5.7.11 Complexes of D-fructose 1-phosphate with the Pd^{II}(tmen) fragment 134

5.7.12 Complexes of D-fructose 6-phosphate with the Pd^{II}(tmen) fragment 136

5.7.13 Complexes of D-fructose 1,6-bisphosphate with the Pd^{II}(tmen) fragment 137

5.7.14 Complexes of D-ribose 5-phosphate with the Pd^{II}(tmen) fragment 137

5.7.15 Reaction of ethane-1,2-diol with the Zn^{II}(dien) fragment 139

5.7.16 Reaction of glycerol with the Zn^{II}(dien) fragment 139

5.7.17 Reaction of D-threitol with the Zn^{II}(dien) fragment 139

5.7.18 Reaction of erythritol with the Zn^{II}(dien) fragment 140

5.7.19 Reaction of methyl α-D-glucopyranoside with the Zn^{II}(dien) fragment 140

5.7.20 Reaction of methyl β-D-glucopyranoside with the Zn^{II}(dien) fragment 140

5.7.21 Reaction of methyl α-D-mannopyranoside with the Zn^{II}(dien) fragment 141

5.7.22 Reaction of methyl α-D-galactopyranoside with the Zn^{II}(dien) fragment 141

5.7.23 Reaction of methyl β-D-galactopyranoside with the Zn^{II}(dien) fragment 142

5.7.24 Reaction of D-lyxose with the Zn^{II}(dien) fragment 142

5.7.25 Reaction of D-arabinose with the Zn^{II}(dien) fragment 143

5.7.26 Reaction of D-xylose with the Zn^{II}(dien) fragment 144

5.7.27 Reaction of D-ribose with the Zn^{II}(dien) fragment 145

5.7.28 Reaction of D-galactose with the Zn^{II}(dien) fragment 146

5.7.29 Reaction of D-glucose with the Zn^{II}(dien) fragment 147

5.7.30 Reaction of D-mannose with the Zn^{II}(dien) fragment 148

5.7.31 Reaction of D-fructose with the Zn^{II}(dien) fragment 149

5.7.32 Reaction of D-fructose 1-phosphate with the Zn^{II}(dien) fragment 150

5.7.33 Reaction of D-fructose 6-phosphate with the Zn^{II}(dien) fragment 151

5.7.34 Reaction of D-fructose 1,6-bisphosphate with the Zn^{II}(dien) fragment 152

5.7.35 Reaction of D-mannose 6-phosphate with the Zn^{II}(dien) fragment 152

5.7.36 Reaction of D-glucose 6-phosphate with the Zn^{II}(dien) fragment 153

5.7.37 Reaction of α-D-glucose 1-phosphate with the Zn^{II}(dien) fragment 154

5.7.38 Reaction of *rac*-glycerol 1-phosphate with the Zn^{II}(dien) fragment 155

6 Appendix 157

6.1 Packing diagrams of the crystal structures 157

6.2 Crystallographic data 160

Bibliography 161

List of product complexes

1a [ReO(tmen)(β-D-Fru2,3H$_{-2}$1,6P_2H$_2$-κ^3$O^{2,3,P1}$)]$^-$

1b [ReO(en)(β-D-Fru2,3H$_{-2}$1,6P_2H$_2$-κ^3$O^{2,3,P1}$)]$^-$

1c [ReO{(*R*,*R*)-chxn}(β-D-Fru2,3H$_{-2}$1,6P_2H$_2$-κ^3$O^{2,3,P1}$)]$^-$

2a [ReO(tmen)(*rac*-Glyc2,3H$_{-2}$1*P*H-κ^3$O^{2,3,P}$)]

2b [ReO(en)(*rac*-Glyc2,3H$_{-2}$1*P*H-κ$O^{2,3,P}$)]

2c [ReO(phen)(*rac*-Glyc2,3H$_{-2}$1*P*H-κ^3$O^{2,3,P}$)]

3a [Pd(tmen)(α-D-Glc*p*1*P*2,3H$_{-2}$-κ^2$O^{2,3}$)]$^{2-}$

3b [Pd(tmen)(α-D-Glc*p*1*P*3,4H$_{-2}$-κ^2$O^{3,4}$)]$^{2-}$

3c [{Pd(tmen)}$_2${μ-(α-D-Glc*p*1*P*-κO^P:κO'^P)}$_2$]

4a [Pd(tmen)(*rac*-Glyc1*P*2,3H$_{-2}$-κ^2$O^{2,3}$)]$^{2-}$

4b [{Pd(tmen)}$_4${μ-(*rac*-Glyc1*P*H$_{-2}$-κ^2$O^{2,3}$:κO^P:κO'^P)}$_2$]

4c [{Pd(tmen)}$_2${μ-(*rac*-Glyc1*P*-κO^P:κO'^P)}$_2$]

5a [{Pd(tmen)}$_2$(α-D-Glc*p*6*P*1,2;3,4H$_{-4}$-κ^2$O^{1,2}$:κ^2$O^{3,4}$)]$^{2-}$

5b [{Pd(tmen)}$_2$(β-D-Glc*p*6*P*1,2;3,4H$_{-4}$-κ^2$O^{1,2}$:κ^2$O^{3,4}$)]$^{2-}$

5c [Pd(tmen)(α-D-Glc*p*6*P*1,2H$_{-2}$-κ^2$O^{1,2}$)]$^{2-}$

5d [Pd(tmen)(β-D-Glc*p*6*P*1,2H$_{-2}$-κ^2$O^{1,2}$)]$^{2-}$

5e [{Pd(tmen)}$_4${μ-(α-D-Glc*p*6*P*1,2H$_{-2}$-κ^2$O^{1,2}$:κO^P:κO'^P)}$_2$]

5f [{Pd(tmen)}$_2${μ-(α-D-Glc*p*6*P*-κO^P:κO'^P)}$_2$]

5g [{Pd(tmen)}$_2${μ-(β-D-Glc*p*6*P*-κO^P:κO'^P)}$_2$]

6a [{Pd(en)}$_2$(α-D-Glc*p*6*P*1,2;3,4H$_{-4}$-κ^2$O^{1,2}$:κ^2$O^{3,4}$)]$^{2-}$

6b [{Pd(en)}$_2$(β-D-Glc*p*6*P*1,2;3,4H$_{-4}$-κ^2$O^{1,2}$:κ^2$O^{3,4}$)]$^{2-}$

7a [{Pd(tmen)}$_2$(α-D-Glc*p*1,2;3,4H$_{-4}$-κ^2$O^{1,2}$:κ^2$O^{3,4}$)]

7b [{Pd(tmen)}$_2$(β-D-Glc*p*1,2;3,4H$_{-4}$-κ^2$O^{1,2}$:κ^2$O^{3,4}$)]

7c [Pd(tmen)(α-D-Glc*p*1,2H$_{-2}$-κ^2$O^{1,2}$)]

7d [Pd(tmen)(β-D-Glc*p*1,2H$_{-2}$-κ^2$O^{1,2}$)]

7e [{Pd(tmen)}$_2$(α-D-Glc*f*6*P*1,2;5,6H$_{-4}$-κ^2$O^{1,2}$:κ^2$O^{5,6}$)]

8a [{Pd(tmen)}$_2$(β-D-Man*p*6*P*1,2;3,4H$_{-4}$-κ^2$O^{1,2}$:κ^2$O^{3,4}$)]$^{2-}$

8b [Pd(tmen)(α-D-Man*p*6*P*2,3H$_{-2}$-κ^2*O*^{2,3})]$^{2-}$

8c [Pd(tmen)(β-D-Man*p*6*P*1,2H$_{-2}$-κ^2*O*^{1,2})]$^{2-}$

8d [{Pd(tmen)}$_4${μ-(α-D-Man*p*6*P*2,3H$_{-2}$-κ^2*O*^{2,3}:κ*O*^{P}:κ*O*'^{P})}$_2$]

8e [{Pd(tmen)}$_4${μ-(β-D-Man*p*6*P*1,2H$_{-2}$-κ^2*O*^{1,2}:κ*O*^{P}:κ*O*'^{P})}$_2$]

8f [{Pd(tmen)}$_2${μ-(α-D-Man*p*6*P*-κ*O*^{P}:κ*O*'^{P})}$_2$]

8g [{Pd(tmen)}$_2${μ-(β-D-Man*p*6*P*-κ*O*^{P}:κ*O*'^{P})}$_2$]

9a [{Pd(tmen)}$_2$(β-D-Fru*p*1*P*2,3;4,5H$_{-4}$-κ^2*O*^{2,3}:κ^2*O*^{4,5})]$^{2-}$

9b [Pd(tmen)(α-D-Fru*p*1*P*4,5H$_{-2}$-κ^2*O*^{4,5})]$^{2-}$

9c [Pd(tmen)(β-D-Fru*p*1*P*2,3H$_{-2}$-κ^2*O*^{2,3})]$^{2-}$

9d [Pd(tmen)(β-D-Fru*f*1*P*2,3H$_{-2}$-κ^2*O*^{2,3})]$^{2-}$

9e [{Pd(tmen)}$_4${μ-(β-D-Fru*f*1*P*2,3H$_{-2}$-κ^2*O*^{2,3}:κ*O*^{P}:κ*O*'^{P})}$_2$]

9f [{Pd(tmen)}$_2${μ-(β-D-Fru*p*1*P*-κ*O*^{P}:κ*O*'^{P})}$_2$]

9g [{Pd(tmen)}$_2${μ-(β-D-Fru*f*1*P*-κ*O*^{P}:κ*O*'^{P})}$_2$]

10a [Pd(tmen)(β-D-Fru*f*6*P*2,3H$_{-2}$-κ^2*O*^{2,3})]$^{2-}$

10b [{Pd(tmen)}$_4${μ-(β-D-Fru*f*6*P*2,3H$_{-2}$-κ^2*O*^{2,3}:κ*O*^{P}:κ*O*'^{P})}$_2$]

10c [{Pd(tmen)}$_2${μ-(α-D-Fru*f*6*P*-κ*O*^{P}:κ*O*'^{P})}$_2$]

10d [{Pd(tmen)}$_2${μ-(β-D-Fru*f*6*P*-κ*O*^{P}:κ*O*'^{P})}$_2$]

11a [Pd(tmen)(β-D-Fru*f*1,6*P*$_2$2,3H$_{-2}$-κ^2*O*^{2,3})]$^{4-}$

11b [{Pd(tmen)}$_4${μ-(β-D-Fru*f*1,6*P*$_2$2,3H$_{-2}$-κ^2*O*^{2,3}:κ*O*^{P6}:κ*O*'^{P6})}$_2$]$^{4-}$

11c [{Pd(tmen)}$_4${μ-(β-D-Fru*f*1,6*P*$_2$2,3H$_{-2}$-κ^2*O*^{2,3}:κ*O*^{P1}:κ*O*'^{P1})}$_2$]$^{4-}$

12a [Pd(tmen)(α-D-Rib*f*5*P*1,2H$_{-2}$-κ^2*O*^{1,2})]$^{2-}$

12b [Pd(tmen)(β-D-Rib*f*5*P*2,3H$_{-2}$-κ^2*O*^{2,3})]$^{2-}$

12c [{Pd(tmen)}$_4${μ-(α-D-Rib*f*5*P*1,2H$_{-2}$-κ^2*O*^{1,2}:κ*O*^{P}:κ*O*'^{P})}$_2$]

12d [{Pd(tmen)}$_4${μ-(β-D-Rib*f*5*P*2,3H$_{-2}$-κ^2*O*^{2,3}:κ*O*^{P}:κ*O*'^{P})}$_2$]

12e [{Pd(tmen)}$_2${μ-(α-D-Rib*f*5*P*-κ*O*^{P}:κ*O*'^{P})}$_2$]

12f [{Pd(tmen)}$_2${μ-(β-D-Rib*f*5*P*-κ*O*^{P}:κ*O*'^{P})}$_2$]

13 [Zn(dien)(C$_2$H$_4$O$_2$-κ^2*O*^{1,2}]

14 [Zn(dien)(Glyc1,2H$_{-2}$-κ^2*O*^{1,2}]

15 [Zn(dien)(D-ThreH$_{-2}$]

16 [Zn(dien)(ErytH$_{-2}$]

17 [Zn(dien)(Me-α-D-Glc*p*H$_{-2}$]

18 [Zn(dien)(Me-β-D-Glc*p*H$_{-2}$]

19 [Zn(dien)(Me-α-D-Man*p*H$_{-2}$]

20 [Zn(dien)(Me-α-D-Gal*p*H$_{-2}$]

21 [Zn(dien)(Me-β-D-Gal*p*H$_{-2}$]

22a [Zn(dien)(α-D-Lyx*p*1,2H$_{-2}$-κ^2*O*^{1,2})]

22b [Zn(dien)(β-D-Lyx*p*1,2H$_{-2}$-κ^2*O*^{1,2})]

23a [Zn(dien)(α-D-Ara*p*1,2H$_{-2}$-κ^2*O*^{1,2})]

23b [Zn(dien)(β-D-Ara*p*1,2H$_{-2}$-κ^2*O*^{1,2})]

23c [Zn(dien)(β-D-Ara*f*1,2H$_{-2}$-κ^2*O*^{1,2})]

24a [Zn(dien)(α-D-Xyl*p*1,2H$_{-2}$-κ^2*O*^{1,2})]

24b [Zn(dien)(β-D-Xyl*p*1,2H$_{-2}$-κ^2*O*^{1,2})]

24c [Zn(dien)(α-D-Xyl*f*1,2H$_{-2}$-κ^2*O*^{1,2})]

25a [Zn(dien)(α-D-Rib*p*1,2H$_{-2}$-κ^2*O*^{1,2})]

25b [Zn(dien)(β-D-Rib*p*1,2H$_{-2}$-κ^2*O*^{1,2})]

26a [Zn(dien)(α-D-Gal*p*1,2H$_{-2}$-κ^2*O*^{1,2})]

26b [Zn(dien)(β-D-Gal*p*1,2H$_{-2}$-κ^2*O*^{1,2})]

26c [Zn(dien)(α-D-Gal*f*1,2H$_{-2}$-κ^2*O*^{1,2})]

27a [Zn(dien)(α-D-Glc*p*1,2H$_{-2}$-κ^2*O*^{1,2})]

27b [Zn(dien)(β-D-Glc*p*1,2H$_{-2}$-κ^2*O*^{1,2})]

27c [Zn(dien)(α-D-Glc*f*1,2H$_{-2}$-κ^2*O*^{1,2})]

28a [Zn(dien)(α-D-Man*p*2,3H$_{-2}$-κ^2*O*^{2,3})]

28b [Zn(dien)(β-D-Man*p*1,2H$_{-2}$-κ^2*O*^{1,2})]

29a [Zn(dien)(β-D-Fru*p*2,3H$_{-2}$-κ^2*O*^{2,3})]

29b [Zn(dien)(β-D-Fru*f*2,3H$_{-2}$-κ^2*O*^{2,3})]

30 [Zn(dien)(β-D-Fru*f*1*P*2,3H$_{-2}$-κ*O*^{2,3})]$^{2-}$

31 [Zn(dien)(β-D-Fru*f*6*P*2,3H$_{-2}$-κ^2*O*^{2,3})]$^{2-}$

32 [Zn(dien)(β-D-Fru*f*1,6*P*$_2$2,3H$_{-2}$-κ^2*O*^{2,3})]$^{4-}$

33a [Zn(dien)(α-D-Man*p*6*P*2,3H$_{-2}$-κ^2*O*^{2,3})]$^{2-}$

33b [Zn(dien)(β-D-Manp6P1,2H$_{-2}$-κ^{2}O^{1,2})]$^{2-}$

34a [Zn(dien)(α-D-Glc*p*6*P*1,2H$_{-2}$-κ^2*O*^{1,2})]$^{2-}$

34b [Zn(dien)(β-D-Glc*p*6*P*1,2H$_{-2}$-κ^2*O*^{1,2})]$^{2-}$

34c [Zn(dien)(α-D-Glc*f*6*P*1,2H$_{-2}$-κ^2*O*^{1,2})]$^{2-}$

35 [Zn(dien)(α-D-Glc*p*H$_{-2}$*P*1]$^{2-}$

36 [Zn(dien)(*rac*-Glyc1*P*H$_{-2}$-κ^2*O*^{2,3})]$^{2-}$

Abbreviations

ADP	adenosine diphosphate
Ara	arabinose
bpy	2,2'-bipyridine
calc	calculated
Car	carnosine
CIS	coordination-induced shift
COSY	correlation spectroscopy
d	doublet
DFT	density functional theory
dien	diethylenetriamine
en	ethane-1,2-diamine
Eryt	erythritol
f	furanose
FAB	fast atom bombardment
Fru	fructose
Gal	galactose
GIAO	gauge-independent atomic orbital
Glc	glucose
Glyc	glycerol
Glu	glutamic acid
His	histidine
HETCOR	heteronuclear correlation
HMBC	heteronuclear multiple bond correlation
HMQC	heteronuclear multiple quantum coherence
Lyx	lyxose
m	multiplet
Man	mannose

Me_3-tacn	1,4,7-trimethyl-1,4,7-triazacylononane
Me_5-dien	*N*,*N*,*N'*,*N''*,*N''*-pentamethyldiethylenetriamine
MS	mass spectrometry
NADPH	nicotinamide adenine dinucleotide phosphate
NMR	nuclear magnetic resonance
obs	observed
P	phosphate
p	pyranose
PCM	polarisable continuum model
Pd-en	aqueous solution of $[Pd(en)(OH)_2]$
Pd-tmen	aqueous solution of $[Pd(tmen)(OH)_2]$
phen	1,10-phenanthroline
(*R*,*R*)-chxn	(1*R*,2*R*)-cyclohexane-1,2-diamine
rac	racemic
s	singlet
Rib	ribose
RNA	ribonucleic acid
t	triplet
tacn	1,4,7-triazacyclononane
Thre	threitol
tmen	*N*,*N*,*N*',*N*'-tetramethylethane-1,2-diamine
tpb	trispyrazolylborate
tpm	trispyrazolylmethane
Xyl	xylose

1 Introduction

1.1 The biological importance of sugar phosphates

Sugar phosphates play a decisive role in all organisms. Ribose 5-phosphate, for example, is well known as it is part of the RNA backbone. But also in metabolism sugar phosphates are key players due to their important task of storing and transferring energy. Ribose 5-phosphate, as well as fructose 6-phosphate, is an intermediate of the pentose-phosphate pathway which generates NADPH and pentoses from glucose polymers and their degradation products. An alternative to this pathway is glycolysis (Figure 1.1), where the same carbohydrates are degraded into pyruvate thereby providing energy.

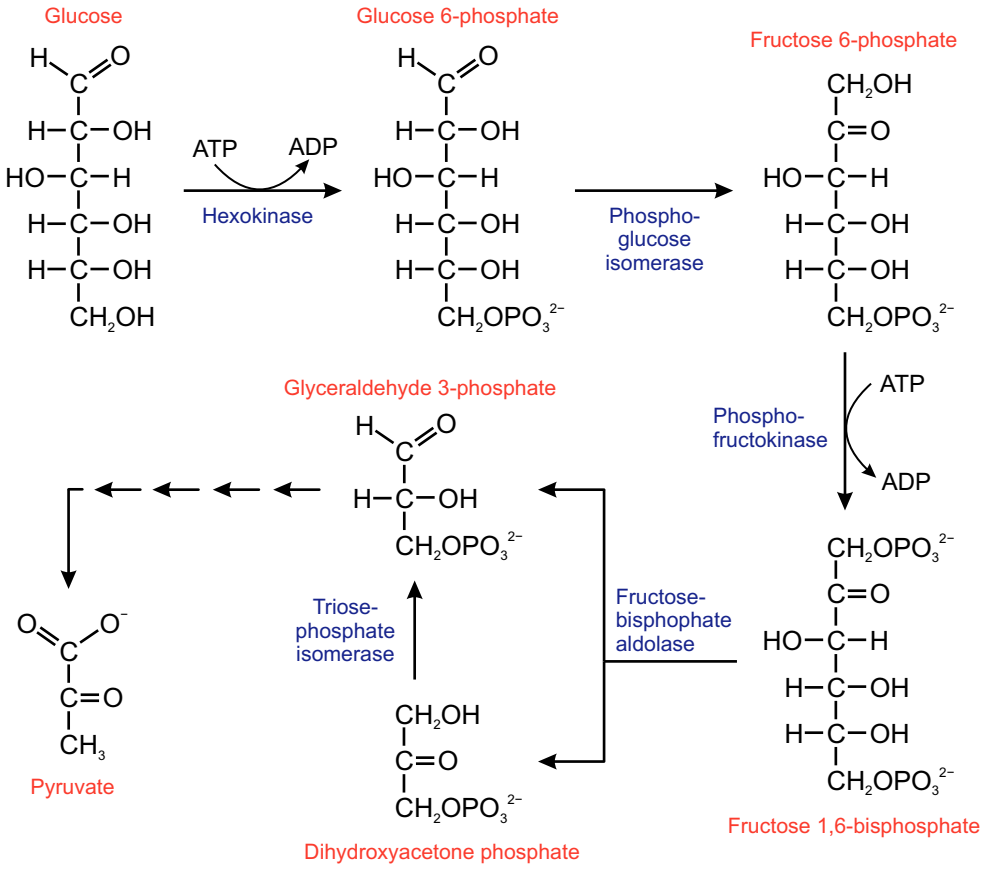

Figure 1.1 Simplified scheme of glycolysis.

The reactions of these pathways are catalysed by enzymes. Some of them contain metal centres in their active site that are essential for the catalysed reaction. There are well documented examples with magnesium(II)[1–9], manganese(II)[10–11], iron(II)[12], and zinc(II) centres[13–24] which are chelated by a sugar, a sugar phosphate or a similar molecule within the substrate-loaded active site of the enzyme. In the case of zinc(II), the available crystal

structures reveal two different possibilities for a sugar phosphate to bind. On the one hand, the phosphate group can coordinate to the metal centre as it is found in fructose 1,6-bisphosphatase[13] and ADP-ribose pyrophosphatase[14]. On the other hand, there is the coordination of the hydroxy functions. In class-II aldolase, for example, a $Zn^{II}(His)_3$ centre is chelated by three hydroxy groups of the open-chain keto form of fructose 1,6-bisphosphate.[15–16] A similar binding pattern was found in L-ribulose-5-phosphate 4-epimerase[17] and glucose-6-phosphate isomerase[18]. In the first example, L-ribulose 5-phosphate coordinates *via* two hydroxy functions to a $Zn^{II}(His)_3$ centre, while in the latter, the open-chain form of fructose 6-phosphate is bound to a $Zn^{II}(His)_3(Glu)$ centre *via* two hydroxy groups. Beside other metalloenzymes containing sugar phosphates as substrates, like D-ribulose-5-phosphate 3-epimerase[19], 3,4-dihydroxy-2-butanone-4-phosphate synthase[20] and mannose-6-phosphate isomerase[21], there are also a few metalloenzymes with a reducing sugar as substrate. Examples are L-rhamnose isomerase[22–23] and glucose dehydrogenase[24].

Nearly all the enzymes mentioned above catalyse key reactions of metabolism. While L-ribulose-5-phosphate 4-epimerase and D-ribulose-5-phosphate 3-epimerase are part of the pentose-phosphate pathway, glucose-6-phosphate isomerase and class-II aldolase catalyse reactions of glycolysis. The latter, for example, is needed to cleave fructose 1,6-bisphosphate into dihydroxyacetone phosphate and D-glyceraldehyde 3-phosphate. In order to understand the molecular mechanism of such a key reaction, it would be important to get more information about the interaction of the substrate with the metal centre. The above-mentioned crystal structure in this case shows the binding pattern only at an intermediate point of the transformation pathway but it gives no information on the initial binding of the ground-state furanose form of fructose 1,6-bisphosphate. A detailed investigation of sugar-phosphate bonding to metal centres such as zinc(II) would help with this issue.

1.2 Coordination chemistry of sugar-phosphate complexes

For this approach, the $Zn^{II}(His)_3$ centre of class-II aldolase can be taken as a starting point. In order to facilitate the experiments, the three histidine ligands are replaced by just one tridentate chelate ligand. Two obvious possibilities are the ligands dien and tacn with each providing three N-donor atoms in one ligand, yielding the metal fragments Zn^{II}(dien) and Zn^{II}(tacn) (dien = diethylenetriamine, tacn = 1,4,7-triazacyclononane) that can be combined with various sugar phosphates. Almost no information is available about such Zn^{II} complexes with sugar phosphates or similar molecules. However, published data[25–27] suggest their existence. Moreover, previous works of *Mayer* and *Herdin* verified the coordination of simple polyols and even a methylated sugar like methyl β-D-ribofuranoside to the Zn^{II}(dien) centre *via* crystal-structure analysis.[28–29] However, the preparation of the necessary crystals was

difficult and time-consuming because of various problems. First of all, the preparation of clear complex solutions was problematic due to the limited solubility of zinc hydroxide in water (solubility product: $L = 1.8 \cdot 10^{-17}$ mol/L). Furthermore, the desired crystals were only obtained from highly concentrated solutions with a resin-like consistency and they were unstable, melting rapidly when exposed to air. Despite these problems, crystal-structure analysis was thought to be the only analytical method to investigate those complexes. UV/VIS spectroscopy was useless because of the electron configuration of Zn^{II} and even NMR spectroscopy did not lead to suitable results since only averaged parameters were obtained on account of a fast metal-ligand exchange.

One possibility to circumvent these problems is to replace Zn^{II} by another metal such as Pd^{II} that was to be shown very appropriate for NMR investigation of complexes with sugars and sugar analogues, as it has already been used in many of those studies.[30–34] Although the Zn^{II}(dien) complexes of polyols and a methylated sugar were found to exhibit a trigonal-bipyramidal coordination sphere,[28–29] they are comparable to the square-planar Pd^{II} complexes since the O–M–O bond angles for both types of complexes are very similar adding up to about 85°.[28–29, 35–36] Recently, it has been shown that several sugar phosphates provided metal-binding sites to the metal fragment Pd^{II}(en) (en = ethane-1,2-diamine).[37–38] Most parts of these studies were limited to the alkaline pH range with only the hydroxy functions coordinating to Pd^{II}(en). However, a few results concerning the coordination of phosphate groups were obtained suggesting that this type of coordination only occurs at lower pH values. Beside a complex of α-D-glucose 1-phosphate with only the phosphate function coordinating to Pd^{II}(en), even a new kind of mixed sugar-core–phosphate ligation exhibiting a seven-membered chelate ring was verified in experiments with D-fructose 1,6-bisphosphate.

Further studies on sugar-phosphate complexes with other metals than Pd^{II} are available. In most of them, metal centres have been found to be exclusively phosphate-binding including Cu^{II}, Mg^{II} and even the strong Lewis acid Al^{III}.[27, 39–41] Only a few more results on sugar-phosphate complexes featuring coordination *via* hydroxy functions are available. It has been shown that ribose 5-phosphate is able to coordinate to Co^{III}(tacn) and Ga^{III}(tacn) forming a tridentate complex.[37, 42–43] Moreover, further complexes of D-fructose 1,6-bisphosphate exhibiting the mixed sugar-core–phosphate chelation have been investigated with the metal fragments Al^{III}(tacn) and Ga^{III}(tacn).[37, 43] All remaining results deal with sugar-phosphate complexes of the $Re^{V}O$ metal fragment. In this context, diolato functions of various sugar phosphates have been found to coordinate to the $Re^{V}O$(L-His) and $Re^{V}O$(L-Car) fragments (L-His = L-histidine, L-Car = L-carnosine).[38] Figure 1.2 summarises the predominant coordination patterns of sugar-phosphate complexes found so far.

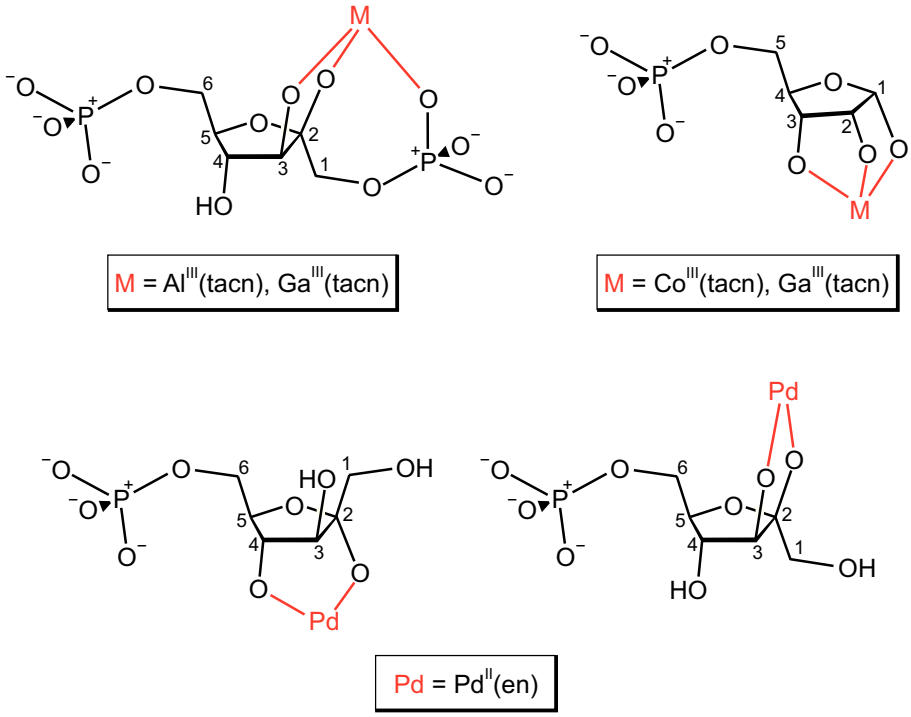

Figure 1.2 Schematic illustration of various coordination patterns of sugar-phosphate complexes known from previous studies.[37–38, 42–43]

Beside the coordination pattern, the configuration of a usual sugar phosphate varies as well. Various isomers of one sugar phosphate exist in solution, namely an α- and β-fructofuranose form and an α- and β-fructopyranose form whereas the pyranose forms of a few sugar phosphates are not accessible as their 6-position is blocked by the phosphate function. Since each isomer of one sugar phosphate existing in solution is able to coordinate to a metal centre, the variety of possible product complexes is large.

1.3 Use of NMR spectroscopy and quantum-chemical calculations

For studies on sugar-phosphate complexes, several analytical methods are available. Beside mass spectrometry and crystal-structure analysis, NMR spectroscopy is especially well suited since it allows the detailed investigation of product equilibria in solution. This is an important quality as the existence of various products in product solutions is usual in those experiments.

Applicable 1D NMR experiments are ^{1}H, $^{13}C\{^{1}H\}$ and $^{31}P\{^{1}H\}$ NMR spectroscopy. ^{13}C NMR spectra play an essential role for complex-species assignment due to the effect of coordination on the ^{13}C NMR signals of carbon atoms bound to coordinating hydroxy functions. This effect is called the coordination-induced shift (CIS). For Pd^{II} diolato complexes, these CIS values usually add up to about 10 ppm in terms of five-membered chelate rings which means that the ^{13}C NMR signals in question are shifted downfield compared to the respective educt

signals.[31] In the case of $Re^{V}O$ complexes, CIS values normally are about 20–25 ppm.[44] Unfortunately, former studies have shown that there are no CIS values for Zn^{II} complexes.[29] Thus, it is difficult to detect the coordinating hydroxy groups of such complexes.

^{1}H NMR spectra are necessary to determine vicinal proton-proton coupling constants $^{3}J_{HH}$ of an associated H–C–C–H fragment occurring in a sugar-phosphate complex. These constants depend on several factors such as the C–C bond length or the H–C–C valence bond angle.[45] However, the most important factor is the dependence on the torsion angle φ_{HH} that is described by the general Karplus equation and the corresponding Karplus curve.[46–47] Since the exact form of this equation, and thus, also the shape of the curve is influenced by electronegative substituents on or near the H–C–C–H fragment, there exist several modified Karplus equations. For sugar-phosphate complexes, the equation of Haasnoot, de Leeuw and Altona[48] should be most suitable because of its carbohydrate origin.

The ^{1}H, $^{31}P\{^{1}H\}$ and $^{13}C\{^{1}H\}$ NMR signals can be assigned by several 2D NMR experiments, namely ^{1}H–^{1}H COSY45, ^{1}H–^{13}C HMQC, ^{1}H–^{13}C HMBC, and ^{31}P–^{1}H HETCOR experiments. Especially the latter can be very important for studies on sugar-phosphate complexes because it is the only way to assign ^{31}P NMR signals of the same intensity to their corresponding complex structures.

NMR spectroscopy is applicable for all diamagnetic sugar-phosphate complexes. In contrast, the application field of mass spectrometry is more limited since it only led to useful results in the case of $Re^{V}O$ complexes of sugar phosphates. The application field of crystal-structure analysis is limited as well since this method is heavily dependent on the quality of isolated crystals and suitable crystals of sugar-phosphate complexes were shown to be difficult to obtain.[38] Regarding Pd^{II} complexes of sugar phosphates, this is problematic since NMR spectroscopy would be the only analytical method to investigate them. To overcome this problem, a procedure based on quantum-chemical calculations was recently developed that allowed the confirmation of experimental NMR parameters such as ^{13}C NMR chemical shifts and vicinal proton-proton coupling constants.[49–50] In this recent work, chemical shifts were calculated for various palladium(II) complexes of glycopyranoses with an accuracy of ± 3 ppm. For palladium, a CEP-4G effective core potential with the corresponding valence basis set was used.[51] Geometries were optimised by the BLYP method and 6-31+G(2d,p) basis sets for all atoms except palladium. GIAO NMR chemical shifts were calculated by the PBE1PBE method and the same basis sets used in the geometry optimisation. Furthermore, a PCM model was used to simulate the influence of the solvent. The resulting chemical shifts were corrected using a linear relationship between the calculated and observed shift values. Although this procedure provided quite accurate values, there were some limitations. For example, it was not possible to entirely consider the effect of the solvent water since the PCM

model used may have missed some of the microscopic processes induced by solvation.[52] However, despite these limitations, this quantum-chemical based procedure seems to be well suited to support NMR investigations of sugar-phosphate complexes with Pd^{II}.

1.4 Aims of this work

As described before, some studies dealing with coordination chemistry of sugar phosphates are available but no analogous complexes of Zn^{II} have been investigated yet. The primary goal of this work is, therefore, to fill this gap. In order to stay close to the active sites of enzymes such as class-II-aldolase, the simple metal fragment Zn^{II}(dien) is used. NMR spectroscopy is used primarily as analytical method since it enables the investigation of both complex equilibria in solution and pH dependence of metal-binding sites. Since this approach is challenging due to the fast metal-ligand exchange and the absence of CIS values, it is necessary to improve the significance of NMR data collected from sugar-phosphate complexes with Zn^{II}. Hence, further experiments are performed with molecules similar to sugar phosphates such as reducing and methylated sugars or polyols. Beside NMR spectroscopy, crystal-structure analysis will be used to get more detailed information about the binding pattern of the complexes.

Additionally, sugar-phosphate complexes of Pd^{II} are investigated since, as described above, the Pd^{II} diolato complexes are comparable to the Zn^{II} diolato complexes. Here, the focus is especially on the pH dependence of the metal-binding sites. As in previous experiments with Pd^{II}(en), various coordination types have already been found at various pH values.[37–38] In this work, the newer fragment Pd^{II}(tmen) (tmen = *N*,*N*,*N'*,*N'*-tetramethylethane-1,2-diamine) is used as, in addition, the results of both palladium(II) fragments can be compared. Product solutions are analysed by NMR spectroscopy while ^{13}C NMR chemical shifts will be confirmed by quantum-chemical calculations.

A further aim of this work is to verify the mixed sugar-core–phosphate ligation that has already been found with the metal fragments Pd^{II}(en), Al^{III}(tacn) and Ga^{III}(tacn). Recently, some results were obtained suggesting the same coordination pattern in complexes of the $Re^{V}O$ fragment with D-fructose 1,6-bisphosphate by using only bidentate spectator ligands N_2 such as en and tmen.[53] However, again, there is no crystal structure verifying this theory. Hence, further experiments are conducted, on the one hand, to synthesise more sugar-phosphate complexes with $Re^{V}ON_2$ fragments, and, on the other hand, to grow crystals confirming the theory about mixed sugar-core–phosphate chelation.

2 Results

2.1 Coordination of sugar phosphates to $Re^{V}ON_2$ fragments

Many studies on the $Re^{V}O$ fragment have been conducted in the last years,[54–82] most of them dealing with the medical significance of its complexes in the field of radiopharmacy. However, in some of these works $Re^{V}O$ complexes of sugars or sugar-like molecules such as polyols or methylated sugars were investigated.[78–82] As a general rule, a further tridentate N-ligand, such as diethylenetriamine or trispyrazolylborate, was used in those complexes as a spectator ligand to provide only two remaining binding sites for the sugar or sugar-like molecule. In later works this model was changed, as, instead of N-ligands, amino-acid ligands such as L-histidine and L-carnosine were used. Thus, it was also possible to obtain sugar-phosphate complexes with the $Re^{V}O$ fragment.[38]

In this work, the denticity of the ligands was changed. Thus, a bidentate N-ligand N_2 was used to provide three remaining binding sites for the sugar-phosphate ligands. The idea behind this approach was to get complexes exhibiting mixed sugar-core–phosphate chelation that have already been obtained by using the fragments Al^{III}(tacn) and Ga^{III}(tacn). In a recent work this concept has already been found to be promising.[53]

2.1.1 Coordination of D-fructose 1,6-bisphosphate

First of all, reactions of D-fructose 1,6-bisphosphate with various $Re^{V}ON_2$ fragments (N_2 = en, (*R*,*R*)-chxn, tmen) were performed to reconstruct the experiments of a previous study.[53] The equimolar reaction of the precursor compound *trans*-[$ReOCl_3(PPh_3)_2$] with tmen, D-fructose 1,6-bisphosphate and two equivalents of triethylamine in methanol led to a clear blue solution. After the solvent was removed, a blue residue was obtained that was redissolved in methanol-d_4 for NMR investigation. The ^{13}C and ^{31}P NMR spectra obtained are shown in Figure 2.1. CIS values of 21.1 ppm for C2 and 28.1 ppm for C3 clearly indicated the coordination of D-fructose 1,6-bisphosphate through O2 and O3 to the $Re^{V}O$(tmen) fragment. Furthermore, the ^{1}H-coupled ^{31}P NMR spectrum showed a triplet for P6 with ^{31}P–^{1}H coupling constants between 3 and 5 Hz as well as a doublet of doublets for P1 with ^{31}P–^{1}H coupling constants of 23.8 and 7.9 Hz. In comparison to the educt spectrum, the multiplicity of the P6 signal did not change. Since the phosphate group of P6 was able to rotate freely, the ^{31}P–^{1}H coupling constants were averaged over various spatial positions of the phosphate function, which obviously applied to both the educt form and the product complex. In contrast, the phosphate group of P1 must have been in a fixed position due to the high difference between

its two $^{31}P–^{1}H$ coupling constants. A coordination of this phosphate group to the $Re^{V}O$(tmen) fragment seemed to be the only possible reason for this result. A further analysis of the blue residue *via* mass spectrometry confirmed this hypothesis, as the synthesised product complex was clearly assigned as the sodium salt of the [ReO(tmen)(β-D-Fru2,3H$_{-2}$1,6P_2H$_2$-κ$^3O^{2,3,P1}$)]$^-$ monoanion (**1a**) that is shown in Figure 2.2. As illustrated in this scheme, the two phosphate groups were mono-protonated on account of the high acidity of the rhenium(V) centre.

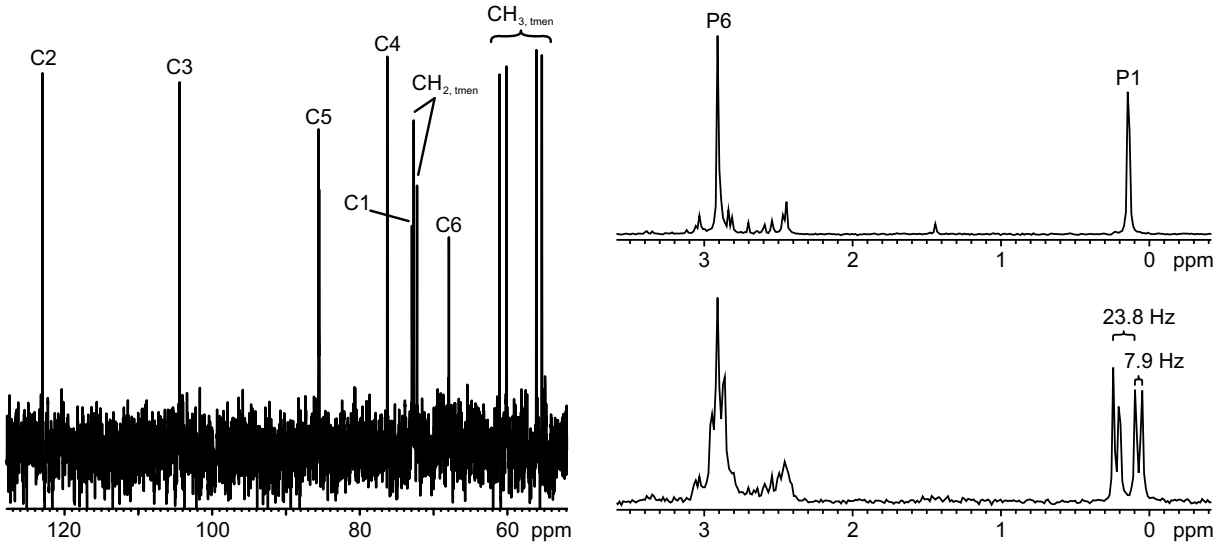

Figure 2.1 ^{13}C NMR spectrum (left), $^{31}P\{^{1}H\}$ NMR spectrum (right, top) and ^{31}P NMR spectrum (right, bottom) of [ReO(tmen)(β-D-Fru2,3H$_{-2}$1,6P_2H$_2$-κ$^3O^{2,3,P1}$)]$^-$ (**1a**) in methanol-d_4 with $^{31}P–^{1}H$ NMR coupling constants ($^3J_{P,H}$/Hz).

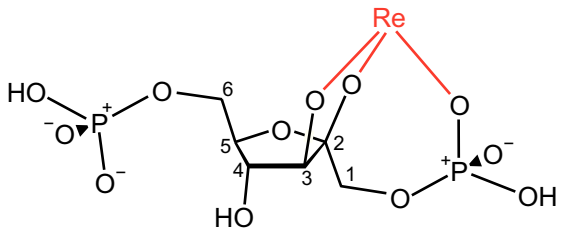

1a / 1b / 1c

Re = $Re^{V}ON_2$ (N_2 = tmen, en, (*R*,*R*)-chxn)

Figure 2.2 Structure of [ReON$_2$(β-D-Fru2,3H$_{-2}$1,6P_2H$_2$-κ$^3O^{2,3,P1}$)]$^-$ (N_2 = tmen (**1a**), en (**1b**), (*R*,*R*)-chxn (**1c**)).

Experiments with the spectator ligands en and (*R*,*R*)-chxn led to similar results. In both cases the reaction resulted in a clear brown solution. Although the brown colour, as known from previous studies, indicated that the reaction was not successful, product signals for the [ReO(en)(β-D-Fru2,3H$_{-2}$1,6P_2H$_2$-κ$^3O^{2,3,P1}$)]$^-$ anion (**1b**) and the [ReO{(*R*,*R*)-chxn}(β-D-Fru2,3H$_{-2}$1,6P_2H$_2$-κ$^3O^{2,3,P1}$)]$^-$ anion (**1c**) were observed in ^{13}C and ^{31}P NMR spectra. The CIS

values as well as the coupling constants and the multiplicity of the $^{31}P\{^{1}H\}$ NMR signals were nearly identical to the results of the experiments with tmen. Thus, the corresponding spectra are not additionally illustrated here. The ^{13}C and ^{31}P NMR chemical shifts of all three products are summarised in Table 2.1. The values are consistent with the ones obtained in a previous work.[53]

Table 2.1 ^{13}C and ^{31}P NMR chemical shifts (δ/ppm) of the product complexes **1a**, **1b** and **1c** from the reactions of *trans*-$[ReOCl_3(PPh_3)_2]$, D-fructose 1,6-bisphosphate, triethylamine and one of the spectator ligands tmen, en and (*R*,*R*)-chxn in methanol. $\Delta\delta$ is the shift difference of the product complex and the free D-fructose 1,6-bisphosphate. Bold-printed $\Delta\delta$ values indicate the metal-binding site.

	isomer	N-ligand		C1	C2	C3	C4	C5	C6	P1	P6
	β-D-Fru*f*1,6P_2		δ	66.0	101.5	76.0	74.5	80.1	65.4	3.8	3.7
1a	β-D-Fru*f*1,6P_2	tmen	δ	72.5	122.6	104.1	75.9	85.2	67.6	0.1	2.9
			$\Delta\delta$	6.5	**21.1**	**28.1**	1.4	5.1	2.2	**–3.7**	–0.8
1b	β-D-Fru*f*1,6P_2	en	δ	72.7	122.9	102.3	77.1	85.5	67.8	2.4	3.1
			$\Delta\delta$	6.7	**21.4**	**26.3**	2.6	5.4	2.4	**–1.4**	–0.6
1c	β-D-Fru*f*1,6P_2	(*R*,*R*)-chxn	δ	72.4	122.5	101.6	76.9	85.1	67.3	2.0	3.1
			$\Delta\delta$	6.4	**21.0**	**25.6**	2.4	5.0	1.9	**–1.8**	–0.6

2.1.2 Coordination of *rac*-glycerol 1-phosphate

Unfortunately, it was not possible to grow crystals of the product complexes **1a**, **1b** or **1c**. Hence, the experiments were repeated with glycerol 1-phosphate. Although this compound is actually not a sugar phosphate, it is a well suited model of that part of fructose 1,6-bisphosphate that was able to coordinate to $Re^{V}ON_2$ fragments as is shown in Figure 2.3.

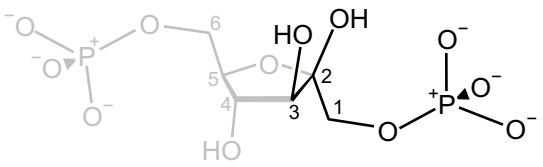

Figure 2.3 Schematic illustration of the similarity between D-glycerol 1-phosphate and D-fructose 1,6-bisphosphate.

As expected, the equimolar reaction of *trans*-$[ReOCl_3(PPh_3)_2]$ with tmen, *rac*-glycerol 1-phosphate and two equivalents of triethylamine in methanol led to a clear blue solution. With the solvent removed, a blue residue was obtained that was redissolved in acetone. After removing colourless crystals of by-products such as triphenylphosphane, blue crystals of

[ReO(tmen)(*rac*-Glyc2,3H$_{-2}$1*P*H-κ^3*O*^{2,3,P})] (**2a**) · 2 H_2O formed within 3–4 hours. Their structure is shown in Figure 2.4.

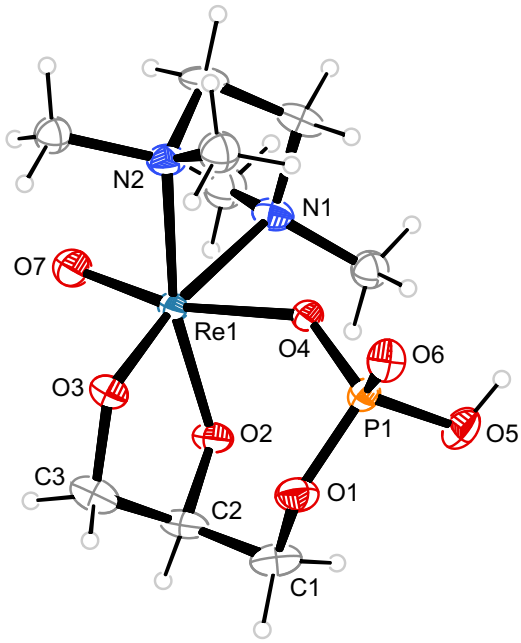

Figure 2.4 Structure of [ReO(tmen)(*rac*-Glyc2,3H$_{-2}$1*P*H-κ^3*O*^{2,3,P})] (**2a**) in crystals of the dihydrate (50 % probability ellipsoids). Distances (Å) and angles (°): Re1–O2 1.941(3), Re1–O3 1.954(3), Re1–O4 2.067(3), Re1–O7 1.678(3), Re1–N1 2.230(4), Re1–N2 2.224(4), P1–O1 1.587(3), P1–O4 1.528(3), P1–O5 1.558(3), P1–O6 1.483(3), O2–Re1–O3 82.26(13), O2–Re1–O4 85.24(12), O3–Re1–O4 88.40(12), O2–Re1–O7 106.18(14), O3–Re1–O7 101.51(14), O2–Re1–N1 95.71(14), O4–Re1–N1 81.36(12), O7–Re1–N1 88.77(13), O3–Re1–N2 97.67(13), O4–Re1–N2 79.87(12), O7–Re1–N2 88.48(13), N1–Re1–N2 81.69(15); chelate torsion angle (°): O2–C2–C3–O3: –37.9(5).

The compound crystallised in the monoclinic space group $P2_1/c$ and, thus, contained both the D- and the L-glycerol 1-phosphate form. It was assumed that using a racemic mixture of the educt was a requirement to obtain such crystals. The phosphate group was mono-protonated as well as in the product complex of D-fructose 1,6-bisphosphate, which was verified by high-resolution mass spectrometry, since signals only for the mono-protonated form were observed. Furthermore, the phosphate group participated in a hydrogen-bonding network that was completed by two water molecules. A short hydrogen bond was formed between the O5H group and one water molecule. An illustration of the hydrogen-bonding network is given in Figure 6.1 within the Appendix. Table 2.2 summarises the distances and angles of the hydrogen bonds. For NMR investigation, the blue crystals were dissolved in D_2O yielding a blue solution of about pH 5 that was stable at 4 °C for several hours. The ^{13}C and ^{31}P NMR signals that are shown in Figure 2.5 are comparable to those of the D-fructose 1,6-bisphosphate experiments. The signals of C2 and C3 are characterised by CIS values of 18.6 and 24.7 ppm, respectively, which clearly indicated the coordination of the corresponding

hydroxy functions to the $Re^{V}O$(tmen) fragment. The coordination of the phosphate group was again verified by a doublet of doublets for P1 in the $^{31}P\{^{1}H\}$ NMR spectrum with $^{31}P–^{1}H$ coupling constants of 23.8 and 6.9 Hz. The ^{13}C and ^{31}P NMR chemical shifts of **2a** are summarised in Table 2.3. The values are consistent with the ones obtained in a previous work.[53]

Table 2.2 Distances (Å) and angles (°) of hydrogen bonds in **2a** · 2 H_2O. Standard deviations of the last digit are given in parentheses. Values without standard deviation are related to hydrogen atoms at calculated positions. D: donor, A: acceptor.

D	H	A	D–H	H···A	D···A	D–H···A
O5	H85	O91^{i}	0.84	1.68	2.522(5)	175.0
O91	H911	O92^{ii}	0.89	1.81	2.697(5)	177.7
O91	H912	O3^{iii}	0.85	1.80	2.656(5)	179.9
O92	H921	O6^{iv}	0.85(4)	1.94(4)	2.771(5)	168(5)
O92	H922	O6^{i}	0.79(4)	2.01(4)	2.778(5)	163(6)

Symmetry code: (i) –*x*+1, –*y*, –*z*; (ii) –*x*+1, *y*+½, –*z*+½; (iii) –*x*+1, –*y*+1, –*z*; (iv) *x*, –*y*+½, *z*+½.

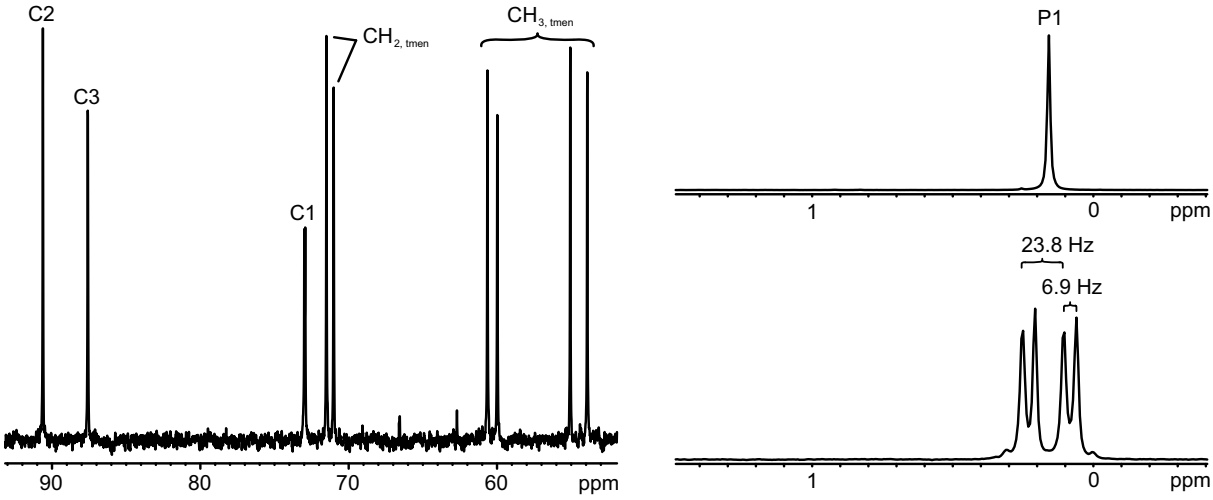

Figure 2.5 ^{13}C NMR spectrum (left), $^{31}P\{^{1}H\}$ NMR spectrum (right, top) and ^{31}P NMR spectrum (right, bottom) of [ReO(tmen)(*rac*-Glyc2,3H$_{-2}$1*P*H-κ^{3}*O*^{2,3,P})] (**2a**) in D_2O with $^{31}P–^{1}H$ NMR coupling constants ($^{3}J_{P,H}$/Hz).

Experiments with the spectator ligands en and phen led to similar results. In the case of en, a clear blue solution was obtained. By reducing the solvent to 4–5 mL, the solution turned brown. Nevertheless, product signals for [ReO(en)(*rac*-Glyc2,3H$_{-2}$1*P*H-κ*O*^{2,3,P})] (**2b**) were observed in ^{13}C and ^{31}P NMR spectra. Since the CIS values and also the coupling constants and the multiplicity of the $^{31}P\{^{1}H\}$ NMR signals were nearly identical to the results of the experiments with tmen, the corresponding spectra are not additionally illustrated here. Table

2.3 lists the ^{13}C and ^{31}P NMR chemical shifts of **2b**. A schematic illustration of **2b** is given in Figure 2.6. The values are consistent with the ones obtained in a previous work.[53]

Table 2.3 ^{13}C and ^{31}P NMR chemical shifts (δ/ppm) of the product complexes **2a** and **2b** from the reactions of *trans*-[$ReOCl_3(PPh_3)_2$], *rac*-glycerol 1-phosphate, triethylamine and one of the spectator ligands tmen and en in methanol. $\Delta\delta$ is the shift difference of the product complex and the free *rac*-glycerol 1-phosphate. Bold-printed $\Delta\delta$ values indicate the metal-binding site.

	isomer	N-ligand		C1	C2	C3	P1
	rac-Glyc1*P*		δ	65.3	72.0	62.9	5.9
2a	*rac*-Glyc1*P*	tmen	δ	73.0	90.6	87.6	0.2
			$\Delta\delta$	7.7	**18.6**	**24.7**	**–5.7**
2b	*rac*-Glyc1*P*	en	δ	72.3	91.6	86.1	4.3
			$\Delta\delta$	7.0	**19.6**	**23.2**	**–1.6**

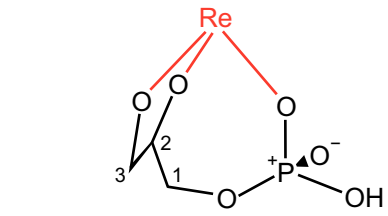

2a / 2b / 2c

Re = $Re^{V}ON_2$ (N_2 = tmen, en, phen)

Figure 2.6 Structure of [$ReON_2$(*rac*-Glyc2,3H$_{-2}$1*P*H-$\kappa^3O^{2,3,P}$)] (N_2 = tmen (**2a**), en (**2b**), phen (**2c**)).

The reaction of phen with *trans*-[$ReOCl_3(PPh_3)_2$], *rac*-glycerol 1-phosphate and triethylamine in methanol led to a clear, yellow-brown solution. By removing the solvent, a brown residue was obtained that was washed and redissolved in methanol. Finally, green crystals of [ReO(phen)(*rac*-Glyc2,3H$_{-2}$1*P*H-$\kappa^3O^{2,3,P}$)] (**2c**) · MeOH formed within two weeks. Their structure is shown in Figure 2.7. Again, the compound crystallised in the monoclinic space group $P2_1/c$. As already seen in the previous structures, the phosphate group was mono-protonated, which was verified by high-resolution mass spectrometry since signals only for the mono-protonated form had been observed. Within the crystal structure, centro-symmetric dimers of **2c** formed *via* two short hydrogen bonds between the O6H group and $O5^i$ as well as the $O6^iH$ group and O5. Table 2.4 summarises the distances and angles of the hydrogen bonds observed. An illustration of the hydrogen-bonding network is given in Figure 6.2 within the Appendix. Unfortunately, the green crystals were indissoluble in any solvent. Thus, analysis *via* NMR spectroscopy was impossible. Even NMR spectra of the concentrated reaction solution did not show any product signals.

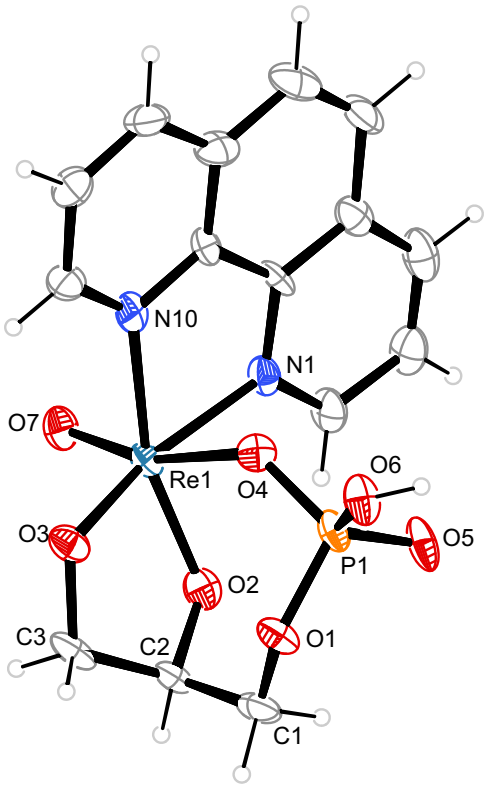

Figure 2.7 Structure of [ReO(phen)(*rac*-Glyc2,3H$_{-2}$1*P*H-κ^3*O*^{2,3,P})] (**2c**) in crystals of **2c** · MeOH (50 % probability ellipsoids). Distances (Å) and angles (°): Re1–O2 1.917(6), Re1–O3 1.957(6), Re1–O4 2.102(6), Re1–O7 1.690(6), Re1–N1 2.129(6), Re1–N10 2.158(7), P1–O1 1.583(6), P1–O4 1.527(6), P1–O5 1.490(7), P1–O6 1.558(7), O2–Re1–O3 82.7(3), O2–Re1–O4 88.2(2), O3–Re1–O4 85.5(2), O2–Re1–O7 106.8(3), O3–Re1–O7 103.8(3), O2–Re1–N1 93.6(3), O4–Re1–N1 78.1(3), O7–Re1–N1 92.8(3), O3–Re1–N10 100.7(3), O4–Re1–N10 73.3(2), O7–Re1–N10 90.9(3), N1–Re1–N10 77.7(3). chelate torsion angle (°): O2–C2–C3–O3 –32.2(9).

Table 2.4 Distances (Å) and angles (°) of hydrogen bonds in **2c** · MeOH. Standard deviations of the last digit are given in parentheses. Values without standard deviation are related to hydrogen atoms at calculated positions. D: donor, A: acceptor.

D	H	A	D–H	H···A	D···A	D–H···A
O6	H86	O5^{i}	0.81(4)	1.68(5)	2.495(8)	179(11)
O8	H88	O3^{i}	0.84	1.84	2.681(9)	173.7

Symmetry code: (i) –*x*, –*y*, –*z*.

2.1.3 Coordination of further sugar phosphates

The experiments conducted with D-fructose 1,6-bisphosphate and *rac*-glycerol 1-phosphate were repeated with further sugar phosphates. Unfortunately, none of these experiments were successful. In the case of D-fructose 6-phosphate, D-mannose 6-phosphate and α-D-glucose 1-

phosphate, either colourless solutions were obtained which indicated a redox reaction of Re^{V}, or the yellow suspension of the educts did not change at all for several days. In experiments with D-glucose 6-phosphate, a greenish blue solution was obtained by refluxing the reaction mixture for 1 hour. However, the colour turned back to yellow at room temperature within half an hour. The analysis *via* ^{13}C NMR spectroscopy of the reaction mixture was impossible due to a poor signal-to-noise ratio. With the reaction of D-ribose 5-phosphate, actually, a blue solution was obtained but the possible product degraded within several minutes, which was indicated by decolouration of the solution. No product signals were found in NMR spectra. As a result, obtaining a tridentate coordination of a triolato function to a $Re^{V}ON_2$ fragment, as realised with the metal fragments Co^{III}(tacn) and Ga^{III}(tacn) (see Figure 1.2), seemed to be impossible. In summary, the only way found for a sugar phosphate to coordinate to a $Re^{V}ON_2$ fragment was *via* the facial coordination pattern of a diolato function combined with a phosphate group. Beside fructose 1,6-bisphophate and glycerol 1-phosphate, there is also fructose 1-phosphate which complies with this requirement. However, experiments with D-fructose 1-phosphate were not successful as only colourless solutions were obtained. The poor solubility of the educt D-fructose 1-phosphate in methanol was assumed to be a possible reason since only the barium salt was available.

2.2 Coordination of sugar phosphates to the Pd^{II}(tmen) fragment

Sugar-phosphate complexes of Pd^{II}(en) have already been investigated in an earlier work.[37–38] The study, however, was mainly restricted to the alkaline pH range. In this work Pd^{II}(tmen) was used for conducting a detailed analysis with one metal fragment in the whole pH range. Compared to Pd^{II}(en), in Pd^{II}(tmen) the N-bonded H atoms are substituted by methyl groups. As a result, complex species stabilities are modified due to, first, an increased steric demand in the direction of the bonded diolate and, second, the impossibility of forming hydrogen bonds. Furthermore, Pd-tmen showed a higher resistance to reduction to Pd^{0}, yielding NMR spectra of a much higher quality that can be analysed in more detail.[35] In recent studies Pd-tmen was used for analysing the chelation sites of several sugars and sugar-like molecules such as polyols, amino sugars, sugar amino acids, methylated sugars and deoxy sugars.[35–36, 83–85] In all of them the Pd^{II}(tmen) fragment is coordinated by diolato functions forming five-ring chelates or six-ring chelates. This binding pattern was verified by several crystal-structure analyses as well as NMR spectroscopy. The presence of a five-ring palladacyle was clearly indicated by a CIS of about 10 ppm for the ^{13}C NMR signals of carbon atoms bound to coordinating hydroxy functions. The coordination of a phosphate group to Pd^{II}(tmen) has not been investigated so far. However, as described in the introduction, a complex with α-D-

glucose 1-phosphate coordinating to Pd^{II}(en) *via* the phosphate function has recently been observed.[38]

In this work several sugar phosphates were investigated in the presence of Pd^{II}(tmen). Since the focus was on the pH dependence of the complexes formed, the same stoichiometric ratio was used in each reaction. In order to avoid high concentrations of free sugar phosphates in product solutions, all reactions of this work were performed under Pd^{II}(tmen)-excess conditions. Thus, a molar Pd^{II}(tmen):sugar-phosphate ratio of 3:1 was used. The pH was varied by adding various stoichiometric amounts of nitric acid.

^{13}C NMR chemical shifts of product complexes were verified by quantum-chemical calculations. Detailed information about the general procedure of the calculations including the methods and basis sets used is given in Chapter 5.3. It should be mentioned that only the complexes with exclusive coordination of the hydroxy functions were analysed by this procedure for two reasons. Firstly, the phosphate-coordinating species exhibited too many atoms, which would have caused overly long calculation times. Secondly, the coordination of a phosphate group caused only a very small change of the ^{13}C NMR chemical shifts up to 2 ppm which was too small to detect it *via* quantum-chemical calculations since the accuracy of the procedure added up to ±3.5 ppm. Furthermore, the calculation of ^{31}P NMR chemical shifts was not successful most probably due to their high dependence on the phosphate group's degree of protonation.

2.2.1 Coordination of α-D-glucose 1-phosphate

The Pd^{II}(tmen) experiments were started with the non-reducing sugar phosphate α-D-glucose 1-phosphate, since its complexes with Pd^{II}(en) have already been investigated at various pH values.[38] Moreover, it is configurationally restricted to the α-pyranose form. Hence, only this form had to be considered for coordination to Pd^{II}(tmen), which resulted in a simplified analysis of NMR spectra.

The dissolution of α-D-glucose 1-phosphate in Pd-tmen (molar Pd^{II}(tmen):sugar-phosphate ratio of 3:1) resulted in the formation of two monometallated species in nearly the same concentration. The first product (51%) was the five-ring chelate [Pd(tmen)(α-D-Glc*p*1*P*2,3H$_{-2}$-κ^2*O*^{2,3})]$^{2-}$ (**3a**) and the second product (49%) was the corresponding κ^2*O*^{3,4} chelate (**3b**). Both products are shown in Figure 2.8. The ^{13}C NMR chemical shifts listed in Table 2.5 clearly confirmed the chelation sites as there were CIS values of 9.8 and 8.8 ppm for C2 and C3 of **3a**, and CIS values of 10.5 and 9.6 ppm for C3 and C4 of **3b**, respectively. Furthermore, the calculated ^{13}C NMR chemical shifts also given in Table 2.5 supported the

species assignment. Compared to results with Pd^{II}(en),[38] only the ratio of the two products was different. In those experiments the κ$O^{3,4}$ chelate was the main species (70%).

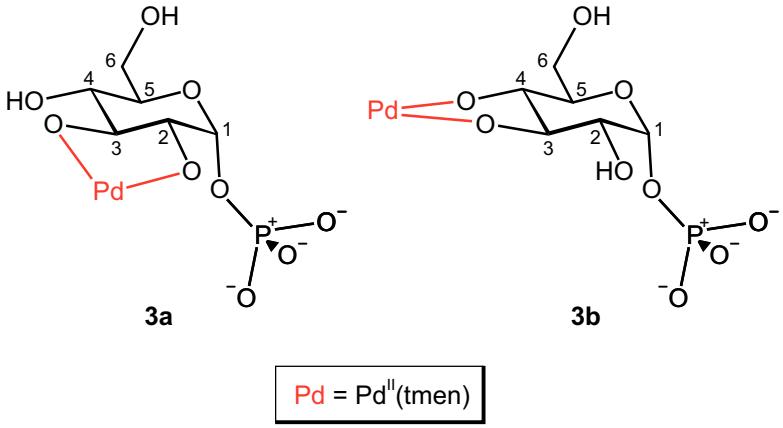

3a **3b**

Figure 2.8 Products from the reaction of Pd-tmen with α-D-glucose 1-phosphate at the molar ratio of 3:1.

Table 2.5 ^{13}C and ^{31}P NMR chemical shifts observed (δ_{obs}/ppm) and calculated (δ_{calc}/ppm) of the product complexes **3a**, **3b** and **3c** from the reactions of Pd-tmen and α-D-glucose 1-phosphate (molar ratio 3:1) with various stoichiometric amounts of nitric acid in D_2O. Shifts calculated were determined by the procedure given in Chapter 5.3. $\Delta\delta$ is the shift difference of the product complex and the free α-D-glucose 1-phosphate. Bold-printed $\Delta\delta$ values indicate the metal-binding site.

	isomer	chelation site		C1	C2	C3	C4	C5	C6	P1
	α-D-Glc*p*1*P*		δ	94.2	72.9	72.6	70.4	73.8	61.4	4.2
3a	α-D-Glc*p*1*P*	$\kappa^2O^{2,3}$	δ_{obs}	94.9	82.7	81.4	72.8	72.5	61.4	3.7
			δ_{calc}	96.9	83.8	81.7	73.6	70.3	61.3	–
			$\Delta\delta$	0.7	**9.8**	**8.8**	2.4	−1.3	0.0	−0.5
3b	α-D-Glc*p*1*P*	$\kappa^2O^{3,4}$	δ_{obs}	94.4	75.0	83.1	80.0	74.6	61.7	4.0
			δ_{calc}	93.0	76.6	80.5	78.4	74.3	62.8	–
			$\Delta\delta$	0.2	2.1	**10.5**	**9.6**	0.8	0.3	−0.2
3c	α-D-Glc*p*1*P*	κO^P:$\kappa O'^P$	δ_{obs}	95.5	72.1	73.5	70.0	73.5	61.1	11.2
			$\Delta\delta$	1.3	−0.8	0.9	−0.4	−0.3	−0.3	**7.0**

Several coupling constants of **3a** and **3b** were determined from ^{1}H NMR spectra. They are listed in Table 2.6. All of them were similar to the coupling constants of the free α-D-glucose 1-phosphate due to the fact that both products, as well as the educt, were α-pyranose forms.

Table 2.6 Coupling constants (*J*/Hz) of the α-D-glucose-1-phosphate part of product complexes **3a**, **3b** and **3c** in D_2O compared to the values of the free α-D-glucose 1-phosphate that were obtained from a previous work[86].

	$^3J_{1,P}$	$^3J_{1,2}$	$^4J_{2,P}$	$^3J_{2,3}$	$^3J_{3,4}$	$^3J_{4,5}$	$^3J_{5,6a}$	$^3J_{5,6b}$	$^2J_{6a,6b}$
α-D-Glc*p*1*P*	7.4	3.5	1.8	9.8	9.7	10.1	5.3	2.3	−12.3
3a	7.2	3.4	–	9.2	9.5	9.8	–	–	–
3b	7.5	3.6	–	9.3	9.5	10.0	–	–	–
3c	7.2	3.5	2.4	9.8	9.1	10.1	5.1	2.2	–

In order to investigate the pH dependence of the metal-binding sites of the α-D-glucose 1-phosphate complexes, further reactions were performed. While the molar ratio of Pd^{II}(tmen) and α-D-glucose 1-phosphate was kept at 3:1, various stoichiometric amounts of nitric acid were added to the product solution. By adding 3 equivalents, the pH changed to 7 and the NMR signals of the two products **3a** and **3b** vanished. Instead, signals of a third species were observed. The ^{13}C NMR shifts were nearly the same as those from the free α-D-glucose-1-phosphate form. However, the ^{31}P NMR signal observed was shifted downfield by 7.0 ppm in comparison to the signal of the free form. The same ^{13}C and ^{31}P NMR signals were found in appropriate experiments with Pd-en conducted in a previous work.[38] There, fortunately, yellow crystals were isolated from a mixture of Pd-en with α-D-glucose 1-phosphate and nitric acid at a pH of 7 yielding the structure of [{Pd(en)}$_2${μ-(α-D-Glc*p*1*P*-κO^P:κO'^P)}$_2$] in crystals with 13 H_2O shown in Figure 2.9.

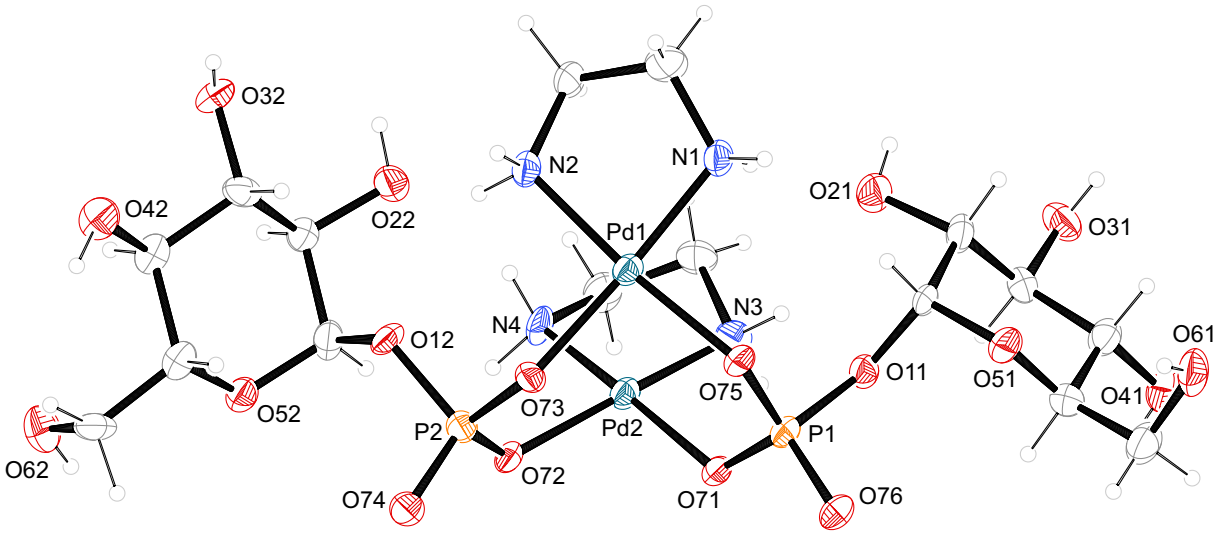

Figure 2.9 Structure of [{Pd(en)}$_2${μ-(α-D-Glc*p*1*P*-κO^P:κO'^P)}$_2$] in crystals with 13 H_2O obtained in an earlier work[38].

In this structure, two molecules of α-D-glucose 1-phosphate acted as bridging ligands as they connected two Pd^{II}(en) fragments by coordination *via* the phosphate group. Moreover, all

hydroxy functions were protonated and non-coordinating, which explained the absence of CIS values in the ^{13}C NMR spectrum. It was obvious that the CIS value observed in the ^{31}P NMR spectrum indicated the coordination of the phosphate group. It has to be mentioned that both the hydroxy functions of α-D-glucose 1-phosphate and the amino functions of the Pd^{II}(en) fragments took part in a hydrogen-bonding network together with 13 water molecules. The participation of the amino functions seemed to be essential, as, unfortunately, no crystals could be isolated from experiments with Pd^{II}(tmen) whose amino functions were methylated. However, the Pd^{II}(tmen)-complex structure was assumed to be the same as in the Pd^{II}(en) complex, since the NMR results from the sugar-phosphate part of both complexes were identical. A scheme of [{Pd(tmen)}$_2${μ-(α-D-Glc*p*1*P*-κ*O*^{P}:κ*O*'^{P})}$_2$] (**3c**) is shown in Figure 2.10. The appropriate ^{13}C and ^{31}P NMR chemical shifts as well as the $^{3}J_{H,H}$ coupling constants determined are listed in Table 2.5 and Table 2.6, respectively.

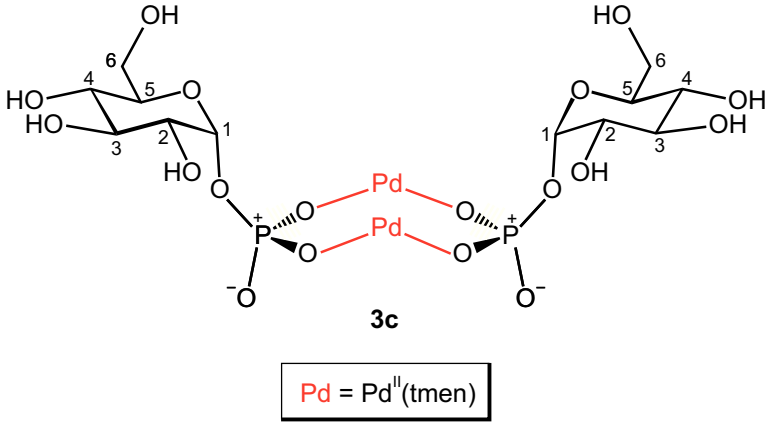

Figure 2.10 Product from the reaction of Pd-tmen with α-D-glucose 1-phosphate and nitric acid at the molar ratio of 3:1:3.

After a scan of the full pH range from 4 to 14, no other products could be clearly assigned. Nevertheless, in the ^{31}P NMR spectra of product solutions with a pH of 8–9, signals of two further species were observed. Their chemical shifts of about 12 ppm indicated that in both complexes the phosphate group coordinated to Pd^{II}. Contrary to first expectations, these signals did not belong to species with mixed sugar-core–phosphate chelation as described in the introduction. It was rather a not—yet—considered combination of the coordination *via* both hydroxy functions and the phosphate group to separate Pd^{II}(tmen) fragments. The results of the following chapters will verify this hypothesis. In the case of α-D-glucose 1-phosphate, the existence of these forms was only speculative since no ^{13}C NMR signals were observed due to the low concentration of the respective products.

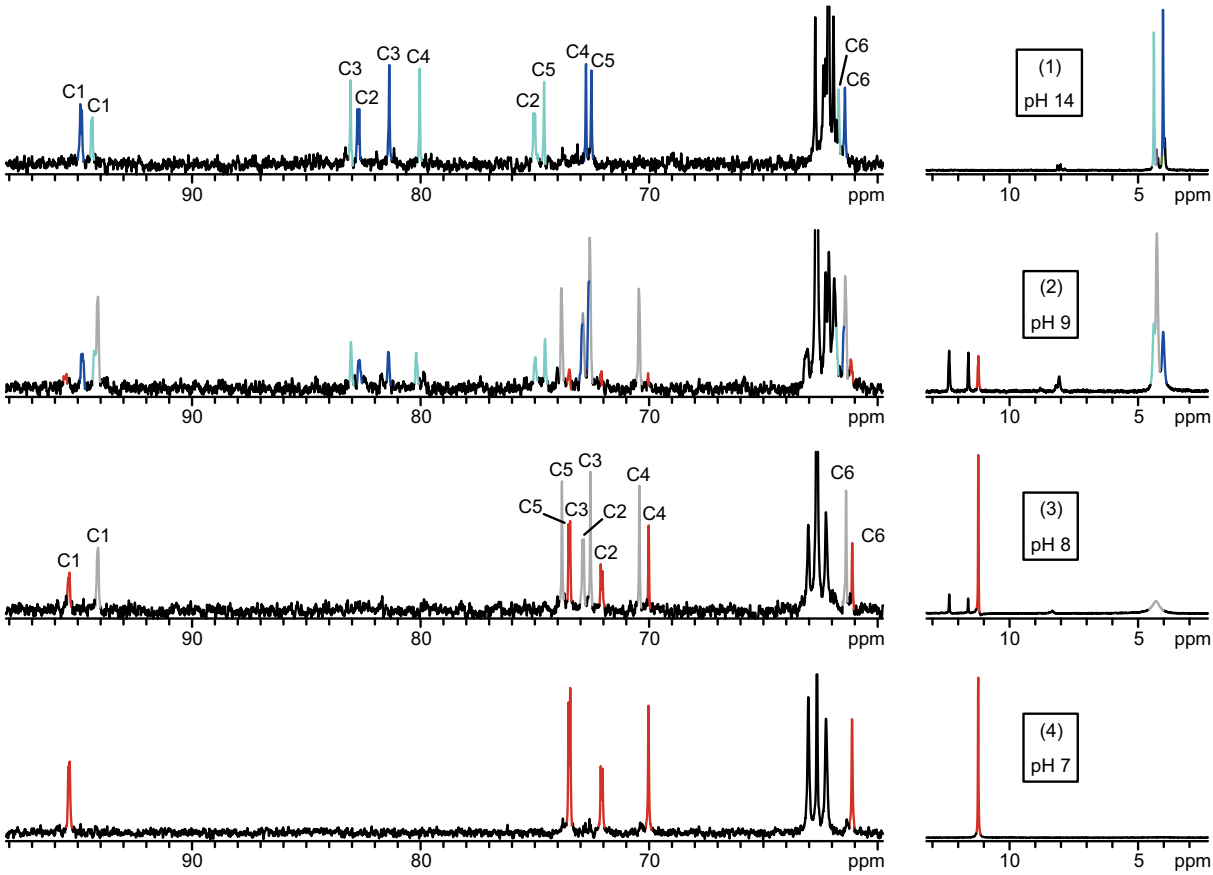

Figure 2.11 ^{13}C and ^{31}P NMR spectra of aqueous solutions from the reactions of Pd-tmen and α-D-glucose 1-phosphate at the molar ratio of 3:1 with various stoichiometric amounts of nitric acid; (1): no addition of nitric acid (pH 14); (2): 2 equivalents of nitric acid (pH 9); (3): 2.5 equivalents of nitric acid (pH 8); (4): 3 equivalents of nitric acid (pH 7). Species assigned are **3a** (marked light blue), **3b** (marked dark blue), **3c** (marked red) and the free α-D-glucose-1-phosphate form (marked grey). Note the split C1 and C2 signals as a result of ^{31}P–^{13}C coupling.

Figure 2.11 gives an overview of ^{13}C and ^{31}P NMR spectra of Pd^{II}(tmen)–α-D-glucose-1-phosphate product solutions at various pH values. It is shown that the products **3a** and **3b** were observed at pH values only above 8. Thus, the coordination of the hydroxy functions seemed to be restricted to this pH range. On the other hand, product **3c** is present at pH values only below 10, which led to the implication that phosphate coordination is limited to this pH range. The transition between these different complexation types was fluent, as there was a small range at pH 9 where all product complexes existed in equilibrium. Finally, it has to be mentioned that, despite the Pd^{II}(tmen)-excess conditions, a high concentration of free α-D-glucose 1-phosphate was observed at pH 8–9.

2.2.2 Coordination of *rac*-glycerol 1-phosphate

rac-Glycerol 1-phosphate is actually not a sugar phosphate but is a suitable model for them as already shown in Chapter 2.1.2. It features one phosphate group and only two hydroxy functions, which should result in a very limited variety of products. Hence, *rac*-glycerol 1-phosphate is eminently suitable to get a basic overview about the pH dependence of the metal-binding sites of sugar-phosphate complexes.

Although *rac*-glycerol 1-phosphate is a racemic mixture of the D- and L-form of glycerol 1-phosphate, only one set of signals was observed in NMR spectra. This applied to possible product species as well. The reaction of *rac*-glycerol 1-phosphate with Pd-tmen (molar Pd^{II}(tmen):glycerol-phosphate ratio of 3:1) led to the formation of only one species, the monometallated [Pd(tmen)(*rac*-Glyc1*P*H$_{-2}$-κ^2*O*^{2,3})]$^{2-}$ anion (**4a**) which is shown in Figure 2.12. Its ^{13}C and ^{31}P NMR chemical shifts are listed in Table 2.7. The CIS values of 8.0 and 8.7 ppm for C2 and C3, respectively, indicated the metal-binding site. The calculated ^{13}C NMR chemical shifts also given in Table 2.7 supported the assignment. In comparison to results with Pd^{II}(en),[38] no significant difference was noticeable.

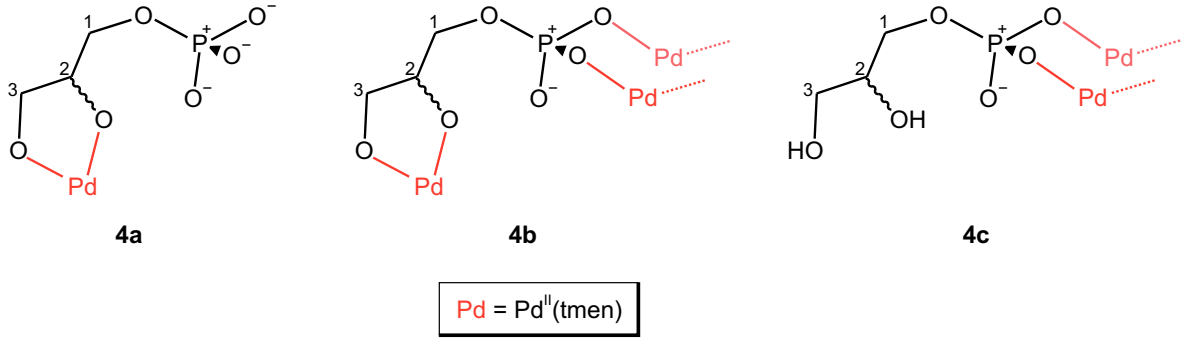

Figure 2.12 Structures and structural fragments of the products from the reactions of Pd-tmen with *rac*-glycerol 1-phosphate at various pH values. About one half of the structure is shown for the products **4b** and **4c**.

After reducing the pH to 6 by adding 3 equivalents of nitric acid, the product signals of **4a** vanished. Instead, signals of the exclusively phosphate-coordinating form [{Pd(tmen)}$_2${μ-(*rac*-Glyc1*P*-κ*O*^{P}:κ*O*'^{P})}$_2$] (**4c**) appeared which was characterised by a CIS of 6.3 ppm for the ^{31}P NMR signal of P1. All NMR chemical shifts determined for **4c** are listed in Table 2.7. Figure 2.12 shows a schematic illustration of **4c**. For reasons of clarity, a structural fragment of about one half of the whole complex containing only one of the two glycerol-1-phosphate ligands is shown there. Another reason for illustrating a structural fragment instead of the whole complex is a general problem that is introduced in the following section.

Table 2.7 ^{13}C and ^{31}P NMR chemical shifts observed (δ_{obs}/ppm) and calculated (δ_{calc}/ppm) of the product complexes **4a**, **4b** and **4c** from the reactions of Pd-tmen and *rac*-glycerol 1-phosphate (molar ratio 3:1) with various stoichiometric amounts of nitric acid in D_2O. Shifts calculated were determined by the procedure given in Chapter 5.3. $\Delta\delta$ is the shift difference of the product complex and the free *rac*-glycerol 1-phosphate. Bold-printed $\Delta\delta$ values indicate the metal-binding site.

	isomer	chelation site		C1	C2	C3	P1
	rac-Glyc*p*1*P*		δ	65.3	72.0	62.9	5.9
4a	*rac*-Glyc*p*1*P*	$\kappa^2O^{2,3}$	δ_{obs}	65.6	80.0	71.6	5.7
			δ_{calc}	65.0	83.5	72.7	–
			$\Delta\delta$	0.3	**8.0**	**8.7**	–0.2
4b	*rac*-Glyc*p*1*P*	$\kappa^2O^{2,3}$:κO^P:$\kappa O'^P$	δ_{obs}	66.6	79.6	71.6	12.0
			$\Delta\delta$	1.3	**7.6**	**8.7**	**6.1**
4c	*rac*-Glyc*p*1*P*	κO^P:$\kappa O'^P$	δ_{obs}	66.7	71.6	62.9	12.2
			$\Delta\delta$	1.4	–0.4	0.0	**6.3**

By scanning the full pH range from 4 to 14, a further product was observed. Its ^{13}C NMR chemical shifts were similar to the ones of **4a** with CIS values of 7.6 and 8.7 ppm for C2 and C3, respectively. However, the ^{31}P NMR signal of this product was shifted as well, resulting in a CIS value of 6.1 ppm. Regarding these NMR results, it was obvious that the exclusive coordination of the hydroxy functions and the exclusive coordination of the phosphate group were combined. This resulted in the complex [{Pd(tmen)}$_4${μ-(*rac*-Glyc1*P*H$_{-2}$-$\kappa^2O^{2,3}$:κO^P:$\kappa O'^P$)}$_2$] (**4b**). It featured two glycerol-1-phosphate ligands that each coordinated to one different Pd^{II}(tmen) fragment *via* the hydroxy groups of C2 and C3. Moreover, the two glycerol-1-phosphate ligands acted as bridging ligands by coordinating to two further Pd^{II}(tmen) fragments *via* their phosphate functions, yielding a kind of ring structure already obtained with the products **3c** and **4c**. Figure 2.12, again, shows a structural fragment of about one half of **4b** containing only one of the two glycerol-1-phosphate ligands for reasons of clarity. This structural fragment could combine with itself to result in **4b** containing four Pd^{II} centres. But, of course, it could also combine with the structural fragment of **4c** given in Figure 2.12 because both of them were available in solution at the pH range 8–9. As a result, it was highly probable that more product complexes existed in solution than sets of signals were observed in the NMR spectra since it was not possible to distinguish between the same structural fragments in different product complexes *via* NMR spectroscopy. Also for that reason, structural fragments and not the whole complexes are shown in Figure 2.12 and all the following Figures of Chapter 2.2.

In Figure 2.13 several ^{13}C and ^{31}P NMR spectra from the reactions of *rac*-glycerol 1-phosphate with Pd-tmen at various pH values are given. It is shown that the coordination of the hydroxy functions was restricted to pH values above 7 as the two products **4a** and **4b** were

observed only at this range. Furthermore, the coordination of the phosphate group, featured in the products **4b** and **4c**, was limited to pH values below 10. Overall, these results were consistent with those of the α-D-glucose-1-phosphate experiments.

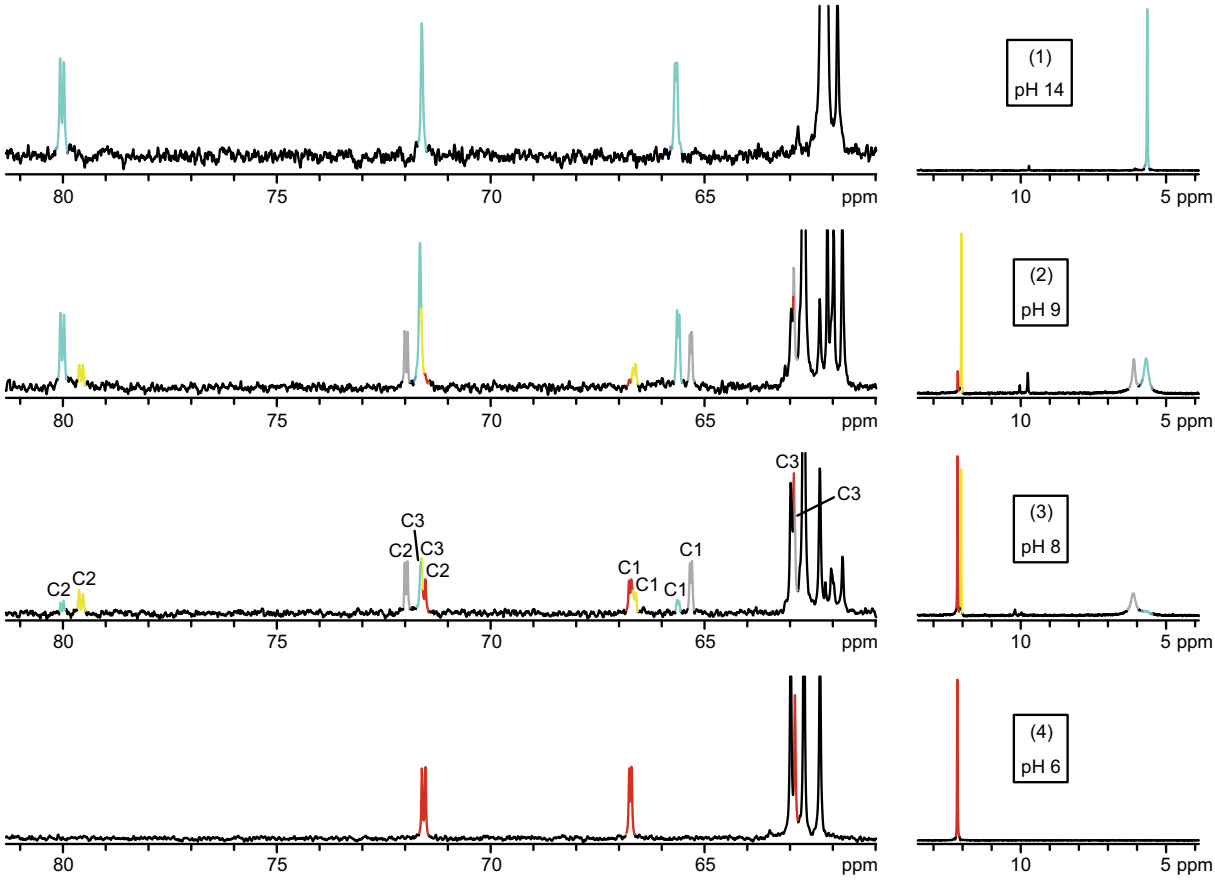

Figure 2.13 ^{13}C and ^{31}P NMR spectra of aqueous solutions from the reactions of Pd-tmen and *rac*-glycerol 1-phosphate at the molar ratio of 3:1 with various stoichiometric amounts of nitric acid; (1): no addition of nitric acid (pH 14); (2): 1.5 equivalents of nitric acid (pH 9); (3): 2 equivalents of nitric acid (pH 8); (4): 3 equivalents of nitric acid (pH 6). Species assigned are **4a** (marked light blue), **4b** (marked yellow), **4c** (marked red) and the free *rac*-glycerol-1-phosphate form (marked grey). Note the split C1 and C2 signals as a result of ^{31}P–^{13}C coupling.

2.2.3 Coordination of D-glucose 6-phosphate

Compared to α-D-glucose 1-phosphate, D-glucose 6-phosphate is phosphorylated at the hydroxy function of C6 instead of C1. The consequences of this change are significant. Since the glucose core is no longer configurationally restricted to the α-pyranose form, the formation of the β-pyranose form and even the furanose forms is possible. However, in aqueous solutions of D-glucose 6-phosphate, practically just the α- and β-pyranose forms were observed *via* NMR spectroscopy with concentrations of 36% and 63%, respectively.

The reaction of D-glucose 6-phosphate and Pd-tmen (molar Pd^{II}(tmen):sugar-phosphate ratio of 3:1) resulted in the formation of three species. The main product was the dimetallated [{Pd(tmen)}$_2$(β-D-Glc*p*6*P*1,2;3,4H$_{-4}$-κ^2*O*^{1,2}:κ^2*O*^{3,4})]$^{2-}$ anion (**5b**) (57%). The two further products were the monometallated κ^2*O*^{1,2} chelates [Pd(tmen)(α-D-Glc*p*6*P*1,2H$_{-2}$-κ^2*O*^{1,2})]$^{2-}$ (**5c**) (11%) and [Pd(tmen)(β-D-Glc*p*6*P*1,2H$_{-2}$-κ^2*O*^{1,2})]$^{2-}$ (**5d**) (32%). Further species were observed after the adjustment of lower pH values by adding stoichiometric amounts of nitric acid. At pH 8 the main species was the β-κ^2*O*^{1,2} product **5e** featuring an additional coordination of the phosphate group. In contrast, the corresponding α-form was not observed at any pH value. Adjusting the pH to values below 8, the two exclusively phosphate-coordinating species **5f** and **5g** formed. Figure 2.14 shows all structures and structural fragments of the products observed. The ^{13}C and ^{31}P NMR chemical shifts of all species are listed in Table 2.8. The CIS values of all ^{13}C NMR signals lay between 8.4 and 12.4 ppm. The ^{31}P NMR CIS values added up to 5.6–5.8 ppm.

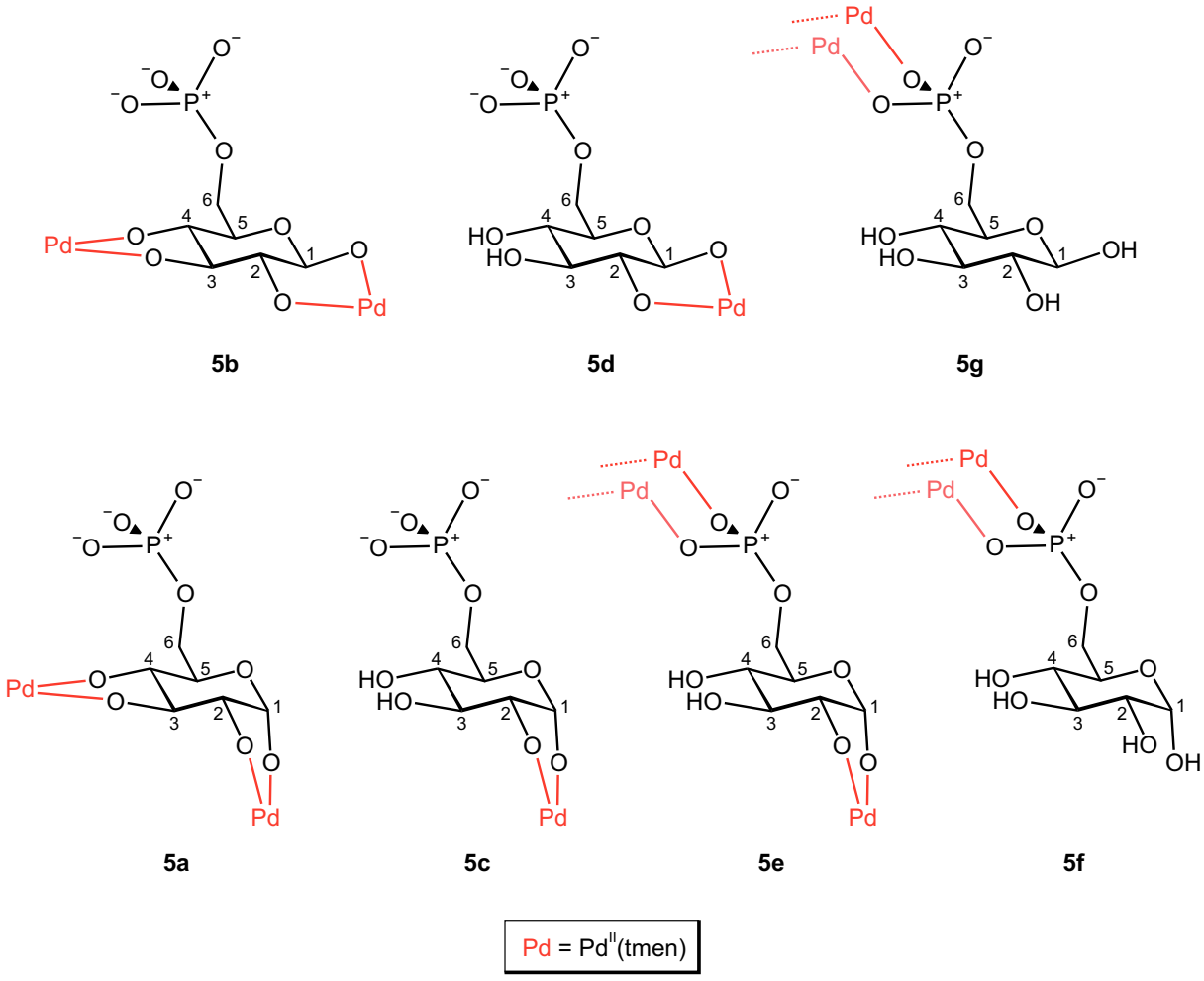

Figure 2.14 Structures and structural fragments of the products from the reactions of Pd-tmen with D-glucose 6-phosphate at various pH values. About one half of the structure is shown for the products **5e**, **5f** and **5g**.

Table 2.8 ^{13}C and ^{31}P NMR chemical shifts observed (δ_{obs}/ppm) and calculated (δ_{calc}/ppm) of the product complexes **5a**, **5b**, **5c**, **5d**, **5e**, **5f** and **5g** from the reactions of Pd-tmen and D-glucose 6-phosphate (molar ratio 3:1) with various stoichiometric amounts of nitric acid in D_2O. Shifts calculated were determined by the procedure given in Chapter 5.3. $\Delta\delta$ is the shift difference of the product complex and the free D-glucose 6-phosphate. Bold-printed $\Delta\delta$ values indicate the metal-binding site.

	isomer	chelation site		C1	C2	C3	C4	C5	C6	P6
	α-D-Glc*p*6*P*		δ	92.9	72.3	72.9	69.7	71.8	63.3	6.3
	β-D-Glc*p*6*P*		δ	96.7	74.9	75.9	69.7	76.1	63.4	6.3
5a	α-D-Glc*p*6*P*	$\kappa^2O^{1,2}$:$\kappa^2O^{3,4}$	δ_{obs}	102.1	84.9	89.9	78.7	72.9	64.0	5.7
			δ_{calc}	102.4	88.9	88.7	80.9	75.3	63.7	–
			$\Delta\delta$	**9.2**	**12.6**	**17.0**	**9.0**	1.1	0.7	−0.6
5b	β-D-Glc*p*6*P*	$\kappa^2O^{1,2}$:$\kappa^2O^{3,4}$	δ_{obs}	105.5	86.4	88.3	80.0	76.5	64.7	5.7
			δ_{calc}	103.6	89.2	90.1	81.9	78.3	64.1	–
			$\Delta\delta$	**8.8**	**11.5**	**12.4**	**10.3**	0.4	1.3	−0.6
5c	α-D-Glc*p*6*P*	$\kappa^2O^{1,2}$	δ_{obs}	102.6	82.3	78.3	69.5	71.2	63.3	6.3
			δ_{calc}	101.9	81.8	78.6	67.9	69.1	61.1	–
			$\Delta\delta$	**9.7**	**10.0**	5.4	−0.2	−0.6	0.0	0.0
5d	β-D-Glc*p*6*P*	$\kappa^2O^{1,2}$	δ_{obs}	105.1	84.4	76.4	70.1	76.8	63.8	6.1
			δ_{calc}	102.7	82.9	77.0	69.7	75.1	61.0	–
			$\Delta\delta$	**8.4**	**9.5**	0.5	0.4	0.7	0.4	−0.2
5e	α-D-Glc*p*6*P*	$\kappa^2O^{1,2}$:κO^P:$\kappa O'^P$	δ_{obs}	102.6	82.2	78.5	69.8	70.9	64.8	12.1
			$\Delta\delta$	**9.7**	**9.9**	5.6	0.1	−0.9	1.5	**5.8**
5f	α-D-Glc*p*6*P*	κO^P:$\kappa O'^P$	δ_{obs}	92.8	72.3	73.2	69.9	71.4	64.7	12.0
			$\Delta\delta$	0.0	0.0	0.3	0.1	−0.5	1.4	**5.7**
5g	β-D-Glc*p*6*P*	κO^P:$\kappa O'^P$	δ_{obs}	96.7	74.9	76.2	69.8	75.6	64.8	11.9
			$\Delta\delta$	−0.1	0.0	0.3	0.2	−0.4	1.4	**5.6**

Table 2.9 Coupling constants (*J*/Hz) of the D-glucose-6-phosphate part of product complexes **5a**, **5b**, **5c**, **5d**, **5e**, **5f** and **5g** in D_2O.

	$^3J_{1,2}$	$^3J_{2,3}$	$^3J_{3,4}$	$^3J_{4,5}$	$^3J_{5,6a}$	$^3J_{5,6b}$	$^3J_{6a,P}$	$^3J_{6b,P}$	$^2J_{6a,6b}$
5a	4.2	8.4	9.4	9.5	7.3	–	3.6	–	−11.5
5b	7.3	9.1	8.9	8.4	7.9	1.9	4.7	5.1	−11.5
5c	3.7	9.2	9.8	9.7	–	5.9	–	3.1	−11.9
5d	7.5	9.0	–	–	–	–	–	–	–
5e	3.7	9.0	9.1	9.8	–	–	–	–	–
5f	3.7	9.4	9.6	–	–	–	–	–	–
5g	8.0	9.4	–	–	–	4.7	–	4.4	−11.4

Several coupling constants of the product complexes observed were determined. They are given in Table 2.9. As expected, the $^{3}J_{1,2}$ coupling constants lie above 7.0 Hz for α-forms and below 4.5 Hz for β-forms.

Figure 2.15 gives an overview of ^{13}C and ^{31}P NMR spectra from Pd^{II}(tmen)–D-glucose-6-phosphate product solutions at various pH values. As seen in the chapters above, the coordination of the phosphate function was limited to the pH range below 10 while the coordination of the hydroxy groups was restricted to pH values above 6. In the pH range between 7 and 9, both coordination types existed, even at the same molecule as shown by **5e**.

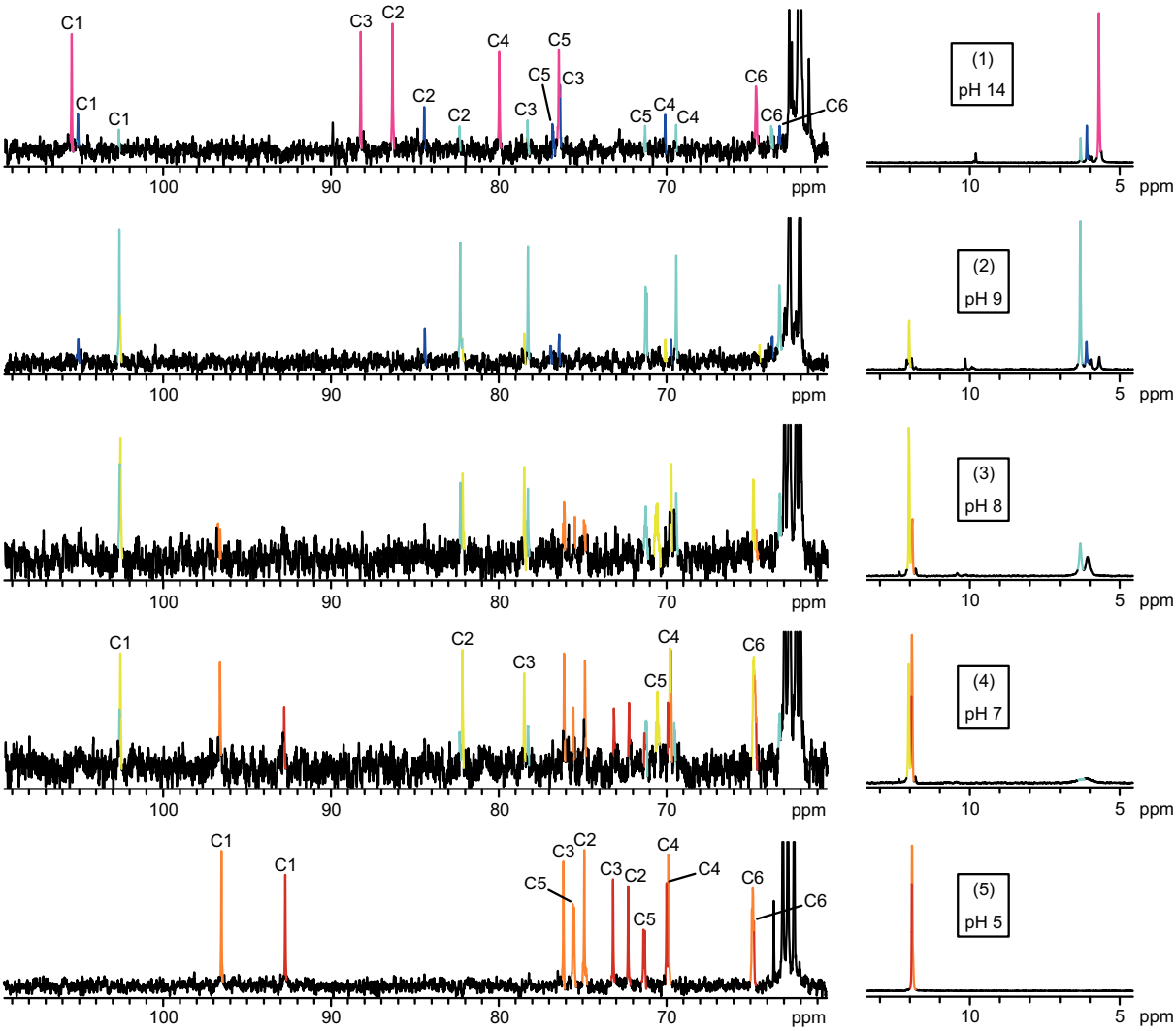

Figure 2.15 ^{13}C and ^{31}P NMR spectra of aqueous solutions from the reactions of Pd-tmen and D-glucose 6-phosphate at the molar ratio of 3:1 with various stoichiometric amounts of nitric acid; (1): no addition of nitric acid (pH 14); (2): 1.5 equivalents of nitric acid (pH 9); (3): 2 equivalents of nitric acid (pH 8); (4): 2.5 equivalents of nitric acid (pH 7); (5): 4 equivalents of nitric acid (pH 5). Species assigned are **5b** (marked magenta), **5c** (marked light blue), **5d** (marked dark blue), **5e** (marked yellow), **5f** (marked red) and **5g** (marked orange). Note the split C5 and C6 signals as a result of ^{31}P–^{13}C coupling.

Surprisingly, the equilibrium between α- and β-forms lay far to the side of the β-forms (8%: 92%) at pH 14. This was in contrast to, on the one hand, the solutions at lower pH values (pH < 10) and, on the other hand, experiments with Pd-en.[38] It was assumed that 3 hours of reaction time were not enough to achieve the final thermodynamic equilibrium. Hence, the reaction at pH 14 was repeated stirring the solutions for various lengths of time. Figure 2.16 shows the ^{13}C NMR spectra obtained.

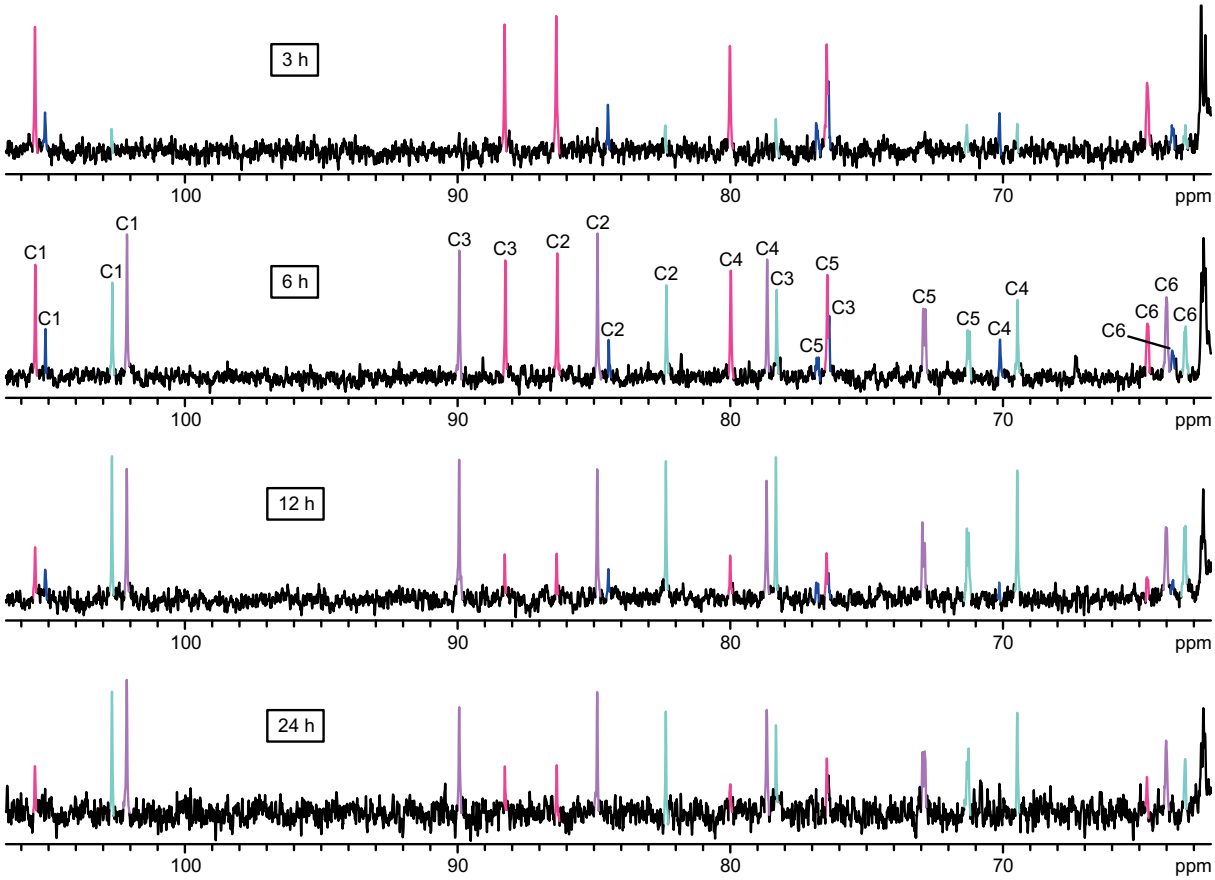

Figure 2.16 ^{13}C and ^{31}P NMR spectra of aqueous solutions from the reaction of Pd-tmen and D-glucose 6-phosphate at the molar ratio of 3:1 (pH 14). The solutions were stirred for various reaction times, namely 3 h, 6 h, 12 h and 24 h. Species assigned are **5a** (marked violet), **5b** (marked magenta), **5c** (marked light blue) and **5d** (marked dark blue). Note the split C5 and C6 signals as a result of ^{31}P–^{13}C coupling.

As clearly shown by the NMR spectra, the assumption was right. After the reaction time of 6 hours, the main species was the dimetallated α-form [{Pd(tmen)}$_2$(α-D-Glc*p*6*P*1,2;3,4H$_{-4}$-κ*O*^{1,2}:κ*O*^{3,4})]$^{2-}$ (**5a**) (see Figure 2.14) that had not been observed after the reaction time of 3 hours. The ^{13}C and ^{31}P NMR chemical shifts as well as the coupling constants found for **5a** are listed in Tables 2.8 and 2.9, respectively. Further product complexes after the reaction time of 6 hours were the dimetallated β-form **5b** and the two monometallated forms **5c** and **5d**. The equilibrium already lay on the side of the α-forms (61%:39%). After 12 hours, the

thermodynamic equilibrium was almost achieved with the α-forms being highly dominant (76%:24%). Within 12 further hours of reaction time the equilibrium did not change significantly.

Since the cause of these long equilibration times—especially at high alkaline pH values—was not clear, several further experiments were conducted investigating the influence of the Pd^{II} fragment, the phosphate function, the pH value and the stoichiometry in more detail.

2.2.3.1 Influence of the pH value and the stoichiometry

The influence of the pH value has already been investigated by the NMR experiments given in Figure 2.15. However, a change of the stoichiometry would also have an effect on the pH, since the decrease of added Pd^{II}(tmen) would also mean a decrease of added hydroxide anions. In order to avoid this problem, the stoichiometry was changed to a molar Pd^{II}(tmen):sugar-phosphate ratio of 2:1 while 2 equivalents of sodium hydroxide were added additionally to obtain almost the same pH as in the previous experiments. The solutions of Pd-tmen with D-glucose 6-phosphate and sodium hydroxide in the molar ratio of 2:1:2 were stirred for various lengths of time between 3 and 24 hours. Figure 2.17 shows the ^{13}C NMR spectra obtained.

The first thing noticed was the remarkably low reaction rate. Even after the reaction time of 3 hours, only 17% of the D-glucose 6-phosphate had reacted. The remaining 83% still existed non-coordinating as the α- and β-educt forms. After 6 hours, the amount of the free D-glucose 6-phosphate forms was still 43%. They vanished after about 24 h. As a result, the additional hydroxide anions in solution seemed to inhibit the reaction. This conclusion was drawn since the NMR spectra of reactions from Pd-tmen with D-glucose 6-phosphate, in the molar ratio of 2:1 without the addition of sodium hydroxide, did not show any signals of educt forms. Hence, not the change of stoichiometry but the further addition of sodium hydroxide is the crucial factor.

The change of the equilibrium between α- and β- product forms over the course of time was similar to the reactions of the molar 3:1 ratio. After 3 hours, only the monometallated β-form **5d** was observed. After 6 hours, the ratio between α- and β-product forms was nearly balanced. A reaction time of 24 hours was necessary to achieve the final thermodynamic equilibrium. At this point only the α-product forms were observed in the ^{13}C NMR spectrum. However, small amounts of the β-product forms were probably still in solution but were obviously not detectable *via* ^{13}C NMR spectroscopy due to a very poor signal-to-noise ratio.

In conclusion, the low reaction rate is not influenced by the change of stoichiometry but is obviously influenced by the concentration of hydroxide anions, and thus, by the pH value.

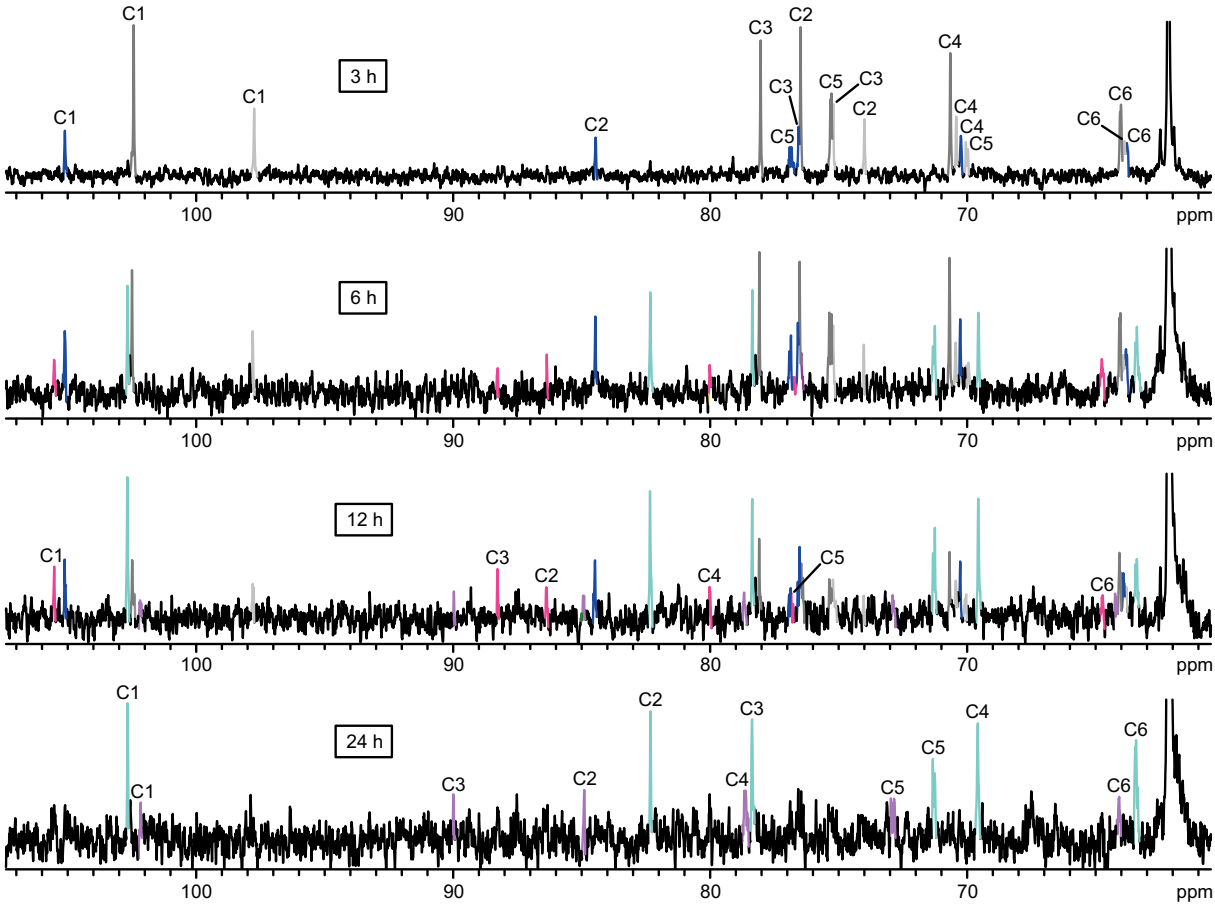

Figure 2.17 ^{13}C and ^{31}P NMR spectra of aqueous solutions from the reaction of Pd-tmen and D-glucose 6-phosphate with the addition of sodium hydroxide at the molar ratio of 2:1:2 (pH 14). The solutions were stirred for various reaction times, namely 3 h, 6 h, 12 h and 24 h. Species assigned are **5a** (marked violet), **5b** (marked magenta), **5c** (marked light blue), **5d** (marked dark blue) and the α- and β-form of the free D-glucose 6-phosphate (marked grey). Note the split C5 and C6 signals as a result of ^{31}P–^{13}C coupling.

It should be mentioned that the signals of the free D-glucose-6-phosphate forms in the NMR spectra of Figure 2.17 were shifted downfield in comparison to educt spectra at neutral pH values. This was due to the deprotonation of the hydroxy functions bound to them. Since the hydroxy groups of C1 had the lowest acid-dissociation constants, they were deprotonated first, and thus, featured the largest shift.

2.2.3.2 Influence of the palladium(II) fragment

In order to investigate the influence of the palladium(II) fragment, the reactions of D-glucose 6-phosphate were repeated with Pd-en. The dissolution of D-glucose 6-phosphate in Pd-en

(molar Pd^{II}(en):sugar-phosphate ratio of 3:1) resulted in the formation of two species: the dimetallated [{Pd(en)}$_2$(α-D-Glc*p*6*P*1,2;3,4H$_{-4}$-κ^2*O*^{1,2}:κ^2*O*^{3,4})]$^{2-}$ anion (**6a**) and the corresponding β-form [{Pd(en)}$_2$(β-D-Glc*p*6*P*1,2;3,4H$_{-4}$-κ^2*O*^{1,2}:κ^2*O*^{3,4})]$^{2-}$ (**6b**), both shown in Figure 2.18. The corresponding ^{13}C and ^{31}P NMR chemical shifts are given in Table 2.10. The results are consistent with the ones obtained in a previous work.[38]

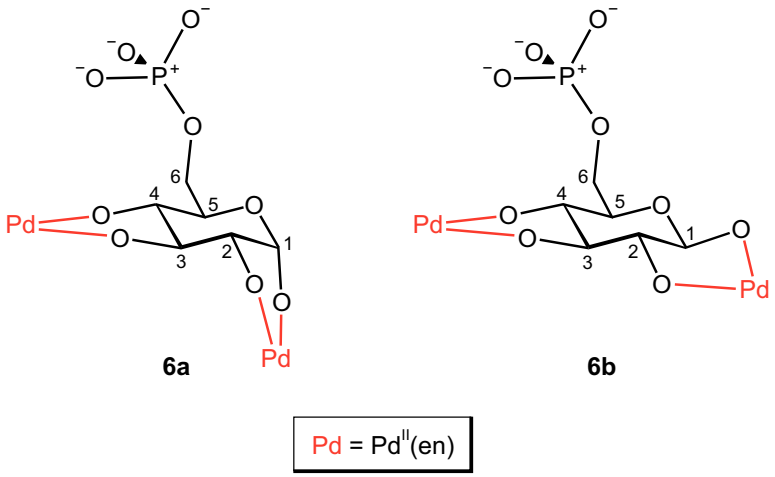

Figure 2.18 Structures of the products from the reaction of Pd-en with D-glucose 6-phosphate at the molar ratio of 3:1.

Table 2.10 ^{13}C and ^{31}P NMR chemical shifts (*δ*/ppm) of the product complexes **6a** and **6b** from the reaction of Pd-en and D-glucose 6-phosphate (molar ratio 3:1) in D_2O. Δ*δ* is the shift difference of the product complex and the free D-glucose 6-phosphate. Bold-printed Δ*δ* values indicate the metal-binding site. The values for **6a** and **6b** are consistent with the ones obtained in a previous work.[38]

	isomer	chelation site		C1	C2	C3	C4	C5	C6	P6
	α-D-Glc*p*6*P*		*δ*	92.9	72.3	72.9	69.7	71.8	63.3	6.3
	β-D-Glc*p*6*P*		*δ*	96.7	74.9	75.9	69.7	76.1	63.4	6.3
6a	α-D-Glc*p*6*P*	κ^2*O*^{1,2}:κ^2*O*^{3,4}	*δ*	103.0	84.9	87.0	79.3	74.7	63.7	5.5
			Δ*δ*	**10.1**	**12.6**	**14.1**	**9.6**	2.9	0.4	−0.8
6b	β-D-Glc*p*6*P*	κ^2*O*^{1,2}:κ^2*O*^{3,4}	*δ*	106.5	85.6	87.6	80.7	76.5	64.3	5.7
			Δ*δ*	**9.8**	**10.7**	**11.7**	**11.0**	0.4	−0.1	−0.6

Table 2.11 Coupling constants (*J*/Hz) of the D-glucose-6-phosphate part of product complexes **6a** and **6b** in D_2O.

	$^3J_{1,2}$	$^3J_{2,3}$	$^3J_{3,4}$	$^3J_{4,5}$	$^3J_{5,6a}$	$^3J_{5,6b}$	$^3J_{6a,P}$	$^3J_{6b,P}$	$^2J_{6a,6b}$
6a	3.7	9.0	9.3	9.4	6.1	2.0	4.0	–	−11.1
6b	7.3	9.3	9.2	9.4	7.4	2.0	4.0	–	−11.2

In this previous study it was possible only to determine a few coupling constants. This time the quality of the NMR spectra was good enough to find almost all of them. They are listed in Table 2.11.

The time-dependent experiments showed that the final equilibrium of the Pd^{II}(en) complexes was obtained much more quickly than in experiments with Pd^{II}(tmen). After 3 hours, the equilibrium already lay on the side of the α-forms. The reaction was finished after 6 hours. Figure 2.19 illustrates the respective ^{13}C NMR spectra.

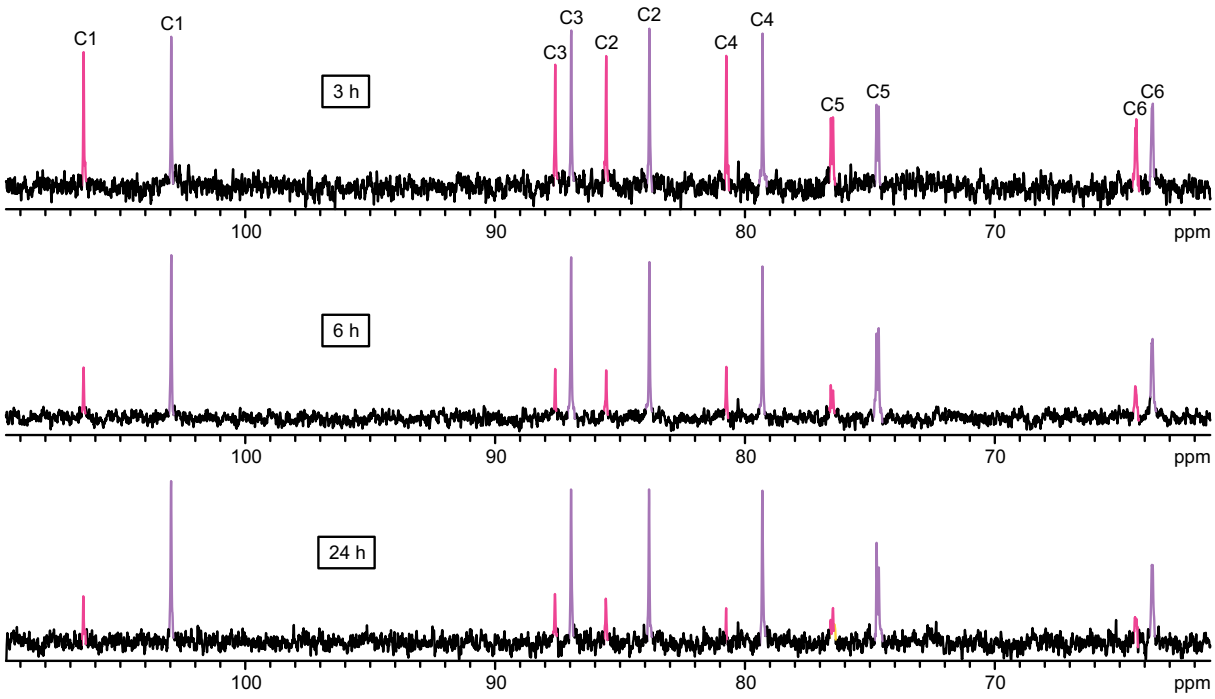

Figure 2.19 ^{13}C and ^{31}P NMR spectra of aqueous solutions from the reaction of Pd-en and D-glucose 6-phosphate at the molar ratio of 3:1 (pH 14). The solutions were stirred for various reaction times, namely 3 h, 6 h and 24 h. Species assigned are **6a** (marked violet) and **6b** (marked magenta). Note the split C5 and C6 signals as a result of ^{31}P–^{13}C coupling.

2.2.3.3 Influence of the phosphate group

The last parameter investigated was the influence of the phosphate group. In this regard, reactions of Pd-tmen with D-glucose were conducted since it is the parental sugar of D-glucose 6-phosphate. The reaction in the molar Pd^{II}(tmen):sugar ratio of 3:1 led to five product complexes, all shown in Figure 2.20. Beside the α- and β-pyranose forms assumed **7a**, **7b**, **7c** and **7d**, the dimetallated α-furanose form **7e** was also obtained. It was even the main species (49%) after the reaction time of 24 hours. The ^{13}C NMR chemical shifts of all five products are given in Table 2.12. They are in agreement with the ones of a previous

work.[36] Since the $^{3}J_{H,H}$ coupling constants have already been published in this work, they are not listed here again. However, they can be found in the Experimental Section of this work.

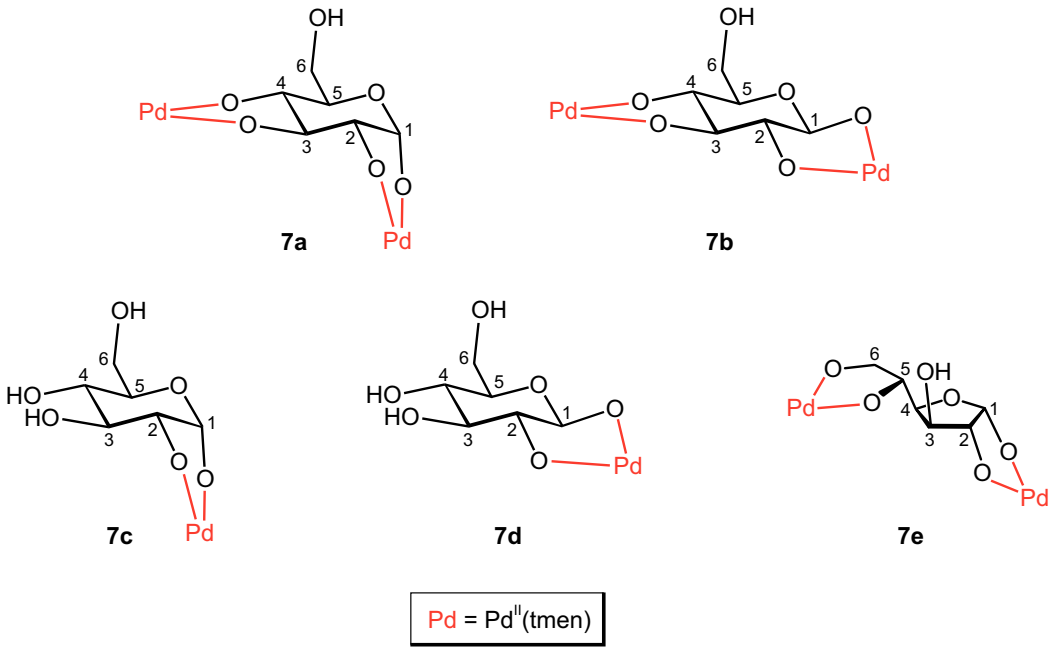

Figure 2.20 Structures of the products from the reaction of Pd-tmen with D-glucose at the molar ratio of 3:1.

Table 2.12 ^{13}C and ^{31}P NMR chemical shifts (δ/ppm) of the product complexes **7a**, **7b**, **7c**, **7d** and **7e** from the reaction of Pd-tmen and D-glucose (molar ratio 3:1) in D_2O. $\Delta\delta$ is the shift difference of the product complex and the free D-glucose. Bold-printed $\Delta\delta$ values indicate the metal-binding site. For the α-furanose educt form only the C1 shift value was available.[87] Thus, the C2–C6 shift values of methyl-α-D-glucofuranose were used for proximity.[88] The values for **7a**–**7e** are consistent with the ones obtained in a previous work.[36]

	isomer	chelation site		C1	C2	C3	C4	C5	C6
	α-D-Glc*p*		δ	92.7	72.1	73.4	70.2	72.0	61.2
	β-D-Glc*p*		δ	96.5	74.7	76.4	70.3	76.6	61.4
	α-D-Glc*f*		δ	97.4	(78.2)	(77.1)	(79.3)	(71.2)	(64.7)
7a	α-D-Glc*p*	$\kappa 2O^{1,2}$:$\kappa^2O^{3,4}$	δ	102.2	85.0	89.8	78.4	73.3	–
			$\Delta\delta$	**9.5**	**12.9**	**16.4**	**8.2**	1.3	–
7b	β-D-Glc*p*	$\kappa^2O^{1,2}$:$\kappa^2O^{3,4}$	δ	105.7	86.6	88.0	79.9	76.8	–
			$\Delta\delta$	**9.2**	**11.9**	**11.6**	**9.6**	0.2	–
7c	α-D-Glc*p*	$\kappa^2O^{1,2}$	δ	102.5	82.0	78.9	70.1	71.4	–
			$\Delta\delta$	**9.8**	**9.9**	5.5	–0.1	–0.6	–
7d	β-D-Glc*p*	$\kappa^2O^{1,2}$	δ	104.9	84.3	77.3	70.8	77.2	–
			$\Delta\delta$	**8.4**	**9.6**	0.9	0.5	0.6	–
7e	α-D-Glc*f*	$\kappa^2O^{1,2}$: $\kappa^2O^{5,6}$	δ	111.8	88.9	80.6	77.6	80.0	73.2
			$\Delta\delta$	**14.4**	(**10.7**)	(3.5)	(–1.7)	(**8.8**)	(**8.5**)

Again, experiments with various reaction times were conducted. Figure 2.21 shows the ^{13}C NMR spectra obtained. The equilibrium between α-pyranose and β-pyranose forms lay far at the side of the β-forms (14%:86%) after 3 hours. After 6 hours, the final thermodynamic equilibrium was still not achieved but the equilibrium already lay on the side of the α-forms (60%:40%). After 24 hours, the reaction was finished with an equilibrium lying far on the side of the α-pyranose forms (84%:16%). The time-dependent ratios were similar to the ones determined by the experiments with D-glucose 6-phosphate. Thus, the low reaction rate at alkaline pH values was independent from the presence of the phosphate group.

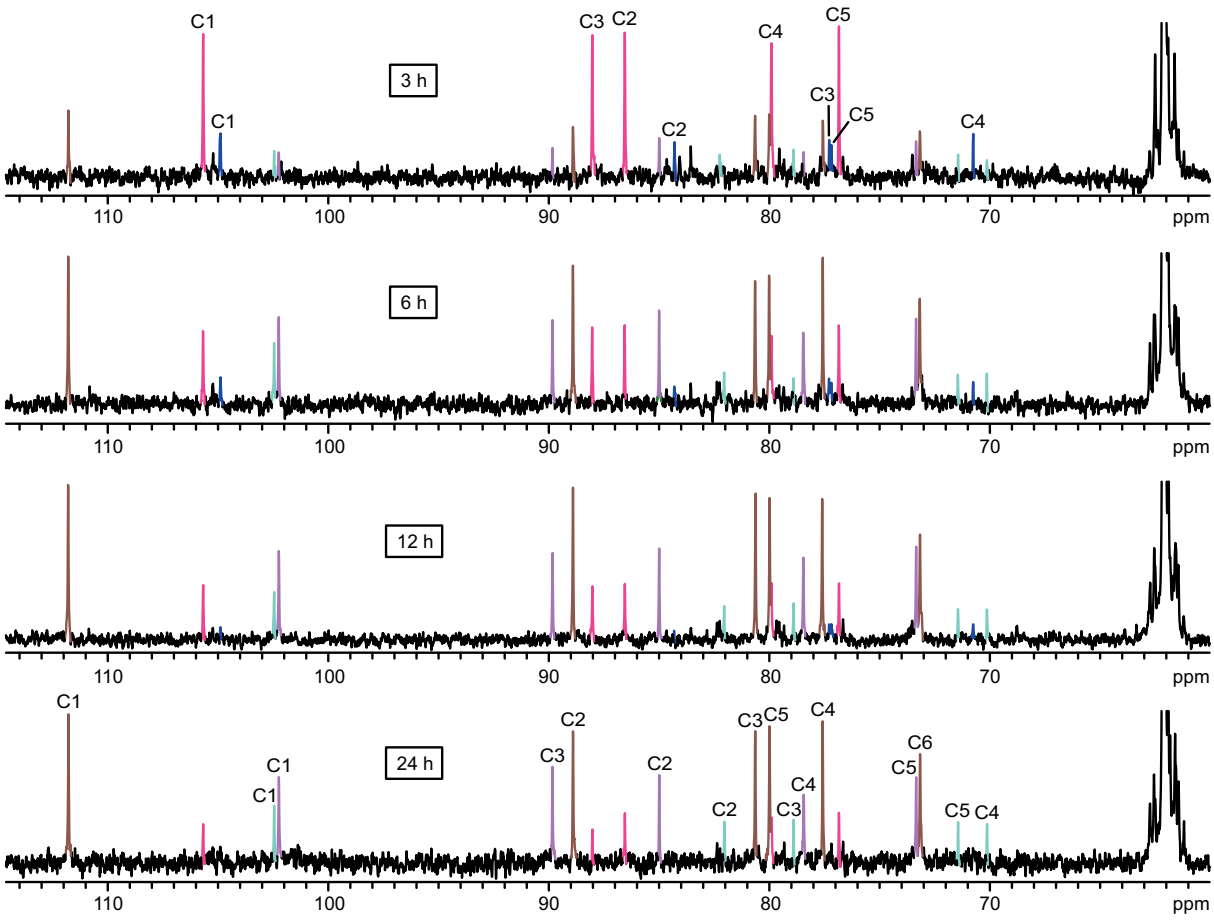

Figure 2.21 ^{13}C and ^{31}P NMR spectra of aqueous solutions from the reaction of Pd-tmen and D-glucose at the molar ratio of 3:1 (pH 14). The solutions were stirred for various reaction times, namely 3 h, 6 h, 12 h and 24 h. Products assigned are **7a** (marked violet), **7b** (marked magenta), **7c** (marked light blue), **7d** (marked dark blue) and **7e** (marked brown).

2.2.4 Coordination of D-mannose 6-phosphate

The sugar phosphate D-mannose 6-phosphate is an epimer of D-glucose 6-phosphate that was investigated in the last chapter. The only difference is the conformation at C2. Thus, the

corresponding hydroxy function of the $^4C_1$-pyranose forms changes from an equatorial to an axial position. Although furanose forms are accessible, the aqueous solution of D-mannose 6-phosphate is only a mixture of the α- and β-pyranose forms (71%:29%). Here, in contrast to D-glucose 6-phosphate, the α-pyranose form is the main species.

The reaction of D-mannose 6-phosphate in Pd-tmen (molar Pd^{II}(tmen):sugar-phosphate ratio of 3:1) resulted in three species. The main species was the monometallated [Pd(tmen)(α-D-Man*p*6*P*2,3H$_{-2}$-κ^2*O*^{2,3})]$^{2-}$ anion (**8b**) (51%). The two minor species were the β-forms [{Pd(tmen)}$_2$(β-D-Man*p*6*P*1,2;3,4H$_{-4}$-κ^2*O*^{1,2}:κ^2*O*^{3,4})]$^{2-}$ (**8a**) (28%) and [Pd(tmen)(β-D-Man*p*6*P*1,2H$_{-2}$-κ^2*O*^{1,2})]$^{2-}$ (**8c**) (21%). Figure 2.22 illustrates the structures of the complexes. The corresponding ^{13}C and ^{31}P NMR chemical shifts are listed in Table 2.13.

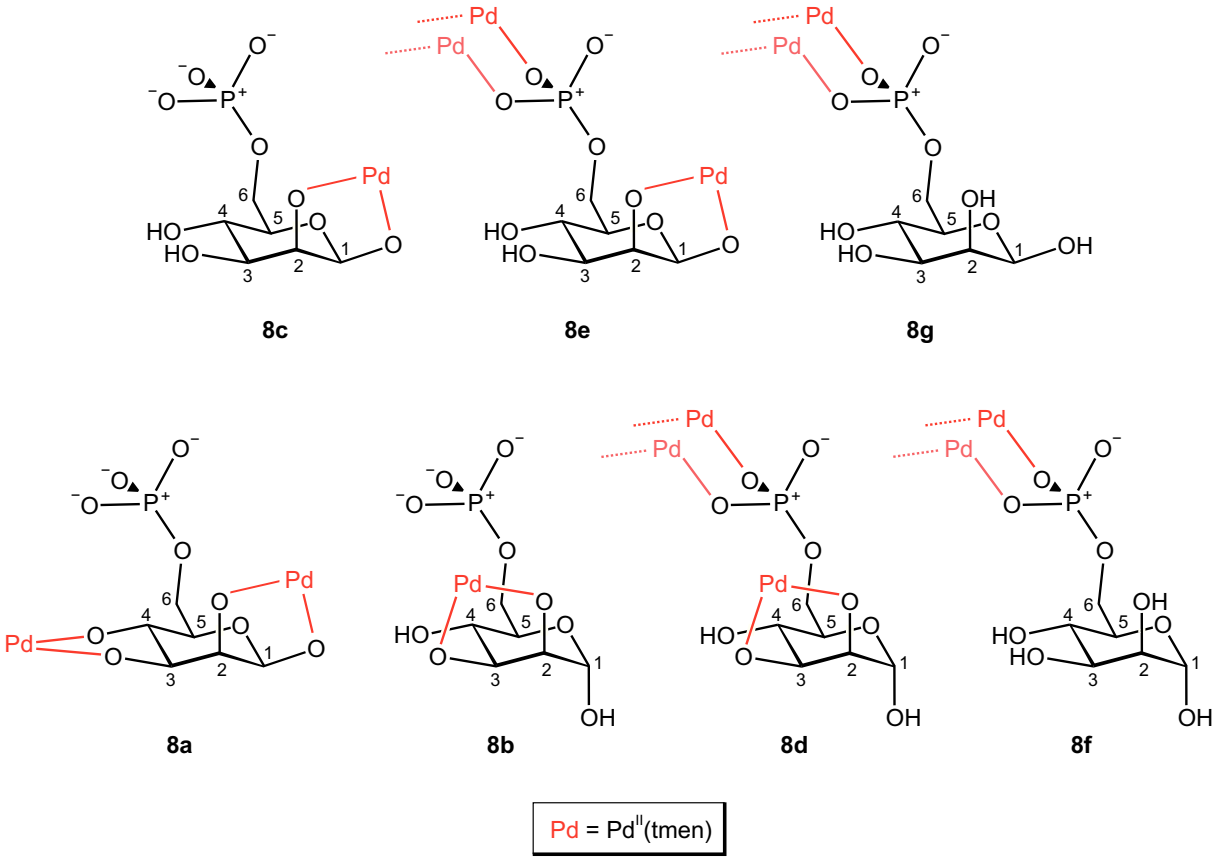

Figure 2.22 Structures and structural fragments of the products from the reactions of Pd-tmen with D-mannose 6-phosphate at various pH values. About one half of the structure is shown for the products **8d**, **8e**, **8f** and **8g**.

The CIS values of all three product complexes that lay between 9.4 and 15.0 ppm clearly assigned the metal-binding sites. The two relatively high CIS values of 13.3 and 15.0 ppm for C1 and C2, respectively, of **8a** were in agreement with the values found for the corresponding Pd^{II}(en) complex.[38] The correct species assignment was confirmed by the quantum-chemical calculation of the ^{13}C NMR chemical shifts. The values calculated are also given in Table

2.13. The formation of the α-$\kappa^2O^{2,3}$ form **8b** had been expected since the formation of a corresponding α-$\kappa^2O^{1,2}$ form was impossible due to the *trans*-orientation of the hydroxy functions of C1 and C2. Nevertheless, the high concentration of **8b** was surprising since in solutions of Pd-en and D-mannose 6-phosphate, the β-$\kappa^2O^{1,2}$ species was the main product, and thus, preferred over the α-$\kappa^2O^{2,3}$ form.[38] However, the reaction of Pd-tmen with the reducing sugar D-mannose also led to product solutions containing the α-$\kappa^2O^{2,3}$ form as the main species.[36]

Table 2.13 ^{13}C and ^{31}P NMR chemical shifts observed (δ_{obs}/ppm) and calculated (δ_{calc}/ppm) of the product complexes **8a**, **8b**, **8c**, **8d**, **8e**, **8f** and **8g** from the reactions of Pd-tmen and D-mannose 6-phosphate (molar ratio 3:1) with various stoichiometric amounts of nitric acid in D_2O. Shifts calculated were determined by the procedure given in Chapter 5.3. $\Delta\delta$ is the shift difference of the product complex and the free D-mannose 6-phosphate. Bold-printed $\Delta\delta$ values indicate the metal-binding site.

	isomer	chelation site		C1	C2	C3	C4	C5	C6	P6
	α-D-Man*p*6*P*		δ	99.9	71.3	70.6	66.9	72.5	63.6	5.6
	β-D-Man*p*6*P*		δ	94.5	72.0	73.3	66.6	76.2	63.6	5.6
8a	β-D-Man*p*6*P*	$\kappa^2O^{1,2}$:$\kappa^2O^{3,4}$	δ_{obs}	107.8	87.0	85.1	76.0	76.5	64.7	5.7
			δ_{calc}	108.3	90.0	86.9	76.2	77.8	64.1	–
			$\Delta\delta$	**13.3**	**15.0**	**11.8**	**9.4**	0.3	1.1	0.1
8b	α-D-Man*p*6*P*	$\kappa^2O^{2,3}$	δ_{obs}	95.1	81.9	80.2	70.5	72.2	64.1	5.9
			δ_{calc}	97.2	80.9	80.1	73.3	73.0	63.4	–
			$\Delta\delta$	0.2	**10.6**	**9.6**	3.6	–0.3	0.5	0.3
8c	β-D-Man*p*6*P*	$\kappa^2O^{1,2}$	δ_{obs}	107.1	83.2	73.1	67.6	75.5	64.1	6.1
			δ_{calc}	107.0	80.1	72.4	69.1	72.8	62.1	–
			$\Delta\delta$	**12.6**	**11.2**	–0.2	1.0	–0.7	0.5	0.3
8d	α-D-Man*p*6*P*	$\kappa^2O^{2,3}$:κO^P:$\kappa O'^P$	δ_{obs}	94.9	81.8	80.3	70.7	72.1	65.9	11.9
			$\Delta\delta$	0.0	**10.5**	**9.7**	3.8	–0.4	2.3	**6.3**
8e	β-D-Man*p*6*P*	$\kappa^2O^{1,2}$:κO^P:$\kappa O'^P$	δ_{obs}	107.0	83.1	73.4	68.0	75.2	66.0	12.1
			$\Delta\delta$	**12.5**	**11.1**	0.1	1.4	–1.0	2.4	**6.5**
8f	α-D-Man*p*6*P*	κO^P:$\kappa O'^P$	δ_{obs}	94.8	71.3	70.7	67.0	72.3	64.9	12.1
			$\Delta\delta$	–0.1	0.0	0.1	0.1	–0.2	1.3	**6.5**
8g	β-D-Man*p*6*P*	κO^P:$\kappa O'^P$	δ_{obs}	94.4	73.5	71.3	66.9	75.8	65.1	12.0
			$\Delta\delta$	–0.1	1.5	–2.0	0.3	–0.4	1.5	**6.4**

Further species were observed in experiments at lower pH values. At pH 8 the two complexes **8d** and **8e** featuring the coordination of both the hydroxy functions and the phosphate group were detected *via* NMR spectroscopy in nearly the same concentration. **8d** was an α-$\kappa^2O^{2,3}$ chelate whereas **8e** was a β-$\kappa^2O^{1,2}$ chelate. Reactions at even lower pH values resulted in the formation of the exclusively phosphate-coordinating species **8f** and **8g**. Figure 2.22 shows

structural fragments of the products **8d**–**8g**. The corresponding ^{13}C and ^{31}P NMR chemical shifts are given in Table 2.13. The ^{13}C NMR shifts lay between 9.7 and 12.5 ppm while the ^{31}P NMR shifts amounted to 6.3–6.5 ppm.

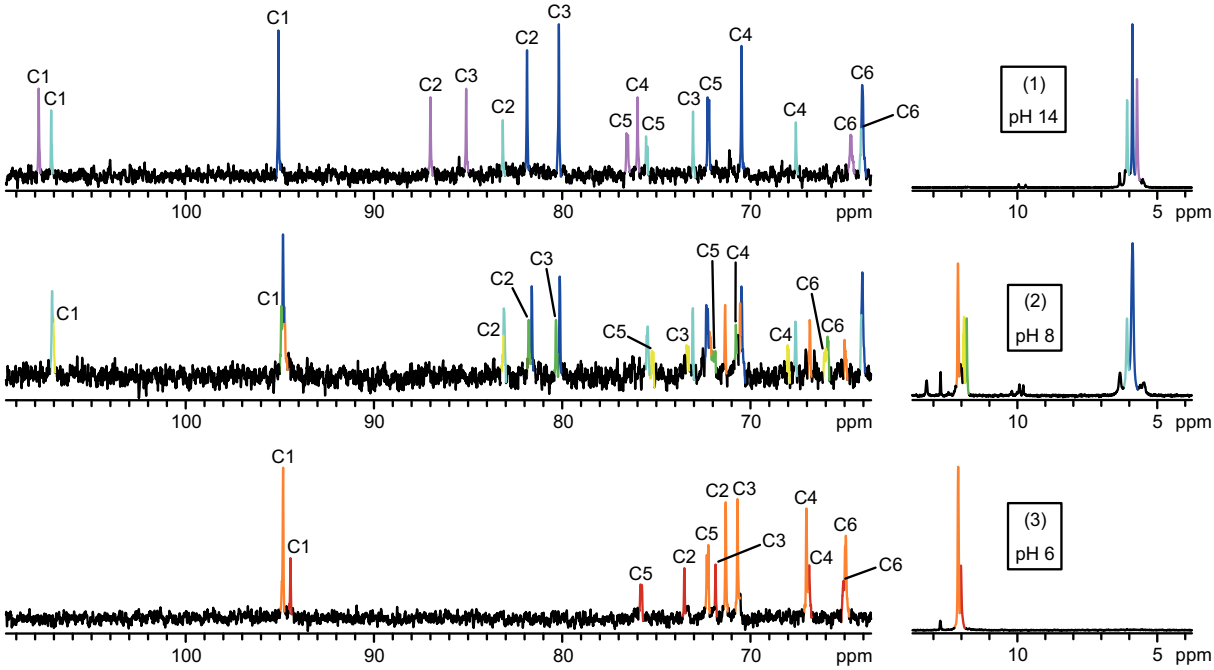

Figure 2.23 ^{13}C and ^{31}P NMR spectra of aqueous solutions from the reactions of Pd-tmen and D-mannose 6-phosphate at the molar ratio of 3:1 with various stoichiometric amounts of nitric acid; (1): no addition of nitric acid (pH 14); (2): 2 equivalents of nitric acid (pH 8); (3): 3 equivalents of nitric acid (pH 6). Species assigned are **8a** (marked violet), **8b** (marked dark blue), **8c** (marked light blue), **8d** (marked green), **8e** (marked yellow), **8f** (marked orange) and **8g** (marked red). Note the split C5 and C6 signals as a result of ^{31}P–^{13}C coupling.

Table 2.14 Coupling constants (*J*/Hz) of the D-mannose-6-phosphate part of product complexes **8a**, **8b**, **8c**, **8d**, **8e**, **8f** and **8g** in D_2O.

	$^3J_{1,2}$	$^3J_{2,3}$	$^3J_{3,4}$	$^3J_{4,5}$	$^3J_{5,6a}$	$^3J_{5,6b}$	$^3J_{6a,P}$	$^3J_{6b,P}$	$^2J_{6a,6b}$
8a	1.3	2.6	9.8	9.6	–	–	–	–	–
8b	1.3	4.0	9.0	9.8	–	–	–	–	–
8c	1.4	3.6	9.9	9.8	–	–	–	–	–
8d	1.1	4.1	8.8	10.1	–	–	–	–	–
8e	1.3	3.5	9.9	9.5	–	–	–	–	–
8f	1.4	–	–	–	–	–	–	–	–
8g	1.2	–	–	–	–	–	–	–	–

Figure 2.23 gives an overview of the ^{13}C and ^{31}P NMR spectra of product solutions at various pH values. As seen above in the experiments with other sugar phosphates, it is shown here

again that the coordination of the hydroxy functions is limited to pH values above 7 while the coordination of the phosphate group is restricted to pH values below 10. Complexes featuring both chelation types were observed only at the pH range around 8.

Finally, the coupling constants determined for all D-mannose 6-phosphate complexes found are listed in Table 2.14. All of them lay in the expected range.

2.2.5 Coordination of D-fructose 1-phosphate

In contrast to the sugar phosphates so far investigated, D-fructose 1-phosphate is not an aldose phosphate but a ketose phosphate, which results in the fact that C2 and not C1 is the anomeric centre. A further difference is the presence of furanose forms. In the previous experiments of this work, furanoses were partly accessible but obviously not stable enough to concentrate in educt or product solutions. In aqueous solutions of D-fructose 1-phosphate, the β-furanose form is available with a concentration of 14% beside the β-pyranose form with 86%. The α-forms were not detectable *via* NMR spectroscopy.

In the product solution from the reaction of Pd-tmen with D-fructose 1-phosphate (molar Pd^{II}(tmen):sugar-phosphate ratio of 3:1) three product complexes were observed. The main species was the monometallated β-furanose form [Pd(tmen)(β-D-Fru*f*1*P*2,3H$_{-2}$-κ^2*O*^{2,3})]$^{2-}$ (**9d**) (55%). The two minor species were the pyranose forms [{Pd(tmen)}$_2$(β-D-Fru*p*1*P*2,3;4,5H$_{-4}$-κ^2*O*^{2,3}:κ^2*O*^{4,5})]$^{2-}$ (**9a**) (26%) and [Pd(tmen)(α-D-Fru*p*1*P*4,5H$_{-2}$-κ^2*O*^{4,5})]$^{2-}$ (**9b**) (19%). Figure 2.24 shows the structures of these complexes. Their ^{13}C and ^{31}P NMR chemical shifts are given in Table 2.15. The CIS values of the three products lay between 7.8 and 13.2 ppm. The species assignment was also confirmed by the quantum-chemical calculation of the ^{13}C NMR chemical shifts also given in Table 2.15. The high concentration of **9d** was expected since in reactions of Pd-tmen with D-fructose the analogous complex was the main species as well. Furthermore, it was noticeable that the monometallated β-pyranose form [Pd(tmen)(β-D-Fru*p*1*P*2,3H$_{-2}$-κ*O*^{2,3})]$^{2-}$ was not observed at high pH values. However, at a pH of 9, small signals for this species **9c** were detected in the ^{13}C NMR spectra. At this pH there were also signals for the β-D-furanose κ^2*O*^{2,3}:κ*O*^{P}:κ*O*'^{P} chelate **9e**, which was the only D-fructose 1-phosphate species found exhibiting the coordination of both hydroxy functions and phosphate group. Experiments at lower pH values led, furthermore, to the exclusively phosphate-coordinating species **9f** and **9g**. Figure 2.24 shows structural fragments of the complexes **9e**–**9g** and the structure of **9c**. The corresponding NMR chemical shifts are listed in Table 2.15. The ^{31}P NMR CIS values of **9e**–**9g** added up to 6.7–6.8 ppm.

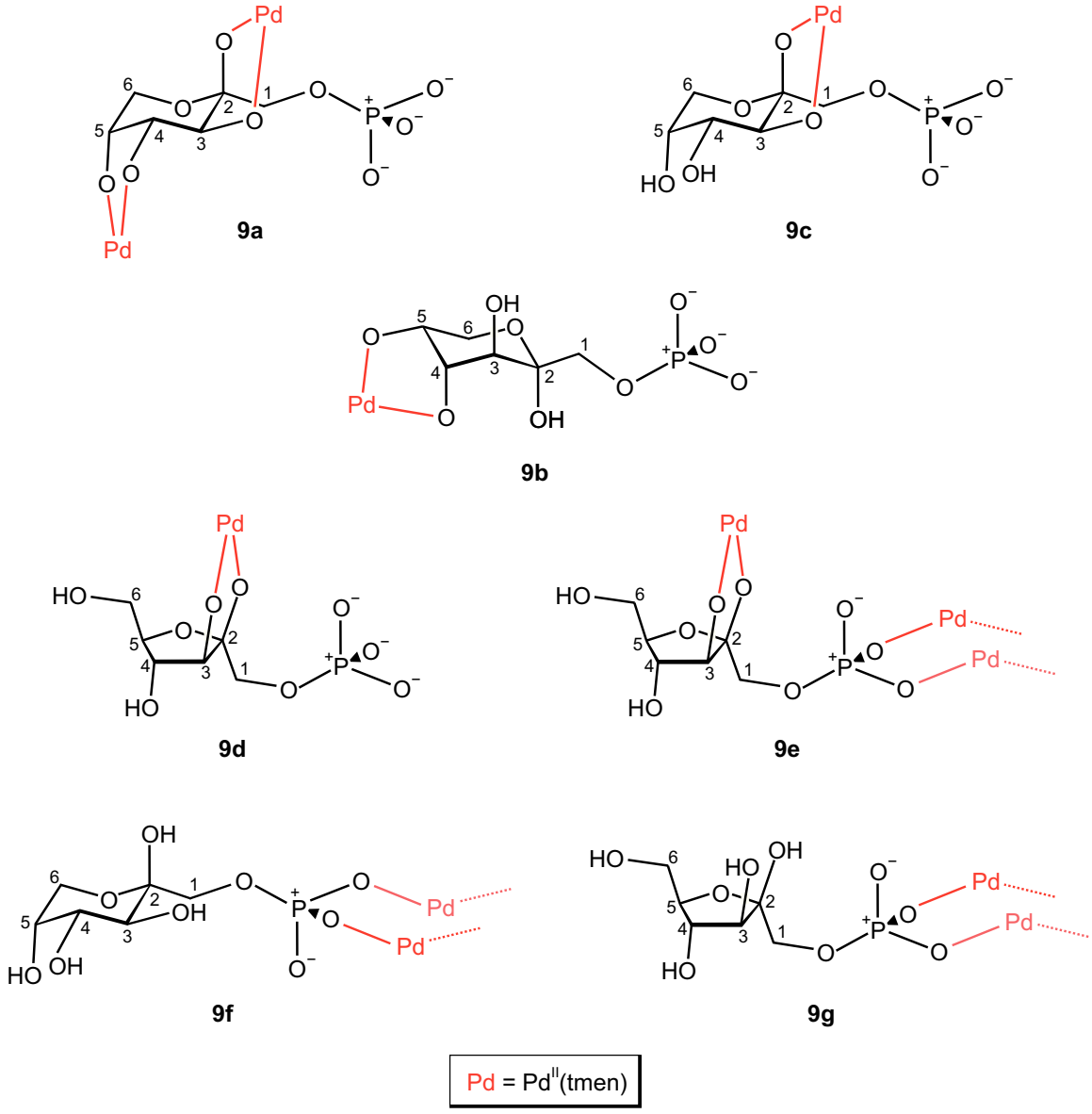

Figure 2.24 Structures and structural fragments of the products from the reactions of Pd-tmen with D-fructose 1-phosphate at various pH values. About one half of the structure is shown for the products **9e**, **9f** and **9g**.

Table 2.16 summarises the coupling constants determined for the products **9b, 9d**, **9e**, **9f** and **9g**. They allowed some conclusions about the conformation of the pyranose or furanose rings of the product species. Thus, it was clearly assigned that the α-$\kappa^2O^{4,5}$ chelate **9b** existed in the $^5C_2$ conformation in contrast to the $^2C_5$ conformation of the β-pyranose products. This result partly explained the unusual chelation site, since the formation of a $\kappa^2O^{2,3}$ or $\kappa^2O^{3,4}$ chelate was impossible due to the *trans*-orientation of the corresponding hydroxy functions. The non-formation of a $\kappa^2O^{2,4}$ form exhibiting a six-membered chelate ring was, however, still unexpected. By analysing the coupling constants of the species **9d**, **9e** and **9g**, the conformation of their furanose rings was determined. For **9g** it was found to be $^4T_3$ while the conformation of **9d** and **9e** was close to ^4E.

Table 2.15 ^{13}C and ^{31}P NMR chemical shifts observed (δ_{obs}/ppm) and calculated (δ_{calc}/ppm) of the product complexes **9a**, **9b**, **9c**, **9d**, **9e**, **9f** and **9g** from the reactions of Pd-tmen and D-fructose 1-phosphate (molar ratio 3:1) with various stoichiometric amounts of nitric acid in D_2O. Shifts calculated were determined by the procedure given in Chapter 5.3. $\Delta\delta$ is the shift difference of the product complex and the free D-fructose 1-phosphate. Bold-printed $\Delta\delta$ values indicate the metal-binding site. For the α-pyranose educt form no chemical shift values were available. Thus, the ^{13}C NMR chemical shifts of α-D-fructopyranose were used for proximity.[36]

	isomer	chelation site		C1	C2	C3	C4	C5	C6	P1
	α-D-Fru*p*1*P*		δ	(65.8)	(98.6)	(70.7)	(71.1)	(61.8)	(61.7)	–
	β-D-Fru*p*1*P*		δ	66.9	98.8	68.3	70.1	69.9	64.1	4.9
	β-D-Fru*f*1*P*		δ	66.5	101.6	76.6	74.7	81.2	63.0	4.6
9a	β-D-Fru*p*1*P*	$\kappa^2O^{2,3}$:$\kappa^2O^{4,5}$	δ_{obs}	69.4	106.6	79.9	83.3	78.3	**–**	5.2
			δ_{calc}	68.7	104.4	80.8	87.8	83.1	64.8	**–**
			$\Delta\delta$	2.5	**7.8**	**10.6**	**13.2**	**8.4**	–	0.3
9b	α-D-Fru*p*1*P*	$\kappa^2O^{4,5}$	δ_{obs}	65.8	98.9	66.7	79.7	72.2	–	6.5
			δ_{calc}	65.0	96.6	68.7	82.7	73.2	63.7	**–**
			$\Delta\delta$	(0.0)	(0.3)	(–4.0)	(**8.6**)	(**10.4**)	–	–
9c	β-D-Fru*p*1*P*	$\kappa^2O^{2,3}$	δ_{obs}	67.7	107.8	76.4	75.8	70.7	–	4.8
			δ_{calc}	67.5	105.0	77.5	76.7	71.9	62.6	**–**
			$\Delta\delta$	0.8	**9.0**	**8.1**	5.7	0.8	–	–0.1
9d	β-D-Fru*f*1*P*	$\kappa^2O^{2,3}$	δ_{obs}	65.3	113.0	87.6	80.2	82.4	63.0	5.1
			δ_{calc}	64.8	110.3	87.0	77.4	79.0	61.2	**–**
			$\Delta\delta$	–1.2	**11.4**	**11.0**	5.5	1.2	0.0	0.5
9e	β-D-Fru*f*1*P*	$\kappa^2O^{2,3}$:κO^P:$\kappa O'^P$	δ_{obs}	65.8	112.5	88.0	80.0	82.7	–	11.3
			$\Delta\delta$	–0.7	**10.9**	**11.4**	5.3	1.5	–	**6.7**
9f	β-D-Fru*p*1*P*	κO^P:$\kappa O'^P$	δ_{obs}	67.3	98.5	68.0	70.0	69.8	64.1	11.7
			$\Delta\delta$	0.4	–0.3	–0.3	–0.1	–0.1	0.0	**6.8**
9g	β-D-Fru*f*1*P*	κO^P:$\kappa O'^P$	δ_{obs}	64.0	101.4	76.2	74.7	81.6	62.8	11.4
			$\Delta\delta$	–2.5	–0.2	–0.4	0.0	0.4	–0.2	**6.8**

Figure 2.25 illustrates the ^{13}C and ^{31}P NMR spectra measured. The fluent passage from phosphate coordination at lower pH values to the coordination of the hydroxy functions at higher pH levels, which was also observed in the previous experiments, was clearly signified. The product fragment **9e** that featured the coordination of the hydroxy groups as well as the phosphate function was observed only at the pH range between 7 and 10.

Table 2.16 Coupling constants (*J*/Hz) of the D-fructose-1-phosphate part of product complexes **9b**, **9d**, **9e**, **9f** and **9g** in D_2O.

	$^3J_{1a,P}$	$^3J_{1b,P}$	$^2J_{1a,1b}$	$^3J_{3,4}$	$^3J_{4,5}$	$^3J_{5,6a}$	$^3J_{5,6b}$	$^2J_{6a,6b}$
9b	–	–	–	3.9	3.5	6.4	10.3	−11.3
9d	2.7	5.1	−10.8	6.3	6.5	–	–	–
9e	–	4.3	−10.6	6.5	6.3	3.0	3.2	–
9f	–	5.3	−10.6	8.3	–	1.9	1.5	−12.8
9g	–	–	–	8.3	7.8	6.5	–	−12.5

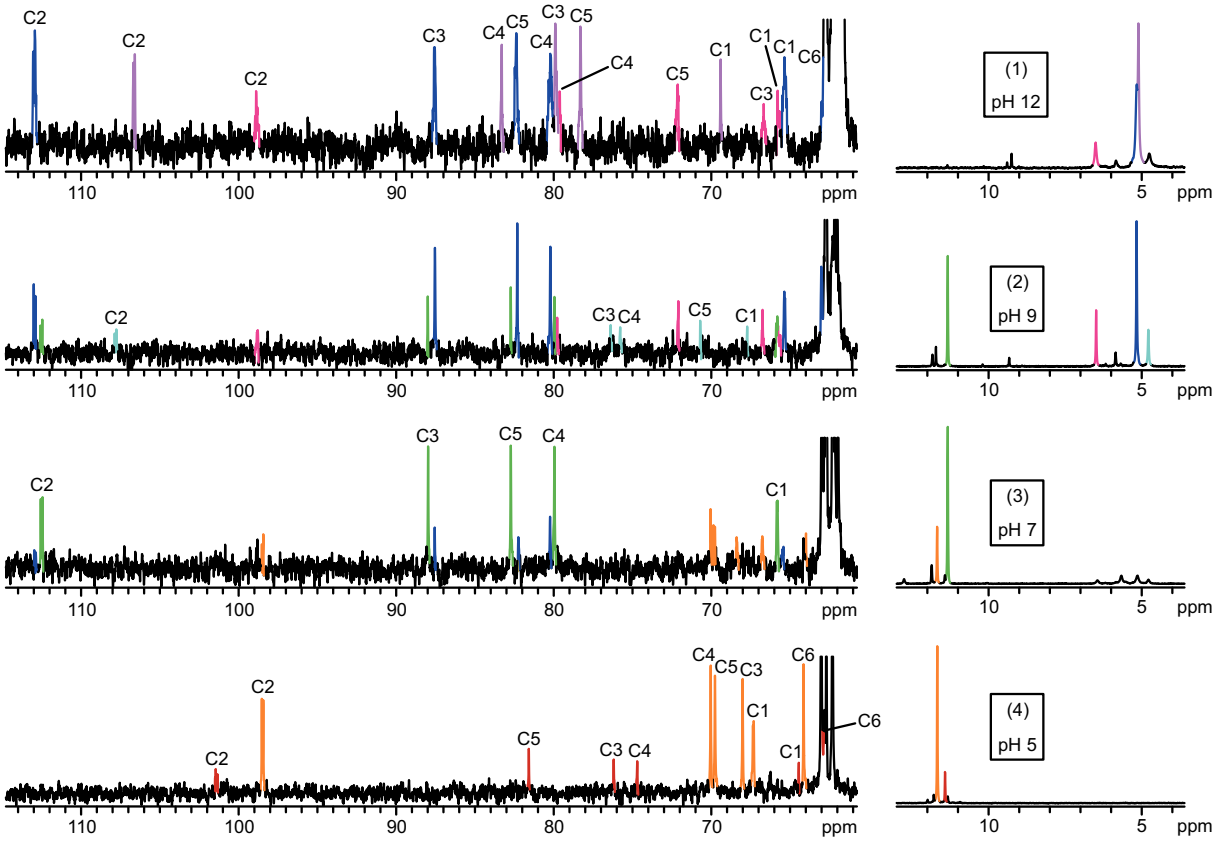

Figure 2.25 ^{13}C and ^{31}P NMR spectra of aqueous solutions from the reactions of Pd-tmen and D-fructose 1-phosphate at the molar ratio of 3:1 with various stoichiometric amounts of nitric acid; (1): no addition of nitric acid (pH 12); (2): 2 equivalents of nitric acid (pH 9); (3): 3 equivalents of nitric acid (pH 7); (4) 4 equivalents of nitric acid (pH 5). Species assigned are **9a** (marked violet), **9b** (marked magenta), **9c** (marked light blue), **9d** (marked dark blue), **9e** (marked green), **9f** (marked orange) and **9g** (marked red). Note the split C1 and C2 signals as a result of ^{31}P–^{13}C coupling.

2.2.6 Coordination of D-fructose 6-phosphate

In contrast to D-fructose 1-phosphate, D-fructose 6-phosphate is phosphorylated at the hydroxy function of C6 instead of C1. As a result, the pyranose forms are no longer accessible. Aqueous solutions of D-fructose 6-phosphate contain the β-furanose form (82%) and the α-furanose form (16%) along with the open-chain keto form in a low concentration.[89]

The dissolution of D-fructose 6-phosphate in Pd-tmen (molar Pd^{II}(tmen):sugar-phosphate ratio of 3:1) resulted in only one species: the monometallated [Pd(tmen)(β-D-Fru*f*6*P*2,3H_{-2}-$\kappa^2O^{2,3}$)]$^{2-}$ anion (**10a**) that is shown in Figure 2.26. Compared to reactions with Pd-en, the formation of only one product was unexpected since in those experiments an α-$\kappa^2O^{1,3}$:$\kappa^2O^{2,4}$ chelate and an α-$\kappa O^{2,4}$ chelate were observed as well.[38]

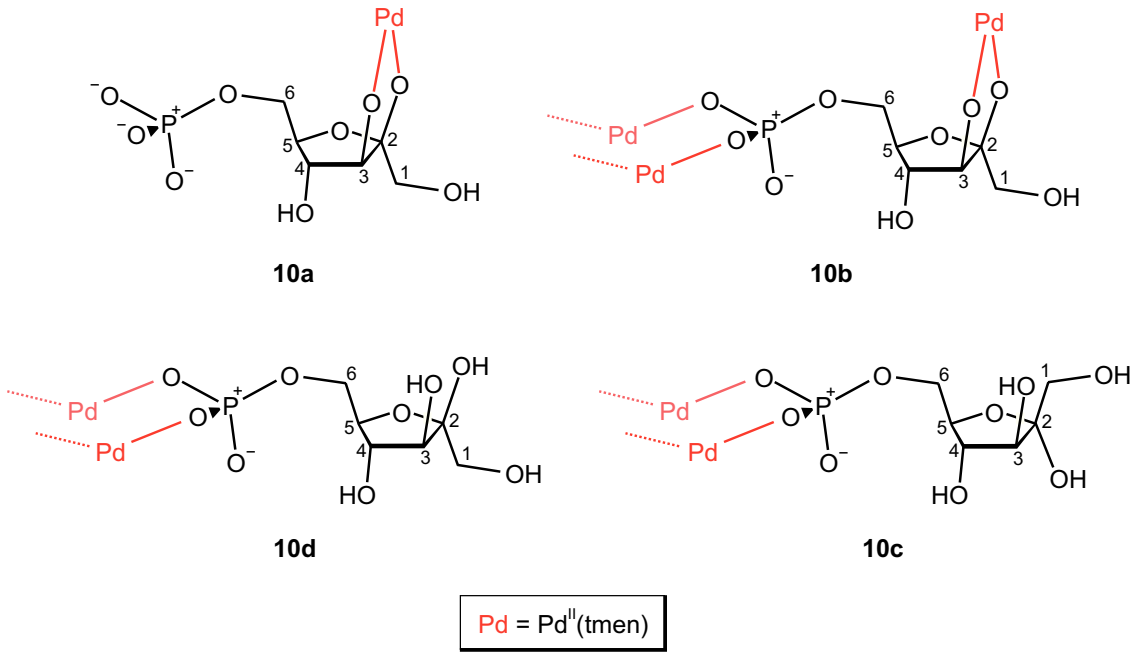

Figure 2.26 Structures and structural fragments of the products from the reactions of Pd-tmen with D-fructose 6-phosphate at various pH values. About one half of the structure is shown for the products **10b**, **10c** and **10d**.

By adding stoichiometric amounts of nitric acid, lower pH values were adjusted yielding further product complexes. At the pH range between 7 and 9 the product species **10b** was observed exhibiting the coordination *via* the hydroxy functions of C2 and C3 as well as the phosphate group. At pH values below 8 the two product fragments **10c** and **10d** were formed featuring the exclusive coordination of the phosphate group. Structural fragments of the three products **10b**–**10d** are illustrated in Figure 2.26. Figure 2.27 gives an overview of the pH dependence of the complexes. Here, it is clearly shown by NMR spectra of product solutions at various pH values that the transformation of one complex to another was achieved by

simply changing the pH of the solution. As a consequence, it was possible to enrich a desired complex simply by setting the pH.

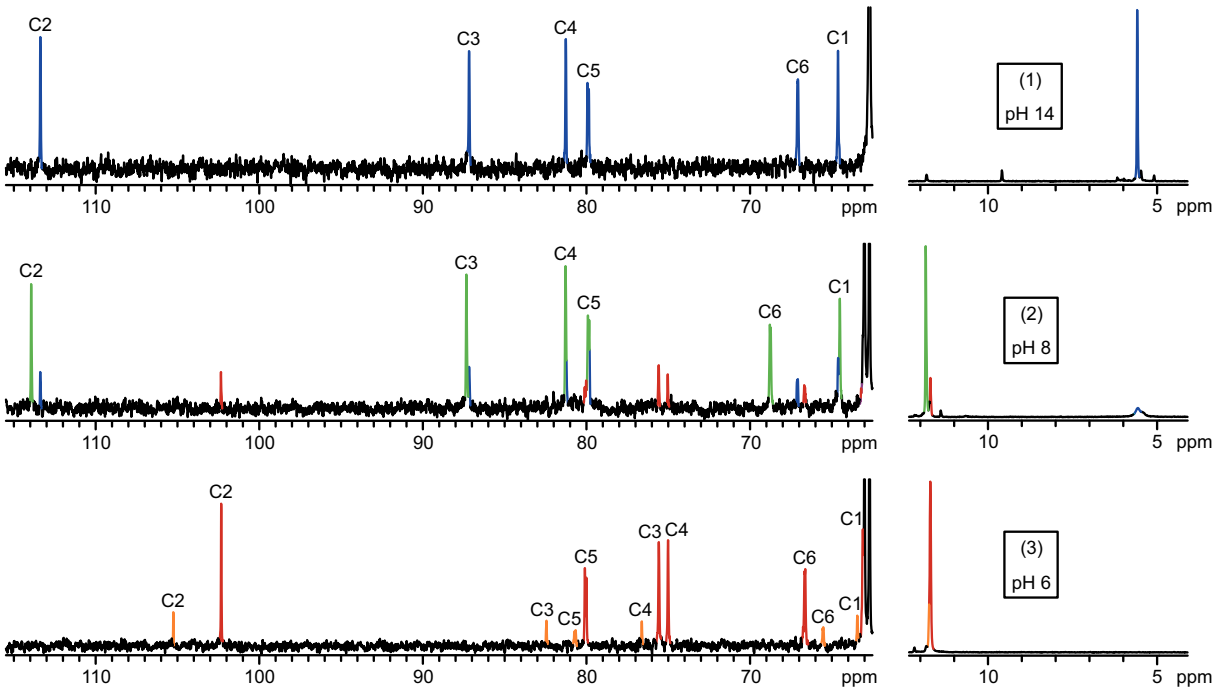

Figure 2.27 ^{13}C and ^{31}P NMR spectra of aqueous solutions from the reactions of Pd-tmen and D-fructose 6-phosphate at the molar ratio of 3:1 with various stoichiometric amounts of nitric acid; (1): no addition of nitric acid (pH 14); (2): 2 equivalents of nitric acid (pH 8); (3) 3 equivalents of nitric acid (pH 6). Species assigned are **10a** (marked dark blue), **10b** (marked green), **10c** (marked orange) and **10d** (marked red). Note the split C5 and C6 signals as a result of ^{31}P–^{13}C coupling.

The coupling constants determined for **10a**, **10b** and **10d** given in Table 2.17 allowed conclusions about the conformation of the furanose rings of these products. The conformation of **10d** was found to be $^4T_3$ while the conformation of **10a** and **10b** lay close to ^4E or $^4T_3$.

Table 2.17 Coupling constants (J/Hz) of the D-fructose-6-phosphate part of product complexes **10a**, **10b** and **10d** in D_2O.

	$^2J_{1a,1b}$	$^3J_{3,4}$	$^3J_{4,5}$	$^3J_{5,6a}$	$^3J_{5,6b}$	$^3J_{6a,P}$	$^3J_{6b,P}$	$^2J_{6a,6b}$
10a	−12.0	7.3	8.3	7.0	4.0	5.6	5.7	−11.0
10b	−11.9	7.0	8.1	–	4.1	–	5.3	−10.8
10d	−11.9	8.5	7.6	–	–	–	–	–

Table 2.18 lists the ^{13}C and ^{31}P NMR chemical shifts of all products found. The ^{13}C NMR CIS values lay between 11.4 and 12.0 ppm and, thus, clearly assigned the metal-binding sites. The ^{31}P NMR CIS values amounted to 6.6–6.8 ppm. The ^{13}C NMR chemical shifts of **10a** were

determined additionally by quantum-chemical calculations. The values obtained, which are also given in Table 2.18, lay very close to the experimental chemical shifts.

Table 2.18 ^{13}C and ^{31}P NMR chemical shifts observed (δ_{obs}/ppm) and calculated (δ_{calc}/ppm) of the product complexes **10a**, **10b**, **10c** and **10d** from the reactions of Pd-tmen and D-fructose 6-phosphate (molar ratio 3:1) with various stoichiometric amounts of nitric acid in D_2O. Shifts calculated were determined by the procedure given in Chapter 5.3. $\Delta\delta$ is the shift difference of the product complex and the free D-fructose 6-phosphate. Bold-printed $\Delta\delta$ values indicate the metal-binding site.

	isomer	chelation site		C1	C2	C3	C4	C5	C6	P1
	α-D-Fru*f*6*P*		δ	63.4	105.1	82.4	76.3	81.0	64.0	5.1
	β-D-Fru*f*6*P*		δ	63.1	102.2	75.6	74.8	80.6	64.9	5.1
10a	β-D-Fru*f*6*P*	$\kappa^2O^{2,3}$	δ_{obs}	64.5	113.6	87.4	81.5	80.0	67.1	5.6
			δ_{calc}	64.8	110.9	87.5	71.7	78.6	67.7	–
			$\Delta\delta$	1.4	**11.4**	**11.8**	6.7	–0.6	2.2	0.5
10b	β-D-Fru*f*6*P*	$\kappa^2O^{2,3}$:κO^P:$\kappa O'^P$	δ_{obs}	64.7	114.2	87.6	81.5	80.1	69.0	11.8
			$\Delta\delta$	1.6	**12.0**	**12.0**	6.7	–0.5	4.1	**6.7**
10c	α-D-Fru*f*6*P*	κO^P:$\kappa O'^P$	δ_{obs}	63.4	105.3	82.4	76.6	80.7	65.5	11.9
			$\Delta\delta$	–0.1	0.2	0.0	0.3	–0.3	1.5	**6.8**
10d	β-D-Fru*f*6*P*	κO^P:$\kappa O'^P$	δ_{obs}	63.1	102.6	75.8	75.3	80.3	66.9	11.7
			$\Delta\delta$	0.0	0.4	0.2	0.5	–0.3	2.0	**6.6**

2.2.7 Coordination of D-fructose 1,6-bisphosphate

Compared to the two previous sugar phosphates investigated, D-fructose 1-phosphate and D-fructose 6-phosphate, D-fructose 1,6-bisphosphate features a phosphorylated hydroxy function at both C1 and C6. However, it is more similar to D-fructose 6-phosphate since the formation of pyranose forms is impossible due to the blocked 6-position. Aqueous solutions of D-fructose 1,6-bisphosphate contain the α-furanose form (13%) and the β-furanose form (86%) with only traces of the open-chain keto form.

As expected, the reaction of Pd-tmen with D-fructose 1,6-bisphosphate (molar Pd^{II}(tmen):sugar-phosphate ratio of 3:1) led to only one product, namely the [Pd(tmen)(β-D-Fru*f*1,6$P_2$2,3H_{-2}-$\kappa^2O^{2,3}$)]$^{4-}$ anion (**11a**). Its structure is shown in Figure 2.28. Signals for an α-$\kappa^2O^{2,4}$ chelate were not observed, which was in agreement with the results from reactions of fructose 6-phosphate with Pd-tmen. However, in experiments with Pd-en, such a six-ring chelate was formed.[38] Since D-fructose 1,6-bisphosphate features two phosphate functions, a decrease of the pH to values between 7–10 should have resulted in at least two further $\kappa^2O^{2,3}$ forms: one of them coordinating to a further Pd^{II}(tmen) fragment *via* its 1-phosphate group

and the other one coordinating *via* its 6-phosphate group. The experiment verified this hypothesis. By adding nitric acid to the 3:1 product solution, the pH was decreased. The resulting ^{13}C NMR spectrum contained signals for three product species. One of them was the already found complex **11a**. The other forms seemed to be the supposed polymetallated complex species **11b** and **11c** (see Figure 2.28) since their signals had nearly the same chemical shifts as the monometallated species. Further evidence was obtained by the ^{31}P NMR spectrum. Two of the signals found and assigned by a $^{31}P^{1}H$ HETCOR NMR experiment exhibited a distinct CIS. These were the signals of the 1-phosphate group and the 6-phosphate group of different product complexes. In order to verify this assignment, Figure 2.29 illustrates the $^{31}P^{1}H$ HETCOR NMR spectrum measured. It should be mentioned that there were two further small ^{31}P NMR signals showing a CIS in the spectra of product solutions of pH 7–10. Unfortunately, the results did not allow a definite assignment. Nevertheless, it was assumed that this product was the $\kappa^2O^{2,3}$ form with both phosphate functions coordinating to Pd^{II}.

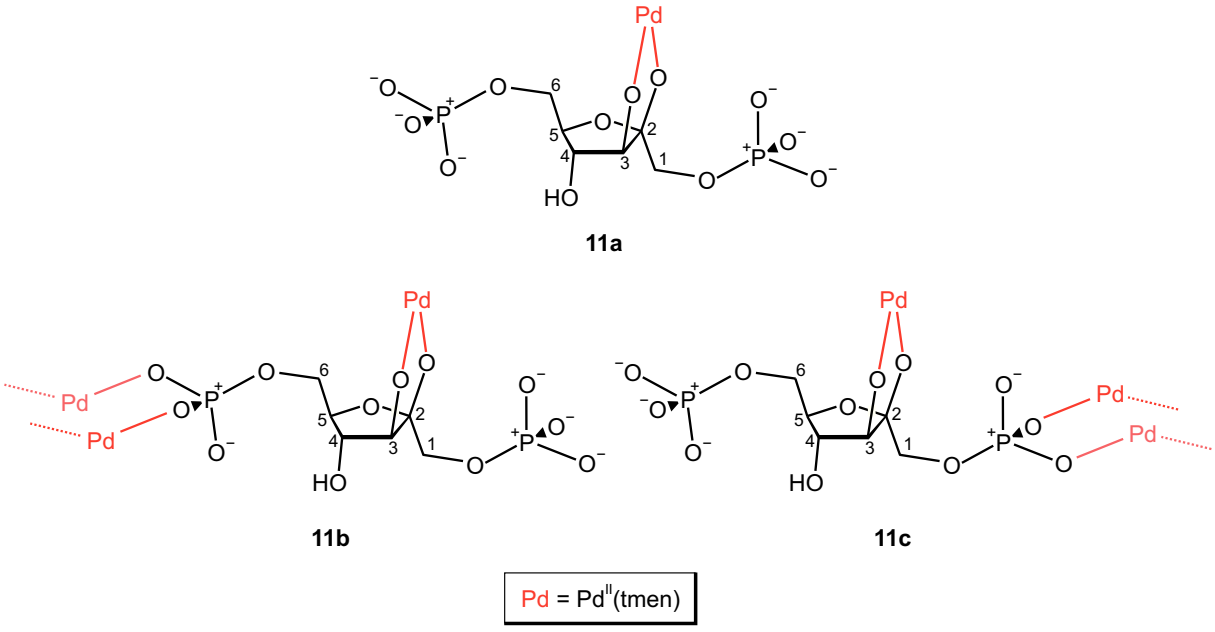

Figure 2.28 Structures and structural fragments of the products from the reactions of Pd-tmen with D-fructose 1,6-bisphosphate at various pH values. About one half of the structure is shown for the products **11b** and **11c**.

The ^{13}C and ^{31}P NMR chemical shifts of all three products assigned are listed in Table 2.19. The ^{13}C NMR CIS values lay between 11.1 and 12.5 ppm. The ^{31}P NMR CIS values added up to 8.1 ppm for the P6 signal of **11b** and 7.7 ppm for the P1 signal of **11c**.

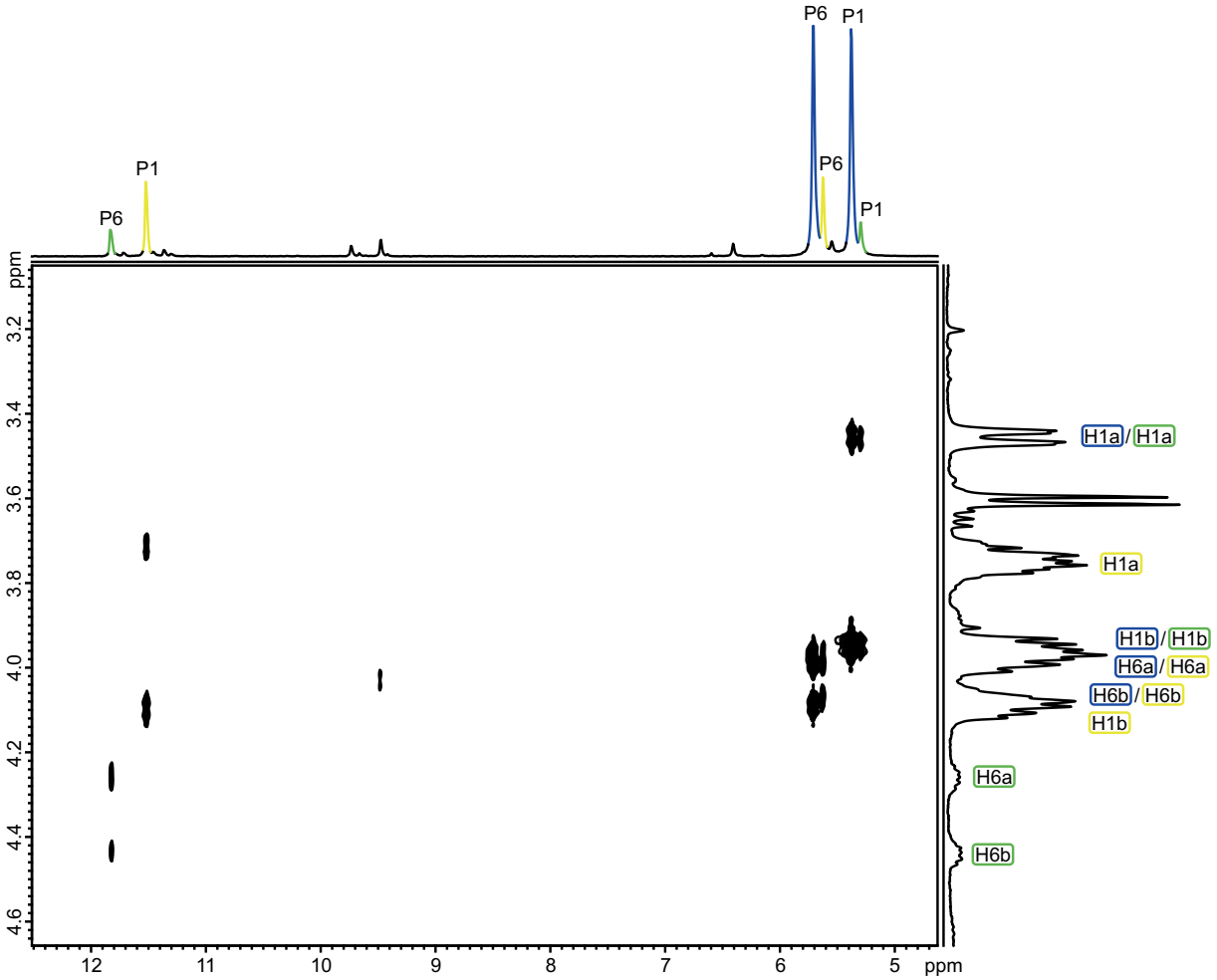

Figure 2.29 $^{31}P^{1}H$ HETCOR NMR spectrum of an aqueous solution from the reaction of Pd-tmen, D-fructose 1,6-bisphosphate and nitric acid at the molar ratio of 3:1:0.75 (pH 10). Species assigned are **11a** (marked dark blue), **11b** (marked green) and **11c** (marked yellow).

Table 2.19 ^{13}C and ^{31}P NMR chemical shifts observed (δ_{obs}/ppm) and calculated (δ_{calc}/ppm) of the product complexes **11a**, **11b** and **11c** from the reactions of Pd-tmen and D-fructose 1,6-bisphosphate (molar ratio 3:1) with various stoichiometric amounts of nitric acid in D_2O. Shifts calculated were determined by the procedure given in Chapter 5.3. $\Delta\delta$ is the shift difference of the product complex and the free D-fructose 1,6-bisphosphate. Bold-printed $\Delta\delta$ values indicate the metal-binding site.

	isomer	chelation site		C1	C2	C3	C4	C5	C6	P1	P6
	β-D-Fru*f*1,6P_2		δ	66.0	101.5	76.0	74.5	80.1	65.4	3.8	3.7
11a	β-D-Fru*f*1,6P_2	$\kappa^2O^{2,3}$	δ_{obs}	66.4	113.4	87.1	81.2	80.0	67.0	5.4	5.7
			δ_{calc}	64.7	110.7	85.1	81.5	80.6	67.5	–	–
			$\Delta\delta$	0.4	**11.9**	**11.1**	6.7	–0.1	1.6	1.6	2.0
11b	β-D-Fru*f*1,6P_2	$\kappa^2O^{2,3}$:κO^{P6}:$\kappa O'^{P6}$	δ_{obs}	66.7	114.0	87.6	81.3	79.9	68.4	5.3	11.8
			$\Delta\delta$	0.7	**12.5**	**11.6**	6.8	–0.2	3.0	1.5	**8.1**
11c	β-D-Fru*f*1,6P_2	$\kappa^2O^{2,3}$:κO^{P1}:$\kappa O'^{P1}$	δ_{obs}	67.0	112.9	87.3	81.1	80.3	67.0	11.5	5.6
			$\Delta\delta$	1.0	**11.4**	**11.3**	6.6	0.2	1.6	**7.7**	1.9

Table 2.20 lists the coupling constants determined for **11a**–**11c**. They allowed conclusions about the conformation of the furanose rings of the product species. The conformation of **11c** was found to be ^4E while the conformation of **11a** and **11b** lay close to ^4E or $^4T_3$.

Table 2.20 Coupling constants (*J*/Hz) of the D-fructose-1,6-bisphosphate part of product complexes **11a**, **11b** and **11c** in D_2O.

	$^2J_{1a,1b}$	$^3J_{1a,P1}$	$^3J_{1b,P1}$	$^3J_{3,4}$	$^3J_{4,5}$	$^3J_{5,6a}$	$^3J_{5,6b}$	$^3J_{6a,P6}$	$^3J_{6b,P6}$	$^2J_{6a,6b}$
11a	−10.7	2.9	5.2	7.1	7.8	4.1	5.2	–	–	–
11b	−10.3	2.8	–	7.1	7.6	–	–	–	–	–
11c	–	–	–	6.6	7.4	–	–	–	–	–

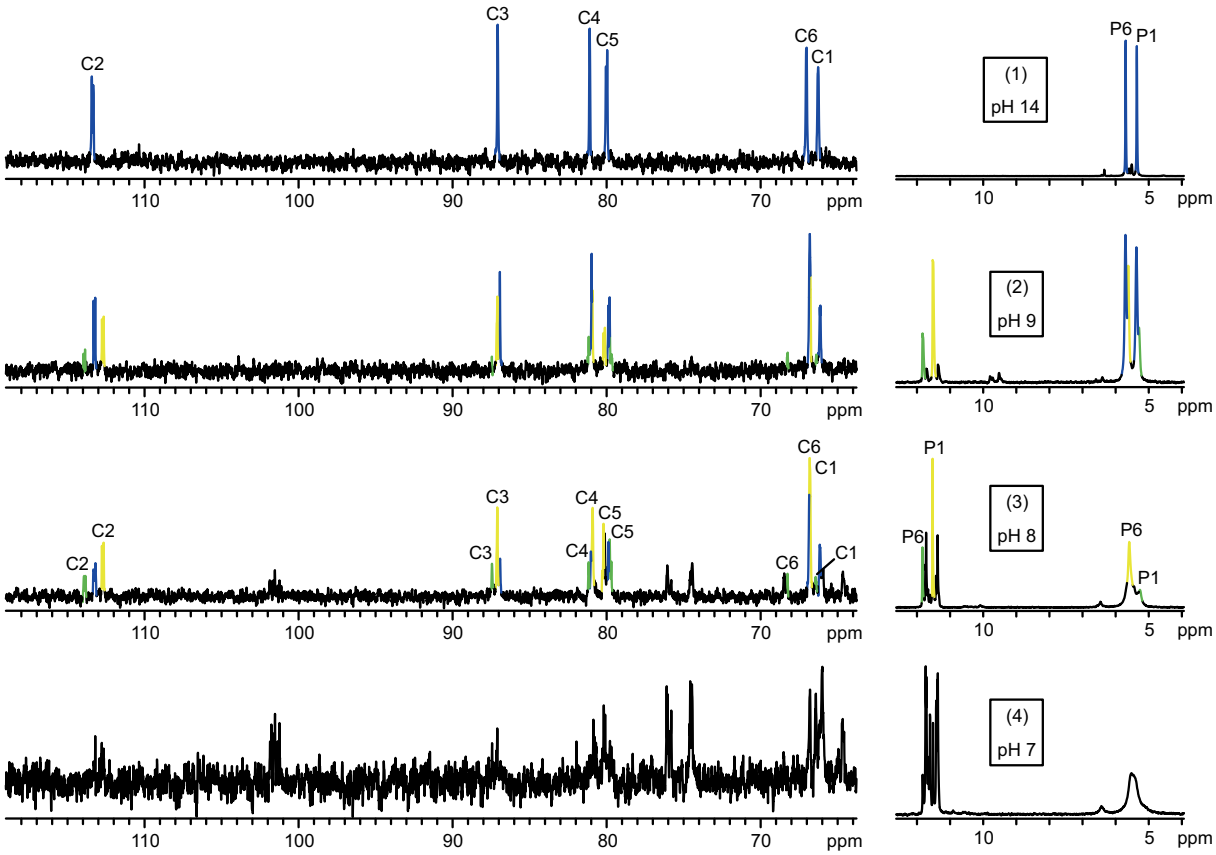

Figure 2.30 ^{13}C and ^{31}P NMR spectra of aqueous solutions from the reactions of Pd-tmen and D-fructose 1,6-bisphosphate at the molar ratio of 3:1 with various stoichiometric amounts of nitric acid; (1): no addition of nitric acid (pH 14); (2): 1 equivalent of nitric acid (pH 9); (3) 1.5 equivalents of nitric acid (pH 8); (4) 2 equivalents of nitric acid (pH 7). Species assigned are **11a** (marked dark blue), **11b** (marked green) and **11c** (marked yellow). Note the split C1, C2, C5 and C6 signals as a result of ^{31}P–^{13}C coupling.

Figure 2.30 gives an overview of the ^{13}C and ^{31}P NMR spectra obtained from product solutions at various pH values. The spectrum of the reaction at pH 7 revealed that there were

products in solution coordinating to Pd^{II} exclusively *via* the phosphate function. However, it was not possible to assign the species unambiguously. The reason for this was the high number of such products formed which caused, on the one hand, the very poor signal-to-noise ratio of the corresponding ^{13}C NMR spectrum and, on the other hand, the overlapping of NMR signals. The high number of products was a consequence of the presence of two phosphate groups on one sugar-phosphate molecule. Thus, at lower pH values, there was one β-furanose complex featuring coordination *via* the 1-phosphate group and a second complex featuring coordination *via* the 6-phosphate group. Of course, a third β-furanose complex featuring coordination *via* both phosphate groups was also possible. The probable formation of three respective α-form complexes led to overall six different possible products at lower pH values whose structural fragments are shown in Figure 2.31. Because of the similarity of the products, their ^{13}C NMR signals for each carbon atom had almost the same chemical shifts making a clear assignment impossible. The ^{31}P NMR spectrum could not help with this issue either due to each product causing two signals with almost all of them lying in the range between 11 and 12 ppm.

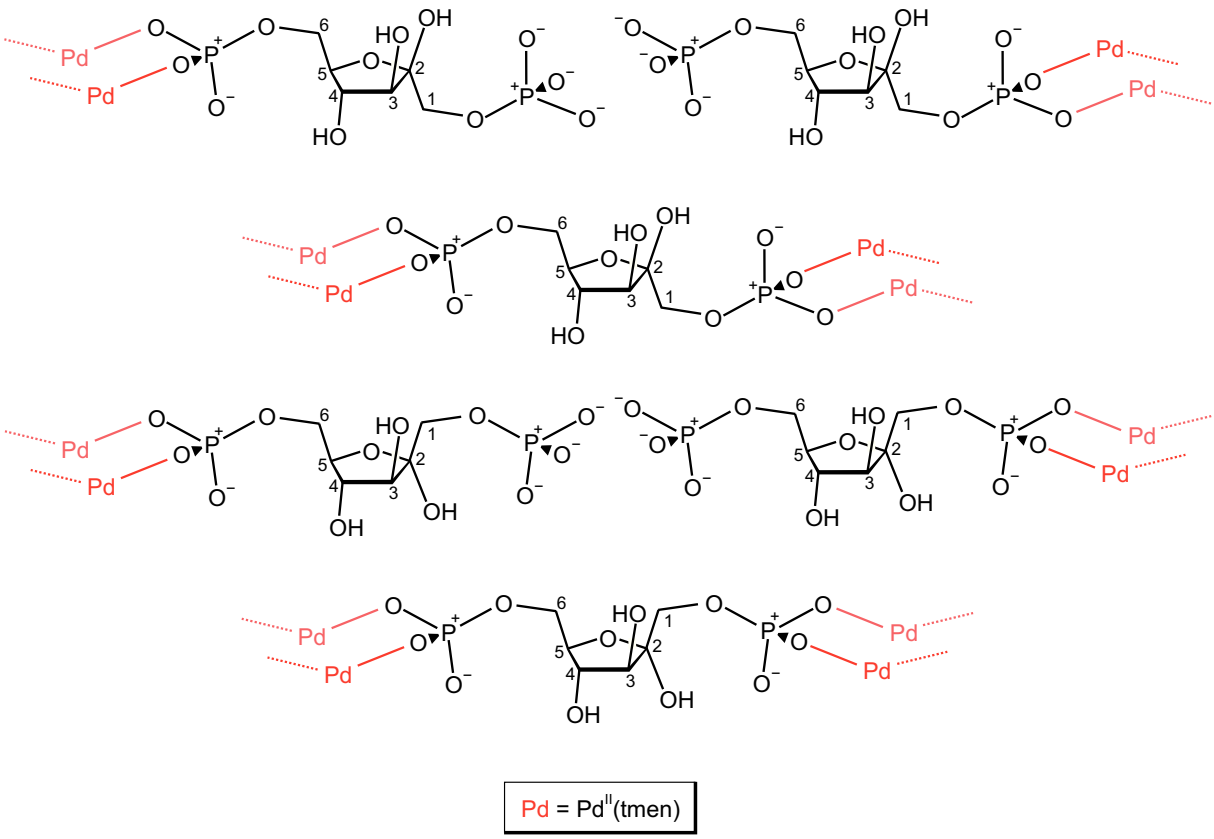

Figure 2.31 Structural fragments of possible product species obtained from the reaction of Pd-tmen with D-fructose 1,6-bisphosphate at pH values below 7.

2.2.8 Coordination of D-ribose 5-phosphate

D-Ribose 5-phosphate was the only pentose phosphate investigated in this work. Since the hydroxy function of C5 is phosphorylated, the formation of pyranose forms is impossible. As a result, aqueous solutions of D-ribose 5-phosphate contain only the α-furanose form (34%) and the β-furanose form (64%) along with the open-chain form in a low concentration.[89]

Dissolving D-ribose 5-phosphate in Pd-tmen (molar Pd^{II}(tmen):sugar-phosphate ratio of 3:1) led to a product solution containing two species. The main product was the monometallated α-$\kappa^2O^{1,2}$-chelate [Pd(tmen)(α-D-Rib*f*5*P*1,2H$_{-2}$-$\kappa^2O^{1,2}$)]$^{2-}$ (**12a**) while the minor species was the β-$\kappa^2O^{2,3}$-chelate [Pd(tmen)(β-D-Rib*f*5*P*2,3H$_{-2}$-$\kappa^2O^{2,3}$)]$^{2-}$ (**12b**). Both product complexes are shown in Figure 2.32. In comparison to reactions with Pd-en, the absence of an α-$\kappa^2O^{1,3}$-chelate was unexpected since it was, in fact, the main species in the product solutions of those experiments.[38] However, it was in agreement with the results of the previous chapters as no six-ring chelate was observed in any experiments with Pd^{II}(tmen) in this work.

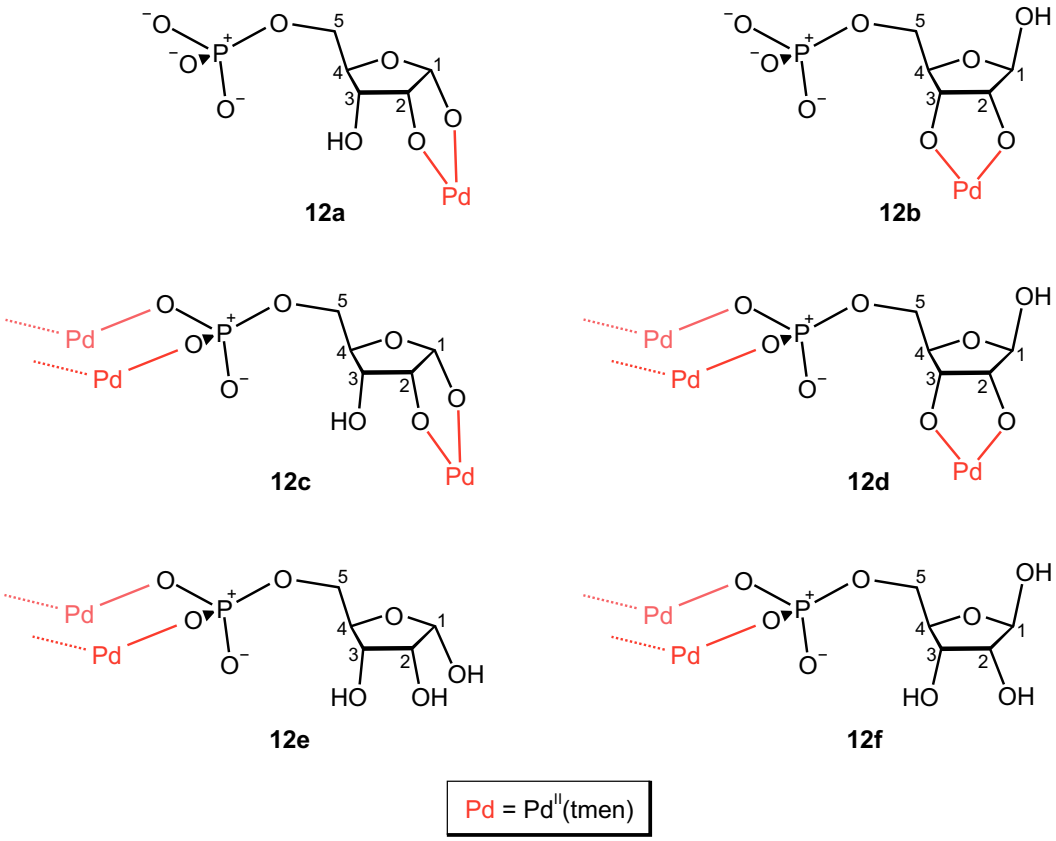

Figure 2.32 Structures and structural fragments of the products from the reactions of Pd-tmen with D-ribose 5-phosphate at various pH values. About one half of the structure is shown for the products **12c**, **12d**, **12e** and **12f**.

Decreasing the pH by adding stoichiometric amounts of nitric acid resulted in overall four further products. At the pH range between 7 and 10 two product species exhibiting

coordination *via* both hydroxy groups and phosphate function were identified: the α-$\kappa^2O^{1,2}$-chelate **12c** and the β-$\kappa^2O^{2,3}$-chelate **12d**. At pH values below 9 the α-species **12e** and the β-species **12f** were observed both exhibiting exclusive phosphate coordination. Figure 2.32 shows structural fragments of all these four products.

In the ^{31}P NMR spectrum of the product solution at pH 9, an additional signal was observed. According to its chemical shift, it belonged to a product complex featuring phosphate coordination. Unfortunately, it was not possible to assign ^{13}C NMR signals to this product.

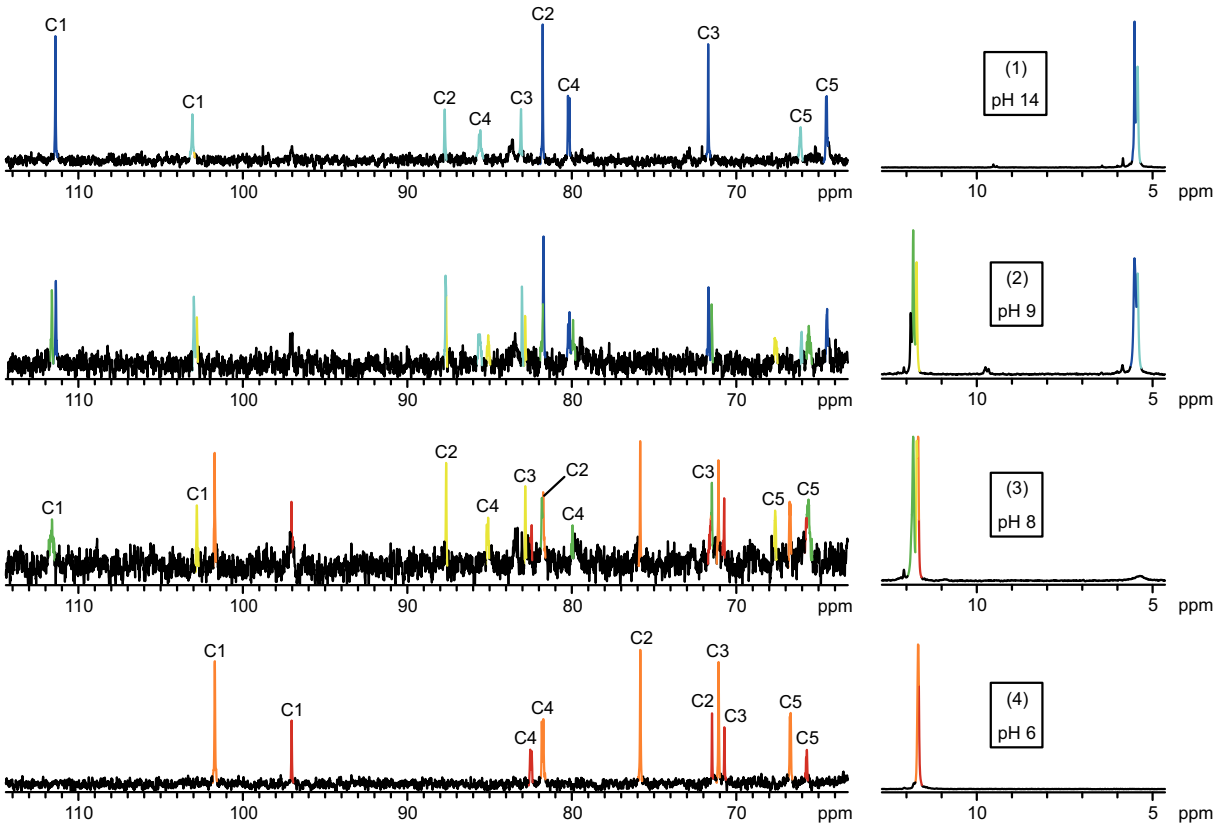

Figure 2.33 ^{13}C and ^{31}P NMR spectra of aqueous solutions from the reactions of Pd-tmen and D-ribose 5-phosphate at the molar ratio of 3:1 with various stoichiometric amounts of nitric acid; (1): no addition of nitric acid (pH 14); (2): 1.5 equivalents of nitric acid (pH 9); (3) 2 equivalents of nitric acid (pH 8); (4) 3 equivalents of nitric acid (pH 6). Species assigned are **12a** (marked dark blue), **12b** (marked light blue), **12c** (marked green), **12d** (marked yellow), **12e** (marked red) and **12f** (marked orange). Note the split C4 and C5 signals as a result of ^{31}P–^{13}C coupling.

An overview of the ^{13}C and ^{31}P NMR spectra of product solutions at various pH values is given in Figure 2.33. As already seen in all other Pd^{II}(tmen) experiments of this work, the coordination type was strongly dependent on the pH. As a result, it was possible to select the metal-binding site, and thus, the product complex simply by adjusting the pH.

Table 2.21 summarises the ^{13}C and ^{31}P NMR signals of all D-ribose 5-phosphate products. All ^{13}C NMR chemical shifts, except for two values, lay between 10.3 and 11.8 ppm. Only the CIS values for the C1 atoms of **12a** and **12c** were a bit higher, reaching 14.4 and 14.6 ppm, respectively. However, these values were in agreement with previous experiments of Pd-en as the CIS value of C1 from the appropriate α-$\kappa^2O^{1,2}$-chelate amounted to 15.2 ppm.[38] The ^{31}P NMR CIS values of the product fragments **12c**–**12f** lay between 6.3 and 6.6 ppm.

Table 2.21 ^{13}C and ^{31}P NMR chemical shifts observed (δ_{obs}/ppm) and calculated (δ_{calc}/ppm) of the product complexes **12a**, **12b**, **12c**, **12d**, **12e** and **12f** from the reactions of Pd-tmen and D-ribose 5-phosphate (molar ratio 3:1) with various stoichiometric amounts of nitric acid in D_2O. Shifts calculated were determined by the procedure given in Chapter 5.3. $\Delta\delta$ is the shift difference of the product complex and the free D-ribose 5-phosphate. Bold-printed $\Delta\delta$ values indicate the metal-binding site.

	isomer	chelation site		C1	C2	C3	C4	C5	P5
	α-D-Rib*f*5*P*		δ	97.0	71.4	70.1	83.3	64.3	5.3
	β-D-Rib*f*5*P*		δ	101.7	76.0	71.3	82.6	65.2	5.3
12a	α-D-Rib*f*5*P*	$\kappa^2O^{1,2}$	δ_{obs}	111.4	81.7	71.7	80.2	64.5	5.6
			δ_{calc}	112.2	81.2	71.9	78.3	65.7	–
			$\Delta\delta$	**14.4**	**10.3**	1.6	–3.1	0.2	0.3
12b	β-D-Rib*f*5*P*	$\kappa^2O^{2,3}$	δ_{obs}	103.1	87.7	83.1	85.6	66.1	5.5
			δ_{calc}	104.5	89.2	84.5	85.2	67.3	–
			$\Delta\delta$	1.4	**11.7**	**11.8**	3.0	0.9	0.2
12c	α-D-Rib*f*5*P*	$\kappa^2O^{1,2}$:κO^P:$\kappa O'^P$	δ_{obs}	111.6	81.7	71.5	79.9	65.6	11.8
			$\Delta\delta$	**14.6**	**10.3**	1.4	–3.4	1.3	**6.5**
12d	β-D-Rib*f*5*P*	$\kappa^2O^{2,3}$:κO^P:$\kappa O'^P$	δ_{obs}	102.8	87.7	82.8	85.1	67.6	11.7
			$\Delta\delta$	1.1	**11.7**	**11.5**	2.5	2.4	**6.4**
12e	α-D-Rib*f*5*P*	κO^P:$\kappa O'^P$	δ_{obs}	97.0	71.5	70.7	83.3	65.7	11.9
			$\Delta\delta$	0.0	0.1	0.6	0.0	1.4	**6.6**
12f	β-D-Rib*f*5*P*	κO^P:$\kappa O'^P$	δ_{obs}	101.7	75.8	71.1	82.5	66.7	11.6
			$\Delta\delta$	0.0	–0.2	–0.2	–0.1	1.5	**6.3**

All coupling constants determined for the products **12a–12f** are listed in Table 2.22. To a certain degree, they allowed conclusions about the conformation of the furanose rings of the products. The conformation of **12a** and **12c** were found to be close to $^1T_2$ while the conformations of **12e** and **12f** both lay close to E_2 or $^3T_2$.

Table 2.22 Coupling constants (*J*/Hz) of the D-ribose-5-phosphate part of product complexes **12a**, **12b**, **12c**, **12d**, **12e** and **12f** in D_2O.

	$^3J_{1,2}$	$^3J_{2,3}$	$^3J_{3,4}$	$^3J_{4,5a}$	$^3J_{4,5b}$	$^3J_{5a,P}$	$^3J_{5b,P}$	$^2J_{5a,5b}$
12a	3.5	6.2	–	–	2.7	–	3.8	−11.4
12b	1.4	–	–	–	–	–	–	–
12c	3.4	6.1	–	–	–	–	–	–
12d	1.3	–	–	–	–	–	–	–
12e	4.0	4.2	5.7	–	–	–	–	–
12f	1.8	4.7	6.4	–	–	–	–	–

2.2.9 Preparation of crystalline compounds

The preparation of crystalline product complexes was not successful even with the addition of several cations such as Ba^{2+}, Sr^{2+}, Ca^{2+}, Mg^{2+}, Cs^+, Li^+, Eu^{3+} and $[Co(NH_3)_6]^{3+}$. Problems were, firstly, the formation of Pd^0 and, secondly, the formation of resin-like precipitations after a few days or weeks. Moreover, product solutions containing α-D-glucose 1-phosphate or *rac*-glycerol 1-phosphate always led to the crystallisation of the free educt form. A further problem occurred in experiments at neutral pH values. Here, the side product $[\{Pd(tmen)\}_2(\mu\text{-}OH)_2](NO_3)_2$ that is shown in Figure 2.34 crystallised in many product solutions.

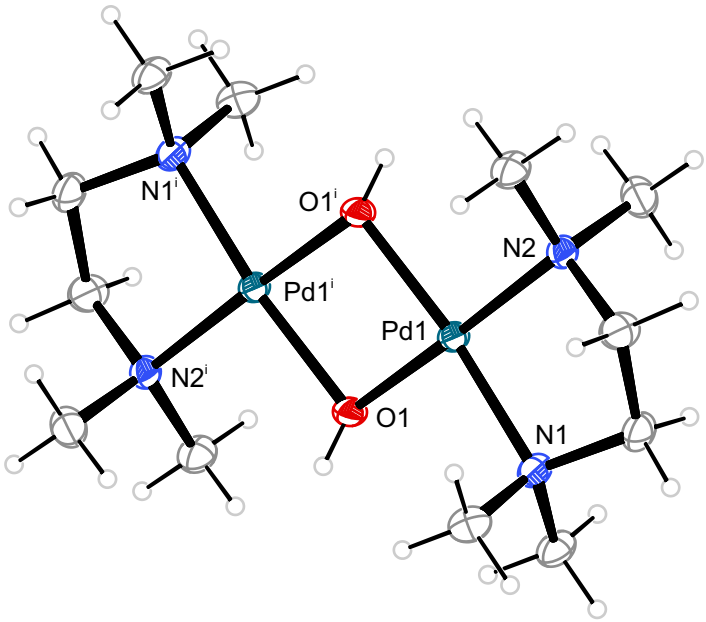

Figure 2.34 Structure of $[\{Pd(tmen)\}_2(\mu\text{-}OH)_2]^{2+}$ in crystals of the dinitrate (50 % probability ellipsoids). Distances (Å) and angles (°): Pd1–O1 2.0168(18), Pd1–O1^i 2.0217(18), Pd1–N1 2.048(2), Pd1–N2 2.047(2), O1–Pd1–O1^i 80.17(7), O1–Pd1–N1 96.94(8), O1^i–Pd1–N2 97.21(8), N1–Pd1–N2 86.14(8). [Symmetry code: (i) $-x, -y, -z$]

The cation had already been crystallised in a previous work.[90] However, crystals of the dinitrate were unknown so far. The structure crystallised in the monoclinic space group $P\,\bar{1}$.

2.3 Coordination of diolato compounds to the Zn^{II}(dien) fragment

Only a few works concerning sugar phosphates coordinating to Zn^{II} are available.[25–29] As described in the introduction, crystal-structure analysis was found to be the only suitable analytical method to investigate those complexes. Appropriate crystal structures of neutral complexes of the form [Zn(dien)(diolate)] exhibiting a trigonal-bipyramidal coordination sphere were obtained with the ligands ethane-1,2-diol, *cis*-1,2-cyclopentanediol, *trans*-1,2-cyclohexanediol, 1,4-anhydroerythritol and methyl β-D-ribofuranoside.[28–29] Thus, only one crystal structure with a diolato ligand featuring non-coordinating hydroxy functions has been obtained so far.

In contrast to previous studies, the experiments of this work showed that it is actually possible to obtain useful results by NMR spectroscopy. Hence, reactions of several sugar phosphates with the Zn^{II}(dien) fragment were conducted and the product solutions obtained were analysed by NMR spectroscopy. In order to heighten the significance of the NMR data obtained, they were compared with results of further experiments that were additionally performed with molecules similar to sugar phosphates, namely polyols, methylated sugars, pentoses and hexoses since no such results were available so far.

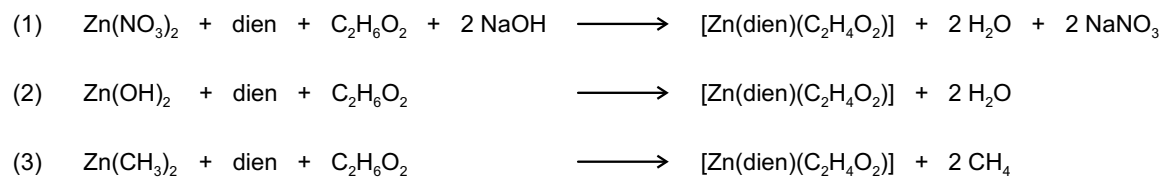

Figure 2.35 Three different reaction variants used for the preparation of product solutions containing Zn^{II}(dien) complexes of polyols, methylated sugars, reducing sugars or sugar phosphates.

The product solutions were obtained by three different reactions given in Figure 2.35 on the example of the educt ethane-1,2-diol. In reaction (1) zinc(II) nitrate was used as the Zn^{II} educt compound. The reaction was carried out in water, adding stoichiometric amounts of diethylenetriamine, ethane-1,2-diol and sodium hydroxide. This procedure was the easiest way to obtain product solutions but was only used for the preparation of NMR samples since the crystallisation of product complexes was disturbed by the remaining nitrate anions. For crystallisation experiments, reactions (2) and (3) were used. The reaction conditions of reaction (2) were the same as in reaction (1) but using zinc(II) hydroxide as the Zn^{II} educt compound which was synthesised from zinc(II) chloride and sodium hydroxide before each

experiment and was used immediately since it was not possible to dissolve old zinc(II) hydroxide in water. In reaction (3) dimethylzinc was used as Zn^{II} educt compound. It was available as a solution in toluene which was removed *in vacuo* and replaced by water while the reaction was carried out under nitrogen atmosphere. Thus, it was the most elaborate reaction variant. However, the product solutions obtained by this reaction led to NMR spectra featuring an improved signal-to-noise ratio compared to spectra of product solutions from reaction (1) or (2). Unfortunately, the disturbing formation of N-glycosides described later on in this work was much more marked in product solutions of reaction (3) than in the ones of reaction (1) or (2). As a result, there was no procedure that generally led to adequate NMR results and, thus, the three reaction variants were tested for each experiment.

2.3.1 Coordination of polyols

In comparison to sugar phosphates, polyols also feature diolato functions that are able to coordinate to a Zn^{II}(dien) fragment but are much simpler and less reactive due to the absence of an aldehyde function and a phosphate group. Thus, they were chosen as a starting point for NMR investigations.

The simplest polyol is ethane-1,2-diol with only two hydroxy functions. The reaction of zinc(II) hydroxide, diethylenetriamine and ethane-1,2-diol in equimolar amounts led to a nearly clear colourless solution. The ^{13}C NMR spectrum of this product solution is shown in Figure 2.36.

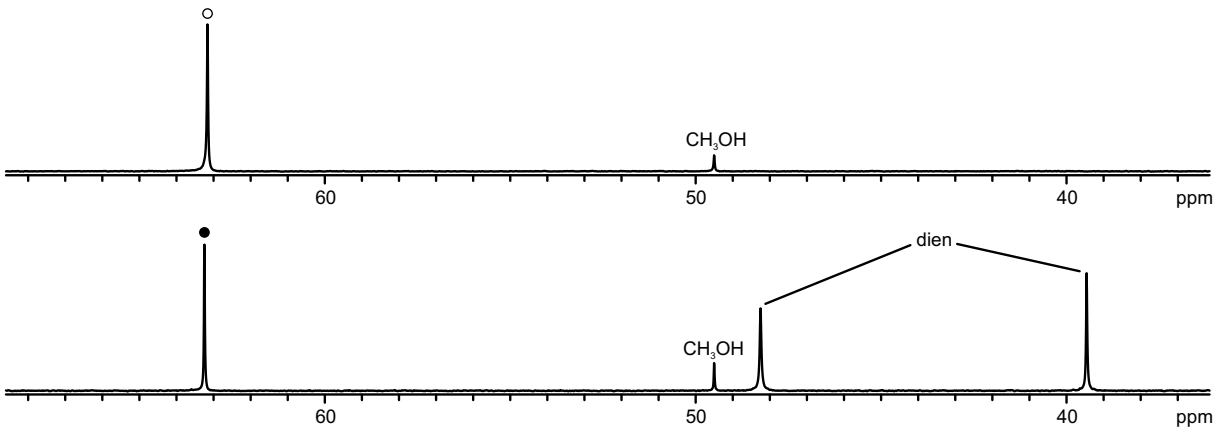

Figure 2.36 top: ^{13}C NMR spectrum of an aqueous solution of ethane-1,2-diol (○). bottom: ^{13}C NMR spectrum of an aqueous solution of zinc(II) hydroxide, diethylenetriamine and ethane-1,2-diol at the molar ratio of 1:1:1. The only product **13** is characterised by two signals for the diethylenetriamine part and one signal for the ethane-1,2-diol part (●).

There was no difference between the ^{13}C NMR chemical shift of the free ethane-1,2-diol and the one for the ethane-1,2-diol part of the product complex as both values added up to 63.2 ppm. However, the product complex [Zn(dien)($C_2H_4O_2$-$\kappa^2O^{1,2}$] **13** was formed which was verified by *Herdin* who obtained crystals of **13** · 1.5 $C_2H_6O_2$ from a similar product solution leading to the same ^{13}C NMR signals.[29] The crystal structure is given in Figure 2.37.

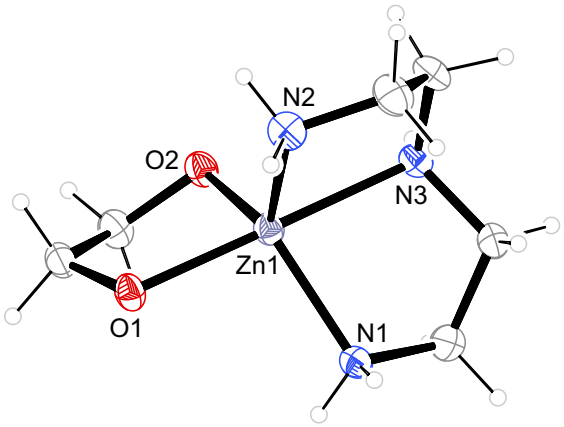

Figure 2.37 Structure of [Zn(dien)($C_2H_4O_2$)] **13** in crystals of **13** · 1.5 $C_2H_6O_2$ obtained in an earlier work.[29]

As *Herdin* had already observed, the Zn^{II} centre of **13** did not cause a coordination-induced shift, which was consistent with results of similar experiments performed with the polyols glycerol, D-threitol and erythritol. The ^{13}C NMR chemical shifts of the product complexes [Zn(dien)(Glyc1,2H$_{-2}$-$\kappa^2O^{1,2}$] **14**, [Zn(dien)(D-ThreH$_{-2}$] **15** and [Zn(dien)(ErytH$_{-2}$] **16** are listed in Table 2.23. All differences between educt and product signals were smaller than 1 ppm. It was noticeable that, only for D-threitol, the difference was exactly 0 ppm for all signals. Moreover, no separation of signals due to the loss of symmetry was observed, which confirmed the hypothesis about the absence of CIS values. Without a CIS it was impossible to unambiguously assign the chelation site of **14**, **15** and **16**. However, since experiments with reducing sugars and sugar phosphates (that will be shown later on) indicated that Zn^{II}(dien) seemed to have a preference for five-ring chelates, it was assumed that glycerol coordinated through O1 and O2. Consequently, the product complexes of D-threitol and erythritol were either κ^2-$O^{1,2}$ or κ^2-$O^{2,3}$ chelates. The formation of a dimetallated species was improbable since no excess of Zn^{II}(dien) was used. Nevertheless, it should be mentioned that, on account of the absence of CIS values, it was possible that various product complexes were formed and led to only one set of NMR signals.

Because of the absence of CIS values, the utility of Zn^{II}(dien) experiments with polyols was very limited. Thus, experiments with further polyols were not conducted.

Table 2.23 ^{13}C NMR chemical shifts of the product complexes **14**, **15** and **16** from the reactions of zinc(II) hydroxide and diethylenetriamine with one of the polyols glycerol, D-threitol and erythritol (molar ratio 1:1:1). $\Delta\delta$ is the shift difference of the product complex and the free polyol.

	polyol		C1	C2	C3	C4
free	Glyc	δ	64.0	73.5	64.0	
14	Glyc	δ	63.6	72.9	63.6	
		$\Delta\delta$	−0.4	−0.6	−0.4	
free	D-Thre	δ	64.0	72.8	72.8	64.0
15	D-Thre	δ	64.0	72.8	72.8	64.0
		$\Delta\delta$	0.0	0.0	0.0	0.0
free	Eryt	δ	64.4	73.5	73.5	64.4
16	Eryt	δ	64.0	73.3	73.3	64.0
		$\Delta\delta$	0.4	−0.2	−0.2	0.4

2.3.2 Coordination of methylated sugars

According to the NMR results obtained from the reactions of Zn^{II}(dien) with polyols, Zn^{II} did not induce coordination-induced shifts that are caused only by the coordination itself. However, if the ligand investigated changes its conformation due to coordination this should lead to a change of ^{13}C NMR chemical shifts anyway and, thus, would verify coordination. Methylated sugars were ligands well suited for this approach. On the one hand, they exhibit furanose or pyranose rings that would twist due to coordination and, on the other hand, they are configurationally restricted and, thus, only one isomer had to be considered for coordination compared to reducing sugars.

Appropriate experiments were conducted with methyl α-D-glucopyranoside, methyl β-D-glucopyranoside, methyl α-D-mannopyranoside, methyl α-D-galactopyranoside and methyl β-D-galactopyranoside. The reaction of dimethylzinc with diethylenetriamine and methyl α-D-glucopyranoside resulted in a nearly clear colourless solution. The ^{13}C NMR spectrum measured is shown in Figure 2.38. Table 2.24 summarises the ^{13}C NMR chemicals shifts of the product complex [Zn(dien)(Me-α-D-Glc*p*H$_{-2}$] **17**. In Figure 2.38, the shift differences between the educt and product signals are clearly visible. They amounted up to 3.0 ppm. Additionally, a ^{13}C NMR spectrum from the free methyl α-D-glucopyranoside at higher pH values was recorded in order to check the influence of the pH value on the educt signals. The corresponding spectrum also shown in Figure 2.38 revealed the influence of the pH value as the signals of the educt were shifted significantly. However, the shifts of the signals caused by the change of pH were obviously different from the shifts caused by coordination.

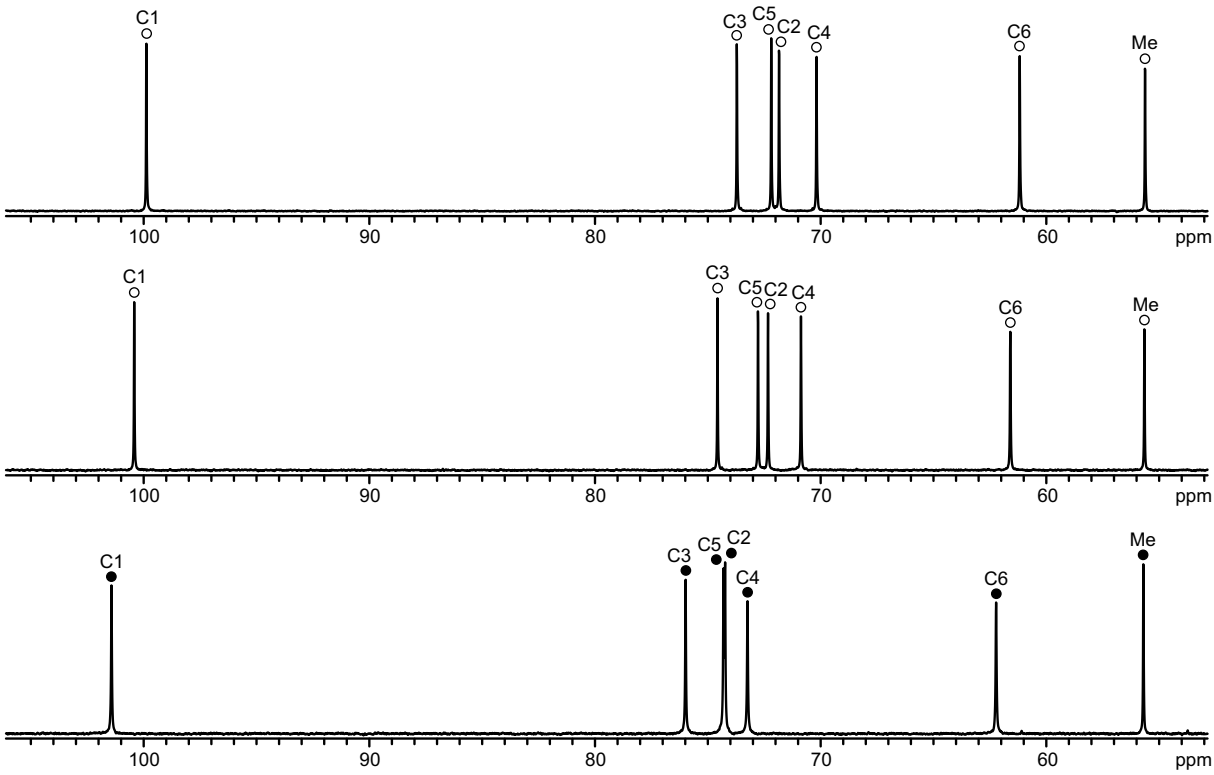

Figure 2.38 ^{13}C NMR spectra; top: an aqueous solution of methyl α-D-glucopyranoside (○). center: an aqueous solution of methyl α-D-glucopyranoside (○) and sodium hydroxide at the molar ratio of 1:2. bottom: an aqueous solution of dimethylzinc, diethylenetriamine and methyl α-D-glucopyranoside at the molar ratio of 2:2:1. The only product assigned is **17** (●).

The ^{13}C NMR spectra of the product solutions obtained from experiments with the methylated sugars methyl β-D-glucopyranoside, methyl α-D-mannopyranoside, methyl α-D-galactopyranoside and methyl β-D-galactopyranoside also contained always one set of signals. The ^{13}C NMR chemical shifts of the corresponding product complexes [Zn(dien)(Me-β-D-Glc*p*H$_{-2}$] **18**, [Zn(dien)(Me-α-D-Man*p*H$_{-2}$] **19**, [Zn(dien)(Me-α-D-Gal*p*H$_{-2}$] **20** and [Zn(dien)(Me-β-D-Gal*p*H$_{-2}$] **21** are given in Table 2.24. The shifts obtained from the signals of C1 and C6 lay between 1.0 and 2.2 ppm. The shifts of the signals for C2, C3, C4 and C5 added up to 0.3–3.5 ppm. The signals of the methyl groups were barely shifted. As assumed, the shift differences between educt and product signals were non-systematic and, thus, they did not allow any conclusion about the metal-binding site. As a result, the complete structures of the products **17**–**21** could not be determined. Possible coordination patterns were the coordination through O2 and O3 or O3 and O4 for all five methylated sugars investigated. Again, it is possible that various product complexes were formed and led to only one set of NMR signals.

Table 2.24 ^{13}C NMR chemical shifts of the product complexes **17**, **18**, **19**, **20** and **21** from the reactions of dimethylzinc and diethylenetriamine with one of the methylated sugars methyl α-D-glucopyranoside, methyl β-D-glucopyranoside, methyl α-D-mannopyranoside, methyl α-D-galactopyranoside and methyl β-D-galactopyranoside (molar ratio 2:2:1). $\Delta\delta$ is the shift difference of the product complex and the free methylated sugar at neutral pH.

	methylated sugar		C1	C2	C3	C4	C5	C6	Me
free	Me-α-D-Glc*p*	δ	99.9	71.8	73.7	70.2	72.2	61.2	55.6
17	Me-α-D-Glc*p*	δ	101.4	74.2	76.0	73.2	74.3	62.2	55.7
		$\Delta\delta$	1.5	2.4	2.3	3.0	2.1	1.0	0.1
free	Me-β-D-Glc*p*	δ	103.8	73.7	76.4	70.3	76.5	61.4	57.8
18	Me-β-D-Glc*p*	δ	105.5	76.1	78.6	73.4	80.0	62.5	57.7
		$\Delta\delta$	1.7	2.4	2.2	3.1	3.5	1.1	−0.1
free	Me-α-D-Man*p*	δ	101.4	70.5	71.2	67.4	73.1	61.6	55.3
19	Me-α-D-Man*p*	δ	103.6	73.5	73.6	70.3	73.4	62.2	55.1
		$\Delta\delta$	2.2	3.0	2.4	2.9	0.3	1.6	−0.2
free	Me-α-D-Gal*p*	δ	100.0	68.8	70.1	69.8	71.3	61.9	55.6
20	Me-α-D-Gal*p*	δ	101.2	71.7	71.3	72.3	73.1	63.0	55.6
		$\Delta\delta$	1.2	2.9	1.2	2.5	1.8	1.1	0.0
free	Me-β-D-Gal*p*	δ	104.4	71.4	73.4	69.3	75.7	61.6	57.8
21	Me-β-D-Gal*p*	δ	105.8	73.8	76.3	71.9	77.8	62.7	57.6
		$\Delta\delta$	1.4	2.4	2.9	2.6	2.1	1.1	−0.2

2.3.3 Coordination of reducing sugars

In contrast to solutions of methylated sugars, aqueous solutions of reducing sugars contain several isomers, namely the α-pyranose form, the β-pyranose form, the α-furanose form and the β-furanose form, that exist in equilibrium. All of these forms should be able to coordinate to a Zn^{II}(dien) fragment. The idea behind these experiments was that the coordination of each isomer is variously preferred. Thus, the ratio of the isomers in solution changed due to coordination, which was detected by NMR spectroscopy.

2.3.3.1 D-Lyxose

Aqueous solutions of D-lyxose contain pyranose forms as well as furanose forms. The main species is the α-D-lyxopyranose (71%) followed by the β-D-lyxopyranose (29%). Only very small amounts of the lyxofuranoses are detectable *via* NMR spectroscopy.

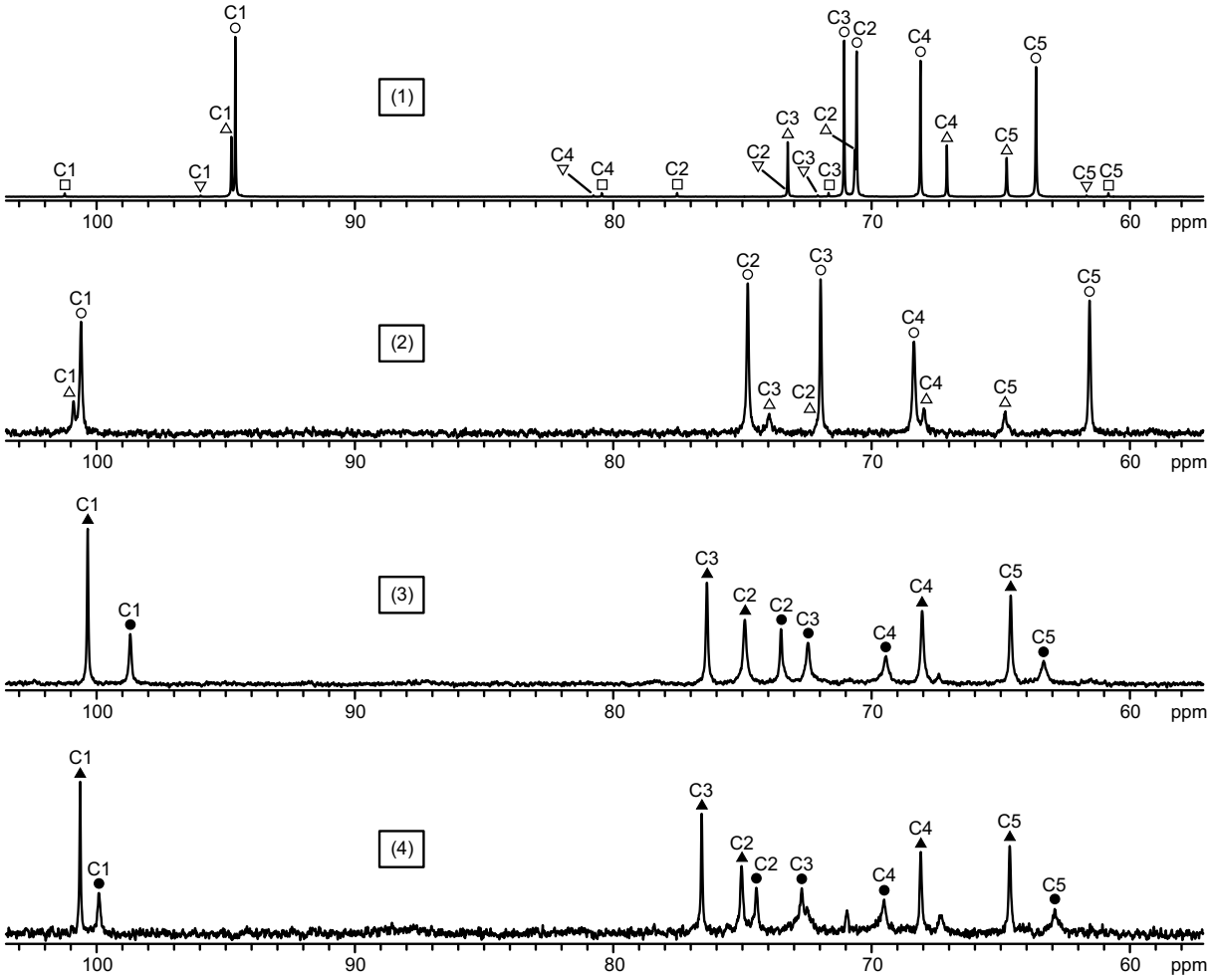

Figure 2.39 ^{13}C NMR spectra; (1): an aqueous solution of D-lyxose. (2): an aqueous solution of D-lyxose and sodium hydroxide at the molar ratio of 1:2. (3): an aqueous solution of dimethylzinc, diethylenetriamine and D-lyxose at the molar ratio of 1:1:1. (4): an aqueous solution of dimethylzinc, diethylenetriamine and D-lyxose at the molar ratio of 2:2:1. Product species assigned are **22a** (●) and **22b** (▲). Free D-lyxose forms assigned are the α-pyranose form (○), the β-pyranose form (△), the α-furanose form (□) and the β-furanose form (▽).

The reactions of dimethylzinc with diethylenetriamine and D-lyxose in the molar ratios 1:1:1 and 2:2:1 both resulted in clear colourless solutions. The ^{13}C NMR spectra measured are shown in Figure 2.39. Signals were assigned for the α-pyranose species **22a** and the β-pyranose species **22b**. It was remarkable that the ^{13}C NMR chemical shifts obtained from the spectrum of the 1:1:1 experiment differed from the ones obtained from the spectrum of the 2:2:1 experiment. Especially the values for C1 and C2 of **22a** differed about 1 ppm. Therefore, the ^{13}C NMR chemicals shifts obtained from both spectra are listed in Table 2.25. Minimal pH differences of both product solutions were assumed to be one reason for this difference. Another reason was thought to be the fast metal-ligand exchange. Thus, the NMR signals would not only represent the product complexes but also small amounts of remaining free D-lyxose. Since the amount of remaining educt is dependent on the stoichiometry used,

this would explain the different ^{13}C NMR chemical shifts. The broadening of the product signals would support this hypothesis.

Table 2.25 ^{13}C NMR chemical shifts of the product complexes **22a** and **22b** from the reactions of dimethylzinc and diethylenetriamine with D-lyxose (molar ratios 1:1:1 and 2:2:1). $\Delta\delta$ is the shift difference of the product complex and the free D-lyxose form at neutral pH.

	isomer	molar ratio		C1	C2	C3	C4	C5
free	α-D-Lyx*p*		δ	94.7	70.6	71.1	68.2	63.7
22a	α-D-Lyx*p*	1:1:1	δ	98.7	73.5	72.5	69.4	63.3
			$\Delta\delta$	4.0	2.9	1.4	1.2	–0.4
22a	α-D-Lyx*p*	2:2:1	δ	99.9	74.5	72.7	69.5	62.9
			$\Delta\delta$	5.2	3.9	1.6	1.3	–0.8
free	β-D-Lyx*p*		δ	94.8	70.7	73.3	67.1	64.8
22b	β-D-Lyx*p*	1:1:1	δ	100.3	74.9	76.4	68.0	64.6
			$\Delta\delta$	5.5	4.2	3.1	0.9	–0.2
22b	β-D-Lyx*p*	2:2:1	δ	100.6	75.0	76.6	68.1	64.7
			$\Delta\delta$	5.8	4.3	3.3	1.0	–0.1

Since Zn^{II} did not induce coordination-induced shifts, the metal-binding sites were only assumed. Due to the hydroxy function of the anomeric carbon atom featuring the lowest acid-dissociation constant, the products were thought to be $\kappa^2O^{1,2}$ chelates when possible. As a result, the two product species **22a** and **22b** were assumed to be [Zn(dien)(α-D-Lyx*p*1,2H$_{-2}$-$\kappa^2O^{1,2}$)] and [Zn(dien)(β-D-Lyx*p*1,2H$_{-2}$-$\kappa^2O^{1,2}$)], respectively. Their structures are shown in Figure 2.40.

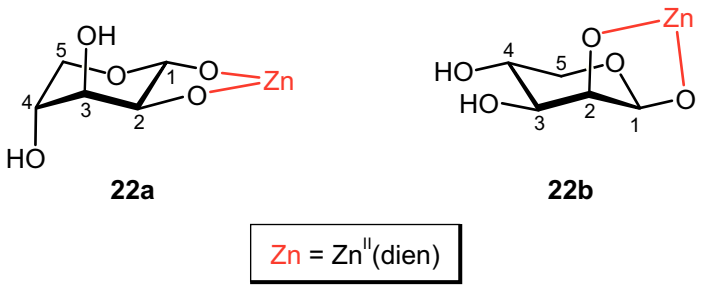

Figure 2.40 Products assumed from the reaction of dimethylzinc and diethylenetriamine with D-lyxose.

The α-pyranose:β-pyranose ratios of the product solutions were found to be 29%:71% for the 1:1:1 reaction and 32%:68% for the 2:2:1 reaction of dimethylzinc with diethylenetriamine and D-lyxose. Compared to the ratio obtained from the educt solution, they were significantly different as the main species in the product solutions was the β-pyranose form **22b** and the main species in the educt solution was the free α-pyranose form. This change of the

equilibrium of the isomers clearly verified that coordination took place. The coordination of the β-pyranose form was privileged.

For comparison, a ^{13}C NMR spectrum of an alkaline solution of D-lyxose is shown in Figure 2.39. It is plainly visible that the increase of pH caused a clear shift of the educt signals. However, the shifts were obviously different from shifts obtained from the measurements of the product solutions. Furthermore, the ratio of the educt forms in solution did not change significantly by varying the pH.

Table 2.26 Coupling constants (*J*/Hz) of the D-lyxose part of product complex **22b** in D_2O. Values of the free form and the idealised forms were obtained from previous works.[36, 91]

	isomer	$^3J_{1,2}$	$^3J_{2,3}$	$^3J_{3,4}$	$^3J_{4,5a}$	$^3J_{4,5b}$	$^2J_{5a,5b}$	conformation
free (exp.)	β-pyr	1.1	2.7	8.5	5.1	9.1	–	$^4C_1$
idealised	β-pyr	1.3	3.5	9.6	4.3	10.1	–	$^4C_1$
idealised	β-pyr	3.1	3.5	4.3	2.5	0.6	–	$^1C_4$
22b	β-pyr	1.2	3.4	8.6	–	10.4	−12.5	$^4C_1$

Some $^3J_{H,H}$ coupling constants of **22b** were determined. In Table 2.26 they are compared with the coupling constants of the free β-lyxopyranose form and the constants of the idealised $^4C_1$ and $^1C_4$ conformations of the β-pyranose form. All these values were obtained from previous works.[36, 91] According to the values determined, the conformation of **22b** is $^4C_1$ which is the same as of the free form.

2.3.3.2 D-Arabinose

The main species in aqueous solutions of D-arabinose is the α-pyranose form (61%). Further isomers are β-D-arabinopyranose (35%), α-D-arabinofuranose (2%) and β-D-arabinofuranose (2%).

The reactions of dimethylzinc with diethylenetriamine and D-arabinose in the molar ratios 1:1:1 and 2:2:1 both led to three product species whereas the product ratios determined from both experiments were equal. The main product was the β-furanose form **23c** (44%). The minor species were the α-pyranose form **23a** (35%) and the β-pyranose form **23b** (21%). The change of concentrations is obvious as the α-furanose form was enriched from 2% in the educt solution to 44% in the product solution. Moreover, the ratio of the pyranose forms shifted slightly to a relatively higher concentration of the β-pyranose form. The products' ^{13}C NMR chemical shifts obtained from both experiments differed from each other as already

seen in the experiments with D-lyxose. Thus, Table 2.27 lists the chemical shifts obtained from both NMR spectra while the spectra are shown in Figure 2.41.

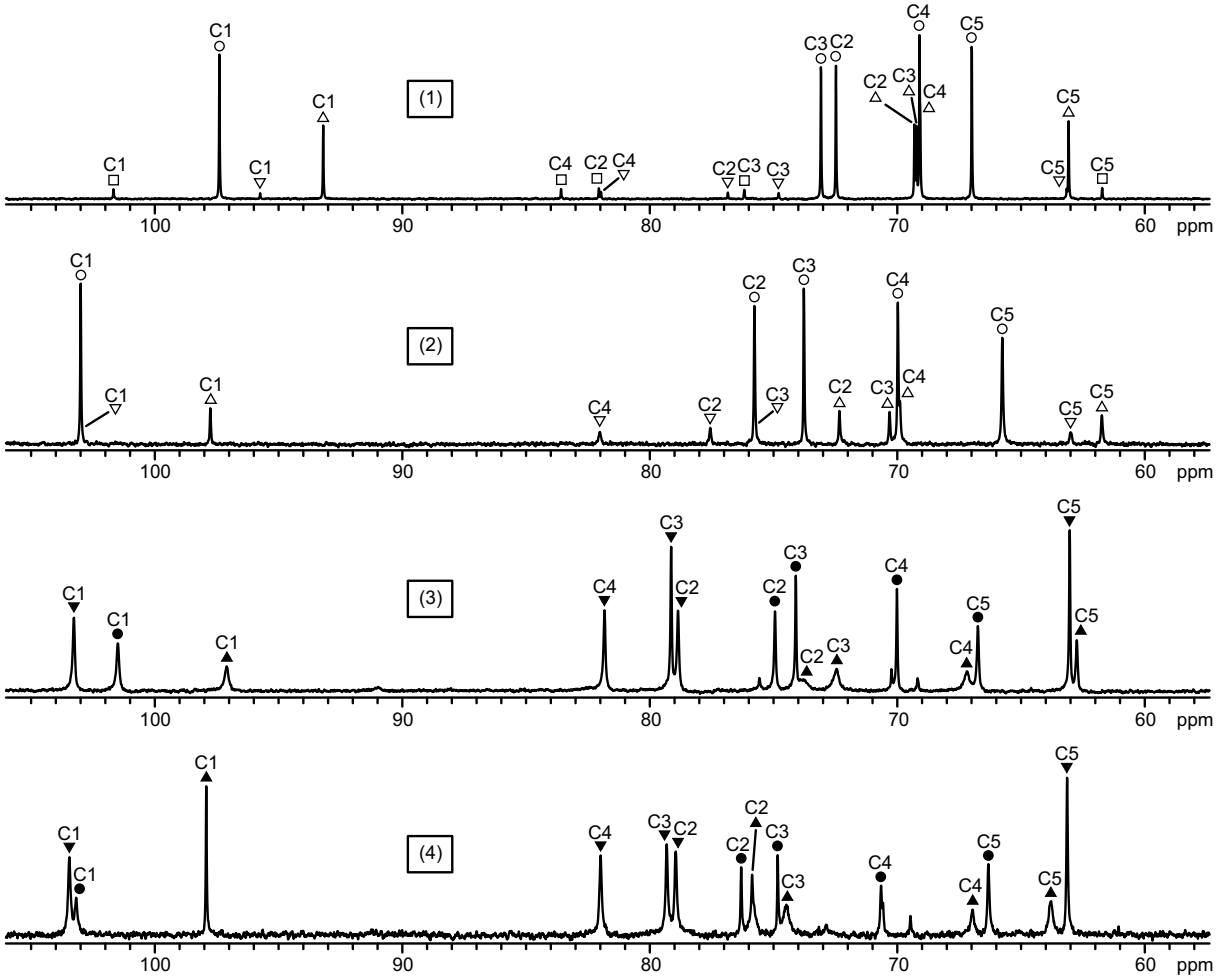

Figure 2.41 ^{13}C NMR spectra; (1): an aqueous solution of D-arabinose. (2): an aqueous solution of D-arabinose and sodium hydroxide at the molar ratio of 1:2. (3): an aqueous solution of dimethylzinc, diethylenetriamine and D-arabinose at the molar ratio of 1:1:1. (4): an aqueous solution of dimethylzinc, diethylenetriamine and D-arabinose at the molar ratio of 2:2:1. Product species assigned are **23a** (●), **23b** (▲) and **23c** (▼). Free D-arabinose forms assigned are the α-pyranose form (○), the β-pyranose form (△), the α-furanose form (□) and the β-furanose form (▽).

The ^{13}C NMR spectrum of an alkaline solution of D-arabinose shown in Figure 2.41 revealed that the shifts of the signals of the free forms caused by the increase of pH were significantly different from the shifts caused by coordination. Furthermore, the ratio of the free forms in solution did not change significantly by changing only the pH.

Again, the chelation sites were only assumed since Zn^{II} did not induce coordination-induced shifts. The products were thought to be $\kappa^2O^{1,2}$ chelates because of the comparatively low acid-dissociation constant of the hydroxy function of C1. Hence, the three product species **23a**,

23b and **23c** were assumed to be [Zn(dien)(α-D-Ara*p*1,2H$_{-2}$-κ^2*O*^{1,2})], [Zn(dien)(β-D-Ara*p*1,2H$_{-2}$-κ^2*O*^{1,2})] and [Zn(dien)(β-D-Ara*f*1,2H$_{-2}$-κ^2*O*^{1,2})], respectively. They are shown in Figure 2.42.

Table 2.27 ^{13}C NMR chemical shifts of the product complexes **23a**, **23b** and **23c** from the reactions of dimethylzinc and diethylenetriamine with D-arabinose (molar ratios 1:1:1 and 2:2:1). $\Delta\delta$ is the shift difference of the product complex and the free D-arabinose form at neutral pH.

	isomer	molar ratio		C1	C2	C3	C4	C5
free	α-D-Ara*p*		δ	97.4	72.5	73.1	69.1	67.0
23a	α-D-Ara*p*	1:1:1	δ	101.5	74.9	74.1	70.0	66.7
			$\Delta\delta$	4.1	2.4	1.0	0.9	–0.3
23a	α-D-Ara*p*	2:2:1	δ	103.2	76.3	74.8	70.7	66.3
			$\Delta\delta$	5.8	3.8	1.7	1.6	–0.7
free	β-D-Ara*p*		δ	93.2	69.2	69.2	69.2	63.1
23b	β-D-Ara*p*	1:1:1	δ	97.1	73.8	72.5	67.2	62.7
			$\Delta\delta$	3.9	4.6	3.3	–2.0	–0.4
23b	β-D-Ara*p*	2:2:1	δ	97.9	75.9	74.5	67.0	63.8
			$\Delta\delta$	4.7	6.7	5.3	–2.2	0.7
free	β-D-Ara*f*		δ	95.6	76.8	74.8	82.0	61.7
23c	β-D-Ara*f*	1:1:1	δ	103.3	78.9	79.1	81.8	63.0
			$\Delta\delta$	7.7	2.1	4.3	–0.2	1.3
23c	β-D-Ara*f*	2:2:1	δ	103.5	79.0	79.3	82.0	63.1
			$\Delta\delta$	7.9	2.2	5.5	0.0	1.4

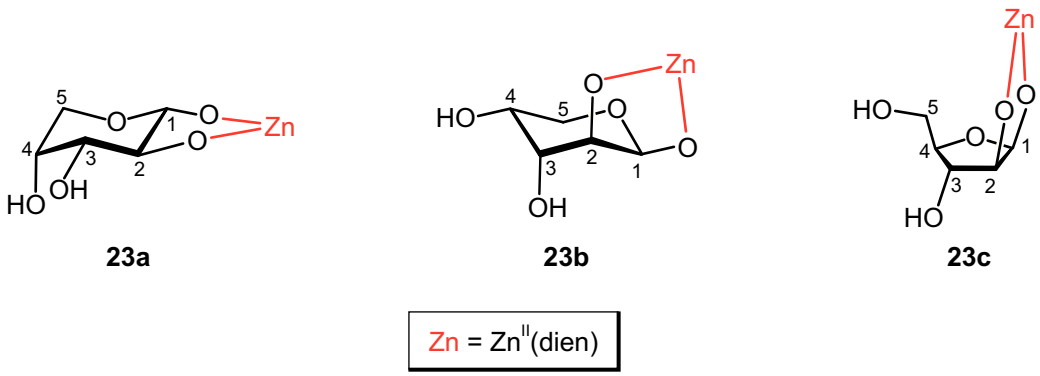

Figure 2.42 Products assumed from the reaction of dimethylzinc and diethylenetriamine with D-arabinose.

Table 2.28 lists the $^3J_{H,H}$ coupling constants determined for **23a**, **23b** and **23c**. They are compared with the values of the free forms and the idealised $^4C_1$ and $^1C_4$ pyranose forms which were all obtained from previous works.[36, 91] The conformation of **23a** was $^1C_4$ and thus, identical to the conformation of the free α-pyranose form. In contrast, the conformation

of the β-pyranose form changed from $^{1}C_4$ for the free form to $^{4}C_1$ for the product species **23b**. This change of conformation was a clear verification of coordination.

Table 2.28 Coupling constants (*J*/Hz) of the D-arabinose part of product complexes **23a**, **23b** and **23c** in D_2O. Values of the free and the idealised forms were obtained from previous works.[36, 91]

	isomer	$^{3}J_{1,2}$	$^{3}J_{2,3}$	$^{3}J_{3,4}$	$^{3}J_{4,5a}$	$^{3}J_{4,5b}$	$^{2}J_{5a,5b}$	conformation
free (exp.)	α-pyr	7.8	9.8	3.6	1.8	1.3	–	$^{1}C_4$
idealised	α-pyr	3.2	4.3	3.5	4.3	10.1	–	$^{4}C_1$
idealised	α-pyr	8.1	9.6	3.2	2.5	0.6	–	$^{1}C_4$
23a	α-pyr	7.2	9.5	3.3	–	–	–	$^{1}C_4$
free (exp.)	β-pyr	3.6	9.3	3.4	2.5	1.7	–	$^{1}C_4$
idealised	β-pyr	1.3	4.3	3.5	4.3	10.1	–	$^{4}C_1$
idealised	β-pyr	3.1	9.6	3.2	2.5	0.6	–	$^{1}C_4$
23b	β-pyr	1.5	4.6	3.5	–	8.1	–	$^{4}C_1$
23c	β-fur	2.2	5.0	–	–	–	–	–

2.3.3.3 D-Xylose

Aqueous solutions of D-xylose contain the α-pyranose form (35%) and the β-pyranose form (65%). Only very small amounts of the xylofuranoses are detectable *via* NMR spectroscopy.

The reaction of dimethylzinc with diethylenetriamine and D-xylose in the molar ratio 1:1:1 resulted in two product species. The main product was the β-pyranose form **24b** (77%) while the minor species was the α-pyranose form **24a** (23%). The reaction in the molar ratio 2:2:1 led to different results. Here, three products were observed. Beside **24a** (24%) and **24b** (49%), there were also signals for the α-furanose species **24c** (27%). Figure 2.43 illustrates the corresponding ^{13}C NMR spectra. The ^{13}C NMR chemical shifts of the three products are given in Table 2.29. It was noticeable that the product ratio of both experiments was different whereas this was not the case in the experiments with D-lyxose and D-arabinose.

A ^{13}C NMR spectrum of an alkaline solution of D-xylose is shown in Figure 2.43 as well. This spectrum clearly verified that the shifts of signals of the free forms caused by the increase of pH were not the same as the shifts caused by coordination. Moreover, no change of the educt ratio induced by the change of pH was observed.

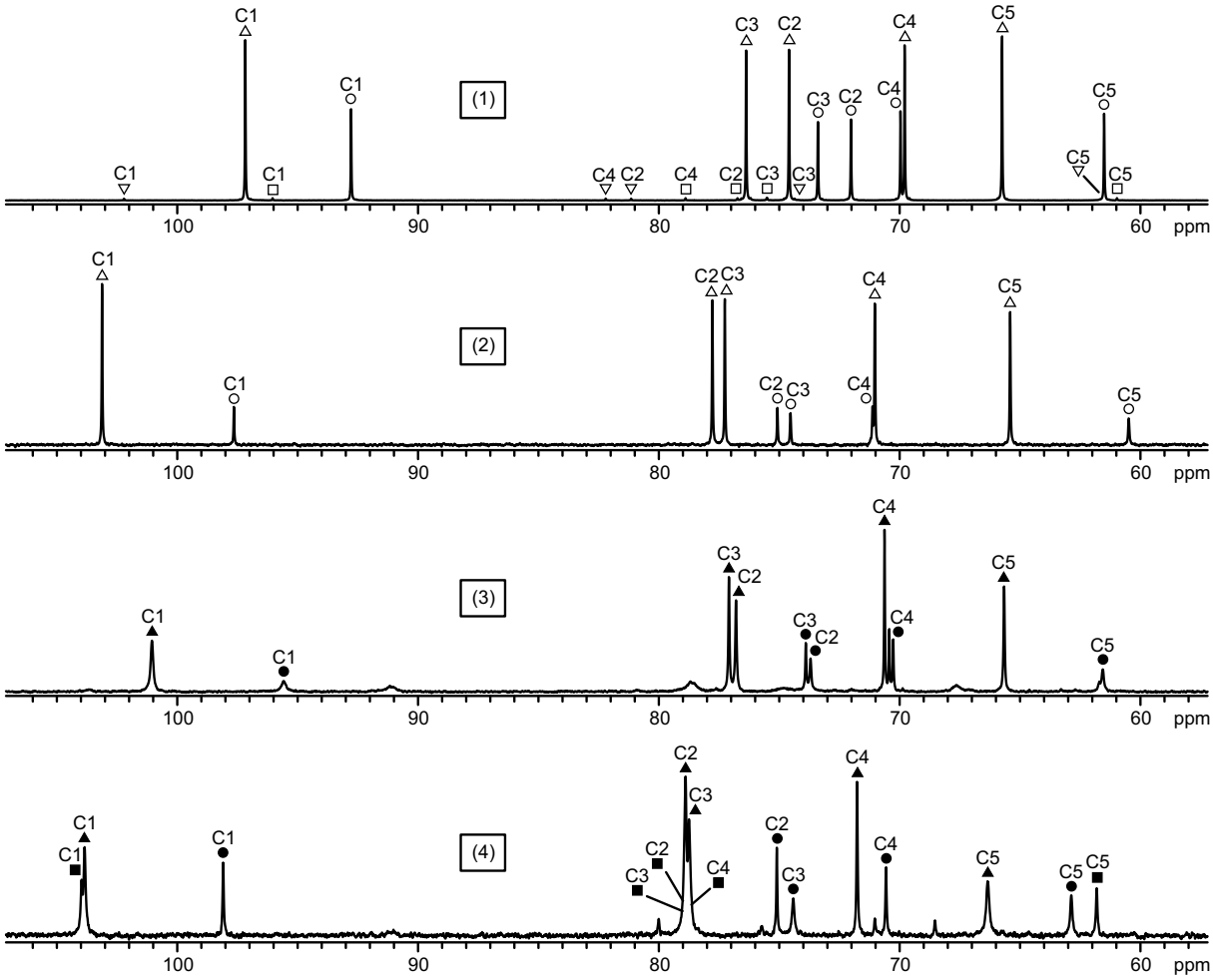

Figure 2.43 ^{13}C NMR spectra; (1): an aqueous solution of D-xylose. (2): an aqueous solution of D-xylose and sodium hydroxide at the molar ratio of 1:2. (3): an aqueous solution of dimethylzinc, diethylenetriamine and D-xylose at the molar ratio of 1:1:1. (4): an aqueous solution of dimethylzinc, diethylenetriamine and D-xylose at the molar ratio of 2:2:1. Product species assigned are **24a** (●), **24b** (▲) and **24c** (■). Free D-xylose forms assigned are the α-pyranose form (○), the β-pyranose form (△), the α-furanose form (□) and the β-furanose form (▽).

Because of the absence of coordination-induced shifts, the metal-binding sites were only assumed. The products were thought to be $\kappa^2O^{1,2}$ chelates due to the comparatively low acid-dissociation constant of the hydroxy function of C1. Thus, the three product species **24a**, **24b** and **24c** were determined to be [Zn(dien)(α-D-Xyl*p*1,2H$_{-2}$-$\kappa^2O^{1,2}$)], [Zn(dien)(β-D-Xyl*p*1,2H$_{-2}$-$\kappa^2O^{1,2}$)] and [Zn(dien)(α-D-Xyl*f*1,2H$_{-2}$-$\kappa^2O^{1,2}$)], respectively. They are shown in Figure 2.44.

Table 2.29 ^{13}C NMR chemical shifts of the product complexes **24a**, **24b** and **24c** from the reactions of dimethylzinc and diethylenetriamine with D-xylose (molar ratios 1:1:1 and 2:2:1). $\Delta\delta$ is the shift difference of the product complex and the free D-xylose form at neutral pH.

	isomer	molar ratio		C1	C2	C3	C4	C5
free	α-D-Xyl*p*		δ	92.8	72.1	73.4	70.0	61.6
24a	α-D-Xyl*p*	1:1:1	δ	95.6	73.7	73.9	70.3	61.6
			$\Delta\delta$	2.8	1.6	0.5	0.3	0.0
24a	α-D-Xyl*p*	2:2:1	δ	98.1	75.1	74.4	70.6	62.9
			$\Delta\delta$	5.3	3.0	1.0	0.6	1.3
free	β-D-Xyl*p*		δ	97.2	74.7	76.4	69.8	65.8
24b	β-D-Xyl*p*	1:1:1	δ	101.0	76.8	77.1	70.6	65.7
			$\Delta\delta$	3.8	2.1	0.7	0.8	–0.1
24b	β-D-Xyl*p*	2:2:1	δ	103.8	78.9	78.7	71.8	66.3
			$\Delta\delta$	6.6	4.2	2.3	2.0	0.5
free	α-D-Xyl*f*		δ	96.1	76.7	75.5	78.9	61.0
24c	α-D-Xyl*f*	2:2:1	δ	104.0	78.9	78.9	78.9	61.8
			$\Delta\delta$	7.9	2.2	3.4	0.0	0.8

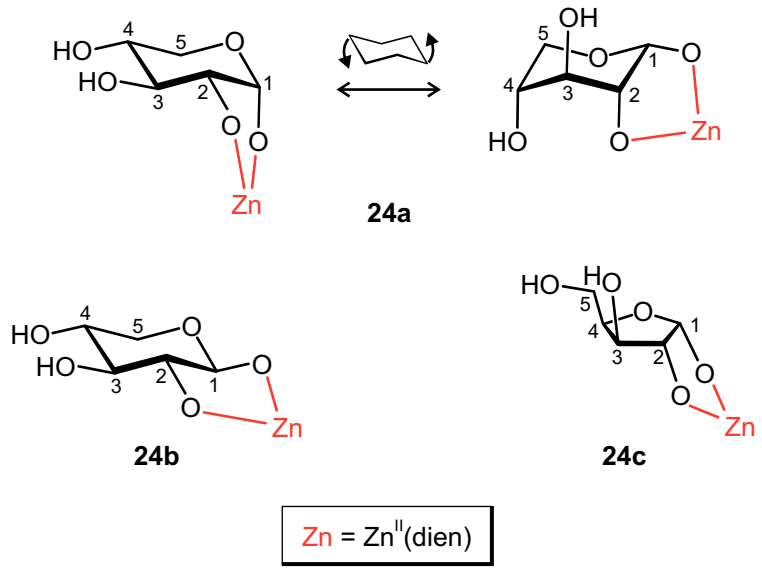

Figure 2.44 Products assumed from the reaction of dimethylzinc and diethylenetriamine with D-xylose.

For the product complexes **24a** and **24b** some $^{3}J_{H,H}$ coupling constants were determined. They are listed in Table 2.30. For comparison, the coupling constants of the free forms and the idealised $^{4}C_{1}$ and $^{1}C_{4}$ forms of the pyranoses obtained from previous works[36, 91] are given in addition. The conformation of **24b** was $^{4}C_{1}$ which is the same as of the educt form. However, the coupling constants of the β-pyranose form lay between both conformation types. Thus, it was assumed that the $^{4}C_{1}$- and the $^{1}C_{4}$ form existed in equilibrium in solution. Such an

equilibrium of pentose complexes had already been found by using Pd^{II} metal fragments in a recent work.[36]

Table 2.30 Coupling constants (*J*/Hz) of the D-xylose part of product complexes **24a** and **24b** in D_2O. Values of the free and the idealised forms were obtained from previous works.[36, 91]

	isomer	$^3J_{1,2}$	$^3J_{2,3}$	$^3J_{3,4}$	$^3J_{4,5a}$	$^3J_{4,5b}$	$^2J_{5a,5b}$	conformation
free (exp.)	α-pyr	3.7	9.8	9.1	5.1	10.2	–	$^4C_1$
idealised	α-pyr	3.1	9.8	9.6	4.3	10.1	–	$^4C_1$
idealised	α-pyr	1.3	4.3	4.3	2.5	0.6	–	$^1C_4$
24a	α-pyr	2.4	6.6	7.5	–	–	–	$^4C_1 \rightleftharpoons {}^1C_4$
free (exp.)	β-pyr	7.8	9.2	9.0	5.6	10.5	–	$^4C_1$
idealised	β-pyr	8.1	9.8	9.6	4.3	10.1	–	$^4C_1$
idealised	β-pyr	3.2	4.3	4.3	2.5	0.6	–	$^1C_4$
24b	β-pyr	7.5	9.2	9.3	5.4	10.5	–	$^4C_1$

2.3.3.4 D-Ribose

D-Ribose was the last pentose investigated in this work. The main species in aqueous solutions is the β-pyranose form (59%). Further isomers in smaller concentrations are α-D-ribopyranose (22%) α-D-ribofuranose (6%) and β-D-ribofuranose (13%).

The reaction of dimethylzinc with diethylenetriamine and D-ribose in the molar ratio 1:1:1 led to two product species, namely the α-pyranose form **25a** (63%) and the β-pyranose form **25b** (37%). In the 2:2:1 reaction the α-pyranose:β-pyranose ratio was 91%:9%. In both ^{13}C NMR spectra shown in Figure 2.45 further signals were obtained. Unfortunately, it was not possible to assign their corresponding structure due to the large broadening of these signals. Either they belonged to a furanose product form not identified or to an unwanted by-product. The formation of such N-glycosides is described in more detail in Chapter 2.3.3.7. Table 2.31 gives the ^{13}C NMR chemical shifts of **25a** and **25b** obtained from the spectra of both reactions.

A ^{13}C NMR spectrum of an alkaline solution of D-ribose given in Figure 2.45 confirmed that the shifts of the signals of the free forms caused by the increase of pH were not the same as the shifts caused by coordination. Furthermore, a change of the ratio of the free forms induced by the change of pH was not observed.

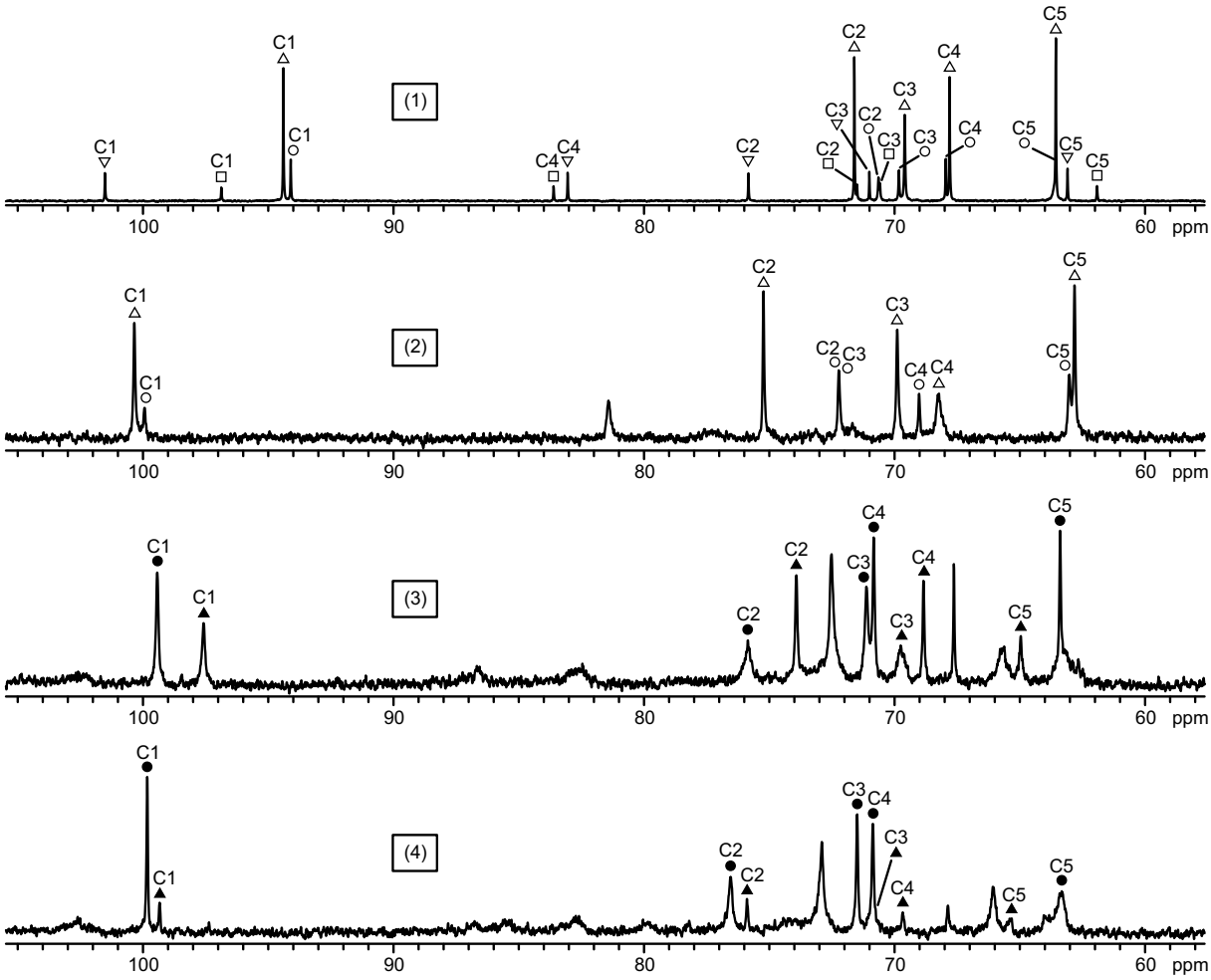

Figure 2.45 ^{13}C NMR spectra; (1): an aqueous solution of D-ribose. (2): an aqueous solution of D-ribose and sodium hydroxide at the molar ratio of 1:2. (3): an aqueous solution of dimethylzinc, diethylenetriamine and D-ribose at the molar ratio of 1:1:1. (4): an aqueous solution of dimethylzinc, diethylenetriamine and D-ribose at the molar ratio of 2:2:1. Product species assigned are **25a** (●) and **25b** (▲). Free D-ribose forms assigned are the α-pyranose form (○), the β-pyranose form (△), the α-furanose form (□) and the β-furanose form (▽).

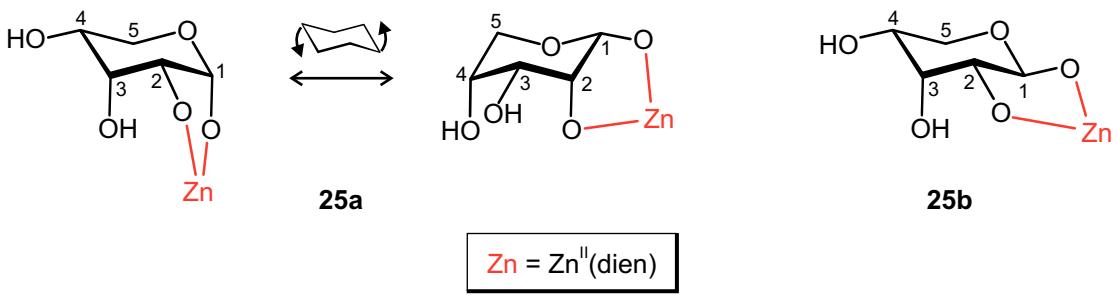

Figure 2.46 Products assumed from the reaction of dimethylzinc and diethylenetriamine with D-ribose.

Due to the absence of coordination-induced shifts, the metal-binding sites were only assumed. The products were thought to be $\kappa^2O^{1,2}$ chelates because of the relatively low acid-dissociation constant of the hydroxy function of C1. As a result, the two product species **25a**

and **25b** were determined to be [Zn(dien)(α-D-Rib*p*1,2H$_{-2}$-κ^2*O*^{1,2})] and [Zn(dien)(β-D-Rib*p*1,2H$_{-2}$-κ^2*O*^{1,2})], respectively. Both structures are shown in Figure 2.46.

Table 2.31 ^{13}C NMR chemical shifts of the product complexes **25a** and **25b** from the reactions of dimethylzinc and diethylenetriamine with D-ribose (molar ratios 1:1:1 and 2:2:1). $\Delta\delta$ is the shift difference of the product complex and the free D-ribose form at neutral pH.

	isomer	molar ratio		C1	C2	C3	C4	C5
free	α-D-Rib*p*		δ	94.1	70.6	69.8	68.0	63.6
25a	α-D-Rib*p*	1:1:1	δ	99.4	75.9	71.1	70.8	63.4
			$\Delta\delta$	5.3	5.3	1.3	2.8	−0.2
25a	α-D-Rib*p*	2:2:1	δ	99.8	76.5	71.5	70.9	63.3
			$\Delta\delta$	5.7	5.9	1.7	2.9	−0.3
free	β-D-Rib*p*		δ	94.4	71.6	69.6	67.8	63.6
25b	β-D-Rib*p*	1:1:1	δ	97.6	73.9	69.8	68.8	65.0
			$\Delta\delta$	3.2	2.3	0.2	1.0	1.4
25b	β-D-Rib*p*	2:2:1	δ	99.3	75.9	70.8	69.7	65.3
			$\Delta\delta$	4.9	4.3	1.2	1.9	1.7

Table 2.32 lists the $^3J_{H,H}$ coupling constants determined for product complexes **25a** and **25b**. For comparison, the coupling constants of the free forms and the idealised $^4C_1$ and $^1C_4$ forms of the pyranoses are given. These values were obtained from previous studies.[36, 91] While the free $^4C_1$ and $^1C_4$ α-pyranose forms existed in conformational equilibrium in solution, the conformation of the α-pyranose product species **25b** was $^4C_1$. Unfortunately, it was not possible to determine the conformation of **25a** due to some ambiguous coupling constants.

Table 2.32 Coupling constants (*J*/Hz) of the D-ribose part of product complexes **25a** and **25b** in D_2O. Values of the free and the idealised forms were obtained from previous works.[36, 91]

	isomer	$^3J_{1,2}$	$^3J_{2,3}$	$^3J_{3,4}$	$^3J_{4,5a}$	$^3J_{4,5b}$	$^2J_{5a,5b}$	conformation
free (exp.)	α-pyr	2.1	3.0	3.0	2.6	5.3	–	$^4C_1 \rightleftharpoons {}^1C_4$
idealised	α-pyr	3.1	3.5	3.5	4.3	10.1	–	$^4C_1$
idealised	α-pyr	1.3	3.5	3.2	2.5	0.6	–	$^1C_4$
25a	α-pyr	1.3	2.5	2.5	3.2	–	−11.7	–
free (exp.)	β-pyr	6.5	3.3	3.2	4.4	8.8	–	$^4C_1 \rightleftharpoons {}^1C_4$
idealised	β-pyr	8.1	3.5	3.5	4.3	10.1	–	$^4C_1$
idealised	β-pyr	3.2	3.5	3.2	2.5	0.6	–	$^1C_4$
25b	β-pyr	–	–	–	5.3	10.5	−10.9	$^4C_1$

2.3.3.5 D-Galactose

After experiments with the four pentoses, D-galactose was the first hexose whose complexes with the Zn^{II}(dien) fragment were investigated in this work. Aqueous solutions of D-galactose contain the α-pyranose form (29%), the β-pyranose form (64%), the α-furanose form (3%) and the β-furanose form (4%).

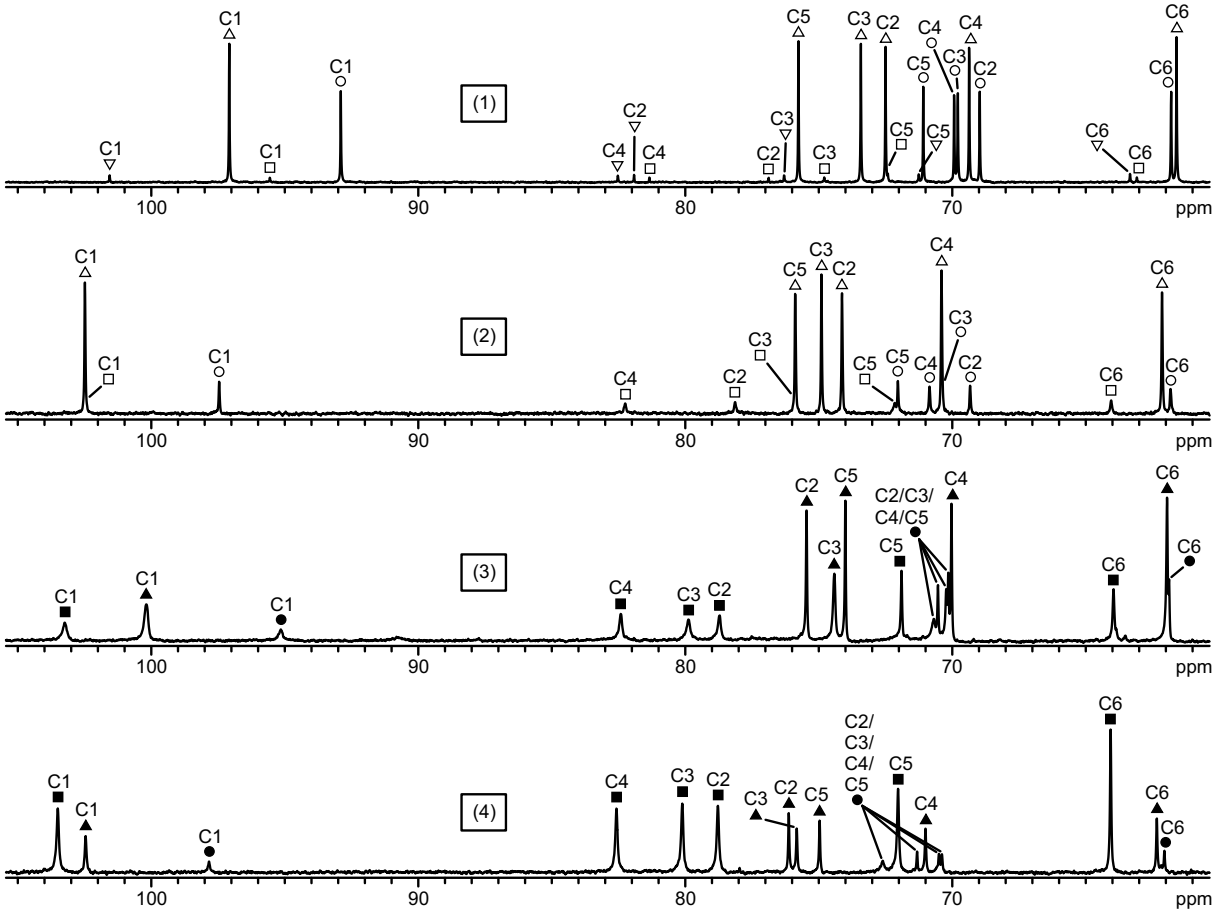

Figure 2.47 ^{13}C NMR spectra; (1): an aqueous solution of D-galactose. (2): an aqueous solution of D-galactose and sodium hydroxide at the molar ratio of 1:2. (3): an aqueous solution of dimethylzinc, diethylenetriamine and D-galactose at the molar ratio of 1:1:1. (4): an aqueous solution of dimethylzinc, diethylenetriamine and D-galactose at the molar ratio of 2:2:1. Product species assigned are **26a** (●), **26b** (▲) and **26c** (■). Free D-galactose forms assigned are the α-pyranose form (○), the β-pyranose form (△), the α-furanose form (□) and the β-furanose form (▽).

The reaction of dimethylzinc with diethylenetriamine and D-galactose in the molar ratio of 1:1:1 resulted in three product species, namely the α-pyranose form **26a** (15%), the β-pyranose form **26b** (57%) and the α-furanose form **26c** (28%). The product ratio found in the 2:2:1 experiment was different as, here, **26c** (68%) was the main species followed by **26b** (26%) and **26a** (6%). Figure 2.47 illustrates the corresponding ^{13}C NMR spectra. The ^{13}C

NMR chemical shifts of **26a**, **26b** and **26c** obtained from the spectra of both experiments are given in Table 2.33.

Table 2.33 ^{13}C NMR chemical shifts of the product complexes **26a**, **26b** and **26c** from the reactions of dimethylzinc and diethylenetriamine with D-galactose (molar ratios 1:1:1 and 2:2:1). $\Delta\delta$ is the shift difference of the product complex and the free D-galactose form at neutral pH.

	isomer	molar ratio		C1	C2	C3	C4	C5	C6
free	α-D-Gal*p*		δ	92.9	69.0	69.8	69.9	71.1	61.8
26a	α-D-Gal*p*	1:1:1	δ	95.5		70.2 / 70.3 / 70.5 / 71.0			61.9
			$\Delta\delta$	2.6	–	–	–	–	0.1
26a	α-D-Gal*p*	2:2:1	δ	97.8		70.4 / 70.5 / 71.3 / 72.6			62.1
			$\Delta\delta$	4.9	–	–	–	–	0.3
free	β-D-Gal*p*		δ	97.1	72.5	73.4	69.4	75.8	61.8
26b	β-D-Gal*p*	1:1:1	δ	100.2	75.5	74.4	70.0	74.0	62.0
			$\Delta\delta$	3.1	3.0	1.0	0.6	–1.8	1.2
26b	β-D-Gal*p*	2:2:1	δ	102.5	76.1	75.8	71.0	74.9	62.3
			$\Delta\delta$	5.4	3.6	2.4	1.6	–0.9	1.5
free	α-D-Gal*f*		δ	95.6	76.9	74.8	81.3	72.4	63.1
26c	α-D-Gal*f*	1:1:1	δ	103.2	78.7	79.9	82.4	71.9	64.0
			$\Delta\delta$	7.6	1.8	5.1	1.1	–0.5	0.9
26c	α-D-Gal*f*	2:2:1	δ	103.5	78.8	80.1	82.6	72.0	64.1
			$\Delta\delta$	7.9	1.9	5.3	1.3	–0.4	1.0

The ^{13}C NMR spectrum of an alkaline solution of D-galactose also given in Figure 2.47 verified that the shifts of the product complexes were not only caused by the change of pH. Furthermore, a significant change of the ratio of the free forms was not observed in this spectrum.

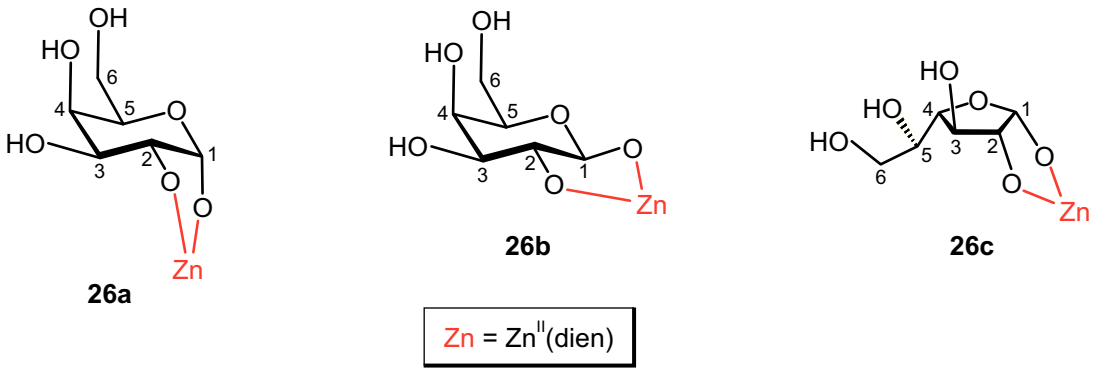

Figure 2.48 Products assumed from the reaction of dimethylzinc and diethylenetriamine with D-galactose.

Since coordination-induced shifts were not induced by Zn^{II}, the chelation sites were only assumed. The three product species **26a**, **26b** and **26c** were thought to be [Zn(dien)(α-D-Gal*p*1,2H$_{-2}$-κ^2*O*^{1,2})], [Zn(dien)(β-D-Gal*p*1,2H$_{-2}$-κ^2*O*^{1,2})] and [Zn(dien)(α-D-Gal*f*1,2H$_{-2}$-κ^2*O*^{1,2})], respectively, and are shown in Figure 2.48. The products were assumed to be κ^2*O*^{1,2} chelates due to the comparatively low acid-dissociation constant of the hydroxy function of C1.

Table 2.34 Coupling constants (*J*/Hz) of the D-galactose part of product complexes **26a, 26b** and **26c** in D_2O.

	$^3J_{1,2}$	$^3J_{2,3}$	$^3J_{3,4}$	$^3J_{4,5}$	$^3J_{5,6a}$	$^3J_{5,6b}$	$^2J_{6a,6b}$
26a	3.6	–	–	–	–	–	–
26b	7.3	9.8	3.6	–	–	–	–
26c	2.1	–	3.2	3.1	–	–	–

Some $^3J_{H,H}$ coupling constants of the three product complexes were determined and are given in Table 2.34. All of them lay in the expected range.

2.3.3.6 D-Glucose

In aqueous solutions of D-glucose, furanose forms are not detectable *via* NMR spectroscopy. The main species is the β-pyranose form (64%) followed by the α-pyranose form (36%).

The reaction of dimethylzinc with diethylenetriamine and D-glucose in the molar ratio of 1:1:1 led to two product species. The main species was the β-pyranose form **27b** (79%) and the minor species was the α-pyranose form **27a** (21%). In the 2:2:1 experiment the product ratio was similar (20%:71%). However, small signals of an additional species were observed which was identified as the α-furanose form **27c** (9%). Figure 2.49 shows the ^{13}C NMR spectra recorded. The ^{13}C NMR chemical shifts of the three products obtained from the spectra of both experiments are given in Table 2.35.

Figure 2.49 also shows the ^{13}C NMR spectrum of an alkaline solution of D-glucose. It confirmed that the shifts of the product complexes were not only caused by the change of pH. Moreover, a significant change of the ratio of the free forms was not observed in this spectrum.

Because of the absence of coordination-induced shifts, the chelation sites were only assumed. The three product species **27a**, **27b** and **27c** were thought to be [Zn(dien)(α-D-Glc*p*1,2H$_{-2}$-κ^2*O*^{1,2})], [Zn(dien)(β-D-Glc*p*1,2H$_{-2}$-κ^2*O*^{1,2})] and [Zn(dien)(α-D-Glc*f*1,2H$_{-2}$-κ^2*O*^{1,2})], respectively. Their structures are shown in Figure 2.50. The products were assumed to be

$\kappa^2O^{1,2}$ chelates due to the relatively low acid-dissociation constant of the hydroxy function of C1.

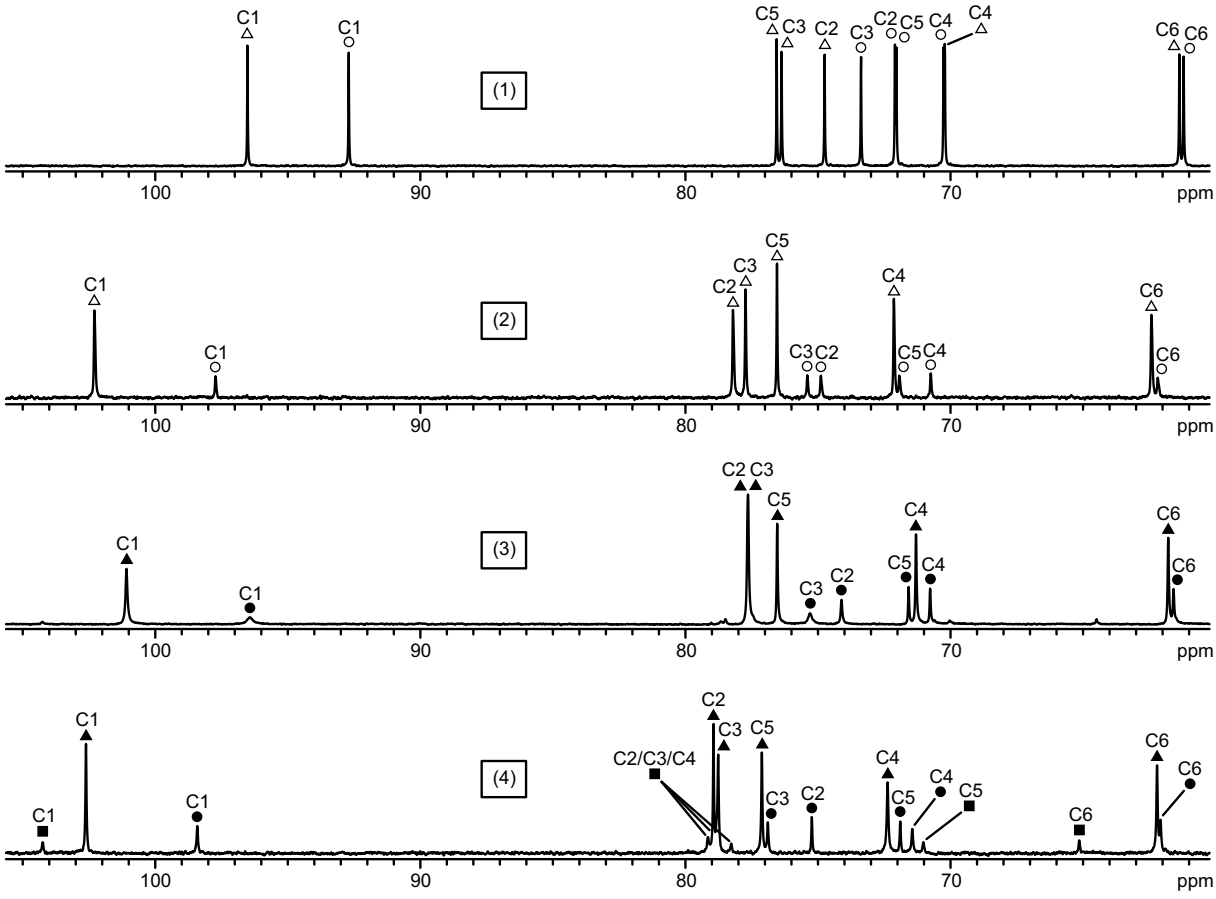

Figure 2.49 ^{13}C NMR spectra; (1): an aqueous solution of D-glucose. (2): an aqueous solution of D-glucose and sodium hydroxide at the molar ratio of 1:2. (3): an aqueous solution of dimethylzinc, diethylenetriamine and D-glucose at the molar ratio of 1:1:1. (4): an aqueous solution of dimethylzinc, diethylenetriamine and D-glucose at the molar ratio of 2:2:1. Product species assigned are **27a** (●), **27b** (▲) and **27c** (■). Free D-glucose forms assigned are the α-pyranose form (○) and the β-pyranose form (△).

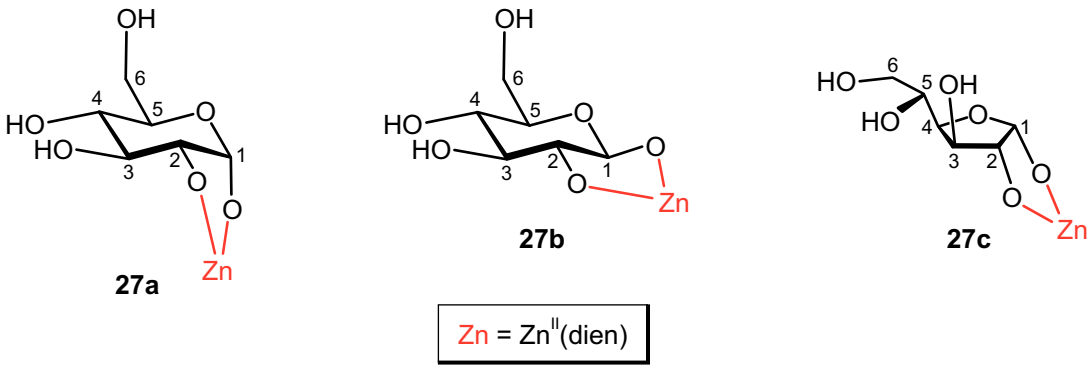

Figure 2.50 Products assumed from the reaction of dimethylzinc and diethylenetriamine with D-glucose.

Table 2.35 ^{13}C NMR chemical shifts of the product complexes **27a**, **27b** and **27c** from the reactions of dimethylzinc and diethylenetriamine with D-glucose (molar ratios 1:1:1 and 2:2:1). $\Delta\delta$ is the shift difference of the product complex and the free D-glucose form at neutral pH. The chemical shifts of free α-D-glucofuranose were adopted from earlier works.[87–88] Since appropriate values were not available for C2–C6, the chemical shifts of methyl α-D-glucofuranoside were used instead.

	isomer	molar ratio		C1	C2	C3	C4	C5	C6
free	α-D-Glc*p*		δ	92.7	72.1	73.4	70.2	72.0	61.2
27a	α-D-Glc*p*	1:1:1	δ	96.4	74.1	75.3	70.8	71.6	61.6
			$\Delta\delta$	3.7	2.0	1.9	0.6	−0.4	0.4
27a	α-D-Glc*p*	2:2:1	δ	98.4	75.2	76.9	71.4	71.9	62.2
			$\Delta\delta$	5.7	3.1	3.5	1.2	−0.1	1.0
free	β-D-Glc*p*		δ	96.5	74.7	76.4	70.3	76.6	61.4
27b	β-D-Glc*p*	1:1:1	δ	101.1	77.6	77.6	71.3	76.5	61.8
			$\Delta\delta$	4.6	2.9	1.2	1.0	−0.1	0.4
27b	β-D-Glc*p*	2:2:1	δ	102.6	78.9	78.8	72.4	77.1	62.2
			$\Delta\delta$	6.1	4.2	2.4	2.1	0.5	0.8
free	α-D-Glc*f*		δ	97.4	(78.2)	(77.1)	(79.3)	(71.2)	(64.7)
27c	α-D-Glc*f*	2:2:1	δ	104.2	78.3 / 78.9 / 79.3			71.0	65.1
			$\Delta\delta$	6.8	–	–	–	(−0.2)	(0.4)

Some $^{3}J_{H,H}$ coupling constants of the product complexes **27a**, **27b** and **27c** were determined and are given in Table 2.36. All of them lay in the expected range.

Table 2.36 Coupling constants (*J*/Hz) of the D-glucose part of product complexes **27a, 27b** and **27c** in D_2O.

	$^{3}J_{1,2}$	$^{3}J_{2,3}$	$^{3}J_{3,4}$	$^{3}J_{4,5}$	$^{3}J_{5,6a}$	$^{3}J_{5,6b}$	$^{2}J_{6a,6b}$
27a	3.7	–	–	–	–	–	–
27b	7.2	9.0	9.2	9.3	6.4	2.0	−12.0
27c	2.6	–	–	–	–	–	–

As mentioned in Chapter 2.2.3, the main species in a solution of D-glucose or D-glucose 6-phosphate in Pd-tmen were α-forms. However, to achieve the final equilibrium it was necessary to stir the solution for almost 24 hours. After a reaction time of only 2 hours, the equilibrium still lay on the side of the β-pyranose forms as in the case of the educt solution. Thus, the reaction of dimethylzinc and diethylenetriamine with D-glucose was repeated with a reaction time of 24 hours. Unfortunately, it was not possible to analyse the corresponding ^{13}C NMR spectrum on account of a very poor signal-to-noise ratio probably caused by the side reactions discussed in Chapters 2.3.3.7 and 2.3.5. As a result, a clear answer to the question of whether the α-pyranose product form or the β-pyranose product form is more energetically favourable was not found.

2.3.3.7 D-Mannose

Aqueous solutions of D-mannose contain the α-pyranose form (67%) and the β-pyranose form (33%). Only very small amounts of the mannofuranoses are detectable *via* NMR spectroscopy.

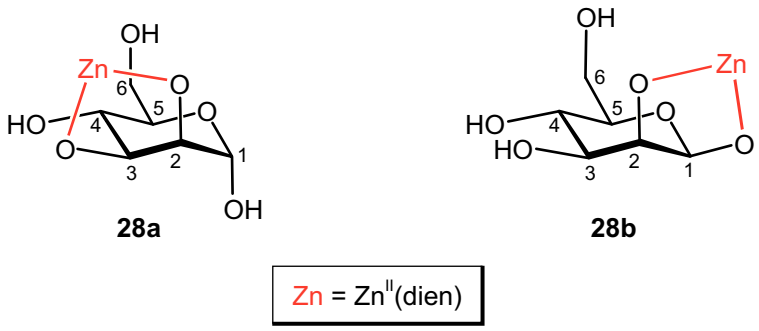

Figure 2.51 Products assumed from the reaction of dimethylzinc and diethylenetriamine with D-mannose.

Table 2.37 ^{13}C NMR chemical shifts of the product complexes **28a** and **28b** from the reactions of dimethylzinc and diethylenetriamine with D-mannose (molar ratios 1:1:1 and 2:2:1). Δδ is the shift difference of the product complex and the free D-mannose form at neutral pH.

	isomer	molar ratio		C1	C2	C3	C4	C5	C6
free	α-D-Man*p*		δ	94.7	71.3	70.8	67.5	73.0	61.6
28a	α-D-Man*p*	1:1:1	δ	98.9	72.1	72.1	68.8	74.5	62.0
			Δδ	4.2	0.8	1.3	1.3	1.5	0.4
28a	α-D-Man*p*	2:2:1	δ	99.7	72.3	72.0	69.1	75.1	62.2
			Δδ	5.0	1.0	1.2	1.6	2.1	0.6
free	β-D-Man*p*		δ	94.3	71.8	73.7	67.2	76.8	61.6
28b	β-D-Man*p*	1:1:1	δ	99.6	75.7	76.8	68.2	75.7	62.0
			Δδ	5.3	3.9	3.1	1.0	−1.1	0.4
28b	β-D-Man*p*	2:2:1	δ	99.7	75.8	76.9	68.3	75.8	62.0
			Δδ	5.4	4.0	3.2	1.1	−1.0	0.4

The product solution from the reaction of dimethylzinc with diethylenetriamine and D-mannose in the molar ratio 1:1:1 contained only two product species, namely the α-pyranose form **28a** (19%) and the β-pyranose form **28b** (81%). No signals of furanose species were observed. The 2:2:1 experiment led to a nearly identical product ratio (18%:82%). **28b** was assumed to be the $\kappa^2O^{1,2}$ chelate [Zn(dien)(β-D-Man*p*1,2H$_{-2}$-$\kappa^2O^{1,2}$)] due to the low acid-dissociation constant of the hydroxy function of C1. In contrast, the α-pyranose species **28a** could not be a $\kappa^2O^{1,2}$ chelate since the vicinal hydroxy functions of C1 and C2 were in *trans* position. Thus, this product was thought be [Zn(dien)(α-D-Man*p*2,3H$_{-2}$-$\kappa^2O^{2,3}$)] with the α-

mannopyranose form coordinating through O2 and O3 to the Zn^{II} centre. According to experiments of Pd-tmen with D-mannose,[36] this $\kappa^2O^{2,3}$ chelation should be preferred over an equally possible $\kappa^2O^{3,4}$ chelation. The reason for this preference is the favoured *cis* position of the vicinal O2 and O3 hydroxy groups compared to the *trans* position of O3 and O4. The structures of the products are shown in Figure 2.51.

Table 2.37 lists the ^{13}C NMR chemical shifts of **28a** and **28b** obtained from both experiments. The corresponding ^{13}C NMR spectra are given in Figure 2.52.

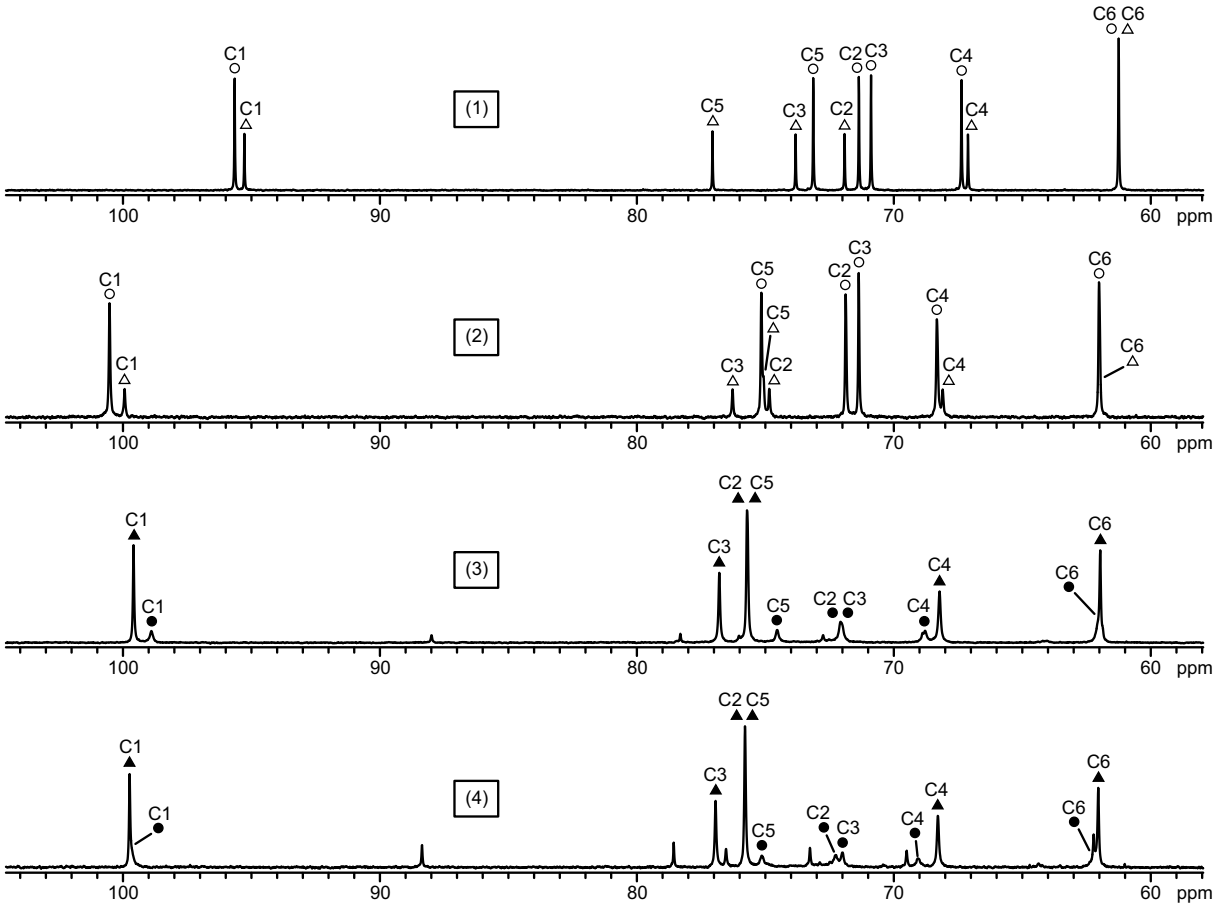

Figure 2.52 ^{13}C NMR spectra; (1): an aqueous solution of D-mannose. (2): an aqueous solution of D-mannose and sodium hydroxide at the molar ratio of 1:2. (3): an aqueous solution of dimethylzinc, diethylenetriamine and D-mannose at the molar ratio of 1:1:1. (4): an aqueous solution of dimethylzinc, diethylenetriamine and D-mannose at the molar ratio of 2:2:1. Product species assigned are **28a** (●) and **28b** (▲). Free D-mannose forms assigned are the α-pyranose form (○) and the β-pyranose form (△).

The ^{13}C NMR spectrum of an alkaline solution of D-mannose given in Figure 2.52 confirmed that the shifts of the product complexes were not only caused by the change of pH. Moreover, the ratio of the free forms in this solution was the same as in the educt solution at neutral pH.

A few coupling constants of the two product complexes were determined. They are listed in Table 2.38 and lay in the expected range.

Table 2.38 Coupling constants (*J*/Hz) of the D-mannose part of product complexes **28a** and **28b** in D_2O.

	$^3J_{1,2}$	$^3J_{2,3}$	$^3J_{3,4}$	$^3J_{4,5}$	$^3J_{5,6a}$	$^3J_{5,6b}$	$^2J_{6a,6b}$
28a	–	–	–	–	–	2.3	−12.0
28b	–	–	–	–	5.9	1.7	−12.0

It should be mentioned that signals of a further species were observed in both product spectra. This species was characterised by an extraordinarily large upfield shift of the signal for C1 that added up to about −6 ppm. After comparison with other works,[84–85] it was assumed that this species was the product complex of a by-product formed by the reaction of D-mannose and diethylenetriamine. The reaction is given in Figure 2.53. This reaction is known as a synthesis of N-glycosides and had already been conducted with the diethylenetriamine-like molecule 1,4,7-triazacyclononane and D-glucose in works of *Yano*.[92] Several experiments showed that the formation of these by-products was more pronounced in reactions with dimethylzinc than in reactions with zinc hydroxide or zinc nitrate. A high concentration of N-glycosides was very undesirable since they were also able to coordinate to Zn^{II}. However, in most cases, it was possible to get either only low concentrations of them or to avoid them completely by optimising reaction conditions or changing the reaction type.

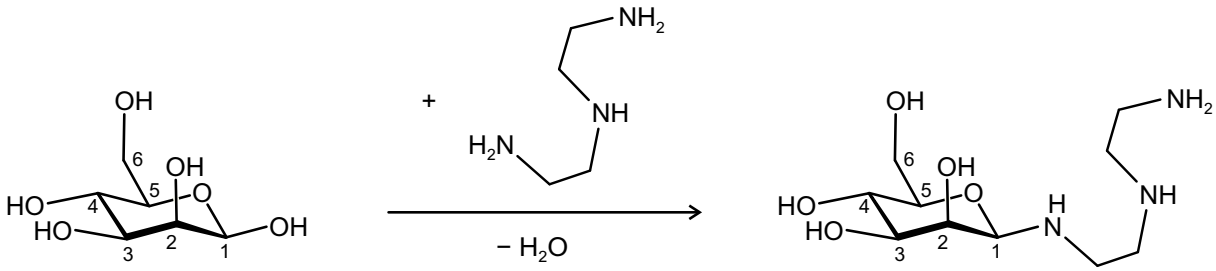

Figure 2.53 Side reaction of the two educts diethylenetriamine and D-mannose, yielding an N-glycoside.

2.3.3.8 D-Fructose

D-Fructose was the only ketose investigated in this work. The main species in aqueous solutions of D-fructose is the β-pyranose form (73%). Further species are the β-furanose form (20%), the α-furanose form (5%) and the α-pyranose form (2%).

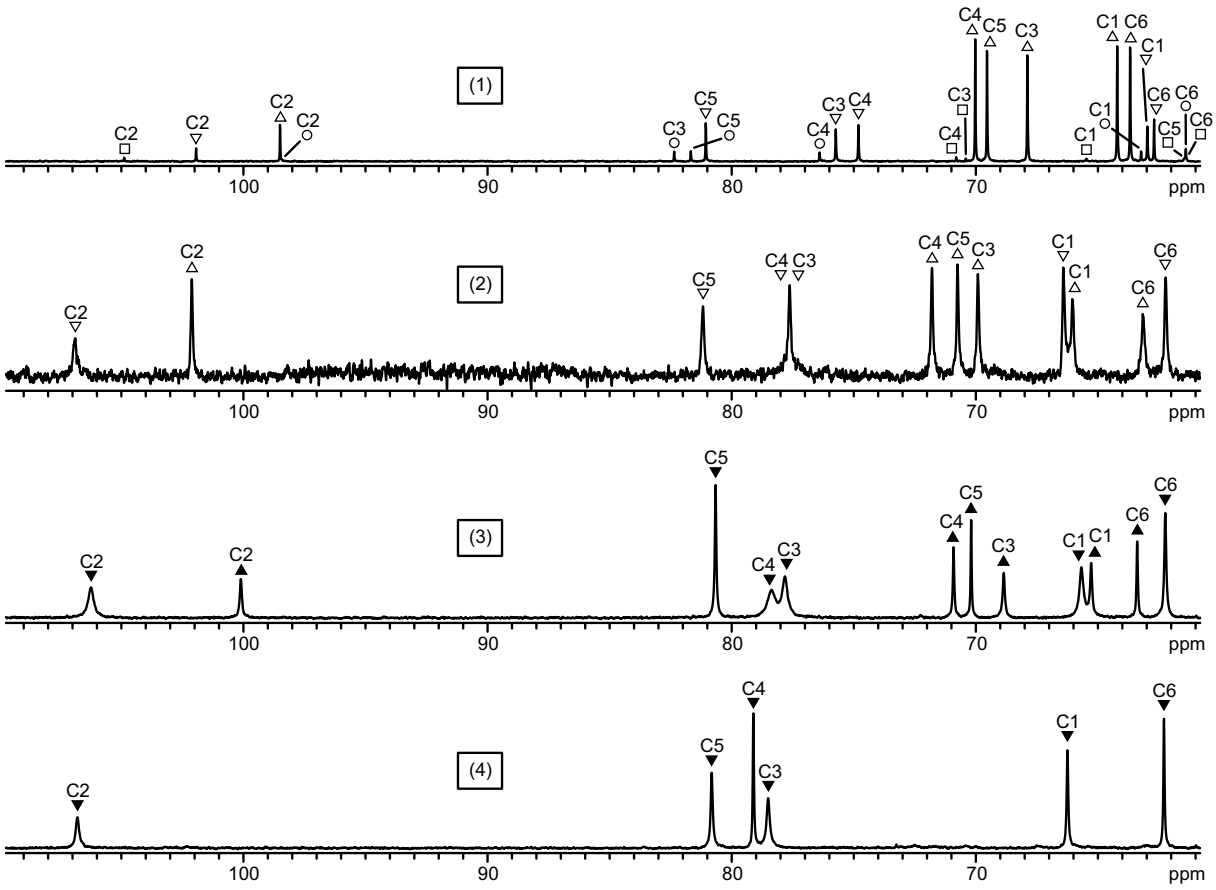

Figure 2.54 ^{13}C NMR spectra; (1): an aqueous solution of D-fructose. (2): an aqueous solution of D-fructose and sodium hydroxide at the molar ratio of 1:2. (3): an aqueous solution of dimethylzinc, diethylenetriamine and D-fructose at the molar ratio of 1:1:1. (4): an aqueous solution of dimethylzinc, diethylenetriamine and D-fructose at the molar ratio of 2:2:1. Product species assigned are **29a** (▲) and **29b** (▼). Free D-fructose forms assigned are the α-pyranose form (○), the β-pyranose form (△), the α-furanose form (□) and the β-furanose form (▽).

The product solution from the reaction of dimethylzinc with diethylenetriamine and D-fructose in the molar ratio 1:1:1 contained two species, namely the β-furanose form **29b** (66%) and the β-pyranose form **29a** (34%). Reducing the concentration of D-fructose in solution led to a different result, since in the ^{13}C NMR spectrum of the 2:2:1 experiment only signals for **29b** were observed. The ^{13}C NMR spectra of both experiments are shown in Figure 2.54. Table 2.39 summarises the corresponding ^{13}C NMR chemical shifts obtained from the spectra of both experiments. The enrichment of the β-furanose form was expected since the sugar core of D-fructose is very similar to the one of D-arabinose and, as seen in Chapter 2.3.3.2, the main species in product solutions of D-arabinose with the Zn^{II}(dien) fragment was also the β-furanose species. The products **29a** and **29b** are illustrated in Figure 2.55. They were thought to be the complexes [Zn(dien)(β-D-Fru*p*2,3H$_{-2}$-κ^2*O*^{2,3})] and [Zn(dien)(β-D-Fru*f*2,3H$_{-2}$-κ^2*O*^{2,3})], respectively. Due to the absence of coordination-induced shifts, the chelation sites were only assumed.

Table 2.39 ^{13}C NMR chemical shifts of the product complexes **29a** and **29b** from the reactions of dimethylzinc and diethylenetriamine with D-fructose (molar ratios 1:1:1 and 2:2:1). $\Delta\delta$ is the shift difference of the product complex and the free D-fructose form at neutral pH.

	isomer	molar ratio		C1	C2	C3	C4	C5	C6
free	β-D-Fru*p*		δ	64.5	98.7	68.2	70.3	69.8	64.0
29a	β-D-Fru*p*	1:1:1	δ	65.3	100.1	68.9	70.9	70.2	63.4
			$\Delta\delta$	0.8	1.4	0.7	0.6	0.4	−0.6
free	β-D-Fru*f*		δ	63.3	102.1	76.0	75.1	81.3	63.0
29b	β-D-Fru*f*	1:1:1	δ	65.8	106.2	77.8	78.4	80.7	62.2
			$\Delta\delta$	1.5	4.1	1.8	3.3	−0.6	−0.8
29b	β-D-Fru*f*	2:2:1	δ	66.3	106.8	78.5	79.1	80.8	62.3
			$\Delta\delta$	3.0	4.7	2.5	4.0	−0.5	−0.7

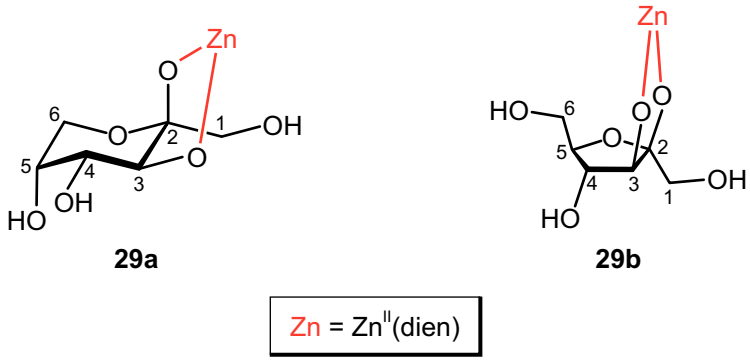

Figure 2.55 Products assumed from the reaction of dimethylzinc and diethylenetriamine with D-fructose.

A ^{13}C NMR spectrum of an alkaline solution of D-fructose is given in Figure 2.54. It verified that the shifts of the product complexes were not only caused by the change of pH. Moreover, the ratio of the free forms in this solution was nearly the same as in the educt solution at neutral pH.

Table 2.40 Coupling constants (*J*/Hz) of the D-fructose part of product complexes **29a** and **29b** in D_2O.

	$^2J_{1a,1b}$	$^3J_{3,4}$	$^3J_{4,5}$	$^3J_{5,6a}$	$^3J_{5,6b}$	$^2J_{6a,6b}$
29a	–	9.9	3.5	–	–	–
29b	−11.5	6.9	–	3.5	2.0	−12.2

Several coupling constants of **29a** and **29b** were determined and are listed in Table 2.40. All of them lay in the expected range.

2.3.4 Coordination of sugar phosphates

As described in the last chapters, it was possible to gain valuable insights from the NMR analysis of complexes of polyols, methylated sugars and reducing sugars with the Zn^{II}(dien) fragment. This knowledge was used afterwards to interpret the NMR spectra of product solutions from experiments with sugar phosphates. Since the experiments with Pd-tmen in Chapter 2.2 showed that the coordination of sugar phosphates to Pd^{II}(tmen) occurs at almost the whole pH range, it was assumed that this is also the case for the Zn^{II}(dien) fragment. Thus, the reactions of sugar phosphates with Zn^{II}(dien) were conducted at various pH values. Unfortunately, the experiments at neutral and acid pH ranges were not successful, as described in more detail in the following chapter.

2.3.4.1 D-Fructose 1-phosphate

The first sugar phosphate investigated was D-fructose 1-phosphate. The analogy to D-fructose that was treated in the last chapter is obvious. The only difference between both molecules is the phosphorylation at O1. Aqueous solutions of D-fructose 1-phosphate contain the β-pyranose form (86%) and the β-furanose form (14%).

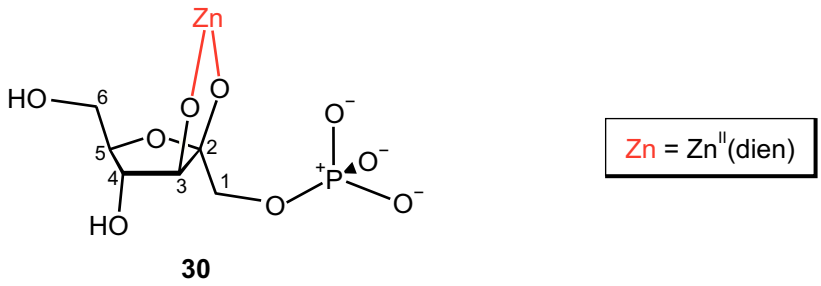

30

Figure 2.56 Product assumed from the reaction of zinc nitrate hexahydrate, sodium hydroxide and diethylenetriamine with D-fructose 1-phosphate.

The reaction of zinc nitrate hexahydrate and sodium hydroxide with diethylenetriamine and D-fructose 1-phosphate in the molar ratio 2:4:2:1 resulted only in the β-furanose form $[Zn(dien)(\beta\text{-D-Fru}f1P2,3H_{-2}\text{-}\kappa^2O^{2,3})]^{2-}$ (**30**), which is shown in Figure 2.56. The enrichment of this species was consistent with that of the experiments with D-fructose. Unfortunately, it was impossible to analyse the NMR spectra of the 1:2:1:1 experiment due to a very poor signal-to-noise ratio. Thus, the probable formation of the β-pyranose product species $[Zn(dien)(\beta\text{-D-Fru}p1P2,3H_{-2}\text{-}\kappa^2O^{2,3})]^{2-}$ could not be confirmed. The ^{13}C NMR chemical shifts of **30** are given in Table 2.41. Figure 2.57 shows the corresponding spectrum.

Table 2.41 ^{13}C NMR chemical shifts of the product complex **30** from the reaction of zinc nitrate hexahydrate, sodium hydroxide and diethylenetriamine with D-fructose 1-phosphate (molar ratio 2:4:2:1). $\Delta\delta$ is the shift difference of the product complex and the free D-fructose-1-phosphate form at neutral pH.

	isomer	molar ratio		C1	C2	C3	C4	C5	C6
free	β-D-Fru*f*1*P*		δ	66.5	101.6	76.6	74.7	81.2	63.0
30	β-D-Fru*f*1*P*	2:4:2:1	δ	69.3	105.8	79.4	79.0	80.0	62.1
			$\Delta\delta$	2.8	4.2	2.8	4.3	−1.2	−0.9

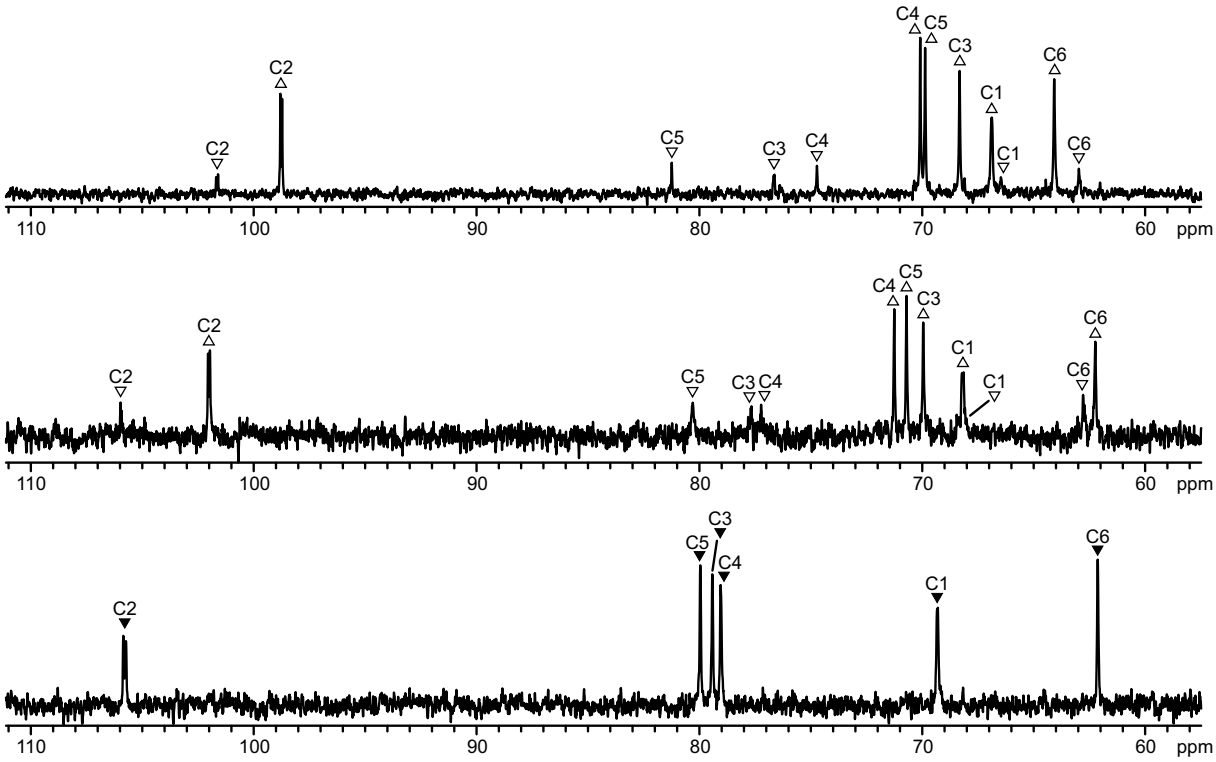

Figure 2.57 ^{13}C NMR spectra; (top): an aqueous solution of D-fructose 1-phosphate. (center): an aqueous solution of D-fructose 1-phosphate and sodium hydroxide at the molar ratio of 1:2. (bottom): an aqueous solution of zinc nitrate hexahydrate, sodium hydroxide, diethylenetriamine and D-fructose 1-phosphate at the molar ratio of 2:4:2:1. The only product species assigned is **30** (▼). Free D-fructose-1-phosphate forms assigned are the β-pyranose form (△) and the β-furanose form (▽). Note the split C1 and C2 signals as a result of ^{31}P–^{13}C coupling.

As with the experiments with reducing sugars, a ^{13}C NMR spectrum of an alkaline solution of D-fructose 1-phosphate was measured additionally to check the influence of the pH. The spectrum is shown in Figure 2.57. It is clearly verified that the shifts of the product complex were not only caused by the change of pH. Furthermore, no change of the ratio of the free forms was achieved by changing only the pH.

Some coupling constants of **30** were determined and are listed in Table 2.42. All of them lay in the expected range.

Table 2.42 Coupling constants (*J*/Hz) of the D-fructose-1-phosphate part of product complex **30** in D_2O.

	$^3J_{1a,P}$	$^3J_{1b,P}$	$^2J_{1a,1b}$	$^3J_{3,4}$	$^3J_{4,5}$	$^3J_{5,6a}$	$^3J_{5,6b}$	$^2J_{6a,6b}$
30	–	–	–	6.9	7.4	–	2.3	–12.8

The experiments in Chapter 2.2.5 showed that D-fructose 1-phosphate was able to coordinate to the Pd^{II}(tmen) fragment at neutral pH values. Hence, it was assumed that a coordination to the Zn^{II}(dien) fragment is also possible at the neutral pH range. Figure 2.58 shows two ^{13}C NMR spectra, namely the educt spectrum of D-fructose 1-phosphate at neutral pH and the spectrum of the solution from the reaction of zinc nitrate hexahydrate, sodium hydroxide and diethylenetriamine with D-fructose 1-phosphate which was set to pH 8 by adding stoichiometric amounts of nitric acid. It is clearly visible that there were no significant shift differences of the ^{13}C NMR signals. Furthermore, no change of the ratio between β-pyranose form and β-furanose form was observed, which verified that no reaction took place. As a result, D-fructose 1-phosphate was able to coordinate to Zn^{II}(dien) only at alkaline pH values but not at the neutral pH range, which was a clear difference to the experiments with Pd-tmen. Fructose 1-phosphate probably coordinated to the Zn^{II}(dien) fragment *via* the phosphate group at acidic pH values, but unfortunately, it was not possible to verify this *via* ^{31}P NMR spectroscopy since no significant CIS values were observed. It should be mentioned that these results were obtained in the experiments with all further sugar phosphates as well. Thus, only the experiments at alkaline pH values are presented in the following chapters.

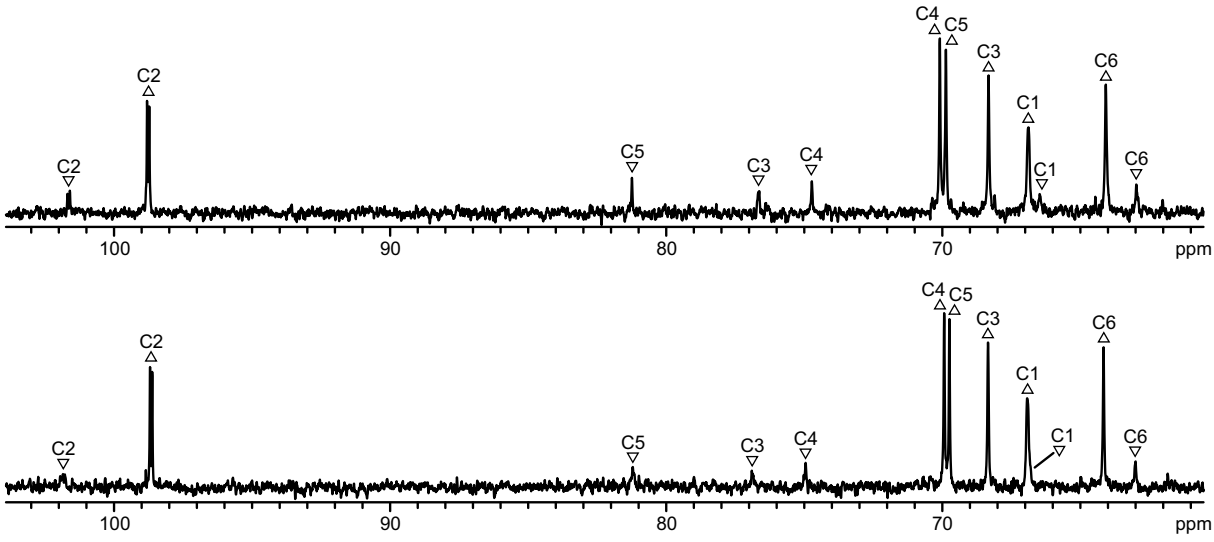

Figure 2.58 ^{13}C NMR spectra; (top): an aqueous solution of D-fructose 1-phosphate. (bottom): an aqueous solution of zinc nitrate hexahydrate, sodium hydroxide, diethylenetriamine, D-fructose 1-phosphate and nitric acid at the molar ratio of 2:4:2:1:2.5 (pH 8). Free D-fructose-1-phosphate forms assigned are the β-pyranose form (△) and the β-furanose form (▽). Note the split C1 and C2 signals as a result of ^{31}P–^{13}C coupling.

2.3.4.2 D-Fructose 6-phosphate

Compared with D-fructose 1-phosphate, D-fructose 6-phosphate is phosphorylated at the hydroxy function of C6 instead of C1. Hence, the pyranose forms are not accessible. Aqueous solutions of D-fructose 6-phosphate contain the β-furanose form (82%) beside the α-furanose form (16%) and the open-chain keto form in a low concentration.[89]

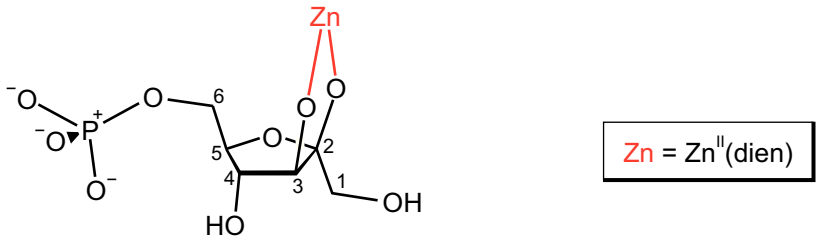

31

Figure 2.59 Product assumed from the reaction of zinc nitrate hexahydrate, sodium hydroxide and diethylenetriamine with D-fructose 6-phosphate.

The product solutions from the reactions of zinc nitrate hexahydrate, sodium hydroxide and diethylenetriamine with D-fructose 6-phosphate in the molar ratios 1:2:1:1 and 2:4:2:1 both resulted in only one product species, namely the β-furanose form [Zn(dien)(β-D-Fru*f*6*P*2,3H$_{-2}$-κ^2*O*^{2,3})]$^{2-}$ (**31**), which is shown in Figure 2.59. The high concentration of this species was expected as the results were consistent with those obtained in experiments with D-fructose and D-fructose 1-phosphate. The ^{13}C NMR chemical shifts of **31** are listed in Table 2.43. Figure 2.60 shows the ^{13}C NMR spectrum.

Table 2.43 ^{13}C NMR chemical shifts of the product complex **31** from the reactions of zinc nitrate hexahydrate, sodium hydroxide and diethylenetriamine with D-fructose 6-phosphate (molar ratios 1:2:1:1 and 2:4:2:1). Δδ is the shift difference of the product complex and the free D-fructose-6-phosphate form at neutral pH.

	isomer	molar ratio		C1	C2	C3	C4	C5	C6
free	β-D-Fru*f*6*P*		δ	63.1	102.2	75.6	74.8	80.6	64.9
31	β-D-Fru*f*6*P*	1:2:1:1	δ	66.5	106.3	77.0	78.5	78.5	65.3
			Δδ	3.4	4.1	1.4	3.7	−2.1	0.4
31	β-D-Fru*f*6*P*	2:4:2:1	δ	66.7	106.6	77.2	78.8	78.5	65.4
			Δδ	3.6	4.4	1.6	4.0	−2.1	0.5

An additional ^{13}C NMR spectrum of an alkaline solution of D-fructose 6-phosphate that is shown in Figure 2.60 verified that the shifts of the product complex were not caused only by the change of pH.

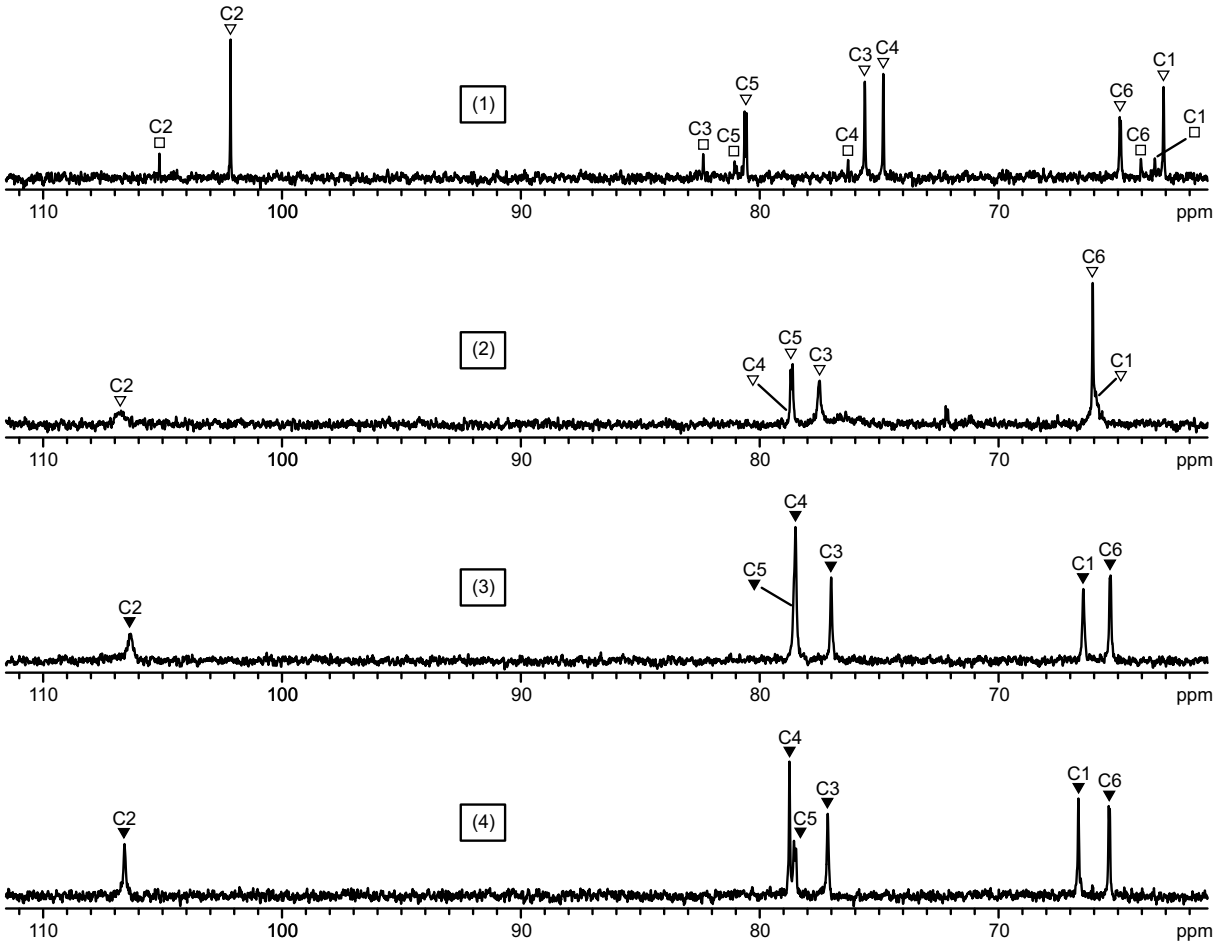

Figure 2.60 ^{13}C NMR spectra; (1): an aqueous solution of D-fructose 6-phosphate. (2): an aqueous solution of D-fructose 6-phosphate and sodium hydroxide at the molar ratio of 1:2. (3): an aqueous solution of zinc nitrate hexahydrate, sodium hydroxide, diethylenetriamine and D-fructose 6-phosphate at the molar ratio of 1:2:1:1. (4): an aqueous solution of zinc nitrate hexahydrate, sodium hydroxide, diethylenetriamine and D-fructose 6-phosphate at the molar ratio of 2:4:2:1. The only product species assigned is **31** (▼). Free D-fructose-6-phosphate forms assigned are the α-furanose form (□) and the β-furanose form (▽). Note the split C5 and C6 signals as a result of ^{31}P–^{13}C coupling.

Table 2.44 lists several coupling constants determined for **31**. All of them lay in the expected range.

Table 2.44 Coupling constants (*J*/Hz) of the D-fructose-6-phosphate part of product complex **31** in D_2O.

	$^2J_{1a,1b}$	$^3J_{3,4}$	$^3J_{4,5}$	$^3J_{5,6a}$	$^3J_{5,6b}$	$^3J_{6a,P}$	$^3J_{6b,P}$	$^2J_{6a,6b}$
31	−11.5	6.8	–	5.7	2.5	5.2	5.0	−11.5

2.3.4.3 D-Fructose 1,6-bisphosphate

In comparison to the two previous sugar phosphates investigated, D-fructose 1-phosphate and D-fructose 6-phosphate, D-fructose 1,6-bisphosphate is phosphorylated at the hydroxy functions of both C1 and C6. However, since the formation of pyranose forms is impossible due to the blocked 6-position, it is more similar to D-fructose 6-phosphate. Aqueous solutions of D-fructose 1,6-bisphosphate contain the β-furanose form (86%) beside the α-furanose form (13%) and only traces of the open-chain keto form.

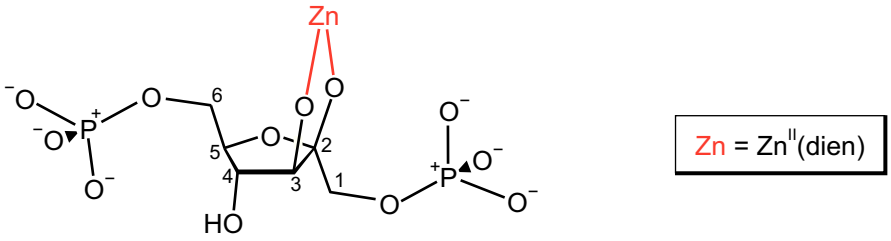

32

Figure 2.61 Product assumed from the reaction of zinc nitrate hexahydrate, sodium hydroxide and diethylenetriamine with D-fructose 1,6-bisphosphate.

The reactions of zinc nitrate hexahydrate, sodium hydroxide and diethylenetriamine with D-fructose 1,6-bisphosphate in the molar ratios of 1:2:1:1 and 2:4:2:1 both resulted only in one product species: the β-furanose form $[Zn(dien)(\beta\text{-D-Fru}f1,6P_2 2,3H_{-2}\text{-}\kappa^2O^{2,3})]^{4-}$ (**32**). Its structure is shown in Figure 2.61. This result was consistent with the experiments with D-fructose, D-fructose 1-phosphate and D-fructose 6-phosphate. Table 2.45 summarises the ^{13}C NMR chemical shifts of **32**. The corresponding ^{13}C NMR spectrum is shown in Figure 2.62.

Table 2.45 ^{13}C NMR chemical shifts of the product complex **32** from the reactions of zinc nitrate hexahydrate, sodium hydroxide and diethylenetriamine with D-fructose 1,6-bisphosphate (molar ratios 1:2:1:1 and 2:4:2:1). $\Delta\delta$ is the shift difference of the product complex and the free D-fructose-1,6-bisphosphate form at neutral pH.

	isomer	molar ratio		C1	C2	C3	C4	C5	C6
free	β-D-Fru*f*1,6P_2		δ	66.0	101.5	76.0	74.5	80.1	65.4
32	β-D-Fru*f*1,6P_2	1:2:1:1	δ	69.7	105.8	78.3	78.7	78.0	65.4
			$\Delta\delta$	3.7	4.3	2.3	4.2	−1.9	0.0
32	β-D-Fru*f*1,6P_2	2:4:2:1	δ	69.9	105.8	78.5	78.9	78.0	65.3
			$\Delta\delta$	3.9	4.3	2.5	4.4	−1.9	−0.1

An additional ^{13}C NMR spectrum of an alkaline solution of D-fructose 1,6-bisphosphate was measured and is illustrated in Figure 2.62. It confirmed that the shifts of the product complex were not caused only by the change of pH.

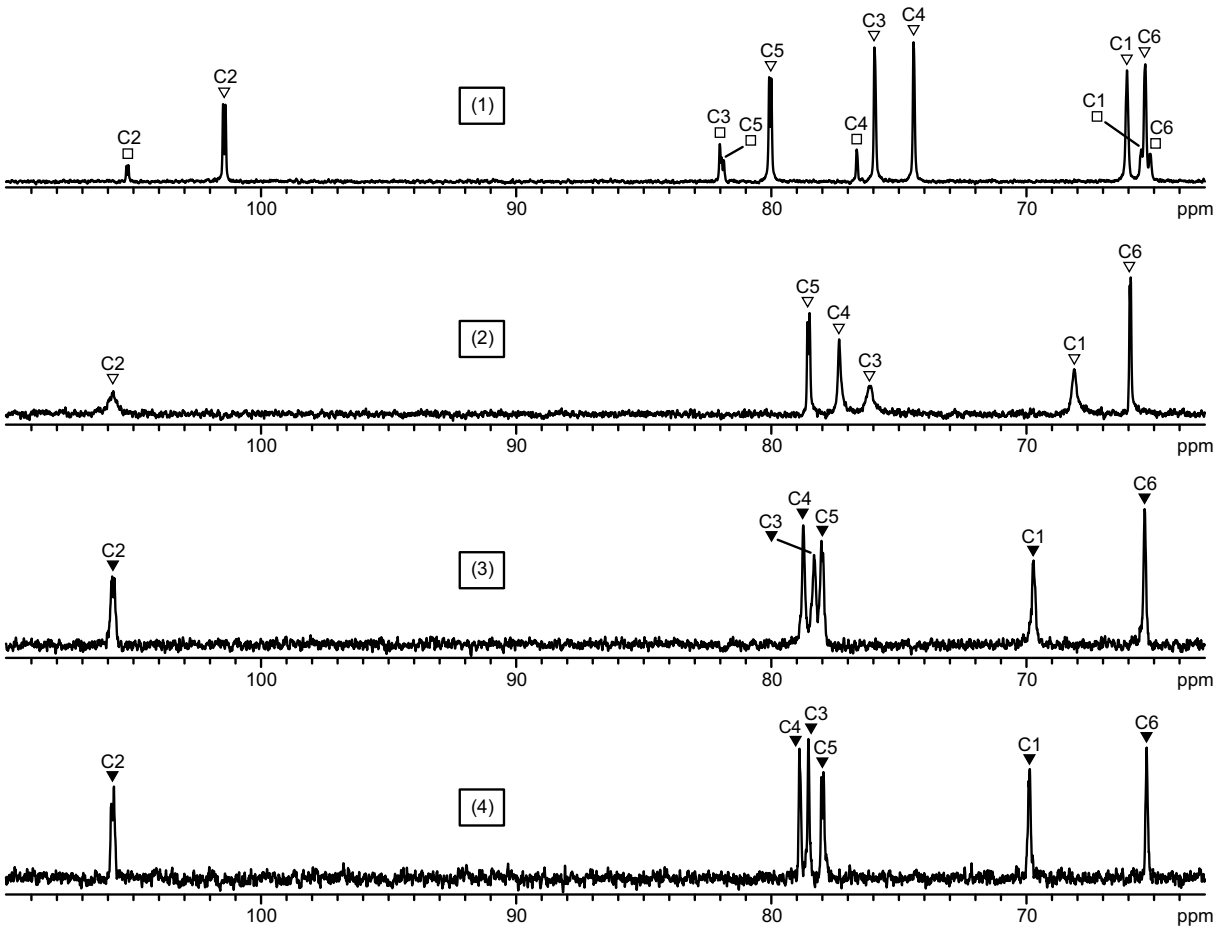

Figure 2.62 ^{13}C NMR spectra; (1): an aqueous solution of D-fructose 1,6-bisphosphate. (2): an aqueous solution of D-fructose 1,6-bisphosphate and sodium hydroxide at the molar ratio of 1:2. (3): an aqueous solution of zinc nitrate hexahydrate, sodium hydroxide, diethylenetriamine and D-fructose 1,6-bisphosphate at the molar ratio of 1:2:1:1. (4): an aqueous solution of zinc nitrate hexahydrate, sodium hydroxide, diethylenetriamine and D-fructose 1,6-bisphosphate at the molar ratio of 2:4:2:1. The only product species assigned is **32**. Free D-fructose-1,6-bisphosphate forms assigned are the α-furanose form (□) and the β-furanose form (▽). Note the split C1, C2, C5 and C6 signals as a result of ^{31}P–^{13}C coupling.

Table 2.46 lists several coupling constants of **32** which were determined from the NMR spectra of the product solutions. All of them lay in the expected range.

Table 2.46 Coupling constants (*J*/Hz) of the D-fructose-1,6-bisphosphate part of product complex **32** in D_2O.

	$^2J_{1a,1b}$	$^3J_{1a,P1}$	$^3J_{1b,P1}$	$^3J_{3,4}$	$^3J_{4,5}$	$^3J_{5,6a}$	$^3J_{5,6b}$	$^3J_{6a,P6}$	$^3J_{6b,P6}$	$^2J_{6a,6b}$
32	–	–	–	7.4	8.9	1.2	4.1	4.8	4.2	−10.5

2.3.4.4 D-Mannose 6-phosphate

Aqueous solutions of D-mannose 6-phosphate contain only the α-pyranose form (71%) and the β-pyranose form (29%) although the furanose forms are accessible.

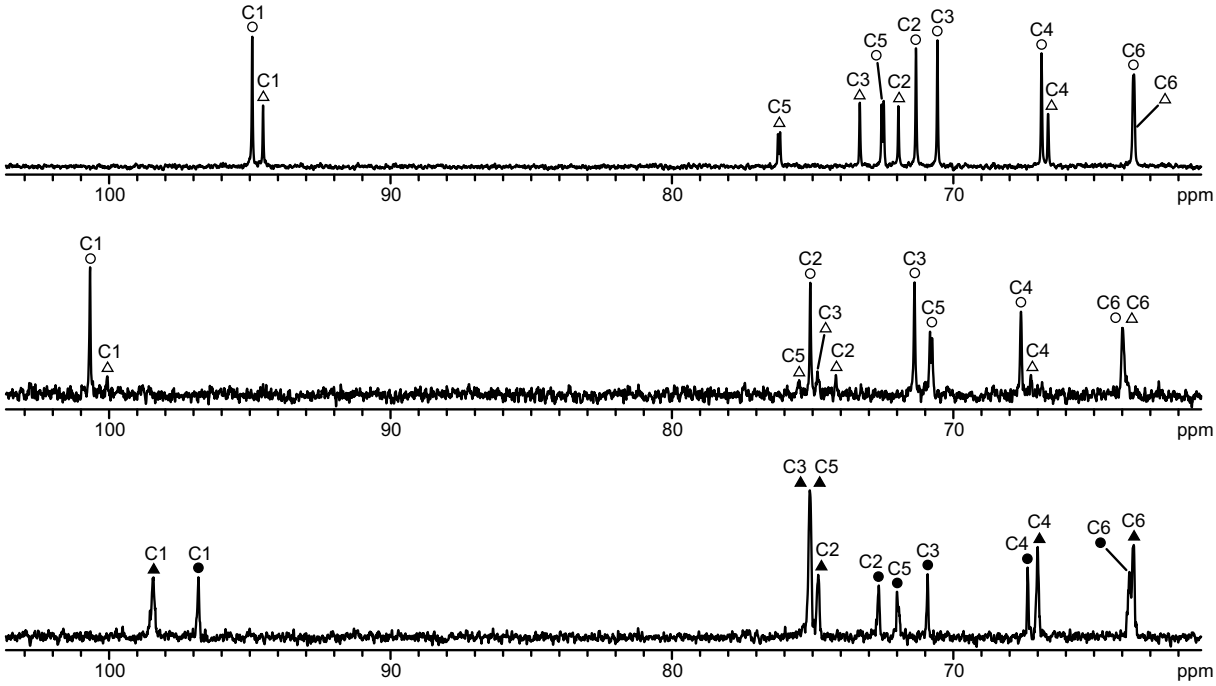

Figure 2.63 ^{13}C NMR spectra; (top): an aqueous solution of D-mannose 6-phosphate. (center): an aqueous solution of D-mannose 6-phosphate and sodium hydroxide at the molar ratio of 1:2. (bottom): an aqueous solution of zinc nitrate hexahydrate, sodium hydroxide, diethylenetriamine and D-mannose 6-phosphate at the molar ratio of 2:4:2:1. Product species assigned are **33a** (●) and **33b** (▲). Free D-mannose-6-phosphate forms assigned are the α-pyranose form (○) and the β-pyranose form (△). Note the split C5 and C6 signals as a result of ^{31}P–^{13}C coupling.

The product solution from the reaction of zinc nitrate hexahydrate, sodium hydroxide and diethylenetriamine with D-mannose 6-phosphate in the molar ratio 2:4:2:1 contained two product species. The main species was the β-pyranose form **33b** (64%) and the minor species was the α-pyranose form **33a** (36%). No signals of furanose species were observed. The ^{13}C NMR spectrum is shown in Figure 2.63. Table 2.47 lists the corresponding ^{13}C NMR chemical shifts. Unfortunately, it was impossible to analyse the NMR spectra of the 1:2:1:1 experiment of zinc nitrate hexahydrate, sodium hydroxide and diethylenetriamine with D-mannose 6-phosphate due to a very poor signal-to-noise ratio.

The NMR spectra obtained were very similar to these from the experiments with D-mannose. According to those results, the β-pyranose form **33b** was assumed to be the $\kappa^2O^{1,2}$ chelate $[Zn(dien)(\beta\text{-D-Man}p6P1,2H_{-2}\text{-}\kappa^2O^{1,2})]^{2-}$ while the α-pyranose form **33a** was thought to be the

$\kappa^2O^{2,3}$ chelate [Zn(dien)(α-D-Man*p*6*P*2,3H$_{-2}$-κ$O^{2,3}$)]$^{2-}$. The structures of the products are shown in Figure 2.64.

Table 2.47 ^{13}C NMR chemical shifts of the product complexes **33a** and **33b** from the reaction of zinc nitrate hexahydrate, sodium hydroxide and diethylenetriamine with D-mannose 6-phosphate (molar ratio 2:4:2:1). Δδ is the shift difference of the product complex and the free D-mannose-6-phosphate form at neutral pH.

	isomer	molar ratio		C1	C2	C3	C4	C5	C6
free	α-D-Man*p*6*P*		δ	94.7	71.3	70.8	67.5	73.0	61.6
33a	α-D-Man*p*6*P*	2:4:2:1	δ	96.8	72.6	70.9	67.4	72.0	63.7
			Δδ	5.0	1.0	1.2	1.6	2.1	0.6
free	β-D-Man*p*6*P*		δ	94.3	71.8	73.7	67.2	76.8	61.6
33b	β-D-Man*p*6*P*	2:4:2:1	δ	98.4	74.8	75.1	67.0	75.1	63.6
			Δδ	5.4	4.0	3.2	1.1	−1.0	0.4

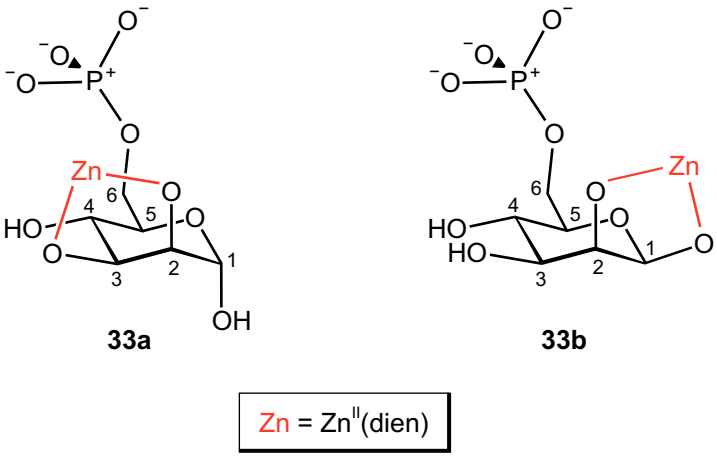

Figure 2.64 Products assumed from the reaction of zinc nitrate hexahydrate, sodium hydroxide and diethylenetriamine with D-mannose 6-phosphate.

A ^{13}C NMR spectrum of an alkaline solution of D-mannose 6-phosphate is illustrated in Figure 2.63 and verifies that the shifts of the product complexes were not caused only by the change of pH. Furthermore, the ratio of the free forms did not change significantly by simply setting the pH to alkaline values.

Table 2.48 Coupling constants (*J*/Hz) of the D-mannose-6-phosphate part of product complexes **33a** and **33b** in D_2O.

	$^3J_{1,2}$	$^3J_{2,3}$	$^3J_{3,4}$	$^3J_{4,5}$	$^3J_{5,6a}$	$^3J_{5,6b}$	$^3J_{6a,P}$	$^3J_{6b,P}$	$^2J_{6a,6b}$
33a	–	–	7.9	9.4	–	–	–	–	–
33b	–	3.4	10.0	10.0	–	–	–	–	–

A few coupling constants determined for **33a** and **33b** are listed in Table 2.48. All of them lay in the expected range.

2.3.4.5 D-Glucose 6-phosphate

D-Glucose 6-phosphate is similar to D-mannose 6-phosphate since the only difference is the orientation of the hydroxy function of C2. In aqueous solutions of D-glucose 6-phosphate, the β-pyranose form (63%) is the main species followed by the α-pyranose form (36%). Furanose forms are accessible but are not observed *via* NMR spectroscopy.

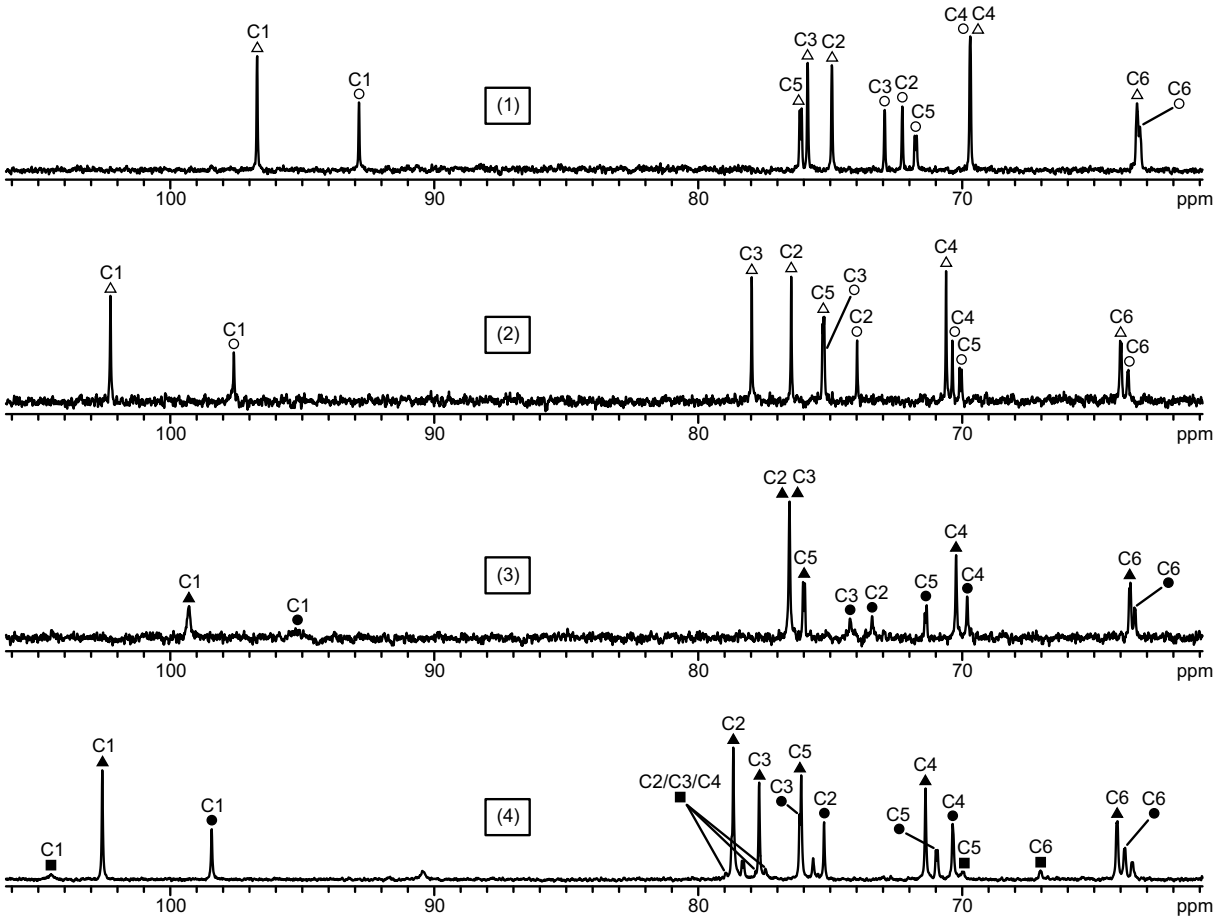

Figure 2.65 ^{13}C NMR spectra; (1): an aqueous solution of D-glucose 6-phosphate. (2): an aqueous solution of D-glucose 6-phosphate and sodium hydroxide at the molar ratio of 1:2. (3): an aqueous solution of zinc nitrate hexahydrate, sodium hydroxide, diethylenetriamine and D-glucose 6-phosphate at the molar ratio of 1:2:1:1. (4): an aqueous solution of zinc nitrate hexahydrate, sodium hydroxide, diethylenetriamine and D-glucose 6-phosphate at the molar ratio of 2:4:2:1. Product species assigned are **34a** (●), **34b** (▲) and **34c** (■). Free D-glucose-6-phosphate forms assigned are the α-pyranose form (○) and the β-pyranose form (△). Note the split C5 and C6 signals as a result of ^{31}P–^{13}C coupling.

The reaction of zinc nitrate hexahydrate, sodium hydroxide and diethylenetriamine with D-glucose 6-phosphate in the molar ratio 1:2:1:1 led to two product species, namely the β-pyranose form **34b** (67%) and the α-pyranose form **34a** (33%). Different results were obtained from the spectra of the 2:4:2:1 experiment. Here, the α-furanose species **34c** (7%) was additionally observed beside **34a** (30%) and **34b** (63%). Table 2.49 lists the ^{13}C NMR chemical shifts of all three products. The corresponding ^{13}C NMR spectra are shown in Figure 2.65. It should be mentioned that there were signals of a further species in the ^{13}C NMR spectrum of the 2:4:2:1 experiment. However, these signals belonged only to an N-glycosidic by-product. The formation of these by-products has already been described in Chapter 2.3.3.7.

Table 2.49 ^{13}C NMR chemical shifts of the product complexes **34a**, **34b** and **34c** from the reactions of zinc nitrate hexahydrate, sodium hydroxide and diethylenetriamine with D-glucose 6-phosphate (molar ratios 1:2:1:1 and 2:4:2:1). $\Delta\delta$ is the shift difference of the product complex and the free D-glucose-6-phosphate form at neutral pH. Since appropriate values were not available for the α-furanose form, the chemical shifts of α-glucofuranose (C1) and methyl α-D-glucofuranoside (C2–C6) were used instead.[87–88]

	isomer	molar ratio		C1	C2	C3	C4	C5	C6
free	α-D-Glc*p*6*P*		δ	92.9	72.3	72.9	69.7	71.8	63.3
34a	α-D-Glc*p*6*P*	1:2:1:1	δ	95.3	73.4	74.2	69.8	71.4	63.5
			$\Delta\delta$	2.4	1.1	1.3	0.1	–0.4	0.2
34a	α-D-Glc*p*6*P*	2:4:2:1	δ	98.5	75.2	76.1	70.2	71.1	63.7
			$\Delta\delta$	5.6	2.9	3.2	0.5	–0.7	0.4
free	β-D-Glc*p*6*P*		δ	96.7	74.9	75.9	69.7	76.1	63.4
34b	β-D-Glc*p*6*P*	1:2:1:1	δ	99.3	76.5	76.5	70.2	76.0	63.6
			$\Delta\delta$	2.6	1.6	0.6	0.5	–0.1	0.2
34b	β-D-Glc*p*6*P*	2:4:2:1	δ	102.6	78.7	77.7	71.4	76.1	64.1
			$\Delta\delta$	5.9	3.8	1.8	1.7	0.0	0.7
free	α-D-Glc*f*6*P*		δ	(97.4)	(78.2)	(77.1)	(79.3)	(71.2)	(64.7)
34c	α-D-Glc*f*6*P*	2:4:2:1	δ	104.5	77.5 / 77.9 / 79.0			70.0	67.1
			$\Delta\delta$	7.1	–	–	–	(–1.2)	2.4

The results obtained were consistent with the results from the experiments of D-glucose. According to those, the β-pyranose form **34b** was assumed to be the $\kappa^2O^{1,2}$ chelate [Zn(dien)(β-D-Glc*p*6*P*1,2H$_{-2}$-$\kappa^2O^{1,2}$)]$^{2-}$. The species **34a** and **34c** were thought to be the complex anions [Zn(dien)(α-D-Glc*p*6*P*1,2H$_{-2}$-$\kappa^2O^{1,2}$)]$^{2-}$ and [Zn(dien)(α-D-Glc*f*6*P*1,2H$_{-2}$-$\kappa^2O^{1,2}$)]$^{2-}$, respectively. The products are shown in Figure 2.66.

Figure 2.65 gives a ^{13}C NMR spectrum of an alkaline solution of D-glucose 6-phosphate. It is clearly visible that the shifts of the product complexes were not caused only by the change of pH. Moreover, the ratio of the free forms did not change significantly.

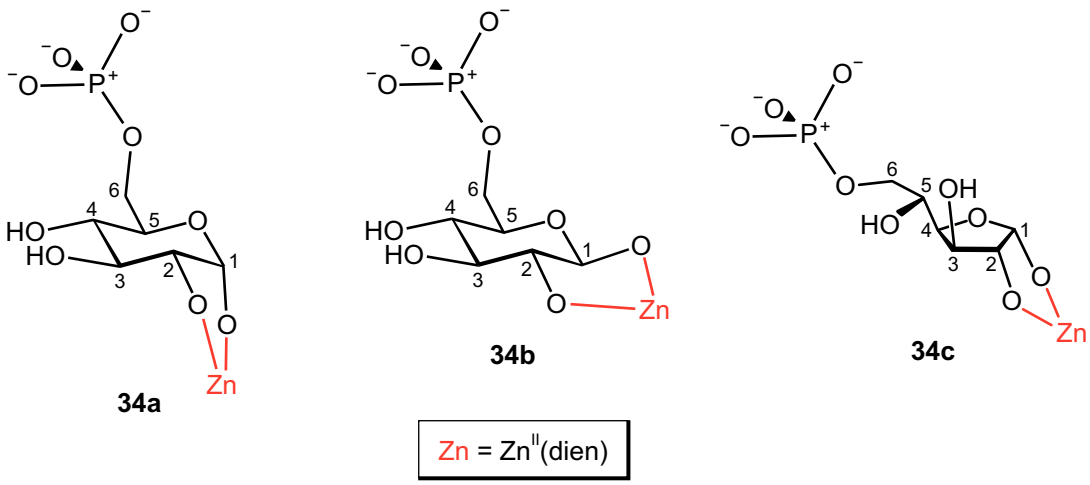

Figure 2.66 Products assumed from the reaction of zinc nitrate hexahydrate, sodium hydroxide and diethylenetriamine with D-glucose 6-phosphate.

A few coupling constants of **34a** and **34b** were determined and are listed in Table 2.50. They confirmed the species assignment.

Table 2.50 Coupling constants (*J*/Hz) of the D-glucose-6-phosphate part of product complexes **34a** and **34b** in D_2O.

	$^3J_{1,2}$	$^3J_{2,3}$	$^3J_{3,4}$	$^3J_{4,5}$	$^3J_{5,6a}$	$^3J_{5,6b}$	$^3J_{6a,P}$	$^3J_{6b,P}$	$^2J_{6a,6b}$
34a	3.5	–	–	–	–	–	–	–	–
34b	7.7	9.0	–	–	–	–	–	–	–

Compared to the experiments with D-glucose 6-phoshpate and Pd-tmen (Chapter 2.2.3), the results obtained were very surprising since, there, the α-pyranose product forms had a higher concentration than the β-pyranose forms. However, the final equilibrium was achieved only after stirring for almost 24 hours. Hence, the reaction of zinc nitrate hexahydrate, sodium hydroxide and diethylenetriamine with D-glucose 6-phosphate was repeated with a reaction time of 24 hours. Unfortunately, the analysis of the corresponding ^{13}C NMR spectrum was impossible due to a very poor signal-to-noise ratio as was also the case in the experiments of D-glucose with the Zn^{II}(dien) fragment.

2.3.4.6 α-D-Glucose 1-phosphate

Compared to glucose 6-phosphate, α-D-glucose 1-phosphate is phosphorylated at the hydroxy function of C1 instead of C6. Thus, it is configurationally restricted to the α-pyranose form.

The product solution from the reaction of dimethylzinc, diethylenetriamine and α-D-glucose 1-phosphate in the molar ratio 2:2:1 contained only the product species $[Zn(dien)(\alpha\text{-D-Glc}p\text{H}_{-2}P1]^{2-}$ (**35**). Because of the absence of CIS values, it was impossible to assign the metal-binding site. Possible coordination patterns were the coordination through O2 and O3 or O3 and O4. These results were comparable with the ones obtained from the experiments with Me-α-D-glucopyranoside described in Chapter 2.3.2. The ^{13}C NMR spectrum measured is illustrated in Figure 2.67. Table 2.51 gives the corresponding ^{13}C NMR chemical shifts.

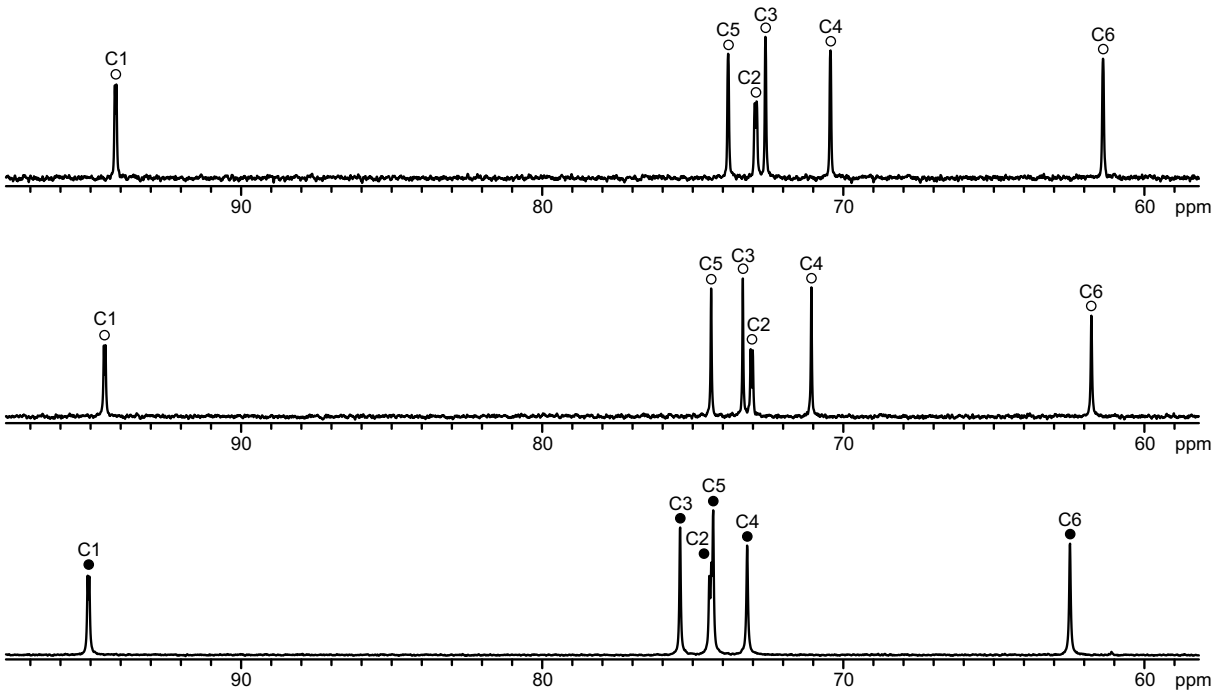

Figure 2.67 ^{13}C NMR spectra; (top): an aqueous solution of α-D-glucose 1-phosphate (○). (center): an aqueous solution of α-D-glucose 1-phosphate and sodium hydroxide at the molar ratio of 1:2. (bottom): an aqueous solution of dimethylzinc, diethylenetriamine and α-D-glucose 1-phosphate at the molar ratio of 2:2:1. The only product species assigned is **35** (●). Note the split C1 and C2 signals as a result of ^{31}P–^{13}C coupling.

Table 2.51 ^{13}C NMR chemical shifts of the product complex **35** from the reaction of dimethylzinc and diethylenetriamine with α-D-glucose 1-phosphate (molar ratio 2:2:1). $\Delta\delta$ is the shift difference of the product complex and the free α-D-glucose-1-phosphate form at neutral pH.

	isomer	molar ratio		C1	C2	C3	C4	C5	C6
free	α-D-Glc*p*1*P*		δ	94.2	72.9	72.6	70.4	73.8	61.4
35	α-D-Glc*p*1*P*	2:2:1	δ	95.1	74.3	75.4	73.2	74.4	62.5
			$\Delta\delta$	0.9	1.4	2.8	2.8	0.6	1.1

As with all the other experiments with sugar phosphates, an additional ^{13}C NMR spectrum of an alkaline solution of α-D-glucose 1-phosphate, which is shown in Figure 2.67, was

measured to check the influence of the pH. According to this spectrum it was verified that the shifts of the product complex were not caused only by the change of pH.

Table 2.52 Coupling constants (*J*/Hz) of the α-D-glucose-1-phosphate part of product complex **35** in D_2O compared to the values of the free α-D-glucose 1-phosphate that were obtained from a previous work[86].

	$^3J_{1,P}$	$^3J_{1,2}$	$^4J_{2,P}$	$^3J_{2,3}$	$^3J_{3,4}$	$^3J_{4,5}$	$^3J_{5,6a}$	$^3J_{5,6b}$	$^2J_{6a,6b}$
α-D-Glc*p*1*P*	7.4	3.5	1.8	9.8	9.7	10.1	5.3	2.3	−12.3
35	7.4	3.3	1.9	9.7	9.2	9.6	6.5	–	−12.2

Table 2.52 lists several coupling constants determined for **35**. All of them lay in the expected range.

2.3.4.7 *rac*-Glycerol 1-phosphate

rac-Glycerol 1-phosphate is a suitable model for sugar phosphates. Exhibiting one phosphate group and only two hydroxy functions it provides only few possible metal-binding sites.

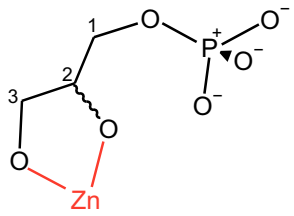

36

Zn = Zn^{II}(dien)

Figure 2.68 Product assumed from the reaction of zinc nitrate hexahydrate, sodium hydroxide and diethylenetriamine with *rac*-glycerol 1-phosphate.

The reaction of zinc nitrate hexahydrate, sodium hydroxide, diethylenetriamine and *rac*-glycerol 1-phosphate in the molar ratio of 2:4:2:1 led to only one product, namely the monometallated $[Zn(dien)(rac\text{-}Glyc1PH_{-2}\text{-}\kappa^2O^{2,3})]^{2-}$ ion (**36**) that is shown in Figure 2.68.

Table 2.53 ^{13}C NMR chemical shifts of the product complex **36** from the reaction of zinc nitrate hexahydrate, sodium hydroxide and diethylenetriamine with *rac*-glycerol 1-phosphate (molar ratio 2:4:2:1). $\Delta\delta$ is the shift difference of the product complex and the free *rac*-glycerol-1-phosphate form at neutral pH.

	isomer	molar ratio		C1	C3	C3
free	*rac*-Glyc1*P*		δ	65.3	72.0	62.9
36	*rac*-Glyc1*P*	2:4:2:1	δ	65.4	72.0	63.0
			$\Delta\delta$	0.1	0.0	0.1

Figure 2.69 shows the ^{13}C NMR spectrum of **36**. The ^{13}C NMR chemical shifts determined are listed in Table 2.53. There are almost no shift differences between signals of the free form and the ones of the product species. These results were consistent with the ones obtained from the experiments with polyols described in Chapter 2.3.1.

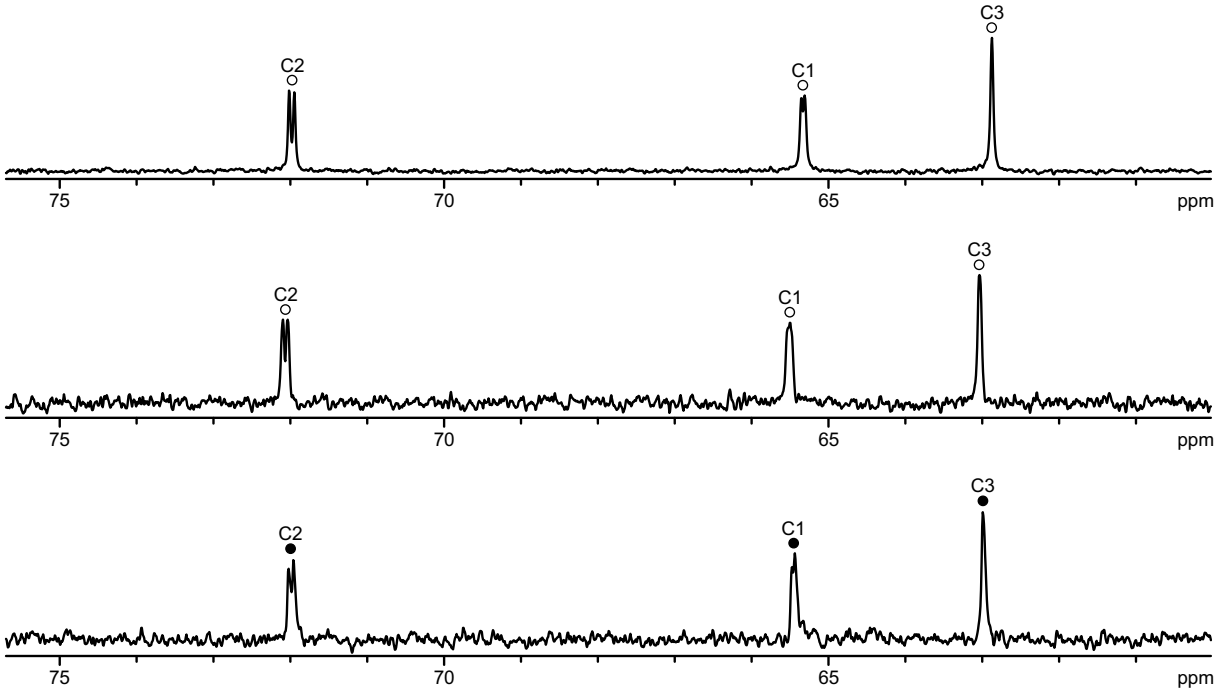

Figure 2.69 ^{13}C NMR spectra; (top): an aqueous solution of *rac*-glycerol 1-phosphate (○). (center): an aqueous solution of *rac*-glycerol 1-phosphate and sodium hydroxide at the molar ratio of 1:2. (bottom): an aqueous solution of zinc nitrate hexahydrate, sodium hydroxide, diethylenetriamine and *rac*-glycerol 1-phosphate at the molar ratio of 2:4:2:1. The only product species assigned is **36** (●). Note the split C1 and C2 signals as a result of ^{31}P–^{13}C coupling.

2.3.4.8 D-Ribose 5-phosphate

Several experiments with D-ribose 5-phosphate were conducted but, unfortunately, all of them resulted in NMR spectra with a very poor signal-to-noise ratio. Thus, an analysis of those spectra was impossible.

2.3.5 Preparation of crystalline compounds

The preparation of crystalline product complexes was not successful. Several reasons for this have already been described in the Introduction. The main problem was the formation of crystalline by-products such as zinc hydroxide or free sugar ligand that was observed after a

few days or weeks. Further observations led to the assumption that a special equilibrium has to be considered for the product solutions which is given in Figure 2.70. The formation of the $[Zn(dien)_2]^{2+}$ cation was undeniable since it crystallised in any product solution containing anions such as nitrate or chloride. A consecutive reaction of the equilibrium assumed that is also given in Figure 2.70 would explain the formation of zinc hydroxide and free sugar ligand.

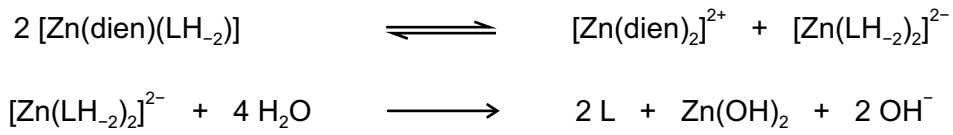

Figure 2.70 Side reactions resulting in zinc hydroxide and free sugar ligand (L).

These side reactions made it impossible to crystallise the desired product even in experiments with methylated sugars which are not so reactive as reducing sugars.

2.3.6 Experiments with further spectator ligands

Some of the experiments with the Zn^{II}(dien) fragment presented in Chapter 2.3.1–2.3.5 were conducted additionally using further spectator ligands. Beside diethylenetriamine, the ligands 1,4,7-triazacyclononane (tacn), 1,4,7-trimethyl-1,4,7-triazacylononane (Me_3-tacn), *N*,*N*,*N*′,*N*″,*N*″-pentamethyldiethylenetriamine (Me_5-dien), trispyrazolylborate (tpb) and trispyrazolylmethane (tpm) were used, among others. Unfortunately, these experiments always resulted in suspensions instead of clear solutions. The reasons for this were varied. The ligands tacn and Me_3-tacn were not suitable for the trigonal-bipyramidal coordination sphere of the product complexes. As far as the other ligands, their solubility in water was obviously insufficient.

3 Discussion

3.1 Coordination of sugar phosphates to $Re^{V}ON_2$ fragments

The use of bidentate spectator ligands N_2 such as ethane-1,2-diamine (en), *N*,*N*,*N'*,*N'*-tetramethylethane-1,2-diamine (tmen) or 1,10-phenanthroline (phen) in $Re^{V}O$ experiments led to $Re^{V}ON_2$ fragments that combined with sugar phosphates. Three positions remained for the coordination of a sugar phosphate to an $Re^{V}ON_2$ fragment. Moreover, there were only two possible binding patterns known from previous works[37, 42–43] that would allow a sugar phosphate to act as a tridentate ligand. They are both shown in Figure 3.1.

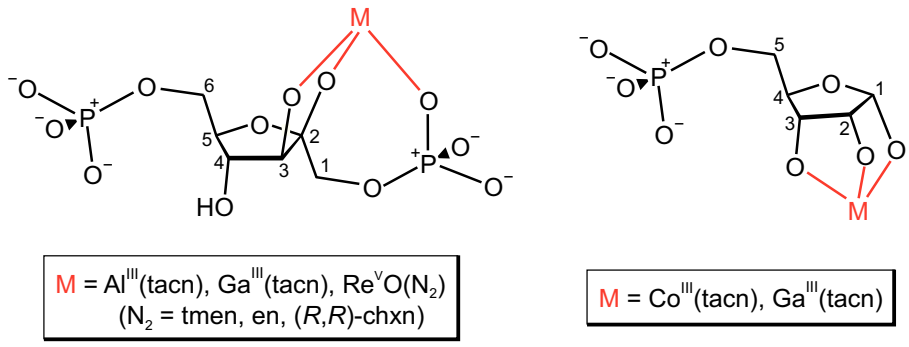

Figure 3.1 Possible tridentate binding patterns of sugar phosphates coordinating to various metal fragments.

The first possibility is the coordination *via* three hydroxy functions as it is realised in ribose-5-phosphate complexes of Co^{III}(tacn) and Ga^{III}(tacn).[37] The synthesis of complexes exhibiting this coordination pattern, however, was not possible by using $Re^{V}ON_2$ metal fragments. Reasons for this were only assumed. Since a rhenium(V) centre is significantly bigger than a cobalt(III) or gallium(III) centre, the possible bonding pattern provided by ribose 5-phosphate could have been too rigid to build a Re^{V} complex. In contrast, the bonding pattern of D-fructose 1,6-bisphosphate featuring two hydroxy functions and one phosphate group was obviously flexible enough to coordinate to the big rhenium(V) centre since it was possible to synthesise appropriate product complexes with the spectator ligands en, tmen, and (1*R*,2*R*)-cyclohexane-1,2-diamine ((*R*,*R*)-chxn). It was unexpected that a successful synthesis of complexes with D-fructose 1-phosphate could not be achieved since they would have featured the same bonding pattern as D-fructose-1,6-bisphosphate complexes. The reason was speculative. It was possible that the solubility in methanol of the barium salt of D-fructose 1-phosphate used was insufficient or that, perhaps, the accessibility of pyranose forms made a difference since, at least, the β-pyranose form is the main species in aqueous solutions of D-fructose 1-phosphate. However, experiments with the model glycerol 1-phosphate confirmed the results obtained with D-fructose 1,6-bisphosphate, as two crystal structures were obtained

with the spectator ligands tmen and phen. No crystal structures were available so far with tmen or phen coordinating to an $Re^{V}O$ centre. There were only crystal structures with en and 2,2'-bipyridine (bpy).[93–94] The Re–N distances in [ReO(OCH$_3$)(ox)(bpy)] (ox = oxalate) added up to 2.126 and 2.131 Å and, thus, lay in the same range as the values obtained for [ReO(phen)(*rac*-Glyc2,3H$_{-2}$1*P*H-κ^3*O*^{2,3,P})] (**2c**) that amounted to 2.129 and 2.158 Å. The Re–N distances 2.230 and 2.224 Å determined for [ReO(tmen)(*rac*-Glyc2,3H$_{-2}$1*P*H-κ^3*O*^{2,3,P})] (**2a**) were a bit longer, even when compared to the Re–N distances of [ReO$_2$en$_2$]Cl that were obtained from a previous work[94] and added up to 2.154 and 2.150 Å. However, the comparatively long Re–N distances of the product complexes with tmen were not unexpected since this tendency was also observed in appropriate palladium(II) complexes.[36] The two crystal structures obtained were the first ones exhibiting a phosphate group coordinating to an $Re^{V}O$ centre. In the only crystal structure available so far featuring a similar element, a diester of phosphoric acid coordinated to an $Re^{V}O$ centre.[95] Here, the Re–OP distance amounted to 1.988 Å and, thus, it was only a little shorter than the values determined for **2a** (2.067 Å) and **2c** (2.102 Å). Furthermore, the phosphate group was in *trans*-position to the oxido ligand in all three structures. All further Re–O bond lengths lay in the range expected from previous studies.[38, 44, 81–82]

The ^{13}C NMR CIS values of the product complexes obtained lay between 18.6 and 28.1 ppm. These values were quite consistent with the CIS values of sugar-phosphate complexes with the $Re^{V}O$(L-His) and $Re^{V}O$(L-Car) fragments that added up to 17.3–25.6 ppm.[38] The ^{31}P NMR CIS values of the complexes synthesised that lay between −1.4 and −5.7 ppm were remarkably dependent on the spectator ligand used which was verified by the CIS values of glycerol 1-phosphate complexes with the spectator ligands en and tmen that amounted to −1.6 and −5.7 ppm, respectively. In comparison with ^{31}P NMR CIS values of sugar-phosphate complexes with further metal centres, it should be mentioned that the $Re^{V}O$ complexes were more similar to complexes of Al^{III} and Ga^{III} with CIS values of −6.7 and −4.4 ppm,[37] respectively, than to complexes of Pd^{II} with CIS values of 5.6–8.1 ppm. This tendency was also observed by comparing ^{31}P–^{1}H coupling constants, as the coupling constants of the fructose-1,6-bisphosphate complex with the $Re^{V}O$ fragment synthesised in this work added up to 6.9 and 23.8 Hz which was closer to the values of the corresponding Al^{III} complex (4.7 and 24.7 Hz) than to the values of the corresponding Pd^{II} complex (13 and 14 Hz).[37]

3.2 The pH dependence of sugar-phosphate complexes with the Pd^{II}(tmen) metal fragment

The main difference between the investigation of the coordination of sugar phosphates to Pd^{II} in this work and the experiments in previous works[37–38] was the systematic analysis of

various pH ranges. Moreover, with Pd^{II}(tmen) instead of Pd^{II}(en) a different metal fragment was used, which also led to partly different results. One example for this was the formation of an as—yet—unknown type of complex that featured the simultaneous coordination of hydroxy functions and phosphate functions of one sugar-phosphate molecule to separate metal centres. These special products had not been observed in any experiments with the Pd^{II}(en) fragment.

The experiments with Pd^{II}(tmen) showed that these products only occurred at pH values between 7 and 10. This was due to the fact that, firstly, the coordination of the hydroxy functions was limited to pH values above 7 and, secondly, the phosphate group coordinated to Pd^{II} only at pH values below 10. Thus, below pH 7, only products with exclusive phosphate coordination were formed while, above pH 10, only products with exclusive coordination of the hydroxy functions were observed. This result is summarised in Figure 3.2.

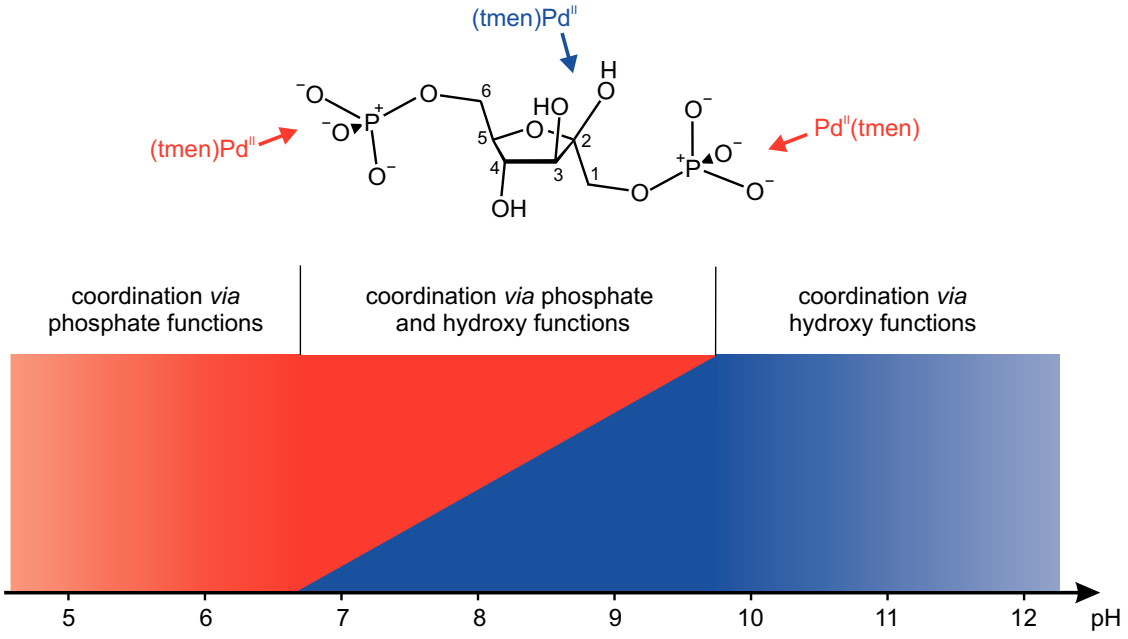

Figure 3.2 Schematic illustration of the pH dependence of sugar-phosphate complexes with the Pd^{II}(tmen) metal fragment on the example of β-D-fructose 1,6-bisphosphate.

The transformation of one complex to another by changing the pH of the solution was plainly visible in all series of spectra shown in Chapter 2.2. As a consequence, it was possible to enrich a desired complex simply by setting the pH. The reasons for this pH dependence were assumed to be the following: a hydroxy function is only able to coordinate to Pd^{II} when it is deprotonated which is not the case at pH values lower than 7. Regarding the pH dependence of the phosphate-group coordination, its explanation is more difficult. First of all, a phosphate group should absolutely be able to coordinate to Pd^{II} at high pH levels. Since this did not

occur, there must be a competitive ligand which coordinates to the metal rather than the phosphate. The hydroxy functions of the sugar core would be insufficient to prevent phosphate ligation since a coordinating phosphate function was not observed at high excess of Pd-tmen either. Finally, the responsible ligand was found to be the hydroxide anion with high signals for [Pd(tmen)(OH)$_2$] in ^{13}C NMR spectra verifying this theory. As a result, the coordination of a hydroxide ligand to Pd^{II} is obviously more favoured than the coordination of phosphate.

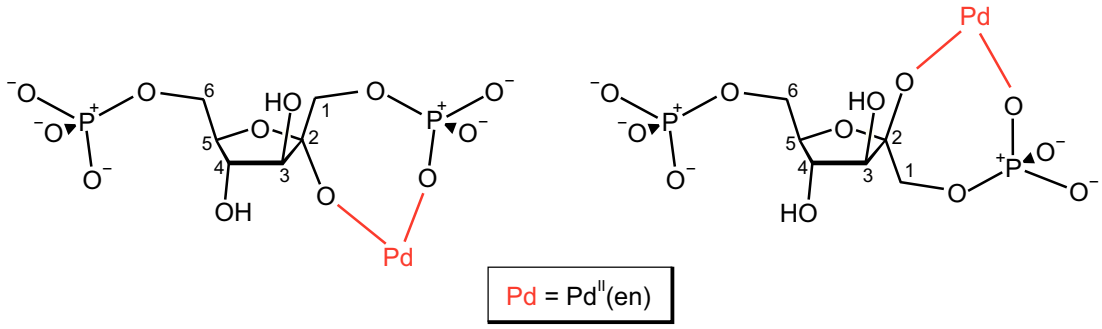

Figure 3.3 Mixed sugar-core–phosphate chelation found in product complexes of D-fructose 1,6-bisphosphate with the Pd^{II}(en) metal fragment.[37, 38]

One interesting result obtained in the experiments of sugar-phosphate complexes with the Pd^{II}(en) fragment in a previous study was the observation of a mixed sugar-core–phosphate chelation type.[37–38] This special coordination type, that is shown in Figure 3.3, was observed only in product solutions of D-fructose 1,6-bisphosphate at pH 10. The product was characterised by a CIS value of about 6 ppm for the ^{31}P NMR signal of P1. Actually, signals with a shift of nearly 6 ppm were observed in the ^{31}P NMR spectra of several Pd^{II}(tmen) product solutions of this work as well, but, unfortunately, the concentration of the related product species was always too low. As a result, no ^{13}C NMR chemical shifts of such a product were observed and, thus, the formation of sugar-phosphate complexes with Pd^{II}(tmen) featuring mixed sugar-core–phosphate chelation could not be verified.

3.3 Chelation preferences of sugar phosphates in complexes with the Pd^{II}(tmen) metal fragment at alkaline pH values

One important difference was recognised by comparing the results from the experiments of sugar-phosphate complexes with Pd^{II}(tmen) obtained in this work with the results of the appropriate Pd^{II}(en) experiments from previous works[37–38]: no single six-ring chelate was observed in the product solutions of sugar phosphates and Pd^{II}(tmen). This was unexpected since in experiments with Pd^{II}(en) the formation of six-ring chelates was shown to be

favoured over the formation of the alternative five-ring chelates. In experiments with ribose 5-phosphate, arabinose 5-phosphate and fructose 6-phosphate, the products exhibiting six-ring chelates were always the main species. Only in the case of D-fructose 1,6-bisphosphate, was the κ^2-$O^{2,3}$ species preferred over the κ^2-$O^{2,4}$ species. However, the preference of Pd^{II}(tmen) for five-ring chelates was confirmed by experiments with reducing sugars performed in a recent work.[36] There, the product solutions of experiments with D-ribose and D-fructose did not contain any six-ring chelate as well. Nevertheless, signals for the κ^2-$O^{1,3}$ species of α-D-arabinofuranose were observed. A reason for the various preferences of the metal fragments Pd^{II}(tmen) and Pd^{II}(en) could only be assumed.

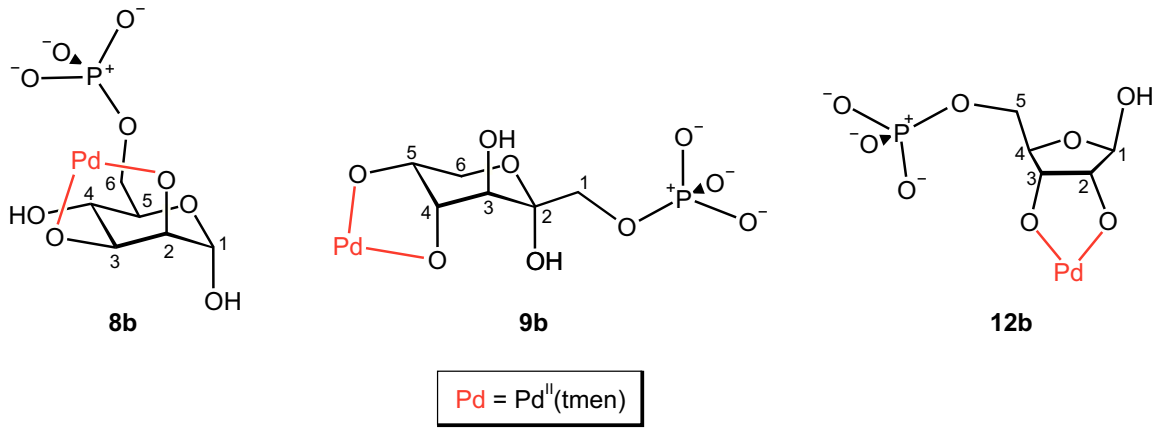

Figure 3.4 Non-phosphate coordinating Pd^{II}(tmen) product species obtained with non-coordinating anomeric hydroxy function.

Concerning the chelation preferences of sugar phosphates at alkaline pH values, further general observations have been made. First of all, the amount of polymetallated species rose with increasing excess of Pd^{II}(tmen) which was expected. The coordination of the first metal fragment always included the hydroxy function of the anomeric carbon atom when possible due to its comparatively low acid-dissociation constant. Thus, monometallated forms with a non-coordinating anomeric hydroxy group were formed only when the coordination *via* this group was not possible as was the case for the α-D-glucose 1-phosphate complexes, since the anomeric hydroxy function was blocked by the phosphate group, but also for the κ^2-$O^{2,3}$ chelate of α-D-mannopyranose 6-phosphate **8b**, the κ^2-$O^{4,5}$ chelate of α-D-fructopyranose 1-phosphate **9b** and the κ^2-$O^{2,3}$ chelate of β-D-ribofuranose 5-phosphate **12b**. The latter three are shown in Figure 3.4. There, it is clearly visible that coordination *via* the anomeric hydroxy functions was not possible due to the *trans*-diaxial position of the affected hydroxy functions. Nevertheless, the formation of **9b** with a concentration of 19% was unexpected since three hydroxy functions were in axial positions and, with the β-pyranose and β-furanose product forms, there were two alternative forms that should have been much more stable. However,

also in reactions of Pd-tmen and Pd-teen (teen = *N*,*N*,*N'*,*N'*-tetraethylethane-1,2-diamine) with D-fructose conducted in a previous work,[36] this κ^2-$O^{4,5}$ species was obtained in concentrations of 16% and 20%, respectively.

One further noticeable observation concerning the chelation preferences was the high concentration of the κ^2-$O^{2,3}$ chelate of β-D-fructofuranose 1-phosphate **9d** shown in Figure 3.5 which was the main species in product solutions of D-fructose 1-phosphate. This was partly unexpected since no signals for furanose species were observed in the spectra of the experiments with both D-glucose 6-phosphate and D-mannose 6-phosphate. However, the stability of **9d** was consistent with the results of appropriate experiments with D-fructose.[36] As discussed in previous works, this high stability could be explained with the formation of an intramolecular hydrogen bond O6–H···O3.[36, 96]

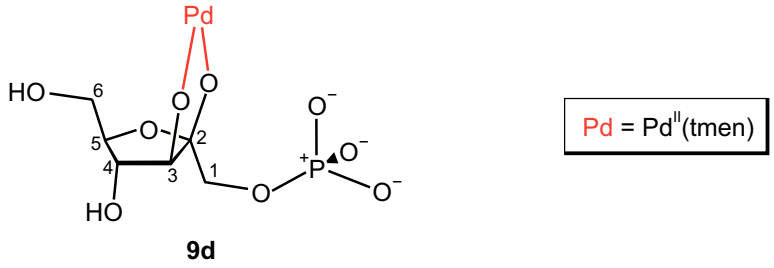

9d

Figure 3.5 Product species **9d** observed in solutions of D-fructose 1-phosphate in Pd-tmen.

One rule established in a previous study[36] was the preference of the coordination *via* hydroxy functions in *cis*-vicinal position over the coordination *via* hydroxy functions in *trans*-vicinal position. This rule is consistent with the results of this work as can be seen in the experiments of D-mannose 6-phosphate and D-glucose 6-phosphate. As mentioned above, the [Pd(tmen)(α-D-Man*p*6*P*2,3H$_{-2}$-$\kappa^2O^{2,3}$)]$^{2-}$ anion (**8b**) was formed only because the coordination of the α-pyranose form through O1 and O2 was impossible. However, coordination through O3 and O4 was actually possible but signals for a κ^2-$O^{3,4}$ chelate were not observed. Thus, for coordination, the *cis*-vicinal position of O2 and O3 was obviously favoured over the *trans*-vicinal position of O3 and O4. This tendency was also observed in D-glucose 6-phosphate experiments as the monometallated and dimetallated α-pyranose forms were preferred over the appropriate β-pyranose forms (all species shown in Figure 3.6). This was unexpected since the β-forms were assumed to be particularly stable due to, firstly, the anomeric effect and, secondly, the fact that all hydroxy functions were in equatorial positions. However, the *cis*-vicinal position of the chelating hydroxy functions was obviously more important for achieving an energetically favourable species. Furthermore, the results obtained in experiments with D-glucose were the same, confirming that this tendency was independent of the existence of a phosphate group. Nevertheless, it should be mentioned that the equilibrium

was achieved only after the reaction time of 12 hours. This unusual delay will be discussed in detail in the next chapter.

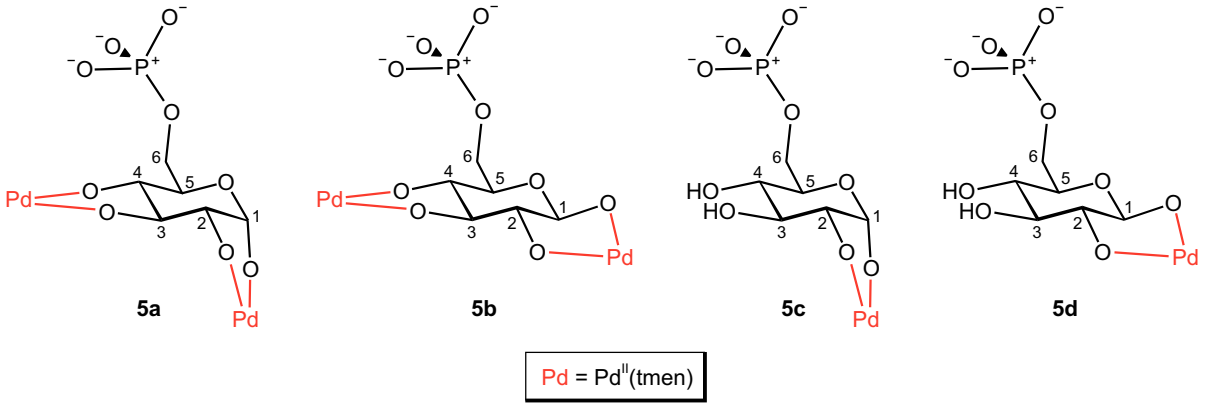

Figure 3.6 Non-phosphate coordinating Pd^{II}(tmen) product species observed in solutions of D-glucose 6-phosphate in Pd-tmen.

3.4 Equilibration times in experiments with D-glucose and D-glucose 6-phosphate

As observed in the reactions of Pd-tmen with sugars or sugar analogues conducted in this work and in several previous works,[35–36, 83–84] the final equilibrium between the product species was generally reached after 2–3 hours. So it was unexpected that in reactions with D-glucose 6-phosphate at alkaline pH values this point was achieved not before 12 hours. Furthermore, similar experiments with D-glucose confirmed that this observation was independent of the existence of a phosphate group. In order to explain this unusual property, it was necessary to look at the equilibria existing in solution. A schematic overview is given in Figure 3.7.

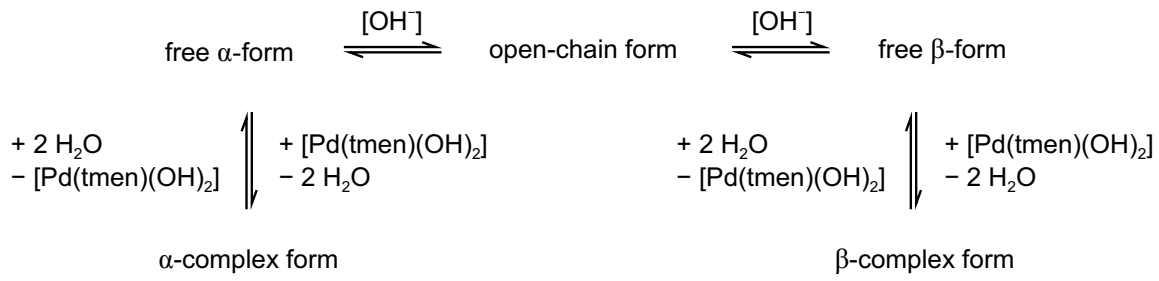

Figure 3.7 Schematic overview of equilibria existing in product solutions of D-glucose 6-phosphate and [Pd(tmen)$(OH)_2$].

Since the β-pyranose form was the main species in solutions of free D-glucose, it was expected that the equilibrium of the product forms in product solutions of Pd-tmen also lay at the side of the β-pyranose forms directly after the reactants were combined. Since the α-pyranose product species were energetically privileged compared to the β-pyranose product species, the equilibrium shifted towards the side of the α-forms within several hours. Thus, α-complex species transformed into β-complex species by the following procedure: First, the β-complex species split into the free β-form and the Pd^{II}(tmen) fragment. Second, the free β-pyranose form converted into the open-chain form which subsequently transformed into the α-pyranose form. Finally, this free α-form coordinated to a Pd^{II}(tmen) metal fragment, yielding an α-complex species. The decisive point is that the equilibrium of the free glucose forms lay on the side of the β-forms as the equilibrium of the product species lay on the side of the α-forms. Hence, the free α-pyranose form converted to the β-pyranose form before it could coordinate to a Pd^{II}(tmen) fragment, which was especially the case at alkaline pH values since the adjustment of the equilibrium state between free α- and β-forms is accelerated by hydroxide anions.[97]

The equilibration time of experiments in Pd-tmen was much longer than the time of reactions in Pd-en since the formation of Pd^{II}(en) complexes with sugars or sugar analogues is, in general, energetically more preferred than the formation of Pd^{II}(tmen) complexes. This hypothesis was verified by all hydroxy functions of D-glucose 6-phosphate coordinating to an Pd^{II}(en) fragment in reactions of this sugar phosphate in excess Pd-en as only dimetallated species were observed. In contrast, reactions of D-glucose 6-phosphate in excess Pd-tmen partly resulted in monometallated species although there was still a large amount of [Pd(tmen)$(OH)_2$] remaining in solution which was assigned by ^{13}C NMR spectroscopy. As a result, the equilibrium of the complex formation, that is given in Figure 3.8 on the example of [Pd(en)$(OH)_2$], lay more on the side of the free ligand in the case of Pd^{II}(tmen) than in the case of Pd^{II}(en).

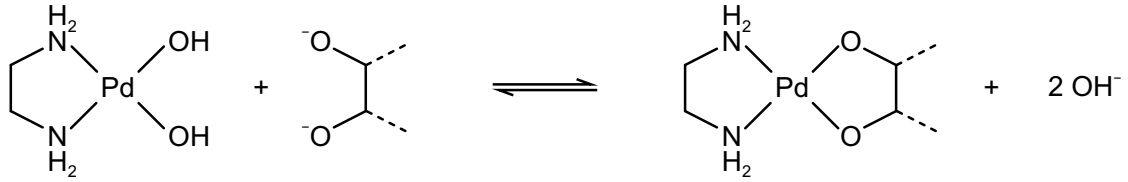

Figure 3.8 Equilibrium of the complex formation at alkaline pH values on the example [Pd(en)$(OH)_2$] and a diolate.

This equilibrium also answered the question of why an excess of sodium hydroxide resulted in a lower formation of complex species, since an increase of hydroxide anions shifted the equilibrium to the side of the free ligand form.

Finally, it should be mentioned that the existence of longer equilibration times was also possible in experiments of D-glucose or D-glucose 6-phosphate with the Zn^{II}(dien) metal fragment caused by the same reasons as mentioned above since, in these experiments, the equilibrium still lay on the side of the β-forms after a reaction time of 2 hours. However, it was not possible to verify this hypothesis due to a very poor signal-to-noise ratio of the NMR spectra obtained from experiments with a reaction time of 24 hours.

3.5 Experiments with the Zn^{II}(dien) metal fragment

The experiments with the Zn^{II}(dien) metal fragment were the most problematic part of this work. First of all, the preparation of crystalline product complexes was not possible on account of the reasons mentioned in Chapter 2.3.5. Moreover, adjusting the right stoichiometry in the experiments was often complicated by the poor solubility of zinc hydroxide in water and the species assignment of ^{13}C NMR signals was aggravated due to the absence of systematic CIS values known from the experiments with other metal ions such as palladium(II). This problem was even exacerbated by a fast metal-ligand exchange that resulted in partly averaged ^{13}C NMR chemical shifts. Thus, it was highly probable that, especially in experiments with an equimolar Zn^{II}(dien):sugar ratio, one set of signals was induced by both free sugar ligand and coordinating sugar ligand. This hypothesis was supported by the fact that, in some cases, the ratio of species in product solutions from experiments with a Zn^{II}(dien):sugar ratio of 1:1 and 2:1 differed from each other although dimetallation was not possible as observed, for example, in the spectra of D-fructose.

In the case of ^{13}C NMR spectroscopy it was further a problem that the chemical shifts of the signals were partly dependent on the pH of the solution. The signals of anomeric carbon atoms were the worst affected by these pH dependent shifts, which was most probably due to the fact that their hydroxy functions had the lowest acid-dissociation constants. However, an additional NMR measurement of an alkaline solution of the free educt form was conducted for all experiments with sugars or sugar phosphates leading in every case to ^{13}C NMR chemical shifts that were different from the shifts observed in the ^{13}C NMR spectra of the corresponding product solution. As a result, the product signals must have been shifted by coordination. The fact that these shifts were not observed in the experiments with polyols suggested the assumption that they were caused by torsions of the furanose or pyranose rings which were a consequence of complex formation. Unfortunately, these shifts were not systematic with the result that they only indicated coordination but did not give any hint for the chelation site. In order to assign the chelation site anyway, it was generally assumed that the sugar or sugar phosphate coordinated *via* the hydroxy function of the anomeric carbon atom when possible because of its low acid-dissociation constant. All assignments based on

this assumption as well as the deduced chelation preferences that are discussed in the following chapter seemed to be convincing.

It was observed in most of the experiments that the ^{13}C NMR chemical shifts of a product species differed in dependence on the Zn^{II}(dien):sugar ratio. The reason for this unusual observation was not absolutely clear. Nevertheless, two reasons were assumed that have already been mentioned above. On the one hand, the pH values of the product solutions could have been slightly different which led to different ^{13}C NMR chemical shifts of the product complexes since these shifts were partly dependent on the pH. On the other hand, it was discussed above that probably one set of ^{13}C NMR signals was induced by both free sugar ligand and coordinating sugar ligand. Since the amount of free sugar ligand would have been naturally lower in the 2:1 experiment than in the 1:1 experiment, this could have resulted in a change of shifts.

Finally, it should be mentioned that the experiments with the Zn^{II}(dien) fragment were limited to the alkaline pH range for two reasons. Firstly, it was discovered that, in contrast to experiments with Pd-tmen, no coordination of the hydroxy functions took place at pH values lower than 10 as can be seen exemplarily in the experiments with D-fructose 1-phosphate. Thus, coordination at these pH values was only possible *via* the phosphate groups but their coordination to Zn^{II} did not induce ^{31}P NMR CIS values as observed in the experiments with Pd-tmen. Furthermore, a change of the ratio between different sets of signals was not observed in any NMR spectrum making it impossible to verify or to investigate the coordination of sugar phosphates to the Zn^{II}(dien) metal fragment *via* phosphate groups.

3.6 Chelation preferences of sugars and sugar phosphates in complexes with the Zn^{II}(dien) metal fragment

The ^{13}C NMR spectra obtained from the experiments with the Zn^{II}(dien) fragment allowed conclusions about the chelation preferences of sugars and sugar phosphates. First of all, only five-ring chelates were formed in all experiments. The formation of alternative six-ring chelates, obviously, did not take place as no single α-furanose product species was observed in experiments with D-arabinose, D-fructose and D-fructose phosphates. This is illustrated by the example of D-fructose-1,6-bisphosphate in Figure 3.9.

As reported in Chapter 2.3.4.3, the reaction of D-fructose 1,6-bisphosphate and Zn^{II}(dien) resulted in the formation of only one product species, namely the β-furanose form [Zn(dien)(β-D-Fru*f*1,6$P_2$2,3H_{-2}-$\kappa^2O^{2,3}$)]$^{4-}$ (**32**), which was a five-ring chelate. Due to the phosphate-blocked hydroxy functions of carbon atoms 1 and 6, only one other coordination

was possible: the coordination of the α-furanose form through O2 and O4 exhibiting a six-membered chelate ring. However, since signals for this product were not observed, it had to be concluded that the formation of five-ring chelates was clearly privileged in the case of the Zn^{II}(dien) fragment. Moreover, this conclusion was consistent with the results of Pd^{II}(tmen) experiments, which emphasised the comparability of the two metal fragments.

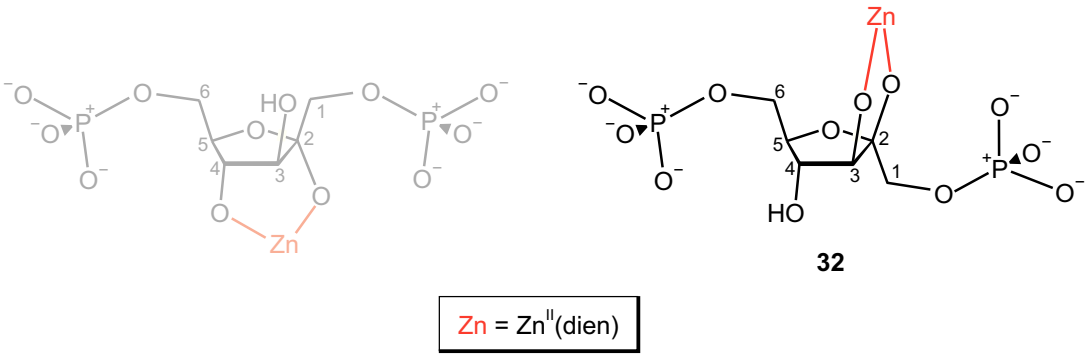

Figure 3.9 Comparison between the five-ring chelate [Zn(dien)(β-D-Fru*f*1,6$P_2$2,3H$_{-2}$-κ^2*O*^{2,3})]$^{4-}$ (**32**) obtained in experiments of this work and the possible six-ring chelate [Zn(dien)(α-D-Fru*f*1,6$P_2$2,4H$_{-2}$-κ^2*O*^{2,4})]$^{4-}$ which was not observed.

A further obvious result was the general enrichment of κ^2-*O*^{1,2} furanose species (or κ^2-*O*^{2,3} furanose species in the case of D-fructose or D-fructose phosphates) with the third hydroxy function directly bound to the furanose ring being in *trans*-position to the chelate ring. This is schematically illustrated in Figure 3.10.

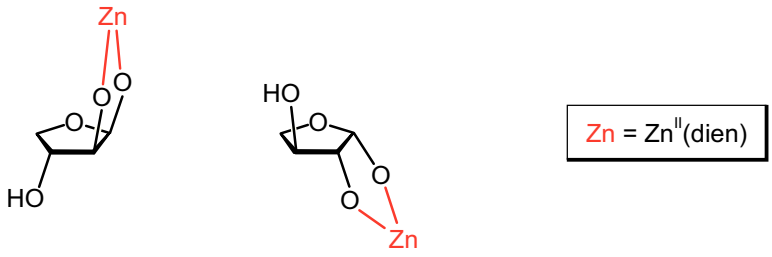

Figure 3.10 Schematic illustration of the furanose configuration especially preferred in product solutions of Zn^{II}(dien) with sugars or sugar phosphates.

Regarding pyranose complexes, it was noticed that species whose coordinating hydroxy functions were oriented in *cis*-vicinal positions instead of the alternative *trans*-vicinal positions were often privileged. However, the number of axial and equatorial hydroxy functions of the complex species was also a decisive parameter for the energetic preference. In contrast, the anomeric effect seemed to be rather unimportant. Finally, in particular cases, there was an influence of intramolecular hydrogen bonds. All conclusions drawn are

discussed in detail on the example of pentoses, hexoses and sugar phosphates in the following chapters.

3.6.1 Pentoses

In this work experiments with the pentoses D-lyxose, D-arabinose, D-xylose and D-ribose were conducted. The molar Zn^{II}(dien):pentose ratios used in the reactions were 1:1 and 2:1. As discussed in Chapter 3.5, it is highly probable that in the case of the 1:1 experiments, one set of ^{13}C NMR signals was induced by both free pentose and coordinating pentose. Hence, the product ratios of the 2:1 experiments were used for the following discussion. Figure 3.11 summarises the product ratios determined from the NMR spectra of the pentose experiments.

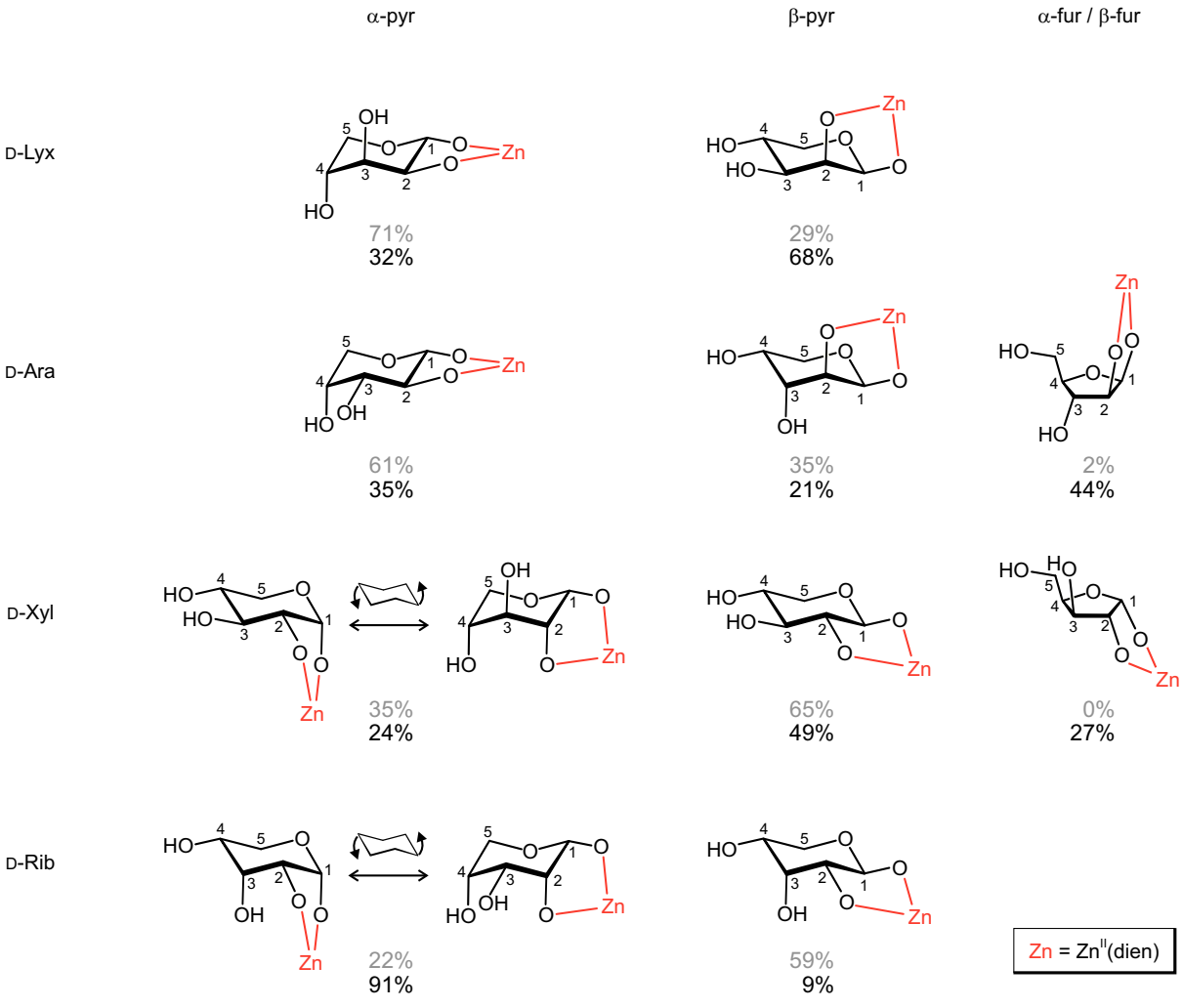

Figure 3.11 Schematic overview about the product ratios of pentose complexes with the Zn^{II}(dien) metal fragment obtained in this work (printed in black). Ratios determined for solutions containing only the free pentose are printed in grey.

The only two furanose species observed were the κ^2-$O^{1,2}$ chelates of the β-arabinofuranose form and the α-xylofuranose form. As mentioned above, this was explained by them being the only two possible κ^2-$O^{1,2}$ chelates with the hydroxy function of C3 being in *trans*-position to the chelate ring. Moreover, it was observed that the arabinofuranose product was the main species (44%) while the xylofuranose product was only a minor species (27%). Here, it had to be considered that the alternative pyranose product forms of D-xylose were energetically more privileged than the ones of D-arabinose because of the lower number of axial hydroxy functions. This applied especially to the β-D-xylopyranose form with its four equatorial hydroxy groups.

Beside these two furanose species, all other product complexes obtained were pyranose species. In the case of D-lyxose, the β-pyranose product species was preferred over the α-pyranose form since the β-form coordinated *via* hydroxy functions in *cis*-vicinal position and featured only one axial hydroxy function. For D-arabinose, the argumentation was a bit different since the α-pyranose product species exhibited the lower number of axial hydroxy functions while, in terms of the β-pyranose form, the chelation was realised *via* hydroxy functions in *cis*-vicinal positions. Finally, the α-pyranose complex was preferred. However, compared to the α-pyranose:β-pyranose ratio observed in the educt solution, the equilibrium changed slightly to the side of the β-pyranose form. Regarding the pyranose products of D-xylose, the issue was similar to that of D-arabinose. The α-pyranose form coordinated *via cis*-vicinal hydroxy groups to the Zn^{II}(dien) fragment while the β-complex was stabilised by four equatorial hydroxy functions. Again, the latter point was more important and the β-pyranose form was the main species in product solutions of D-xylose.

Compared to the other pentoses, the results obtained from the experiments with D-ribose were different. Here, the α-pyranose form, which coordinated *via cis*-vicinal hydroxy groups, was significantly preferred over the β-pyranose form, although it featured one more axial hydroxy group. It was assumed that, in this case, the α-pyranose form was especially stabilised by an intramolecular hydrogen bond O4–H···O2. This argumentation was also used in a recent work concerning sugar complexes of Pd^{II}.[36] There, crystal-structure analyses supported the hypothesis.

As published in recent studies[35–36], pentose complexes of Pd^{II}(tmen) are able to fluctuate between $^4C_1$ and $^1C_4$ conformation in aqueous solution. The results of this work showed that this is also possible for pentose complexes of Zn^{II}(dien), since the coupling constants determined for [Zn(dien)(α-D-Xyl*f*1,2H$_{-2}$-$\kappa^2O^{1,2}$)] were averaged values of the $^4C_1$ and the $^1C_4$ conformer. The existence of an equilibrium between the two conformers of this α-xylopyranose complex was actually unexpected since only the $^4C_1$ conformation of α-xylopyranose was observed in solutions of the free D-xylose. This shift of equilibrium was

explained with similar argumentation as used in terms of the stability of the furanose species mentioned above. Thus, κ^2-$O^{1,2}$ species were energetically privileged when the hydroxy functions of C2 and C3 were positioned *trans*-equatorial. Since this was realised in the $^1C_4$ conformation of the α-xylopyranose complex species, it would explain the stability of this conformer in spite of the presence of three axial hydroxy functions. Indeed, this conformer was also stabilised by the intramolecular hydrogen bond O4–H···O2. Concerning the κ^2-$O^{1,2}$ chelate of α-D-arabinopyranose, however, none of the two conformers exhibited a similar hydrogen bond. Nevertheless, the equilibrium was shifted completely to the side of $^4C_1$ conformer while, in solutions of the free D-arabinose, only the $^1C_4$ conformer was observed. Since, furthermore, the number of axial hydroxy groups is equal for both conformers, the only explanation for the $^4C_1$ conformer's stability was the *trans*-equatorial orientation of O2 and O3. The influence of this special configuration was confirmed by the results obtained in the experiments with D-lyxose.

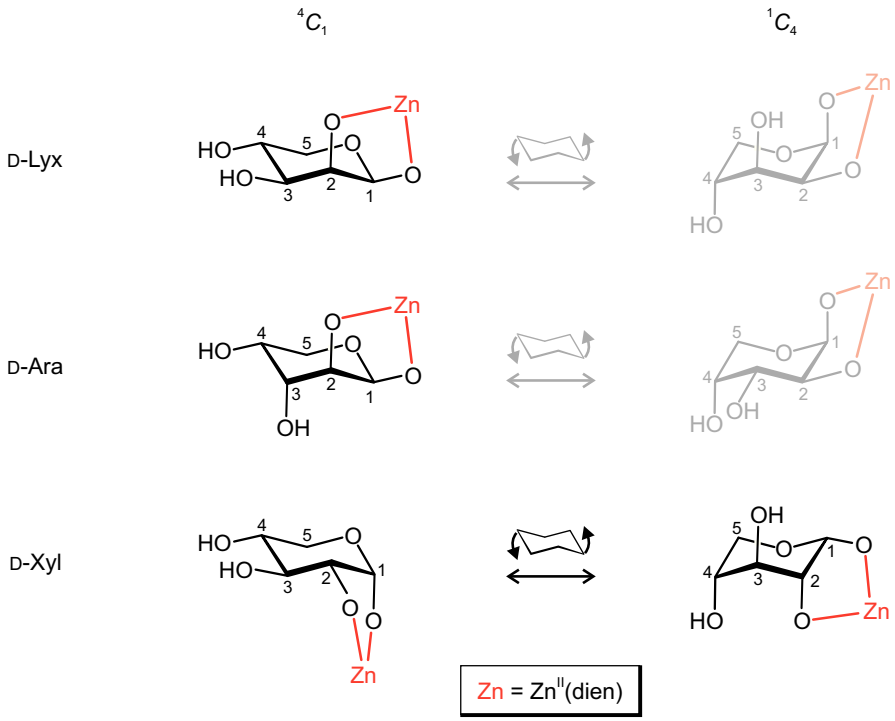

Figure 3.12 Schematic overview about the κ^2-$O^{1,2}$ chelates detected in product solutions of Zn^{II}(dien) and D-lyxose, D-arabinose or D-xylose.

As can be seen in Figure 3.12, neither the $^4C_1$ nor the $^1C_4$ conformer of D-lyxose featured a *trans*-equatorial orientation of O2 and O3. Thus, the conformer with the lowest number of axial hydroxy functions should have been energetically privileged. Since, this number is the same for coordinating and free forms, the tendency of the equilibrium between $^4C_1$ and $^1C_4$ conformer should have been the same for product solutions and solutions of the free D-lyxose.

And indeed, this was the case, as in both solutions the equilibrium was shifted completely to side of the $^4C_1$ conformer which exhibited the lower number of axial hydroxy functions.

Finally, it should be mentioned that the coupling constants determined for [Zn(dien)(α-D-Rib*p*1,2H$_{-2}$-κ^2*O*^{1,2})] (**25a**), which also would have been able to fluctuate, did not allow any conclusion about the distribution of conformation. Thus, this product was not considered in this discussion

3.6.2 Hexoses

The product ratios determined from the NMR spectra of the hexose experiments are given in Figure 3.13. At first glance, it is recognised that the three furanose species determined had the same configuration as found in complexes of the pentoses: the hydroxy function of C3 (or C4 in the case of D-fructose) was in *trans*-position to the chelate ring. For D-mannose, such a configuration was not possible and, thus, no furanose product species formed. The stability of these furanose forms was remarkable as the two product forms [Zn(dien)(α-D-Gal*f*1,2H$_{-2}$-κ^2*O*^{1,2})] (**26c**) and [Zn(dien)(β-D-Fru*f*2,3H$_{-2}$-κ^2*O*^{2,3})] (**29b**) were the main species in their product solutions. Only in the case of D-glucose, was the furanose product form a minor species. However, this was explained by the relatively high stabilisation of the D-glucopyranose complexes due to their high number of equatorial hydroxy functions. This hypothesis was consistent with the results and conclusions of the D-xylose experiments discussed above, which was expected since the configuration of D-xylose and D-glucose is very similar. Thus, the β-pyranose form of D-glucose stabilised by four equatorial hydroxy groups was clearly the main species in product solutions.

Regarding the pyranose forms of D-galactose, the argumentation is the same. Since the β-species featured one more equatorial hydroxy function than the α-species, it was energetically preferred although the α-pyranose form coordinated *via cis*-vicinal hydroxy groups to the Zn^{II}(dien) fragment.

For the last two hexoses investigated, D-mannose and D-fructose, the preference of the respective β-pyranose product form had particular reasons. The α-pyranose species of D-fructose would have been energetically unprivileged due to the axial position of the CH_2OH group. Concerning the α-mannopyranose species, coordination was not possible through O1 because of O1 and O2 being in *trans*-equatorial positions.

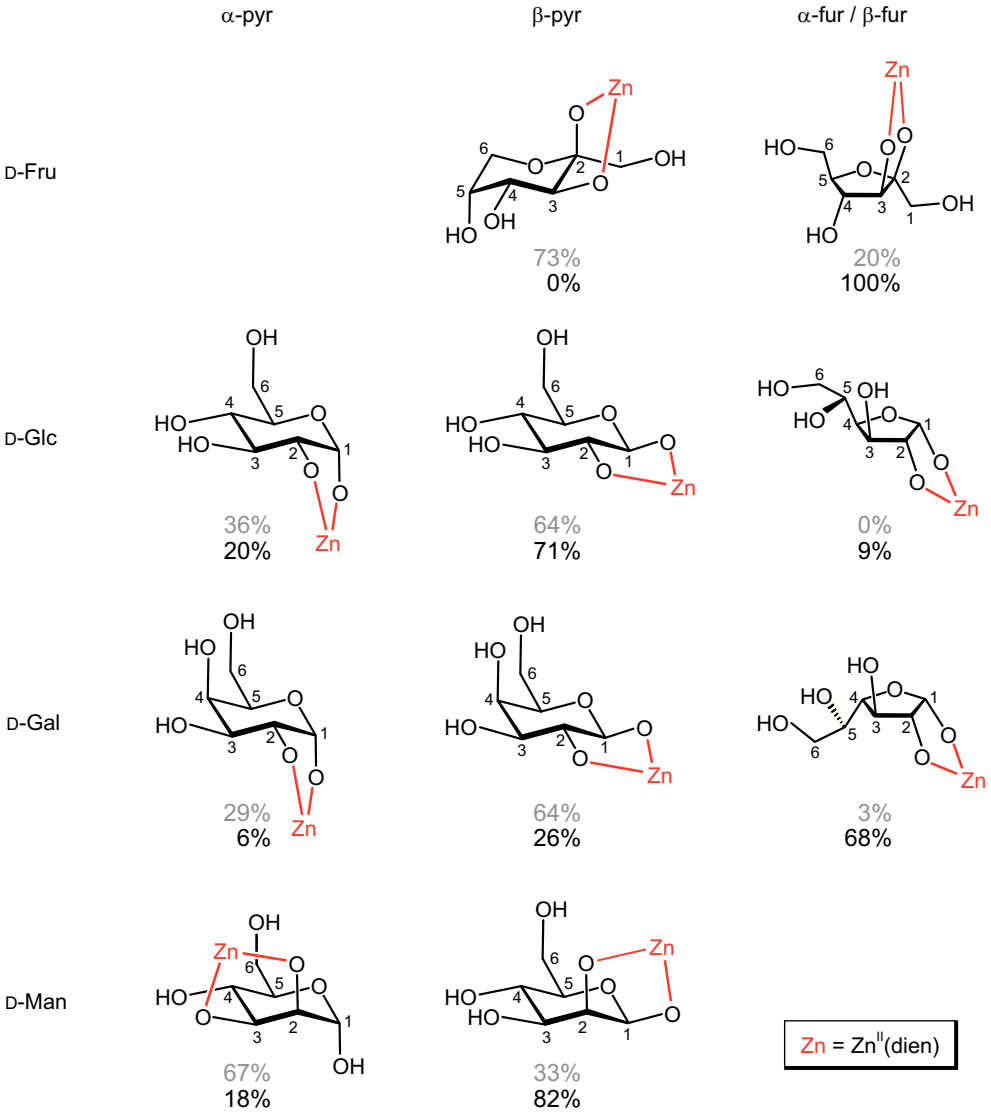

Figure 3.13 Schematic overview about the product ratios of hexose complexes with the Zn^{II}(dien) metal fragment obtained in this work (printed in black). Ratios determined for solutions containing only the free hexose are printed in grey.

3.6.3 Sugar phosphates

Since the results of the experiments with the sugar phosphates D-glucose 6-phosphate, D-mannose 6-phosphate and D-fructose 1-phosphate were very similar to the results obtained with the corresponding sugars, they were not discussed additionally. The preference of the β-furanose product species of D-fructose 6-phosphate and D-fructose 1,6-bisphosphate was due to, firstly, the inaccessibility of pyranose forms and, secondly, the preference of five-ring chelates over six-ring chelates which was discussed at the beginning of Chapter 3.6.

Compared to experiments with the metal fragment Pd^{II}(tmen) at alkaline pH values, the Zn^{II}(dien) results were similar since comparable main species were obtained in the reactions with D-fructose 1-phosphate, D-fructose 6-phosphate and D-fructose 1,6-bisphosphate. Thus, a preference of five-ring chelates was observed for both Pd^{II}(tmen) and Zn^{II}(dien). Further similarities were: the preference of pyranose forms coordinating *via cis*-vicinal hydroxy functions and the existence of equilibria between $^4C_1$ and $^1C_4$ conformers of product species. However, experiments at neutral pH values also revealed clear differences between the two metal fragments as, in contrast to Zn^{II}(dien) experiments, the coordination of hydroxy functions to Pd^{II}(tmen) was also observed at the pH range between 7 and 10. Overall, using the Pd^{II}(tmen) results to support Zn^{II}(dien) experiments was possible, but limited to the alkaline pH range.

3.7 Calculation of NMR chemical shifts

For the DFT-based procedure, the concept of a previous study was used which was well suited for the calculation of ^{13}C NMR chemical shifts of Pd^{II} complexes with sugar analogues.[49] This concept included correcting the calculated shifts by linear regression in order to compensate systematic errors of the procedure. The standard deviation determined from the ^{13}C NMR chemical shifts corrected added up to 1.8 ppm and was a measure of the difference between the chemical shifts obtained from the experiment and the calculation. It was comparable to values of previous works dealing with the calculation of ^{13}C NMR chemical shifts of similar complexes, as the standard deviations of these studies lay between 1.4 and 2.1 ppm.[49–50, 98] It should be mentioned that some of the differences between calculated and experimental values were relatively high. These were the values for C2 of $[\{Pd(tmen)\}_2(\alpha\text{-D-Glc}p6P1,2;3,4H_{-4}\text{-}\kappa^2O^{1,2}\text{:}\kappa^2O^{3,4})]^{2-}$ (4.0 ppm) and for C4 and C5 of $[\{Pd(tmen)\}_2(\beta\text{-D-Fru}p1P2,3;4,5H_{-4}\text{-}\kappa^2O^{2,3}\text{:}\kappa^2O^{4,5})]^{2-}$ (4.5 and 4.8 ppm). Concerning the second product complex, the optimisation of its structure was very complicated since a convergence for just one of three possible conformers was achieved only after many attempts. Thus, it is possible that one of the two other conformers would have led to better results. However, despite the differences between the values obtained from experiment and calculation, the assignment of the NMR signals of the two product complexes affected was unambiguous because of clear CIS values. Beside the three values mentioned above, all further differences between calculated and experimental values were not higher than 3.5 ppm.

The calculations were limited to complexes coordinating to Pd^{II} only *via* hydroxy functions for two reasons. Firstly, an additional coordination of the phosphate group caused only a very small change of the ^{13}C NMR chemical shifts up to 2 ppm which was too small to detect it *via* quantum-chemical calculations. Secondly, the calculation of ^{31}P NMR chemical shifts was not

successful which was most probably due to the strong dependence of these shifts on the phosphate group's degree of protonation.

Beside the calculation of NMR chemical shifts of Pd^{II} product complexes it would also have been possible to calculate the shifts of the $Re^{V}O$ and Zn^{II} product complexes. However, the determination of values calculated of the $Re^{V}O$ products was not necessary since the CIS values have already been supported by crystal-structure analysis, mass spectrometry and the determination of $^{31}P–^{1}H$ coupling constants. The calculation of ^{13}C NMR chemical shifts of Zn^{II} product complexes was not conducted due to the absence of sufficiently high CIS values.

4 Summary

The primary goal of this work was to obtain more knowledge about the coordination chemistry of sugar phosphates in order to gain deeper insight into the initial binding patterns of sugar-phosphate substrates to metal centres of metalloenzymes. To that end, experiments with the Zn^{II}(dien) metal fragment and several sugar phosphates were conducted since Zn^{II} is a well known catalytic centre occurring in many enzymes including class-II aldolase, L-ribulose-5-phosphate 4-epimerase and glucose-6-phosphate isomerase. Experiments were performed with the sugar phosphates D-fructose 1-phosphate, D-fructose 6-phosphate, D-fructose 1,6-bisphosphate, D-mannose 6-phosphate, D-glucose 6-phosphate, α-D-glucose 1-phosphate and D-ribose 5-phosphate. Due to the lack of knowledge about Zn^{II}(dien) complexes of sugars and sugar analogues, additional investigations were performed with the polyols ethane-1,2-diol, glycerol, D-threitol, and erythritol, with the methylated sugars methyl α-D-glucopyranoside, methyl β-D-glucopyranoside, methyl α-D-mannopyranoside, methyl α-D-galactopyranoside, and methyl β-D-galactopyranoside, and with the reducing sugars D-lyxose, D-arabinose, D-xylose, D-ribose, D-glucose, D-mannose, D-galactose, and D-fructose.

Only NMR spectroscopy was used for the analysis of product solutions since no suitable crystals necessary for crystal-structure analysis were obtained, due to the existence of special equilibria in solution causing the formation of crystalline by-products such as zinc hydroxide or free sugar ligand. However, in contrast to a previous study[29], NMR spectroscopy was shown to be quite useful for the analysis of product solutions. In NMR experiments with methylated sugars, pentoses, hexoses and sugar phosphates, small CIS values were observed that were most probably the consequence of ring torsions induced by coordination. Thus, it was possible to verify the coordination of furanose or pyranose rings to the Zn^{II}(dien) fragment by ^{13}C NMR spectroscopy. Although the change of pH induced similar shifts of NMR signals, these shifts were decisively different from the ones caused by coordination. The CIS values found were unsystematic, and thus, it was not possible to assign the metal-chelation site based on them. In order to circumvent this problem, the assumption was made that coordination is always realised *via* the hydroxy function of the anomeric carbon atom, when possible, because of its comparatively low acid-dissociation constant. In addition to unsystematic CIS values, coordination was also clearly verified by the change of ratio between α- and β-furanose forms as well as α- and β-pyranose forms in solution.

This change of ratio allowed conclusions about the chelation preferences of pentoses, hexoses and sugar phosphates to the Zn^{II}(dien) metal fragment. One of them was the preference of five-ring chelates over six-ring chelates as it was clearly verified in reactions with D-fructose 1,6-bisphosphate. Moreover, several examples such as the one of D-fructose showed that

furanose species were enriched in solution when the hydroxy group next to the coordinating hydroxy functions was in *trans*-position to the chelate ring. Further points affected the pyranose complex products. Here, stabilised species were often characterised by either a lower number of axial hydroxy functions or coordination *via cis*-vicinal hydroxy groups. In particular cases, the product complex was stabilised by an intramolecular hydrogen bond. An example for this was the product species [Zn(dien)(α-D-Rib*p*1,2H$_{-2}$-κ$O^{1,2}$)]. In contrast, the anomeric effect seemed to have no importance.

The experiments of sugar phosphates were conducted at various pH values in order to obtain different types of coordination such as exclusive coordination of phosphate groups, exclusive coordination of hydroxy functions, a combination of both or mixed sugar-core–phosphate chelation. Unfortunately, it was impossible to decisively detect the coordination of phosphate groups to Zn^{II}(dien) since no clear ^{31}P NMR CIS values were observed. Furthermore, the coordination of hydroxy functions to the Zn^{II}(dien) fragment was limited to pH values above 10. Hence, significant results were obtained only in the alkaline pH range.

Since the NMR analysis of Zn^{II}(dien) product solutions was partly limited by methodical problems, the experiments with sugar phosphates were additionally performed with the metal fragment Pd^{II}(tmen) that is perfectly suited for NMR analysis. Since the product complexes of the two metal fragments were comparable due to very similar O–M–O bond angles adding up to about 85°,[29, 36] the results obtained with the Pd^{II}(tmen) fragment were able to support the Zn^{II}(dien) experiments. By inducing a coordination-induced shift of about 10 ppm to signals of carbon atoms bound to coordinating hydroxy groups of five-membered chelate rings, indeed, Pd^{II} clearly indicated the metal-chelating site of the sugar-phosphate complexes observed. Some results, such as the preference of five-ring chelates over six-ring chelates, even suggested that the product complexes of both metal fragments were indeed comparable. However, experiments at neutral pH values showed that this was not completely true as, in contrast to Zn^{II}(dien) experiments, the coordination of hydroxy functions to Pd^{II}(tmen) was also observed at the pH range between 7 and 10. Nevertheless, the distributions of species obtained at the alkaline pH range were consistent for both metal fragments in most cases. Regarding the three fructose phosphates investigated, for example, the main species was always the κ$^2O^{2,3}$ chelate of the β-furanose form. A further similarity of the sugar-phosphate complexes of both metal fragments was the less pronounced tendency to form crystals. Concerning the Pd^{II}(tmen) experiments, crystallisation was disabled by the formation of Pd^0, resin-like precipitations, crystals of free ligand or crystals of by-products such as [{Pd(tmen)}$_2$(μ-OH)$_2$](NO$_3$)$_2$.

Since hydroxy groups coordinated to Pd^{II}(tmen) also at neutral pH values, the pH dependence of the metal-chelation sites was investigated in detail. The coordination of a phosphate

function to Pd^{II} was detected *via* the coordination-induced shift of its ^{31}P NMR signal. These shifts lay between 5.6 and 7.0 ppm. Thus, a complete assignment of the metal-chelating sites of the product species was possible at almost the whole pH range. This study revealed that hydroxy functions coordinated to Pd^{II}(tmen) only at pH values higher than 7 since they are only able to coordinate to Pd^{II} when they are deprotonated, which is not the case at pH values lower than 7. In contrast, phosphate groups coordinated to the Pd^{II}(tmen) fragment only at pH values below 10 since the coordination of hydroxide anions was clearly privileged. In the range between pH 7 and 10 both coordination types were observed, even at the same molecule. This simultaneous coordination of hydroxy groups and phosphate functions of one sugar-phosphate molecule to separate metal centres had never been observed in experiments with Pd^{II}(en). In summary, the formation of product complexes was highly dependent on the pH. As a consequence, it was possible to enrich a desired complex simply by adjusting the pH.

In experiments of D-glucose 6-phosphate with Pd-tmen at alkaline pH values, unusually long equilibration times were observed. The energetic preference of the β-pyranose product species was only pretended as these were the main species after 2 hours of reaction time. However, after the reaction time of 24 hours, the equilibrium lay plainly on the side of the α-pyranose product species. Further experiments with D-glucose revealed that this long equilibration time was not dependent on the existence of a phosphate group. It was explained by the fact that the equilibrium of the free glucose forms lay on the side of the β-forms as the equilibrium of the product species lay on the side of the α-forms. Thus, the free α-pyranose form converted to the energetically privileged free β-form before it had the chance to coordinate to a Pd^{II}(tmen) fragment. This effect was observed only at alkaline pH values since the adjustment of the equilibrium state between free α- and β-forms was accelerated by hydroxide anions.

The species assignments of sugar-phosphate complexes with Pd^{II}(tmen) were supported by quantum-chemical calculations based on a recently published procedure which was well suited for the calculation of ^{13}C NMR chemical shifts of Pd^{II} complexes with sugar analogues.[49] In this context, the Gaussian 03 program package[99] was used to perform geometry optimisations and calculations of GIAO NMR chemical shifts. In all calculations, a PCM model was used in order to simulate the influence of the solvent. Several conformers were considered for the determination of the NMR chemical shifts calculated of one product complex. On the basis of special rules obtained from a recent work[49], the shifts of one conformer were chosen to be the best fitting shifts for one complex. Finally, the chemical shifts of all complexes were corrected by linear regression in order to compensate for systematic errors of the procedure. The standard deviation determined from the ^{13}C NMR chemical shifts corrected was 1.8 ppm and represented a measure of the difference between

experimental and calculated chemical shifts. This value was comparable to values of previous studies on the calculation of ^{13}C NMR chemical shifts of similar complexes as those standard deviations lay between 1.4 and 2.1 ppm.[49–50, 95] However, a few of the differences between calculated and experimental values were relatively high, most probably due to problems concerning geometry optimisations. Beside these three values, all further differences between calculated and experimental values were not higher than 3.5 ppm.

Beside Zn^{II} and Pd^{II}, experiments with $Re^{V}O$ were performed also within this work. With them, it was possible to get more knowledge about mixed sugar-core–phosphate chelation as D-fructose 1,6-bisphosphate was found to coordinate to several $Re^{V}ON_2$ centres (N_2 = en, (*R*,*R*)-chxn, tmen) *via* two hydroxy functions and one phosphate group. This special coordination type featured one common five-membered chelate ring and one seven-membered phosphate-containing chelate ring. The product anions [$ReON_2$(β-D-Fru*f*2,3H$_{-2}$1,6P_2H$_2$-κ$^3O^{2,3,P1}$)]$^-$ were characterised by mass spectrometry and NMR spectroscopy with CIS values of 21.0–28.1 ppm for the ^{13}C NMR signals of O2 and O3 and CIS values between −1.8 and −3.7 ppm for the ^{31}P NMR signals of P1. Furthermore, the P1 signal was found as a doublet of doublets with ^{31}P–^{1}H coupling constants of 23.8 and 7.9 Hz. Experiments with the D-fructose 1,6-bisphoshphate model glycerol 1-phosphate resulted in appropriate product complexes that were characterised by very similar NMR parameters and additionally performed high-resolution mass spectrometry. Moreover, crystals were isolated from reactions with the spectator ligands tmen and phen. The crystal structures of the products [ReO(tmen)(*rac*-Glyc2,3H$_{-2}$1*P*H-κ$^3O^{2,3,P}$)] and [ReO(phen)(*rac*-Glyc2,3H$_{-2}$1*P*H-κ$^3O^{2,3,P}$)] were the first to verify mixed sugar-core–phosphate chelation. Unfortunately, appropriate experiments with D-fructose 1-phosphate were not successful although it provided the same metal-chelating site as D-fructose 1,6-bisphosphate and glycerol 1-phosphate. Experiments with further sugar phosphates were also unsuccessful. For D-ribose 5-phosphate, a tridentate coordination of three hydroxy groups was actually assumed to be possible since comparable complexes were obtained with the metal fragments Co^{III}(tacn) and Ga^{III}(tacn).[37, 42–43]

Overall, the aims of this work were achieved. Mixed sugar-core–phosphate chelation was finally verified by crystal-structure analysis. Furthermore, a detailed investigation of sugar-phosphate complexes with Pd^{II}(tmen) allowed new conclusions about metal-chelating sites of sugar phosphates concerning, for example, their pH dependence. And finally, an extensive analysis of the coordination chemistry of Zn^{II}(dien) complexes led to as—yet—unknown basic conclusions concerning chelation preferences of sugars and sugar phosphates that will help to gain deeper insight into the initial binding patterns of sugar-phosphate substrates to the metal centres of metalloenzymes. With Zn^{II}(dien), a new metal fragment for the investigation

of metal-chelating sites of sugars and sugar phosphates was established which is well suited for the modelling of catalytic centres since Zn^{II} occurs in many metalloenzymes.

5 Experimental Section

5.1 Common working techniques

The synthesis of [Pd(en)$(OH)_2$] and [Pd(tmen)$(OH)_2$] as well as all reactions using Me_2Zn were carried out under nitrogen atmosphere using standard Schlenk techniques. All other reactions were performed under normal air conditions. For NMR investigation of Zn^{II} or Pd^{II} product solutions, 1–2 mL of a product solution were prepared and stirred at 4 °C without using inert gas for 2–3 hours if no other time or treatment is mentioned. The solution was subsequently either immediately investigated by NMR spectroscopy or stored at −60 °C. Elemental analyses were performed on an Elementar vario EL elemental analyser. Mass spectra were recorded on a Jeol JMS-700 mass spectrometer.

5.2 Reagents and solvents

(1*R*,2*R*)-cyclohexane-1,2-diamine	99% (ABCR)
1,4,7-triazacylcononane	synthesis
1,4,7-trimethyl-1,4,7-triazacylcononane	synthesis
1,10-phenanthroline monohydrate	≥ 99% (Aldrich)
acetone	≥ 99.5% (Fluka)
adenosine 5'-monophosphate monohydrate	≥ 97% (Sigma)
ammonium perrhenate	99% (ABCR)
barium D-fructose 1-phosphate trihydrate	– (Aldrich)
barium(II) nitrate	99% (Merck)
calcium nitrate tetrahydrate	≥ 99% (Fluka)
caesium nitrate	99.0% (Fluka)
D-arabinose	> 99% (Fluka)
deuterium oxide	99.90% (Eurisotop)
D-fructose	> 99.0% (Fluka)
D-galactose	≥ 99.0% (Fluka)
D-glucose monohydrate	≥ 99.5% (Fluka)
diethylenetriamine	99% (Sigma-Aldrich)
dimethyl zinc	2 M in toluene (Fluka)
disodium α-D-glucose 1-phosphate tetrahydrate	≥ 97% (Sigma)
disodium D-fructose 6-phosphate hydrate	98% (Sigma)
disodium D-glucose 6-phosphate hydrate	≥ 98% (Sigma)
disodium D-mannose 6-phosphate dihydrate	≥ 95% (Carbosynth)

disodium D-ribose 5-phosphate hydrate	≥ 98% (Sigma) / synthesis
disodium *rac*-glycerol 1-phosphate hydrate	> 85.0% (TCI Europe)
D-lyxose	≥ 99% (Fluka)
D-mannose	99% (ABCR)
Dowex®50WX8	50–100 mesh, p.a. (Fluka)
D-ribose	99% (Acros)
D-threitol	97% (Sigma)
D-xylose	≥ 99% (Fluka)
ethane-1,2-diamine	≥ 99.8% (Fluka)
ethanol	99.9% (Fluka)
ethyl acetate	p.a. (Merck)
ethane-1,2-diol	≥ 99.5% (Fluka)
europium(III) nitrate	99.9% (Strem)
glycerol anhydrous	≥ 99.5% (Fluka)
hexamminecobalt(III) chloride	≥ 97% (Fluka)
hydrochloric acid conc.	37% (Biesterfeld Graën)
isopropyl alcohol	≥ 99.5% (Fluka)
lithium nitrate	≥ 99% (Fluka)
magnesium nitrate hexahydrate	> 99.5% (Fluka)
erythritol	99% (Alfa Aesar)
methanol	p.a. (Fluka)
methanol-d_4	99.80% (Eurisotop)
methyl α-D-galactopyranoside	≥ 98.0% (Fluka)
methyl α-D-glucopyranoside	≥ 99% (Fluka)
methyl α-D-mannopyranoside	≥ 99% (Fluka)
methyl β-D-galactopyranoside	≥ 98.0% (Fluka)
methyl β-D-glucopyranoside hydrate	≥ 99% (Fluka)
N,*N*,*N'*,*N''*,*N''*-pentamethyldiethylenetriamine	99% (Aldrich)
N,*N*,*N'*,*N'*-tetramethylethane-1,2-diamine	≥ 99.5% (Sigma-Aldrich)
nitric acid	p.a. (Fluka)
palladium(II) chloride	99.9% (Fluka, Alfa Aesar)
silver(I) oxide	≥ 99% (Merck)
sodium hydroxide	≥ 98% (Fluka)
strontium(II) nitrate	≥ 98% (Fluka)
toluene	p.a. (Fluka)
triethylamine	≥ 99% (Riedel-de Haën)
triphenylphosphane	99% (Acros)
trisodium D-fructose 1,6-bisphosphate octahydrate	≥ 98% (AppliChem)

water, deionised	house installation with ion exchange resin
zinc chloride	> 98% (Fluka)
zinc nitrate hexahydrate	≥ 99% (Fluka)
zinc sulphate heptahydrate	≥ 99.5% (Fluka)

5.3 NMR spectroscopy and species assignment

NMR spectra were recorded at 4 °C on Jeol ECX400/ECP 400 (^{1}H: 400 MHz, ^{13}C{^{1}H}: 100 MHz, ^{31}P: 109 MHz) spectrometers. The signals of methanol, which was added to the sample, were used as an internal secondary reference for the chemical shift. Shift differences in the spectra of palladium(II), zinc(II) and rhenium(V) experiments are given as $\delta(C_{complex}) - \delta(C_{free\ ligand})$. The values for the free ligands were determined in neutral aqueous solution if no special pH or solvent is mentioned.

The ^{1}H, ^{31}P{^{1}H} and ^{13}C{^{1}H} NMR signals were assigned by ^{1}H–^{1}H COSY45, ^{1}H–^{13}C HMQC, ^{1}H–^{13}C HMBC, and ^{31}P–^{1}H HETCOR experiments in D_2O. In order to assign the sets of signals to individual species, first of all, coupling constants J were analysed applying a modified Karplus relationship to identify the correct anomer.[48] Afterwards, the correct chelation site was assigned by using CIS values in the case of the Pd^{II}(tmen) and $Re^{V}O$ experiments. To support the assignments of the Pd^{II}(tmen) experiments, the shifts of the non-phosphate-coordinating species were predicted by a DFT-based procedure.[49–50] The Gaussian 03 program package[99] was used for the calculations. For palladium, a CEP-4G effective core potential with the corresponding valence basis set was used (18 electrons in the valence shell).[51] Geometries were optimised by the B3LYP method and 6-31+G(2d,p) basis sets for all atoms except palladium. Stationary points were confirmed with subsequent frequency analyses. GIAO NMR chemical shifts were calculated by the PBE1PBE method and the same basis sets used in the geometry optimisation. Shifts refer to $\delta = 0$ for tetramethylsilane, calculated by the same procedure. In all calculations, a PCM model was used to simulate the influence of the solvent. For the determination of the calculated NMR chemical shifts of one product complex, several conformers were considered. Based upon special rules obtained from a recent work[49], the shifts of one conformer were chosen to be the best fitting shifts for one complex. Finally, the chemical shifts of all complexes were corrected by linear regression in order to compensate systematic errors of the procedure. The resulting linear relationship between the calculated and experimental shift values is shown in Figure 5.1.

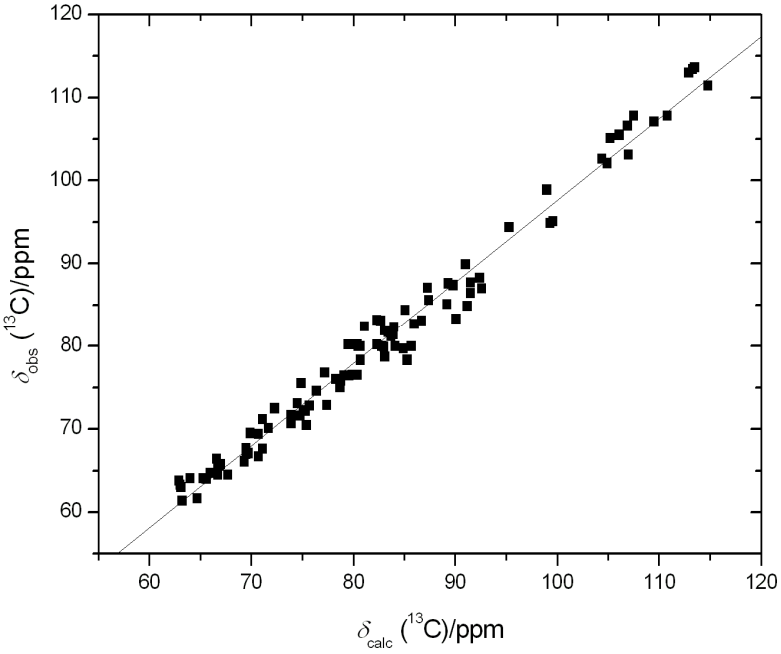

Figure 5.1 Linear correlation between ^{13}C NMR chemical shifts obtained from calculations [δ_{calc}, PBE1PBE/6-31+G(2d,p)] and from the experiment (δ_{obs}). Included are data of all non-phosphate-coordinating species of sugar-phosphate complexes with the Pd^{II}(tmen) metal fragment. The correlation is described by the linear equation δ_{obs} (^{13}C)/ppm = 0.98642 · δ_{calc} (^{13}C)/ppm – 1.04203.

5.4 Crystal-structure determination and refinement

The suitability of the crystals for analysis by x-ray crystallography was checked using a polarisation microscope (Leica MZ6 with polarisation filters). The selected crystals were covered with paraffin oil and mounted on the tip of a glass fibre. They were investigated at 200 K either on a Nonius Kappa CCD diffractometer or an Oxford XCalibur 3 diffractometer with graphite-monochromated Mo K_α radiation (λ = 0.71073 Å). The structures were solved by direct methods (SIR97[100]) and refined by full-matrix, least-squares calculations on F^2 (SHELXL-97[101]). The analyses of the refined structures were performed using PLATON[102], the visualisations were produced using ORTEP-3[103] and SCHAKAL[104]. Further details on the structures are listed in Table 6.1 within the Appendix. The values given there are defined as follows:

$$R(F) = \frac{\sum \left| |F_o| - |F_c| \right|}{\sum |F_o|} \tag{5.1}$$

$$R_{\text{int}} = \frac{\sum \left| F_o^2 - \langle F_o \rangle^2 \right|}{\sum F_o^2} \tag{5.2}$$

$$R_w(F^2) = \sqrt{\frac{\sum w\left(F_o^2 - F_c^2\right)^2}{\sum w\left(F_o^2\right)^2}} \tag{5.3}$$

$$S = \sqrt{\frac{\sum w\left(F_o^2 - F_c^2\right)^2}{N_{\text{hkl}} - N_{\text{parameter}}}} \tag{5.4}$$

The weighting factors *w* and *P* are defined as follows:

$$w = \frac{1}{\sigma^2\left(F_o^2\right) + \left(xP\right)^2 + yP} \tag{5.5}$$

$$P = \frac{\max\left(F_o^2, 0\right) + 2F_c^2}{3} \tag{5.6}$$

In analogy to SHELXL-97, the values of the parameters *x* and *y* were adopted to minimise the variance of $w\left(F_c^2 / F_o^2\right)$ for several (intensity-ordered) groups of reflexes.

The coefficient U_{eq} is defined as:

$$U_{\text{eq}} = \frac{1}{3}\sum_{i=1}^{3}\sum_{j=1}^{3} U_{ij} a_i a_j a_i^* a_j^* \tag{5.7}$$

5.5 Preparation of the precursor compounds

5.5.1 *trans*-[$ReOCl_3(PPh_3)_2$]

The preparation was based on a published procedure.[105] Ammonium perrhenate (2.68 g, 10.00 mmol) and concentrated hydrochloric acid (20 mL) were heated in ethanol (100 mL) under reflux until the perrhenate was dissolved. After adding a solution of triphenylphosphane (15.74 g, 60.00 mmol) in hot ethanol (40 mL at 60 °C), the clear solution immediately turned into a green-yellow suspension. After 1/2 h of reflux, a yellow solid of *trans*-[$ReOCl_3(PPh_3)_2$] was filtered off and washed twice with hot ethanol and acetone. The yield was 7.52 g (90%). Elemental Analysis: calcd. for $C_{36}H_{31}Cl_3OP_2Re$: C, 51.90; H, 3.63; Cl, 12.77; found: C, 52.02; H, 3.66; Cl, 12.35.

5.5.2 [$Pd(en)Cl_2$]

The preparation was based on a published procedure.[106] Concentrated hydrochloric acid (10 mL) was added to a brown suspension of palladium(II) chloride (10.16 g, 57.40 mmol) in water (50 mL). Two thirds of a solution of ethane-1,2-diamine (13.5 mL, 202 mmol) in water (30 mL) were added dropwise, yielding a pink precipitate which dissolved after warming to 60 °C and the addition of the remaining ethane-1,2-diamine solution. The mixture was filtrated and adjusted to pH 2 with half-concentrated hydrochloric acid. The reaction tube was stored at 0 °C with a yellow precipitate of [$Pd(en)Cl_2$] forming after 2 h which was filtered off and dried. The remaining solution was again adjusted to pH 2. Further product precipitated in the course of 2 h. The combined yellow solids were dried *in vacuo*. The yield was 9.95 g (73 %). Elemental Analysis: calcd. for $C_2H_8N_2Cl_2Pd$: C, 10.12; H, 3.40; N, 11.80; Cl, 29.86; found: C, 10.15; H, 3.41; N, 11.67; Cl, 29.87.

5.5.3 [$Pd(en)(OH)_2$] (0.3 M)

The preparation was based on a published procedure.[36] A suspension of [$Pd(en)Cl_2$] (1.07 g, 4.50 mmol) and silver(I) oxide (1.15 g, 4.95 mmol) in H_2O (15 mL) was stirred under nitrogen and the exclusion of light at 40 °C for 30 min. AgCl was subsequently removed by filtration through a G4 filter under nitrogen atmosphere, yielding a clear, yellow solution of [$Pd(en)(OH)_2$] (“Pd-en”). The 0.3 M alkaline solution was stored at −60 °C. D_2O was used instead of H_2O for the preparation of [$Pd(en)(OD)_2$]. $^{13}C\{^1H\}$ NMR (D_2O): δ [ppm] = 45.4.

5.5.4 [$Pd(tmen)Cl_2$]

The preparation was based on a published procedure.[36] Concentrated hydrochloric acid (2.50 mL) was added to a brown suspension of palladium(II) chloride (2.50 g, 14.10 mmol) in water

(85 mL). The mixture was stirred for 30 min, yielding a brown solution. A yellow precipitate of [Pd(tmen)Cl_2] formed on the dropwise addition of *N*,*N*,*N'*,*N'*-tetramethylethane-1,2-diamine (3.25 g, 27.97 mmol) in water (90 mL) under stirring. The yellow complex was filtered off after being stirred for 30 min, washed with cold water and dried *in vacuo*. The yield was 3.84 g (93%). Elemental Analysis: calcd. for $C_6H_{16}N_2Cl_2Pd$: C, 24.55; H, 5.49; N, 9.54; Cl, 24.16; found: C, 24.37; H, 5.36; N, 9.50; Cl, 24.12.

5.5.5 [Pd(tmen)$(OH)_2$] (0.3 M)

The preparation was based on a published procedure.[36] A suspension of [Pd(tmen)Cl_2] (1.32 g, 4.50 mmol) and silver(I) oxide (1.15 g, 4.95 mmol) in H_2O (15 mL) was stirred under nitrogen and the exclusion of light at 40 °C for 30 min. AgCl was subsequently removed by filtration through a G4 filter under nitrogen atmosphere, yielding a clear, yellow solution of [Pd(tmen)$(OH)_2$] ("Pd-tmen"). The 0.3 M alkaline solution was stored at −60 °C. D_2O was used instead of H_2O for the preparation of [Pd(tmen)$(OH)_2$]. $^{13}C\{^1H\}$ NMR (D_2O): δ [ppm] = 50.2 (4C, CH_3), 62.1 (2C, CH_2).

5.5.6 Zinc(II) hydroxide

A solution of sodium hydroxide (83.0 mg, 2.08 mmol) in water (5 mL) was added under stirring to a solution of zinc(II) chloride (0.14 g, 1.03 mmol) in water (10 mL), yielding a colourless precipitate of zinc(II) hydroxide which was filtered off and washed with water. It was used immediately for further experiments.

5.5.7 Disodium D-ribose 5-phosphate hydrate

The preparation was based on a published procedure.[107] Adenosine 5'-monophosphate monohydrate (2.00 g, 5.00 mmol) and Dowex (H^+, 50W-X8) (19.60 g) were heated in water (40 mL) under reflux until the AMP was dissolved. The solution was cooled down to RT after stirring for 10 min and the ion-exchange resin was filtered off. The filtrate was cooled down to 4 °C and its pH was adjusted to 7.5 by adding sodium hydroxide solution (1 M). After reducing the solvent to 10 mL *in vacuo*, it was completely removed by freeze-drying, yielding an orange powder of disodium D-ribose 5-phosphate hydrate. The yield was 1.28 g (85%). $^{13}C\{^1H\}$ NMR (D_2O): δ [ppm] = 64.3 (α-C5), 65.2 (β-C5), 70.1 (α-C3), 71.4 (α-C2), 71.3 (β-C3), 76.0 (β-C2), 82.6 (β-C4), 83.3 (α-C4), 97.0 (α-C1), 101.7 (β-C1). $^{31}P\{^1H\}$ NMR (D_2O): δ [ppm] = 5.3 (α-P5, β-P5).

5.6 Preparation of the crystalline complex compounds

5.6.1 [ReO(tmen)(*rac*-Glyc2,3H$_{-2}$1*P*H-κ^3*O*^{2,3,P})] (2a) · 2 H_2O

Disodium *rac*-glycerol 1-phosphate hydrate (108 mg, 0.50 mmol), *trans*-[$ReOCl_3(PPh_3)_2$] (418 mg, 0.50 mmol), *N*,*N*,*N'*,*N'*-tetramethylethane-1,2-diamine (75.0 µL, 0.50 mmol), and NEt_3 (139 µL, 1.00 mmol) in 250 mL methanol were stirred at RT for 48 hours, yielding a clear, blue solution. A blue residue was obtained by removing the solvent which was redissolved in acetone (40 mL). After removing colourless crystals by filtration, blue crystals of [ReO(tmen)(*rac*-Glyc2,3H$_{-2}$1*P*H-κ^3*O*^{2,3,P})] · 2 H_2O formed within 5 hours at RT. The yield was 75 mg (29%).

^{1}H NMR (D_2O): δ [ppm] = 3.91 (dd, 1H, H3a, $^3J_{2,3}$ 6.2 Hz, $^2J_{3a,3b}$ 10.3 Hz), 4.56 (d, 1H, H3b), 4.61–4.76 (m, 3H, H1a, H1b, H2).

^{13}C NMR (D_2O): δ [ppm] = 53.9–60.7 (4C, $CH_{3,\ tmen}$), 71.0–71.6 (2C, $CH_{2,\ tmen}$), 73.0 (C1), 87.6 (C3), 90.6 (C2).

^{31}P NMR (D_2O): δ [ppm] = 0.2.

MS (FAB^+): *m*/*z* = calcd. for $C_9H_{23}O_7N_2P\ ^{185}Re\ [M + H]^+$: 487.0773; found: 487.0726, *m*/*z* = calcd. for $C_9H_{23}O_7N_2P^{187}Re\ [M + H]^+$: 489.0801; found: 489.0803.

5.6.2 [ReO(phen)(*rac*-Glyc2,3H$_{-2}$1*P*H-κ^3*O*^{2,3,P})] (2c) · MeOH

A suspension of disodium *rac*-glycerol 1-phosphate hydrate (108 mg, 0.50 mmol), *trans*-[$ReOCl_3(PPh_3)_2$] (418 mg, 0.50 mmol), 1,10-phenanthroline monohydrate (90.1 mg, 0.50 mmol), and NEt_3 (139 µL, 1.00 mmol) in 250 mL methanol was stirred at RT for 48 hours, yielding a clear, yellow-brown solution. A brown residue was obtained by removing the solvent which was washed with acetone and redissolved in methanol (80 mL). Green crystals of [ReO(phen)(*rac*-Glyc2,3H$_{-2}$1*P*H-κ^3*O*^{2,3,P})] · MeOH formed within 2 weeks at 4 °C. The yield was 71 mg (24%).

MS (FAB^+): *m*/*z* = calcd. for $C_{15}H_{15}O_7N_2P^{185}Re\ [M + H]^+$: 551.0147; found: 551.0163, calcd. for $C_{15}H_{15}O_7N_2P^{187}Re\ [M + H]^+$: 553.0175; found: 553.0220.

5.7 Preparation of the complex compounds in solution

5.7.1 [ReO(tmen)(β-D-Fru2,3H$_{-2}$1,6P_2H_2-κ^3*O*^{2,3,P1})]$^-$ (1a)

A suspension of *N*,*N*,*N'*,*N'*-tetramethylethane-1,2-diamine (75.0 µL, 0.50 mmol), trisodium D-fructose 1,6-bis-phosphate octahydrate (176 mg, 0.50 mmol), *trans*-[$ReOCl_3(PPh_3)_2$] (418 mg, 0.50 mmol), and NEt_3 (208 µL, 1.50 mmol) in 250 mL methanol was stirred at RT for 48

hours, yielding a clear, blue solution. A blue residue containing Na[ReO(tmen)(β-D-Fru2,3H$_{-2}$1,6P_2H$_2$-κ$^3O^{2,3,P1}$)] was obtained after removing the solvent. It was washed with acetone and dissolved in methanol-d$_4$ for NMR investigation.

^{1}H NMR (CD_3OD): δ [ppm] = 5.32–5.53 (m, 3H, H5, H6a, H6b), 5.41 (t, 1H, H4, $^3J_{3,4}$ 6.7 Hz, $^3J_{4,5}$ 7.3 Hz), 5.77 (dd, 1H, H1a, $^3J_{1a,P}$ 23.8 Hz, $^2J_{1a,1b}$ 11.2 Hz), 5.99 (dd, 1H, H1b, $^3J_{1b,P}$ 7.9 Hz), 6.11 (d, 1H, H3).

^{13}C NMR (CD_3OD): δ [ppm] = 67.6 (C6), 72.5 (C1), 75.9 (C4), 85.2 (C5), 104.1 (C3), 122.6 (C2).

^{31}P NMR (CD_3OD): δ [ppm] = 0.1 (P1), 2.9 (P6).

MS (FAB$^+$): m/z = 656.8 [M − Na + 2H]$^+$, 678.7 [M + H]$^+$, 700.7 [M + Na]$^+$, 757.8 [M − Na + 2H + NEt_3]$^+$, 772.8 [M − Na + 2H + tmen]$^+$.

MS (FAB$^-$): m/z = 676.8 [M − H]$^-$, 654.8 [M − Na]$^-$, 560.7 [M − H − tmen]$^-$, 538.7 [M − Na − tmen]$^-$.

5.7.2 [ReO(en)(β-D-Fru2,3H$_{-2}$1,6P_2H$_2$-κ$^3O^{2,3,P1}$)]$^-$ (1b)

A suspension of ethane-1,2-diamine (33.4 µL, 0.50 mmol), trisodium D-fructose 1,6-bisphosphate octahydrate (176 mg, 0.50 mmol), *trans*-[$ReOCl_3(PPh_3)_2$] (418 mg, 0.50 mmol), and NEt_3 (208 µL, 1.50 mmol) in 250 mL methanol was stirred at RT for 48 hours, yielding a clear, brown solution containing the product complex [ReO(en)(β-D-Fru2,3H$_{-2}$1,6P_2H$_2$-κ$^3O^{2,3,P1}$)]$^-$. The solvent was reduced to 4–5 mL, yielding a concentrated brown solution which was immediately investigated by NMR spectroscopy.

^{1}H NMR (CH_3OH): δ [ppm] = 3.89–4.07 (m, 3H, H5, H6a, H6b), 4.04 (dd, 1H, H4, $^3J_{3,4}$ 6.3 Hz, $^3J_{4,5}$ 7.4 Hz), 4.18 (dd, 1H, H1a, $^3J_{1a,P}$ 24.2 Hz, $^2J_{1a,1b}$ 11.1 Hz), 4.44 (dd, 1H, H1b, $^3J_{1b,P}$ 6.1 Hz), 4.71 (d, 1H, H3).

^{13}C NMR (CH_3OH): δ [ppm] = 67.3 (C6), 72.4 (C1), 76.9 (C4), 85.1 (C5), 101.6 (C3), 122.5 (C2).

^{31}P NMR (CH_3OH): δ [ppm] = 2.0 (P1), 3.1 (P6).

5.7.3 [ReO{(*R*,*R*)-chxn}(β-D-Fru2,3H$_{-2}$1,6P_2H$_2$-κ$^3O^{2,3,P1}$)]$^-$ (1c)

A suspension of (1*R*,2*R*)-cyclohexane-1,2-diamine (60.0 µL, 0.50 mmol), trisodium D-fructose 1,6-bisphosphate octahydrate (176 mg, 0.50 mmol), *trans*-[$ReOCl_3(PPh_3)_2$] (418 mg, 0.50 mmol), and NEt_3 (208 µL, 1.5 mmol) in 250 mL methanol was stirred at RT for 48 hours, yielding a clear, brown solution containing the product complex [ReO{(*R*,*R*)-chxn}(β-D-Fru2,3H$_{-2}$1,6P_2H$_2$-κ$^3O^{2,3,P1}$)]$^-$. The solvent was reduced to 4–5 mL, yielding a concentrated brown solution which was immediately investigated by NMR spectroscopy.

^{1}H NMR (CH_3OH): δ [ppm] = 3.87–4.08 (m, 4H, H4, H5, H6a, H6b), 4.18 (dd, 1H, H1a, $^{3}J_{1a,P}$ 24.1 Hz, $^{2}J_{1a,1b}$ 11.1 Hz), 4.45 (dd, 1H, H1b, $^{3}J_{1b,P}$ 6.3 Hz), 4.72 (d, 1H, H3, $^{3}J_{3,4}$ 6.3).

^{13}C NMR (CH_3OH): δ [ppm] = 67.8 (C6), 72.7 (C1), 77.1 (C4), 85.5 (C5), 102.3 (C3), 122.9 (C2).

^{31}P NMR (CH_3OH): δ [ppm] = 2.4 (P1), 3.1 (P6).

5.7.4 [ReO(en)(*rac*-Glyc2,3H$_{-2}$1*P*H-κ^{3}*O*^{2,3,P})] (2b)

A suspension of disodium *rac*-glycerol 1-phosphate hydrate (108 mg, 0.50 mmol), *trans*-[$ReOCl_3(PPh_3)_2$] (418 mg, 0.50 mmol), ethane-1,2-diamine (33.4 µL, 0.05 mmol), and NEt_3 (139 µL, 1.00 mmol) in 250 mL methanol was stirred at RT for 48 hours, yielding a clear, blue solution which turned brown after reducing the solvent to 4–5 mL. The brown solution containing the product complex [ReO(en)(*rac*-Glyc2,3H$_{-2}$1*P*H-κ^{3}*O*^{2,3,P})] was immediately investigated by NMR spectroscopy.

^{13}C NMR (CH_3OH): δ [ppm] = 72.3 (C1), 86.1 (C3), 91.6 (C2).

5.7.5 Complexes of α-D-glucose 1-phosphate with the Pd^{II}(tmen) fragment

Disodium α-D-glucose 1-phosphate tetrahydrate (38 mg, 0.1 mmol) was dissolved in 1 mL Pd-tmen (0.3 M solution in D_2O). For experiments at lower pH, 150 µL (0.30 mmol) nitric acid (2 M) were added. The yellow solutions were stirred under ice cooling for 2–3 hours and subsequently stored at −60 °C.

[Pd(tmen)(α-D-Glc*p*1*P*2,3H$_{-2}$-κ^{2}*O*^{2,3})]$^{2-}$ (3a)

^{1}H NMR (D_2O): δ [ppm] = 3.29 (t, 1H, H4, $^{3}J_{3,4}$ 9.5 Hz, $^{3}J_{4,5}$ 9.8 Hz), 3.31–3.38 (m, 1H, H2), 3.59 (t, 1H, H3, $^{3}J_{2,3}$ 9.2 Hz), 3.62–3.68 (m, 2H, H5, H6a), 3.79–3.86 (m, 1H, H6b), 5.31 (dd, 1H, H1, $^{3}J_{1,2}$ 3.4 Hz, $^{3}J_{1,P}$ 7.2 Hz).

^{13}C NMR (D_2O): δ [ppm] = 61.4 (C6), 72.5 (C5), 72.8 (C4), 81.4 (C3), 82.7 (C2), 94.9 (C1).

^{31}P NMR (D_2O): δ [ppm] = 3.7.

[Pd(tmen)(α-D-Glc*p*1*P*3,4H$_{-2}$-κ^{2}*O*^{3,4})]$^{2-}$ (3b)

^{1}H NMR (D_2O): δ [ppm] = 2.99 (t, 1H, H4, $^{3}J_{3,4}$ 9.5 Hz, $^{3}J_{4,5}$ 10.0 Hz), 3.26–3.38 (m, 2H, H2, H6a), 3.60 (t, 1H, H3, $^{3}J_{2,3}$ 9.3 Hz), 3.62–3.69 (m, 1H, H6b), 3.79–3.86 (m, 1H, H5), 5.22 (dd, 1H, H1, $^{3}J_{1,2}$ 3.6 Hz, $^{3}J_{1,P}$ 7.5 Hz).

^{13}C NMR (D_2O): δ [ppm] = 61.7 (C6), 74.6 (C5), 75.0 (C2), 80.0 (C4), 83.1 (C3), 94.4 (C1).

^{31}P NMR (D_2O): δ [ppm] = 4.0.

[{Pd(tmen)}$_2${μ-(α-D-Glc*p*1*P*-κ*O*^{P}:κ*O*'^{P})}$_2$] (3c)

^{1}H NMR (D_2O): δ [ppm] = 3.50 (t, 1H, H4, $^3J_{3,4}$ 9.1 Hz, $^3J_{4,5}$ 10.1 Hz), 3.63 (dt, 1H, H2, $^3J_{1,2}$ 3.5 Hz, $^3J_{2,3}$ 9.8 Hz, $^4J_{2,P}$ 2.4 Hz), 3.81 (t, 1H, H3), 3.79–3.89 (m, 2H, H6a, H6b), 3.96 (ddd, 1H, H5, $^3J_{5,6a}$ 5.1 Hz, $^3J_{5,6b}$ 2.2 Hz), 5.55 (dd, 1H, H1, $^3J_{1,P}$ 7.2 Hz).

^{13}C NMR (D_2O): δ [ppm] = 61.1 (C6), 70.0 (C4), 72.1 (C2), 73.5 (C3), 73.5 (C5), 95.5 (C1).

^{31}P NMR (D_2O): δ [ppm] = 11.2.

5.7.6 Complexes of *rac*-glycerol 1-phosphate with the Pd^{II}(tmen) fragment

Disodium *rac*-glycerol 1-phosphate hydrate (22 mg, 0.1 mmol) was dissolved in 1 mL Pd-tmen (0.3 M solution in D_2O). For experiments at lower pH, 75.0–150 μL (0.15–0.30 mmol) nitric acid (2 M) were added. The yellow solutions were stirred under ice cooling for 2–3 hours and subsequently stored at −60 °C.

[Pd(tmen)(*rac*-Glyc1*P*2,3H$_{-2}$-κ^2*O*^{2,3})]$^{2-}$ (4a)

^{1}H NMR (D_2O): δ [ppm] = 3.14–3.20 (m, 1H, H3a), 3.37–3.44 (m, 2H, H2, H3b), 3.83–3.90 (m, 1H, H1a), 4.10–4.17 (m, 1H, H1b).

^{13}C NMR (D_2O): δ [ppm] = 65.6 (C1), 71.6 (C3), 80.0 (C2).

^{31}P NMR (D_2O): δ [ppm] = 5.5.

[{Pd(tmen)}$_4${μ-(*rac*-Glyc1*P*H$_{-2}$-κ^2*O*^{2,3}:κ*O*^{P}:κ*O*'^{P})}$_2$] (4b)

^{1}H NMR (D_2O): δ [ppm] = 3.24–3.29 (m, 1H, H3a), 3.45–3.52 (m, 2H, H2, H3b), 4.08–4.15 (m, 1H, H1a), 4.28–4.34 (m, 1H, H1b).

^{13}C NMR (D_2O): δ [ppm] = 66.6 (C1), 71.6 (C3), 79.6 (C2).

^{31}P NMR (D_2O): δ [ppm] = 12.0.

[{Pd(tmen)}$_2${μ-(*rac*-Glyc1*P*-κ*O*^{P}:κ*O*'^{P})}$_2$] (4c)

^{1}H NMR (D_2O): δ [ppm] = 3.69–3.82 (m, 2H, H3a, H3b), 3.98–4.15 (m, 3H, H1a, H1b, H2).

^{13}C NMR (D_2O): δ [ppm] = 62.9 (C3), 66.7 (C1), 71.6 (C2).

^{31}P NMR (D_2O): δ [ppm] = 12.2.

5.7.7 Complexes of D-glucose 6-phosphate with the Pd^{II}(tmen) fragment

Disodium D-glucose 6-phosphate hydrate (30 mg, 0.1 mmol) was dissolved in 1 mL Pd-tmen (0.3 M solution in D_2O). For experiments at lower pH, 75.0–150 μL (0.15–0.30 mmol) nitric acid (2 M) were added. The yellow solutions were stirred at 8 °C for various periods of time between 2–24 hours and subsequently stored at −60 °C.

[{Pd(tmen)}$_2$(α-D-Glc*p*6*P*1,2;3,4H$_{-4}$-κ^2*O*^{1,2}:κ^2*O*^{3,4})]$^{2-}$ (5a)

^{1}H NMR (D_2O): δ [ppm] = 2.70 (m, 1H, H2), 2.93 (t, 1H, H4, $^3J_{4,5}$ 9.5 Hz), 3.68 (ddd, 1H, H6a, $^3J_{5,6a}$ 7.3 Hz, $^3J_{6a,P}$ 3.6 Hz, $^2J_{6a,6b}$ −11.5 Hz), 3.93–4.00 (m, 2H, H5, H6b), 4.87 (dd, 1H, H3, $^3J_{2,3}$ 8.4 Hz, $^3J_{3,4}$ 9.4 Hz), 4.88 (d, 1H, H1, $^3J_{1,2}$ 4.2 Hz).

^{13}C NMR (D_2O): δ [ppm] = 64.0 (C6), 72.9 (C5), 78.7 (C4), 84.9 (C2), 89.9 (C3), 102.1 (C1).

^{31}P NMR (D_2O): δ [ppm] = 5.7.

[{Pd(tmen)}$_2$(β-D-Glc*p*6*P*1,2;3,4H$_{-4}$-κ^2*O*^{1,2}:κ^2*O*^{3,4})]$^{2-}$ (5b)

^{1}H NMR (D_2O): δ [ppm] = 2.90–2.96 (m, 1H, H4), 3.06 (dd, 1H, H2, $^3J_{1,2}$ 7.3 Hz, $^3J_{2,3}$ 9.1 Hz), 3.39 (t, 1H, H3, $^3J_{3,4}$ 8.9 Hz), 3.43 (ddd, 1H, H5, $^3J_{4,5}$ 8.4 Hz, $^3J_{5,6a}$ 7.9 Hz, $^3J_{5,6b}$ 1.9 Hz), 3.58 (ddd, 1H, H6a, $^3J_{6a,P}$ 4.7 Hz, $^2J_{6a,6b}$ −11.5 Hz), 3.96 (ddd, 1H, H6b, $^3J_{6b,P}$ 5.1 Hz), 4.23 (d, 1H, H1).

^{13}C NMR (D_2O): δ [ppm] = 64.7 (C6), 76.5 (C5), 80.0 (C4), 86.4 (C2), 88.3 (C3), 105.5 (C1).

^{31}P NMR (D_2O): δ [ppm] = 5.7.

[Pd(tmen)(α-D-Glc*p*6*P*1,2H$_{-2}$-κ^2*O*^{1,2})]$^{2-}$ (5c)

^{1}H NMR (D_2O): δ [ppm] = 2.82 (dd, 1H, H2, $^3J_{1,2}$ 3.7 Hz, $^3J_{2,3}$ 9.2 Hz), 3.53 (dd, 1H, H4, $^3J_{3,4}$ 9.8 Hz, $^3J_{4,5}$ 9.7 Hz), 3.78–3.91 (m, 2H, H5, H6a), 4.07 (ddd, 1H, H6b, $^3J_{5,6b}$ 5.9 Hz, $^3J_{6b,P}$ 3.1 Hz, $^2J_{6a,6b}$ −11.9 Hz), 4.84 (t, 1H, H3), 5.12 (d, 1H, H1).

^{13}C NMR (D_2O): δ [ppm] = 63.3 (C6), 69.5 (C4), 71.2 (C5), 78.3 (C3), 82.3 (C2), 102.6 (C1).

^{31}P NMR (D_2O): δ [ppm] = 6.3.

[Pd(tmen)(β-D-Glc*p*6*P*1,2H$_{-2}$-κ^2*O*^{1,2})]$^{2-}$ (5d)

^{1}H NMR (D_2O): δ [ppm] = 3.12 (dd, 1H, H2, $^3J_{1,2}$ 7.5 Hz, $^3J_{2,3}$ 9.0 Hz), 3.32–3.44 (m, 4H, H3, H4, H5, H6a), 3.91–4.00 (m, 1H, H6b), 4.42 (d, 1H, H1).

^{13}C NMR (D_2O): δ [ppm] = 63.8 (C6), 70.1 (C4), 76.4 (C3), 76.8 (C5), 84.4 (C2), 105.1 (C1).

^{31}P NMR (D_2O): δ [ppm] = 6.1.

[{Pd(tmen)}$_4${μ-(α-D-Glc*p*6*P*1,2H$_{-2}$-κ^2*O*^{1,2}:κ*O*^{P}:κ*O*'^{P})}$_2$] (5e)

^{1}H NMR (D_2O): δ [ppm] = 2.79 (dd, 1H, H2, $^3J_{1,2}$ 3.7 Hz, $^3J_{2,3}$ 9.0 Hz), 3.51 (dd, 1H, H4, $^3J_{3,4}$ 9.1 Hz, $^3J_{4,5}$ 9.8 Hz), 3.95–4.01 (m, 1H, H5), 4.11–4.26 (m, 2H, H6a, H6b), 4.87 (dd, 1H, H3), 5.14 (d, 1H, H1).

^{13}C NMR (D_2O): δ [ppm] = 64.8 (C6), 69.8 (C4), 70.9 (C5), 78.5 (C3), 82.2 (C2), 102.6 (C1).

^{31}P NMR (D_2O): δ [ppm] = 12.1.

[{Pd(tmen)}$_2${μ-(α-D-Glc*p*6*P*-κ*O*^{P}:κ*O*'^{P})}$_2$] (5f)

^{1}H NMR (D_2O): δ [ppm] = 3.48–3.53 (m, 2H, H2, H4), 3.73 (t, 1H, H3, $^3J_{2,3}$ 9.4 Hz, $^3J_{3,4}$ 9.6 Hz), 3.81 (t, 1H, H3), 3.93–3.99 (m, 1H, H5), 4.08–4.31 (m, 2H, H6a, H6b), 5.22 (d, 1H, H1, $^3J_{1,2}$ 3.7 Hz).

^{13}C NMR (D_2O): δ [ppm] = 64.7 (C6), 69.9 (C4), 71.4 (C5), 72.3 (C2), 73.2 (C3), 92.8 (C1).

^{31}P NMR (D_2O): δ [ppm] = 12.0.

[{Pd(tmen)}$_2${μ-(β-D-Glc*p*6*P*-κ*O*^{P}:κ*O*'^{P})}$_2$] (5g)

^{1}H NMR (D_2O): δ [ppm] = 3.22 (dd, 1H, H2, $^3J_{1,2}$ 8.0 Hz, $^3J_{2,3}$ 9.4 Hz), 3.49–3.62 (m, 3H, H3, H4, H5), 4.09–4.16 (m, 1H, H6a), 4.29 (ddd, 1H, H6b, $^3J_{5,6b}$ 4.7 Hz, $^3J_{6b,P}$ 4.4 Hz, $^2J_{6a,6b}$ −11.4 Hz), 4.67 (d, 1H, H1).

^{13}C NMR (D_2O): δ [ppm] = 64.8 (C6), 69.8 (C4), 74.9 (C2), 75.6 (C5), 76.2 (C3), 96.7 (C1).

^{31}P NMR (D_2O): δ [ppm] = 11.9.

5.7.8 Complexes of D-glucose 6-phosphate with the Pd^{II}(en) fragment

Disodium D-glucose 6-phosphate hydrate (30 mg, 0.1 mmol) was dissolved in 1 mL Pd-en (0.3 M solution in D_2O). The yellow solution was stirred at 8 °C for various periods of time between 2–24 hours and subsequently stored at −60 °C.

[{Pd(en)}$_2$(α-D-Glc*p*6*P*1,2;3,4H$_{-4}$-κ^2*O*^{1,2}:κ^2*O*^{3,4})]$^{2-}$ (6a)

^{1}H NMR (D_2O): δ [ppm] = 2.72 (dd, 1H, H2, $^3J_{1,2}$ 3.7 Hz, $^3J_{2,3}$ 9.0 Hz), 2.97 (t, 1H, H4, $^3J_{3,4}$ 9.3 Hz, $^3J_{4,5}$ 9.4 Hz), 3.67 (ddd, 1H, H6a, $^3J_{5,6a}$ 6.1 Hz, $^3J_{6a,P}$ 4.0 Hz, $^2J_{6a,6b}$ −11.1 Hz), 3.78 (ddd, 1H, H5, $^3J_{5,6b}$ 2.0 Hz), 3.86–3.91 (m, 1H, H6b), 4.31 (t, 1H, H3), 4.94 (d, 1H, H1).

^{13}C NMR (D_2O): δ [ppm] = 63.7 (C6), 74.7 (C5), 79.3 (C4), 84.9 (C2), 87.0 (C3), 103.0 (C1).

^{31}P NMR (D_2O): δ [ppm] = 5.5.

[{Pd(en)}$_2$(β-D-Glc*p*6*P*1,2;3,4H$_{-4}$-κ^2*O*^{1,2}:κ^2*O*^{3,4})]$^{2-}$ (6b)

^{1}H NMR (D_2O): δ [ppm] = 2.97 (dd, 1H, H2, $^3J_{1,2}$ 7.3 Hz, $^3J_{2,3}$ 9.3 Hz), 3.01 (dd, 1H, H4, $^3J_{3,4}$ 9.2 Hz, $^3J_{4,5}$ 9.4 Hz), 3.38 (ddd, 1H, H3), 3.43 (ddd, 1H, H5, $^3J_{5,6a}$ 7.4 Hz, $^3J_{5,6b}$ 2.0 Hz), 3.60 (ddd, 1H, H6a, $^3J_{6a,P}$ 4.0 Hz, $^2J_{6a,6b}$ −11.2 Hz), 3.86–3.91 (m, 1H, H6b), 4.28 (d, 1H, H1).

^{13}C NMR (D_2O): δ [ppm] = 64.3 (C6), 76.5 (C5), 80.7 (C4), 85.6 (C2), 87.6 (C3), 106.5 (C1).

^{31}P NMR (D_2O): δ [ppm] = 5.7.

5.7.9 Complexes of D-glucose with the Pd^{II}(tmen) fragment

D-Glucose monohydrate (20 mg, 0.1 mmol) was dissolved in 1 mL Pd-tmen (0.3 M solution in D_2O). The yellow solution was stirred at 8 °C for various periods of time between 2–24 hours and subsequently stored at −60 °C.

[{Pd(tmen)}$_2$(α-D-Glc*p*1,2;3,4H$_{-4}$-κ^2*O*^{1,2}:κ^2*O*^{3,4})] (7a)

^{1}H NMR (D_2O): δ [ppm] = 2.88 (dd, 1H, H4, $^3J_{3,4}$ 8.9 Hz, $^3J_{4,5}$ 9.7 Hz), 3.86 (ddd, 1H, H5, $^3J_{5,6a}$ 2.6 Hz, $^3J_{5,6b}$ 5.5 Hz), 4.85 (t, 1H, H3, $^3J_{2,3}$ 8.8 Hz), 4.88 (d, 1H, H1, $^3J_{1,2}$ 3.9 Hz).

^{13}C NMR (D_2O): δ [ppm] = 73.3 (C5), 78.4 (C4), 85.0 (C2), 89.8 (C3), 102.2 (C1).

[{Pd(tmen)}$_2$(β-D-Glc*p*1,2;3,4H$_{-4}$-κ^2*O*^{1,2}:κ^2*O*^{3,4})] (7b)

^{1}H NMR (D_2O): δ [ppm] = 2.94 (t, 1H, H4, $^3J_{3,4}$ 9.1 Hz, $^3J_{4,5}$ 9.5 Hz), 3.04 (dd, 1H, H2, $^3J_{1,2}$ 7.3 Hz, $^3J_{2,3}$ 9.1 Hz), 3.29 (ddd, 1H, H5, $^3J_{5,6a}$ 6.8 Hz, $^3J_{5,6b}$ 2.5 Hz), 3.36 (t, 1H, H3), 3.54 (dd, 1H, H6a, $^2J_{6a,6b}$ −12.4 Hz), 3.74 (dd, 1H, H6b), 4.22 (d, 1H, H1).

^{13}C NMR (D_2O): δ [ppm] = 76.8 (C5), 79.9 (C4), 86.6 (C2), 88.0 (C3), 105.7 (C1).

[Pd(tmen)(α-D-Glc*p*1,2H$_{-2}$-κ^2*O*^{1,2})] (7c)

^{1}H NMR (D_2O): δ [ppm] = 2.77 (dd, 1H, H2, $^3J_{1,2}$ 3.9 Hz, $^3J_{2,3}$ 8.8 Hz), 3.32 (dd, 1H, H4, $^3J_{3,4}$ 9.0 Hz, $^3J_{4,5}$ 9.7 Hz), 3.86 (ddd, 1H, H5, $^3J_{5,6a}$ 2.6 Hz, $^3J_{5,6b}$ 5.5 Hz), 4.80 (t, 1H, H3), 5.12 (d, 1H, H1).

^{13}C NMR (D_2O): δ [ppm] = 70.1 (C4), 71.4 (C5), 78.9 (C3), 82.0 (C2), 102.5 (C1).

[Pd(tmen)(β-D-Glc*p*1,2H$_{-2}$-κ^2*O*^{1,2})] (7d)

^{1}H NMR (D_2O): δ [ppm] = 3.05 (dd, 1H, H2, $^3J_{1,2}$ 7.5 Hz, $^3J_{2,3}$ 9.5 Hz), 3.21 (dd, 1H, H4, $^3J_{3,4}$ 8.8 Hz, $^3J_{4,5}$ 9.8 Hz), 3.32 (ddd, 1H, H5, $^3J_{5,6a}$ 5.7 Hz, $^3J_{5,6b}$ 2.2 Hz), 3.33 (dd, 1H, H3), 3.65 (dd, 1H, H6a), 3.80 (dd, 1H, H6b), 4.41 (d, 1H, H1).

^{13}C NMR (D_2O): δ [ppm] = 70.8 (C4), 77.2 (C5), 77.3 (C3), 84.3 (C2), 104.9 (C1).

[{Pd(tmen)}$_2$(α-D-Glc*f*6*P*1,2;5,6H$_{-4}$-κ^2*O*^{1,2}:κ^2*O*^{5,6})] (7e)

^{1}H NMR (D_2O): δ [ppm] = 3.36 (dd, 1H, H6a, $^3J_{5,6a}$ 5.9 Hz, $^2J_{6a,6b}$ −12.2 Hz), 3.43 (dd, 1H, H6b, $^3J_{5,6b}$ 4.0 Hz), 3.58 (ddd, 1H, H5, $^3J_{4,5}$ 6.7 Hz), 3.65 (dd, 1H, H2, H2, $^3J_{1,2}$ 3.0 Hz, $^3J_{2,3}$ 1.4 Hz), 4.30 (dd, 1H, H3, $^3J_{3,4}$ 3.4 Hz), 4.99 (d, 1H, H1), 5.22 (dd, 1H, H4).

^{13}C NMR (D_2O): δ [ppm] = 73.2 (C6), 77.6 (C4), 80.0 (C5), 80.6 (C3), 88.9 (C2), 111.8 (C1).

5.7.10 Complexes of D-mannose 6-phosphate with the Pd^{II}(tmen) fragment

Disodium D-mannose 6-phosphate dihydrate (34 mg, 0.1 mmol) was dissolved in 1 mL Pd-tmen (0.3 M solution in D_2O). For experiments at lower pH, 75.0–150 µL (0.15–0.30 mmol) nitric acid (2 M) were added. The yellow solutions were stirred under ice cooling for 2–3 hours and subsequently stored at −60 °C.

[{Pd(tmen)}$_2$(β-D-Man*p*6*P*1,2;3,4H$_{-4}$-κ^2*O*^{1,2}:κ^2*O*^{3,4})]$^{2-}$ (8a)

^{1}H NMR (D_2O): δ [ppm] = 3.19–3.26 (m, 1H, H5), 3.34 (dd, 1H, H3, $^3J_{2,3}$ 2.6 Hz, $^3J_{3,4}$ 9.8 Hz), 3.52 (t, 1H, H4, $^3J_{4,5}$ 9.6 Hz), 3.78–3.86 (m, 1H, H6a), 3.97 (dd, 1H, H2, $^3J_{1,2}$ 1.3 Hz) 4.00–4.06 (m, 1H, H6b), 4.09 (d, 1H, H1).

^{13}C NMR (D_2O): δ [ppm] = 64.7 (C6), 76.0 (C4), 76.5 (C5), 85.1 (C3), 87.0 (C2), 107.8 (C1).

^{31}P NMR (D_2O): δ [ppm] = 5.7.

[Pd(tmen)(α-D-Man*p*6*P*2,3H$_{-2}$-κ^2*O*^{2,3})]$^{2-}$ (8b)

^{1}H NMR (D_2O): δ [ppm] = 2.95 (dd, 1H, H3, $^3J_{2,3}$ 4.0 Hz, $^3J_{3,4}$ 9.0 Hz), 3.72 (dd, 1H, H2), $^3J_{1,2}$ 1.3 Hz), 3.71–3.76 (m, 1H, H5), 3.98–4.06 (m, 2H, H6a, H6b), 4.41 (t, 1H, H4, $^3J_{4,5}$ 9.8 Hz), 4.92 (d, 1H, H1).

^{13}C NMR (D_2O): δ [ppm] = 64.1 (C6), 70.5 (C4), 72.2 (C5), 80.2 (C3), 81.9 (C2), 95.1 (C1).

^{31}P NMR (D_2O): δ [ppm] = 5.9.

[Pd(tmen)(β-D-Man*p*6*P*1,2H$_{-2}$-κ^2*O*^{1,2})]$^{2-}$ (8c)

^{1}H NMR (D_2O): δ [ppm] = 3.19–3.26 (m, 1H, H5), 3.51 (dd, 1H, H3, $^3J_{2,3}$ 3.6 Hz, $^3J_{3,4}$ 9.9 Hz), 3.80 (t, 1H, H4, $^3J_{4,5}$ 9.8), 3.78–3.86 (m, 1H, H6a), 3.95 (dd, 1H, H2, $^3J_{1,2}$ 1.4 Hz) 4.00–4.06 (m, 1H, H6b), 4.24 (d, 1H, H1).

^{13}C NMR (D_2O): δ [ppm] = 64.1 (C6), 67.6 (C4), 73.1 (C3), 75.5 (C5), 83.2 (C2), 107.1 (C1).

^{31}P NMR (D_2O): δ [ppm] = 6.1.

[{Pd(tmen)}$_4${µ-(α-D-Man*p*6*P*2,3H$_{-2}$-κ^2*O*^{2,3}:κ*O*^{P}:κ*O*'^{P})}$_2$] (8d)

^{1}H NMR (D_2O): δ [ppm] = 2.97 (dd, 1H, H3, $^3J_{2,3}$ 4.1 Hz, $^3J_{3,4}$ 8.8 Hz), 3.71–3.78 (m, 2H, H2, H5), 3.93–3.97 (m, 2H, H6a, H6b), 4.33 (dd, 1H, H4, $^3J_{4,5}$ 10.1 Hz), 4.89 (d, 1H, H1, $^3J_{1,2}$ 1.1 Hz).

^{13}C NMR (D_2O): δ [ppm] = 65.9 (C6), 70.7 (C4), 72.1 (C5), 80.3 (C3), 81.8 (C2), 94.9 (C1).

^{31}P NMR (D_2O): δ [ppm] = 11.9.

[{Pd(tmen)}$_4${μ-(β-D-Man*p*6*P*1,2H$_{-2}$-κ^2*O*^{1,2}:κ*O*^{P}:κ*O*'^{P})}$_2$] (8e)

^{1}H NMR (D_2O): δ [ppm] = 3.31–3.36 (m, 1H, H5), 3.51 (dd, 1H, H3, $^3J_{2,3}$ 3.5 Hz, $^3J_{3,4}$ 9.9 Hz), 3.83–3.87 (m, 1H, H6a), 3.87 (t, 1H, H4, $^3J_{4,5}$ 9.5 Hz), 3.89–3.92 (m, 1H, H2), 3.96–4.00 (m, 1H, H6b), 4.27 (d, 1H, H1, $^3J_{1,2}$ 1.3 Hz).

^{13}C NMR (D_2O): δ [ppm] = 66.0 (C6), 68.0 (C4), 73.4 (C3), 75.2 (C5), 83.1 (C2), 107.0 (C1).

^{31}P NMR (D_2O): δ [ppm] = 12.1.

[{Pd(tmen)}$_2${μ-(α-D-Man*p*6*P*-κ*O*^{P}:κ*O*'^{P})}$_2$] (8f)

^{1}H NMR (D_2O): δ [ppm] = 3.85–3.88 (m, 2H, H3, H4), 3.93–3.95 (m, 2H, H2, H5), 4.13–4.27 (m, 2H, H6a, H6b), 5.17 (d, 1H, H1, $^3J_{1,2}$ 1.4 Hz).

^{13}C NMR (D_2O): δ [ppm] = 64.9 (C6), 67.0 (C4), 70.7 (C3), 71.3 (C2), 72.3 (C5), 94.8 (C1).

^{31}P NMR (D_2O): δ [ppm] = 12.1.

[{Pd(tmen)}$_2${μ-(β-D-Man*p*6*P*-κ*O*^{P}:κ*O*'^{P})}$_2$] (8g)

^{1}H NMR (D_2O): δ [ppm] = 3.48–3.54 (m, 1H, H5), 3.67–3.77 (m, 2H, H2, H4), 3.93–3.95 (m, 1H, H3), 4.09–4.16 (m, 1H, H6a), 4.28–4.34 (m, 1H, H6b), 4.91 (d, 1H, H1, $^3J_{1,2}$ 1.2 Hz).

^{13}C NMR (D_2O): δ [ppm] = 65.1 (C6), 66.9 (C4), 71.3 (C3), 73.5 (C2), 75.8 (C5), 94.4 (C1).

^{31}P NMR (D_2O): δ [ppm] = 12.0.

5.7.11 Complexes of D-fructose 1-phosphate with the Pd^{II}(tmen) fragment

Barium D-fructose 1-phosphate trihydrate (41 mg, 0.1 mmol) was dissolved in 1 mL Pd-tmen (0.3 M solution in D_2O). For experiments at lower pH, 75.0–200 μL (0.15–0.40 mmol) nitric acid (2 M) were added. The yellow solutions were stirred under ice cooling for 2–3 hours and subsequently stored at −60 °C.

[{Pd(tmen)}$_2$(β-D-Fru*p*1*P*2,3;4,5H$_{-4}$-κ^2*O*^{2,3}:κ^2*O*^{4,5})]$^{2-}$ (9a)

^{1}H NMR (D_2O): δ [ppm] = 3.38–3.42 (m, 1H, H5), 3.53–3.58 (m, 1H, H4), 3.61–3.65 (m, 1H, H1a), 3.73–3.86 (m, 3H, H3, H6a, H6b), 4.75–4.81 (m, 1H, H1b).

^{13}C NMR (D_2O): δ [ppm] = 69.4 (C1), 78.3 (C5), 79.9 (C3), 83.3 (C4), 106.6 (C2).

^{31}P NMR (D_2O): δ [ppm] = 5.2.

[Pd(tmen)(α-D-Fru*p*1*P*4,5H$_{-2}$-κ^2*O*^{4,5})]$^{2-}$ (9b)

^{1}H NMR (D_2O): δ [ppm] = 3.21–3.27 (ddd, 1H, H5, $^3J_{4,5}$ 3.5 Hz, $^3J_{5,6a}$ 6.4 Hz, $^3J_{5,6b}$ 10.3 Hz), 3.40–3.46 (m, 1H, H1a), 3.74 (d, 1H, H3, $^3J_{3,4}$ 3.9 Hz), 3.74–3.82 (m, 2H, H1b, H6a), 3.93 (t, 1H, H4), 4.84 (t, 1H, H6b, $^2J_{6a,6b}$ −11.3 Hz).

^{13}C NMR (D_2O): δ [ppm] = 65.8 (C1), 66.7 (C3), 72.2 (C5), 79.7 (C4), 98.9 (C2).

^{31}P NMR (D_2O): δ [ppm] = 6.5.

[Pd(tmen)(β-D-Fru*p*1*P*2,3H$_{-2}$-κ^2*O*^{2,3})]$^{2-}$ (9c)

^{1}H NMR (D_2O): δ [ppm] = 3.20–3.26 (m, 1H, H6a), 3.72–3.78 (m, 2H, H3, H4), 3.91–3.95 (m, 1H, H5), 4.78–4.84 (m, 1H, H6b).

^{13}C NMR (D_2O): δ [ppm] = 67.7 (C1), 70.7 (C5), 75.8 (C4), 76.4 (C3), 107.8 (C2).

^{31}P NMR (D_2O): δ [ppm] = 4.8.

[Pd(tmen)(β-D-Fru*f*1*P*2,3H$_{-2}$-κ^2*O*^{2,3})]$^{2-}$ (9d)

^{1}H NMR (D_2O): δ [ppm] = 3.42–3.49 (dd, 1H, H1a, $^3J_{1a,P}$ 2.7 Hz, $^2J_{1a,1b}$ −10.8 Hz), 3.54 (d, 1H, H3, $^3J_{3,4}$ 6.3 Hz), 3.73–3.86 (m, 3H, H5, H6a, H6b), 4.01 (dd, 1H, H1b, $^3J_{1b,P}$ 5.1 Hz), 4.78 (t, 1H, H4, $^3J_{4,5}$ 6.5 Hz).

^{13}C NMR (D_2O): δ [ppm] = 63.0 (C6), 65.3 (C1), 80.2 (C4), 82.4 (C5), 87.6 (C3), 113.0 (C2).

^{31}P NMR (D_2O): δ [ppm] = 5.1.

[{Pd(tmen)}$_4${μ-(β-D-Fru*f*1*P*2,3H$_{-2}$-κ^2*O*^{2,3}:κ*O*^{P}:κ*O*'^{P})}$_2$] (9e)

^{1}H NMR (D_2O): δ [ppm] = 3.77–3.83 (m, 3H, H1a, H6a, H6b), 3.81 (d, 1H, H3, $^3J_{3,4}$ 6.5 Hz), 3.87 (dt, 1H, H5, $^3J_{4,5}$ 6.3 Hz, $^3J_{5,6a}$ 3.0 Hz, $^3J_{5,6b}$ 3.2 Hz), 4.23 (dd, 1H, H1b, $^3J_{1b,P}$ 4.3 Hz, $^2J_{1a,1b}$ −10.6 Hz), 4.92 (t, 1H, H4).

^{13}C NMR (D_2O): δ [ppm] = 65.8 (C1), 80.0 (C4), 82.7 (C5), 88.0 (C3), 112.5 (C2).

^{31}P NMR (D_2O): δ [ppm] = 11.3.

[{Pd(tmen)}$_2${μ-(β-D-Fru*p*1*P*-κ*O*^{P}:κ*O*'^{P})}$_2$] (9f)

^{1}H NMR (D_2O): δ [ppm] = 3.70 (dd, 1H, H6a, $^3J_{5,6a}$ 1.9 Hz, $^2J_{6a,6b}$ −12.8 Hz), 3.95 (d, 1H, H3, $^3J_{3,4}$ 8.3 Hz), 3.95–4.02 (m, 3H, H1a, H4, H5), 4.06 (dd, 1H, H6b, $^3J_{5,6b}$ 1.5 Hz), 4.09 (dd, 1H, H1b, $^3J_{1b,P}$ 5.3 Hz, $^2J_{1a,1b}$ −10.6 Hz).

^{13}C NMR (D_2O): δ [ppm] = 64.1 (C6), 67.3 (C1), 68.0 (C3), 69.8 (C5), 70.0 (C4), 98.5 (C2).

^{31}P NMR (D_2O): δ [ppm] = 11.7.

[{Pd(tmen)}$_2${μ-(β-D-Fru*f*1*P*-κ*O*^{P}:κ*O*'^{P})}$_2$] (9g)

^{1}H NMR (D_2O): δ [ppm] = 3.66 (dd, 1H, H6a, $^3J_{5,6a}$ 6.5 Hz, $^2J_{6a,6b}$ −12.5 Hz), 3.77–3.84 (m, 2H, H5, H6b), 4.12 (t, 1H, H4, $^3J_{3,4}$ 8.3, $^3J_{4,5}$ 7.8), 4.21 (d, 1H, H3).

^{13}C NMR (D_2O): δ [ppm] = 62.8 (C6), 64.0 (C1), 74.7 (C4), 76.2 (C3), 81.6 (C5), 101.4 (C2).

^{31}P NMR (D_2O): δ [ppm] = 11.4.

5.7.12 Complexes of D-fructose 6-phosphate with the Pd^{II}(tmen) fragment

Disodium D-fructose 6-phosphate hydrate (30 mg, 0.1 mmol) was dissolved in 1 mL Pd-tmen (0.3 M solution in D_2O). For experiments at lower pH, 75.0–150 µL (0.15–0.30 mmol) nitric acid (2 M) were added. The yellow solutions were stirred under ice cooling for 2–3 hours and subsequently stored at −60 °C.

[Pd(tmen)(β-D-Fru*f*6*P*2,3H$_{-2}$-κ^2*O*^{2,3})]$^{2-}$ (10a)

^{1}H NMR (D_2O): δ [ppm] = 3.40 (d, 1H, H1a, $^2J_{1a,1b}$ −12.0 Hz), 3,60 (d, 1H, H3, $^3J_{3,4}$ 7.3 Hz), 3.76–3.82 (m, 1H, H5), 3.77 (d, 1H, H1b), 4.05 (ddd, 1H, H6a, $^3J_{5,6a}$ 7.0 Hz, $^3J_{6a,P}$ 5.6 Hz, $^2J_{6a,6b}$ −11.0 Hz), 4,17 (ddd, 1H, H6b, $^3J_{5,6b}$ 4.0 Hz, $^3J_{6b,P}$ 5.7 Hz), 5.07 (t, 1H, H4, $^3J_{4,5}$ 8.3 Hz).

^{13}C NMR (D_2O): δ [ppm] = 64.5 (C1), 67.1 (C6), 80.0 (C5), 81.5 (C4), 87.4 (C3), 113.6 (C2).

^{31}P NMR (D_2O): δ [ppm] = 5.6.

[{Pd(tmen)}$_4${µ-(β-D-Fru*f*6*P*2,3H$_{-2}$-κ^2*O*^{2,3}:κ*O*^{P}:κ*O*'^{P})}$_2$] (10b)

^{1}H NMR (D_2O): δ [ppm] = 3.32 (d, 1H, H1a, $^2J_{1a,1b}$ −11.9 Hz), 3.53 (d, 1H, H3, $^3J_{3,4}$ 7.0 Hz), 3.73 (d, 1H, H1b), 3.78–3.85 (m, 1H, H5), 4.17–4.24 (m, 1H, H6a), 4.40 (ddd, 1H, H6b, $^3J_{5,6b}$ 4.1 Hz, $^3J_{6b,P}$ 5.3 Hz, $^2J_{6a,6b}$ −10.8 Hz), 4.90 (t, 1H, H4, $^3J_{4,5}$ 8.1 Hz).

^{13}C NMR (D_2O): δ [ppm] = 64.7 (C1), 69.0 (C6), 80.1 (C5), 81.5 (C4), 87.6 (C3), 114.2 (C2).

^{31}P NMR (D_2O): δ [ppm] = 11.8.

[{Pd(tmen)}$_2${µ-(α-D-Fru*f*6*P*-κ*O*^{P}:κ*O*'^{P})}$_2$] (10c)

^{1}H NMR (D_2O): δ [ppm] = 3.60–3.67 (m, 2H, H1a, H1b), 4.06–4.13 (m, 3H, H3, H4, H6a), 4.17–4.23 (m, 2H, H5, H6b).

^{13}C NMR (D_2O): δ [ppm] = 63.4 (C1), 65.5 (C6), 76.6 (C4), 80.7 (C5), 82.4 (C3), 105.3 (C2).

^{31}P NMR (D_2O): δ [ppm] = 11.9.

[{Pd(tmen)}$_2${µ-(β-D-Fru*f*6*P*-κ*O*^{P}:κ*O*'^{P})}$_2$] (10d)

^{1}H NMR (D_2O): δ [ppm] = 3.32 (d, 1H, H1a, $^2J_{1a,1b}$ −11.9 Hz), 3.73 (d, 1H, H1b), 3.93–4.00 (m, 1H, H5), 4.06–4.13 (m, 1H, H6a), 4.14 (d, 1H, H3, $^3J_{3,4}$ 8.5 Hz), 4.17–4.24 (m, 1H, H6b), 4.22 (t, 1H, H4, $^3J_{4,5}$ 7.6 Hz).

^{13}C NMR (D_2O): δ [ppm] = 63.1 (C1), 66.9 (C6), 75.3 (C4), 75.8 (C3), 80.3 (C5), 102.6 (C2).

^{31}P NMR (D_2O): δ [ppm] = 11.7.

5.7.13 Complexes of D-fructose 1,6-bisphosphate with the Pd^{II}(tmen) fragment

Trisodium D-fructose 1,6-bisphosphate octahydrate (55 mg, 0.1 mmol) was dissolved in 1 mL Pd-tmen (0.3 M solution in D_2O). For experiments at lower pH, 75.0–150 µL (0.15–0.30 mmol) nitric acid (2 M) were added. The yellow solutions were stirred under ice cooling for 2–3 hours and subsequently stored at −60 °C.

[Pd(tmen)(β-D-Fru*f*1,6$P_2$2,3H_{-2}-κ^2*O*^{2,3})]$^{4-}$ (11a)

^{1}H NMR (D_2O): δ [ppm] = 3.46 (dd, 1H, H1a, $^3J_{1a,P1}$ 2.9 Hz, $^2J_{1a,1b}$ −10.7 Hz), 3.60 (d, 1H, H3, $^3J_{3,4}$ 7.1 Hz), 3.76 (td, 1H, H5, $^3J_{4,5}$ 7.8 Hz, $^3J_{5,6a}$ 4.1 Hz, $^3J_{5,6b}$ 5.2 Hz), 3.95 (dd, 1H, H1b, $^3J_{1b,P1}$ 5.2 Hz, 3.95–4.03 (m, 1H, H6a), 4.06–4.13 (m, 1H, H6b), 4.85 (t, 1H, H4).

^{13}C NMR (D_2O): δ [ppm] = 66.4 (C1), 67.0 (C6), 80.0 (C5), 81.2 (C4), 87.1 (C3), 113.4 (C2).

^{31}P NMR (D_2O): δ [ppm] = 5.4 (P1), 5.7 (P6).

[{Pd(tmen)}$_4${µ-(β-D-Fru*f*1,6$P_2$2,3H_{-2}-κ^2*O*^{2,3}:κ*O*^{P6}:κ*O*'^{P6})}$_2$]$^{4-}$ (11b)

^{1}H NMR (D_2O): δ [ppm] = = 3.43–3.49 (m, 1H, H1a), 3.65 (d, 1H, H3, $^3J_{3,4}$ 6.6 Hz), 3.83–3.91 (m, 1H, H5), 3.92–3.98 (m, 1H, H1b), 4.21–4.32 (m, 1H, H6a), 4.36–4.47 (m, 1H, H6b), 4.78 (t, 1H, H4, $^3J_{4,5}$ 7.4 Hz).

^{13}C NMR (D_2O): δ [ppm] = 66.7 (C1), 68.4 (C6), 79.9 (C5), 81.3 (C4), 87.6 (C3), 114.0 (C2).

^{31}P NMR (D_2O): δ [ppm] = 5.3 (P1), 11.8 (P6).

[{Pd(tmen)}$_4${µ-(β-D-Fru*f*1,6$P_2$2,3H_{-2}-κ^2*O*^{2,3}:κ*O*^{P1}:κ*O*'^{P1})}$_2$]$^{4-}$ (11c)

^{1}H NMR (D_2O): δ [ppm] = 3.72 (dd, 1H, H1a, $^3J_{1a,P1}$ 2.8 Hz, $^2J_{1a,1b}$ −10.3 Hz), 3.72 (d, 1H, H3, $^3J_{3,4}$ 7.1 Hz), 3.74–3.80 (m, 1H, H5), 3.98–4.04 (m, 1H, H6a), 4.08–4.15 (m, 2H, H1b, H6b), 4.94 (t, 1H, H4, $^3J_{4,5}$ 7.6 Hz).

^{13}C NMR (D_2O): δ [ppm] = 67.0 (C1), 67.0 (C6), 80.3 (C5), 81.1 (C4), 87.3 (C3), 112.9 (C2).

^{31}P NMR (D_2O): δ [ppm] = 5.6 (P6), 11.5 (P1).

^{31}P NMR (CH_3OH): δ [ppm] = 4.3.

5.7.14 Complexes of D-ribose 5-phosphate with the Pd^{II}(tmen) fragment

Disodium D-ribose 5-phosphate hydrate (27 mg, 0.1 mmol) was dissolved in 1 mL Pd-tmen (0.3 M solution in D_2O). For experiments at lower pH, 75.0–150 µL (0.15–0.30 mmol) nitric acid (2 M) were added. The yellow solutions were stirred under ice cooling for 2–3 hours and subsequently stored at −60 °C.

[Pd(tmen)(α-D-Rib*f*5*P*1,2H$_{-2}$-κ^2*O*^{1,2})]$^{2-}$ (12a)

^{1}H NMR (D_2O): δ [ppm] = 3.71 (dd, 1H, H2, $^3J_{1,2}$ 3.5 Hz, $^3J_{2,3}$ 6.2 Hz), 3.90–3.99 (m, 2H, H3, H5a), 4.11 (dt, 1H, H5b, $^3J_{4,5b}$ 2.7 Hz, $^3J_{5,P}$ 3.8 Hz, $^2J_{5a,5b}$ −11.4 Hz), 4.92–4.98 (m, 1H, H4), 5.10 (d, 1H, H1).

^{13}C NMR (D_2O): δ [ppm] = 64.5 (C5), 71.7 (C3), 80.2 (C4), 81.7 (C2), 111.4 (C1).

^{31}P NMR (D_2O): δ [ppm] = 5.6.

[Pd(tmen)(β-D-Rib*f*5*P*2,3H$_{-2}$-κ^2*O*^{2,3})]$^{2-}$ (12b)

^{1}H NMR (D_2O): δ [ppm] = 3.76–3.86 (m, 3H, H2, H3, H5a), 3.99–4.04 (m, 1H, H5b), 4.64–4.69 (m, 1H, H4), 5.30 (d, 1H, H1, $^3J_{1,2}$ 1.4 Hz).

^{13}C NMR (D_2O): δ [ppm] = 66.1 (C5), 83.1 (C3), 85.6 (C4), 87.7 (C2), 103.1 (C1).

^{31}P NMR (D_2O): δ [ppm] = 5.5.

[{Pd(tmen)}$_4${μ-(α-D-Rib*f*5*P*1,2H$_{-2}$-κ^2*O*^{1,2}:κ*O*^{P}:κ*O*'^{P})}$_2$] (12c)

^{1}H NMR (D_2O): δ [ppm] = 3.72 (dd, 1H, H2, $^3J_{1,2}$ 3.4 Hz, $^3J_{2,3}$ 6.1 Hz), 3.91–4.04 (m, 2H, H3, H5a), 4.26–4.41 (m, 1H, H5b), 4.93–5.01 (m, 1H, H4), 5.13 (d, 1H, H1).

^{13}C NMR (D_2O): δ [ppm] = 65.6 (C5), 71.5 (C3), 79.9 (C4), 81.7 (C2), 111.6 (C1).

^{31}P NMR (D_2O): δ [ppm] = 11.8.

[{Pd(tmen)}$_4${μ-(β-D-Rib*f*5*P*2,3H$_{-2}$-κ^2*O*^{2,3}:κ*O*^{P}:κ*O*'^{P})}$_2$] (12d)

^{1}H NMR (D_2O): δ [ppm] = 3.76–3.91 (m, 3H, H2, H3, H5a), 3.97–4.07 (m, 1H, H5b), 4.74–4.79 (m, 1H, H4), 5.31 (d, 1H, H1, $^3J_{1,2}$ 1.3 Hz).

^{13}C NMR (D_2O): δ [ppm] = 67.6 (C5), 82.8 (C3), 85.1 (C4), 87.7 (C2), 102.8 (C1).

^{31}P NMR (D_2O): δ [ppm] = 11.7.

[{Pd(tmen)}$_2${μ-(α-D-Rib*f*5*P*-κ*O*^{P}:κ*O*'^{P})}$_2$] (12e)

^{1}H NMR (D_2O): δ [ppm] = 3.97–4.01 (m, 1H, H5a), 4.13 (dd, 1H, H3, $^3J_{2,3}$ 4.2 Hz, $^3J_{3,4}$ 5.7 Hz), 4.14–4.19 (m, 1H, H5b), 4.21 (dd, 1H, H2, $^3J_{1,2}$ 4.0 Hz) 4.26 (m, 1H, H4), 5.38 (d, 1H, H1).

^{13}C NMR (D_2O): δ [ppm] = 65.7 (C5), 70.7 (C3), 71.5 (C2), 83.3 (C4), 97.0 (C1).

^{31}P NMR (D_2O): δ [ppm] = 11.9.

[{Pd(tmen)}$_2${μ-(β-D-Rib*f*5*P*-κ*O*^{P}:κ*O*'^{P})}$_2$] (12f)

^{1}H NMR (D_2O): δ [ppm] = 4.03 (dd, 1H, H2, $^3J_{1,2}$ 1.8 Hz, $^3J_{2,3}$ 4.7 Hz), 4.06–4.20 (m, 3H, H4, H5a, H5b), 4.31 (dd, 1H, H3, $^3J_{3,4}$ 6.4 Hz), 5.25 (d, 1H, H1).

^{13}C NMR (D_2O): δ [ppm] = 66.7 (C5), 71.1 (C3), 75.8 (C2), 82.5 (C4), 101.7 (C1).

^{31}P NMR (D_2O): δ [ppm] = 11.6.

5.7.15 Reaction of ethane-1,2-diol with the Zn^{II}(dien) fragment

Diethylenetriamine (10.7 µL, 0.1 mmol) and ethane-1,2-diol (5.6 µL, 0.1 mmol) were added to a suspension of zinc hydroxide (10 mg, 0.1 mmol) in water (1 mL), yielding a nearly clear colourless solution which was stirred under ice cooling for 2–3 hours and subsequently stored at −60 °C.

[Zn(dien)($C_2H_4O_2$-$\kappa^2O^{1,2}$] (13)

^{1}H NMR (D_2O): δ [ppm] = 3.64–3.65 (m, 4H, H1a, H1b, H2a, H2b).

^{13}C NMR (D_2O): δ [ppm] = 63.2 (C1, C2).

5.7.16 Reaction of glycerol with the Zn^{II}(dien) fragment

Diethylenetriamine (10.7 µL, 0.10 mmol) and glycerol (7.3 µL, 0.1 mmol) were added to a suspension of zinc hydroxide (10 mg, 0.1 mmol) in water (1 mL), yielding a nearly clear colourless solution which was stirred under ice cooling for 2–3 and subsequently stored at −60 °C.

[Zn(dien)(Glyc1,2H$_{-2}$-$\kappa^2O^{1,2}$] (14)

^{1}H NMR (D_2O): δ [ppm] = 3.47−3.53 (m, 2H, H1a, H3a), 3.58–3.63 (m, 2H, H1b, H3b), 3.68–3.75 (m, 1H, H2).

^{13}C NMR (D_2O): δ [ppm] = 63.6 (C1, C3), 72.9 (C2).

5.7.17 Reaction of D-threitol with the Zn^{II}(dien) fragment

Diethylenetriamine (10.7 µL, 0.1 mmol) and D-threitol (12 mg, 0.1 mmol) were added to a suspension of zinc hydroxide (10 mg, 0.1 mmol) in water (1 mL), yielding a nearly clear colourless solution which was stirred under ice cooling for 2–3 hours and subsequently stored at −60 °C.

[Zn(dien)(D-ThreH$_{-2}$] (15)

^{1}H NMR (D_2O): δ [ppm] = 3.51–3.64 (m, 6H, H1a, H1b, H2, H3, H4a, H4b).

^{13}C NMR (D_2O): δ [ppm] = 64.0 (C1, C4), 72.8 (C2, C3).

5.7.18 Reaction of erythritol with the Zn^{II}(dien) fragment

Diethylenetriamine (10.7 µL, 0.1 mmol) and erythritol (12 mg, 0.1 mmol) were added to a suspension of zinc hydroxide (10 mg, 0.1 mmol) in water (1 mL), yielding a nearly clear colourless solution which was stirred under ice cooling for 2–3 hours and subsequently stored at −60 °C.

[Zn(dien)(ErytH$_{-2}$] (16)

^{1}H NMR (D_2O): δ [ppm] = 3.51–3.60 (m, 4H, H1a, H1b, H4a, H4b), 3.73–3.79 (m, 2H, H2, H3).

^{13}C NMR (D_2O): δ [ppm] = 64.0 (C1, C4), 73.3 (C2, C3).

5.7.19 Reaction of methyl α-D-glucopyranoside with the Zn^{II}(dien) fragment

A solution of dimethyl zinc (1.0 mL, 2.0 mmol, 2M in toluene) was added slowly to a suspension of methyl α-D-glucopyranoside (194 mg, 1.0 mmol) and diethylenetriamine (217 µL, 2.0 mmol) in toluene (5 mL) under nitrogen atmosphere. The solvent was removed *in vacuo* after stirring at 4 °C for 1–2 hours. The precipitate obtained was dissolved in D_2O (2 mL), yielding a clear, colourless solution which was stirred for 1–2 hours under ice cooling and subsequently stored at −60 °C.

[Zn(dien)(Me-α-D-Glc*p*H$_{-2}$] (17)

^{1}H NMR (D_2O): δ [ppm] = 3.09–3.15 (m, 1H, H4), 3.36–3.39 (m, 2H, H2, H3), 3.58 (ddd, 1H, H5, $^{3}J_{4,5}$ 9.1 Hz, $^{3}J_{5,6a}$ 6.4 Hz, $^{3}J_{5,6b}$ 1.9 Hz), 3.69 (dd, 1H, H6a, $^{2}J_{6a,6b}$ −12.0 Hz), 3.88 (dd, 1H, H6b), 4.75 (d, 1H, H1, 2.1 Hz).

^{13}C NMR (D_2O): δ [ppm] = 55.7 (OCH_3), 62.2 (C6), 73.2 (C4), 74.2 (C2), 74.3 (C5), 76,0 (C3), 101.4 (C1).

5.7.20 Reaction of methyl β-D-glucopyranoside with the Zn^{II}(dien) fragment

A solution of dimethyl zinc (1.0 mL, 2.0 mmol, 2M in toluene) was added slowly to a suspension of methyl β-D-glucopyranoside hydrate (203 mg, 1.0 mmol) and diethylenetriamine (217 µL, 2.0 mmol) in toluene (5 mL) under nitrogen atmosphere. The solvent was removed *in vacuo* after stirring at 4 °C for 1–2 hours. The precipitate obtained was dissolved in D_2O (2 mL), yielding a clear, colourless solution which was stirred for 1–2 hours under ice cooling and subsequently stored at −60 °C.

[Zn(dien)(Me-β-D-Glc*p*H$_{-2}$] (18)

^{1}H NMR (D_2O): δ [ppm] = 3.01–3.13 (m, 3H, H2, H3, H4), 3.38 (td, 1H, H5, $^{3}J_{4,5}$ 8.8 Hz, $^{3}J_{5,6a}$ 7.4 Hz, $^{3}J_{5,6b}$ 1.5 Hz), 3.64 (dd, 1H, H6a, $^{2}J_{6a,6b}$ −12.3 Hz), 3.95 (dd, 1H, H6b), 4.28 (d, 1H, H1, $^{3}J_{1,2}$ 7.4 Hz).

^{13}C NMR (D_2O): δ [ppm] = 57.7 (OCH_3), 62.5 (C6), 73.4 (C4), 76.1 (C2), 78.6 (C3), 80.0 (C5), 105.5 (C1).

5.7.21 Reaction of methyl α-D-mannopyranoside with the Zn^{II}(dien) fragment

A solution of dimethyl zinc (1.0 mL, 2.0 mmol, 2M in toluene) was added slowly to a suspension of methyl α-D-mannopyranoside (194 mg, 1.0 mmol) and diethylenetriamine (217 µL, 2.0 mmol) in toluene (5 mL) under nitrogen atmosphere. The solvent was removed *in vacuo* after stirring at 4 °C for 1–2 hours. The precipitate obtained was dissolved in D_2O (2 mL), yielding a clear, colourless solution which was stirred for 1–2 hours under ice cooling and subsequently stored at −60 °C.

[Zn(dien)(Me-α-D-Man*p*H$_{-2}$] (19)

^{1}H NMR (D_2O): δ [ppm] = 3.32 (t, 1H, H4, $^{3}J_{3,4}$ 8.9 Hz, $^{3}J_{4,5}$ 10.1 Hz), 3.38 (s, 3H, OCH_3), 3.49–3.52 (m, 1H, H5), 3.52 (dd, 1H, H3, $^{3}J_{2,3}$ 1.8 Hz), 3.62 (dd, 1H, H2, $^{3}J_{1,2}$ 1.5 Hz), 3.72 (dd, 1H, H6a, $^{3}J_{5,6a}$ 6.2 Hz, $^{2}J_{6a,6b}$ −12.0 Hz), 3.87 (dd, 1H, H6b, $^{3}J_{5,6b}$ 2.0 Hz), 4.72 (s, 1H, H1).

^{13}C NMR (D_2O): δ [ppm] = 55.1 (OCH_3), 62.2 (C6), 70.3 (C4), 73.4 (C5), 73.5 (C2), 73.6 (C3), 103.6 (C1).

5.7.22 Reaction of methyl α-D-galactopyranoside with the Zn^{II}(dien) fragment

A solution of dimethyl zinc (1.0 mL, 2.0 mmol, 2M in toluene) was added slowly to a suspension of methyl α-D-galactopyranoside (194 mg, 1.0 mmol) and diethylenetriamine (217 µL, 2.0 mmol) in toluene (5 mL) under nitrogen atmosphere. The solvent was removed *in vacuo* after stirring at 4 °C for 1–2 hours. The precipitate obtained was dissolved in D_2O (2 mL), yielding a clear, colourless solution which was stirred for 1–2 hours under ice cooling and subsequently stored at −60 °C.

[Zn(dien)(Me-α-D-Gal*p*H$_{-2}$] (20)

^{1}H NMR (D_2O): δ [ppm] = 3.39 (s, 3H, OCH_3), 3.55 (dd, 1H, H2, $^{3}J_{1,2}$ 3.7 Hz, $^{3}J_{2,3}$ 9.8 Hz), 3.61 (dd, 1H, H3, $^{3}J_{3,4}$ 3.5 Hz), 4.71–4.81 (m, 4H, H4, H5, H6a, H6b), 4.75 (d, 1H, H1).

^{13}C NMR (D_2O): δ [ppm] = 55.6 (OCH_3), 63.0 (C6), 71.3 (C3), 71.7 (C2), 72.3 (C4), 73.1 (C5), 101.2 (C1).

5.7.23 Reaction of methyl β-D-galactopyranoside with the Zn^{II}(dien) fragment

A solution of dimethyl zinc (1.0 mL, 2.0 mmol, 2M in toluene) was added slowly to a suspension of methyl β-D-galactopyranoside (194 mg, 1.0 mmol) and diethylenetriamine (217 µL, 2.0 mmol) in toluene (5 mL) under nitrogen atmosphere. The solvent was removed *in vacuo* after stirring at 4 °C for 1–2 hours. The precipitate obtained was dissolved in D_2O (2 mL), yielding a clear, colourless solution which was stirred for 1–2 hours under ice cooling and subsequently stored at −60 °C.

[Zn(dien)(Me-β-D-Gal*p*H$_{-2}$] (21)

^{1}H NMR (D_2O): δ [ppm] = 3.21 (dd, 1H, H2, $^{3}J_{1,2}$ 7.9 Hz, $^{3}J_{2,3}$ 9.1 Hz), 3.38 (dd, 2H, H3, $^{3}J_{3,4}$ 2.4 Hz), 3.55 (s, 3H, OCH_3), 3.57–3.62 (m, 1H, H5), 3.64–3.68 (m, 1H, H4), 3.71–3.85 (m, 2H, H6a, H6b), 4.21 (d, 1H, H1).

^{13}C NMR (D_2O): δ [ppm] = 57.6 (OCH_3), 62.7 (C6), 71.9 (C4), 73.8 (C2), 76.3 (C3), 77.8 (C5), 105.8 (C1).

5.7.24 Reaction of D-lyxose with the Zn^{II}(dien) fragment

A solution of dimethyl zinc (1.0 mL, 2.0 mmol, 2M in toluene) was added slowly to a suspension of D-lyxose (150 mg, 1.0 mmol / 300 mg, 2.0 mmol) and diethylenetriamine (217 µL, 2.0 mmol) in toluene (5 mL) under nitrogen atmosphere. The solvent was removed *in vacuo* after stirring at 4 °C for 1–2 hours. The precipitate obtained was dissolved in D_2O (2 mL), yielding a clear, colourless solution which was stirred for 1–2 hours under ice cooling and subsequently stored at −60 °C.

[Zn(dien)(α-D-Lyx*p*1,2H$_{-2}$-κ^2*O*^{1,2})] (22a)

molar Zn(dien):sugar ratio of 1:1

^{1}H NMR (D_2O): δ [ppm] = 3.57–3.60 (m, 1H, H2), 3.63–3.78 (m, 3H, H4, H5a, H5b), 3.81–3.85 (m, 1H, H3), 4.95 (s, 1H, H1).

^{13}C NMR (D_2O): δ [ppm] = 63.3 (C5), 69.4 (C4), 72.5 (C3), 73.5 (C2), 98.7 (C1).

molar Zn(dien):sugar ratio of 2:1

^{1}H NMR (D_2O): δ [ppm] = 3.56–3.59 (m, 1H, H2), 3.62–3.78 (m, 3H, H4, H5a, H5b), 3.80–3.83 (m, 1H, H3), 5.00 (s, 1H, H1).

^{13}C NMR (D_2O): δ [ppm] = 62.9 (C5), 69.5 (C4), 72.7 (C3), 74.5 (C2), 99.9 (C1).

[Zn(dien)(β-D-Lyx*p*1,2H$_{-2}$-κ^2*O*^{1,2})] (22b)

molar Zn(dien):sugar ratio of 1:1

^{1}H NMR (D_2O): δ [ppm] = 3.14 (t, 1H, H5a, $^3J_{4,5a}$ 10.5 Hz, $^2J_{5a,5b}$ −12.3 Hz), 3.50 (dd, 1H, H3, $^3J_{2,3}$ 3.2 Hz, $^3J_{3,4}$ 8.5 Hz), 3.58 (dd, 1H, H2, $^3J_{1,2}$ 1.2 Hz), 3.71–3.80 (m, 2H, H4, H5b), 4.85 (d, 1H, H1).

^{13}C NMR (D_2O): δ [ppm] = 64.6 (C5), 68.0 (C4), 74.9 (C2), 76.4 (C3), 100.3 (C1).

molar Zn(dien):sugar ratio of 2:1

^{1}H NMR (D_2O): δ [ppm] = 3.13 (dd, 1H, H5a, $^3J_{4,5a}$ 10.4 Hz, $^2J_{5a,5b}$ −12.5 Hz), 3.48 (dd, 1H, H3, $^3J_{2,3}$ 3.4 Hz, $^3J_{3,4}$ 8.6 Hz), 3.58 (dd, 1H, H2, $^3J_{1,2}$ 1.2 Hz), 3.71–3.80 (m, 2H, H4, H5b), 4.85 (d, 1H, H1).

^{13}C NMR (D_2O): δ [ppm] = 64.7 (C5), 68.1 (C4), 75.0 (C2), 76.6 (C3), 100.6 (C1).

5.7.25 Reaction of D-arabinose with the Zn^{II}(dien) fragment

A solution of dimethyl zinc (1.0 mL, 2.0 mmol, 2M in toluene) was added slowly to a suspension of D-arabinose (150 mg, 1.0 mmol / 300 mg, 2.0 mmol) and diethylenetriamine (217 µL, 2.0 mmol) in toluene (5 mL) under nitrogen atmosphere. The solvent was removed *in vacuo* after stirring at 4 °C for 1–2 hours. The precipitate obtained was dissolved in D_2O (2 mL), yielding a clear, colourless solution which was stirred for 1–2 hours under ice cooling and subsequently stored at −60 °C.

[Zn(dien)(α-D-Ara*p*1,2H$_{-2}$-κ^2*O*^{1,2})] (23a)

molar Zn(dien):sugar ratio of 1:1

^{1}H NMR (D_2O): δ [ppm] = 3.29 (dd, 1H, H2, $^3J_{1,2}$ 7.2 Hz, $^3J_{2,3}$ 9.7 Hz), 3.56 (dd, 1H, H3, $^3J_{3,4}$ 3.5 Hz), 3.60–3.65 (m, 1H, H5a), 3.79–3.84 (m, 1H, H5b), 3.84–3.87 (m, 1H, H4), 4.45 (d, 1H, H1).

^{13}C NMR (D_2O): δ [ppm] = 66.7 (C5), 70.0 (C4), 74.1 (C3), 74.9 (C2), 101.5 (C1).

molar Zn(dien):sugar ratio of 2:1

^{1}H NMR (D_2O): δ [ppm] = 3.16 (dd, 1H, H2, $^3J_{1,2}$ 7.2 Hz, $^3J_{2,3}$ 9.5 Hz), 3.51 (dd, 1H, H3, $^3J_{3,4}$ 3.3 Hz), 3.77–3.81 (m, 1H, H4), 3.85–3.92 (m, 2H, H5a, H5b), 4.40 (d, 1H, H1).

^{13}C NMR (D_2O): δ [ppm] = 66.3 (C5), 70.7 (C4), 74.8 (C3), 76.3 (C2), 103.2 (C1).

[Zn(dien)(β-D-Ara*p*1,2H$_{-2}$-κ^2*O*^{1,2})] (23b)

molar Zn(dien):sugar ratio of 1:1

^{1}H NMR (D_2O): δ [ppm] = 3.48 (dd, 1H, H2, $^3J_{1,2}$ 1.2 Hz, $^3J_{2,3}$ 4.6 Hz), 3.54–3.72 (m, 2H, H5a, H5b), 3.87–3.89 (m, 1H, H3), 3.95 (dd, 1H, H4, $^3J_{3,4}$ 3.7 Hz, $^3J_{4,5}$ 7.2 Hz), 5.08 (d, 1H, H1).

^{13}C NMR (D_2O): δ [ppm] = 62.7 (C5), 67.2 (C4), 72.5 (C3), 73.8 (C2), 97.1 (C1).

molar Zn(dien):sugar ratio of 2:1

^{1}H NMR (D_2O): δ [ppm] = 3.40 (dd, 1H, H2, $^3J_{1,2}$ 1.5 Hz, $^3J_{2,3}$ 3.8 Hz), 3.38–3.54 (m, 2H, H5a, H5b), 3.78–3.83 (m, 1H, H3), 3.89 (dd, 1H, H4, $^3J_{3,4}$ 3.5 Hz, $^3J_{4,5a}$ 8.1 Hz), 5.04 (d, 1H, H1).

^{13}C NMR (D_2O): δ [ppm] = 63.8 (C5), 67.0 (C4), 74.5 (C3), 75.9 (C2), 97.9 (C1).

[Zn(dien)(β-D-Ara*f*1,2H$_{-2}$-κ^2*O*^{1,2})] (23c)

molar Zn(dien):sugar ratio of 1:1

^{1}H NMR (D_2O): δ [ppm] = 3.54–3.72 (m, 2H, H5a, H5b), 3.65 (dd, 1H, H2, $^3J_{1,2}$ 2.2 Hz, $^3J_{2,3}$ 5.0 Hz), 3.74–3.78 (m, 1H, H4), 3.78–3.81 (m, 1H, H3), 5.46 (d, 1H, H1).

^{13}C NMR (D_2O): δ [ppm] = 63.0 (C5), 78.9 (C2), 79.1 (C3), 81.8 (C4), 103.3 (C1).

molar Zn(dien):sugar ratio of 2:1

^{1}H NMR (D_2O): δ [ppm] = 3.56–3.70 (m, 2H, H5a, H5b), 3.63 (dd, 1H, H2, $^3J_{1,2}$ 2.2 Hz, $^3J_{2,3}$ 5.0 Hz), 3.74–3.78 (m, 1H, H4), 3.78–3.82 (m, 1H, H3), 5.46 (d, 1H, H1).

^{13}C NMR (D_2O): δ [ppm] = 63.1 (C5), 79.0 (C2), 79.3 (C3), 82.0 (C4), 103.5 (C1).

5.7.26 Reaction of D-xylose with the Zn^{II}(dien) fragment

A solution of dimethyl zinc (1.0 mL, 2.0 mmol, 2M in toluene) was added slowly to a suspension of D-xylose (150 mg, 1.0 mmol / 300 mg, 2.0 mmol) and diethylenetriamine (217 µL, 2.0 mmol) in toluene (5 mL) under nitrogen atmosphere. The solvent was removed *in vacuo* after stirring at 4 °C for 1–2 hours. The precipitate obtained was dissolved in D_2O (2 mL), yielding a clear, colourless solution which was stirred for 1–2 hours under ice cooling and subsequently stored at −60 °C.

[Zn(dien)(α-D-Xyl*p*1,2H$_{-2}$-κ^2*O*^{1,2})] (24a)

molar Zn(dien):sugar ratio of 1:1

^{1}H NMR (D_2O): δ [ppm] = 3.29–3.41 (m, 2H, H2, H5a), 3.53–3.58 (m, 1H, H4), 3.64 (t, 1H, H3, $^3J_{2,3}$ 4.1 Hz, $^3J_{3,4}$ 4.5 Hz), 3.91 (dd, 1H, H5b, $^3J_{4,5b}$ 5.8 Hz, $^2J_{5a,5b}$ −11.0 Hz), 5.17 (d, 1H, H1, $^3J_{1,2}$ 3.1 Hz).

^{13}C NMR (D_2O): δ [ppm] = 61.6 (C5), 70.3 (C4), 73.7 (C2), 73.9 (C3), 95.6 (C1).

molar Zn(dien):sugar ratio of 2:1

^{1}H NMR (D_2O): δ [ppm] = 3.22–3.32 (m, 2H, H2, H5a), 3.43–3.52 (m, 1H, H4), 3.58 (t, 1H, H3, $^{3}J_{2,3}$ 6.6 Hz, $^{3}J_{3,4}$ 7.5 Hz), 3.91 (dd, 1H, H5b, $^{3}J_{4,5b}$ 5.6 Hz, $^{2}J_{5a,5b}$ −10.2 Hz), 5.06 (d, 1H, H1, $^{3}J_{1,2}$ 2.4 Hz).

^{13}C NMR (D_2O): δ [ppm] = 62.9 (C5), 70.6 (C4), 74.4 (C3), 75.1 (C2), 98.1 (C1).

[Zn(dien)(β-D-Xyl*p*1,2H$_{-2}$-κ^2*O*^{1,2})] (24b)

molar Zn(dien):sugar ratio of 1:1

^{1}H NMR (D_2O): δ [ppm] = 3.04 (dd, 1H, H2, $^{3}J_{1,2}$ 7.5 Hz, $^{3}J_{2,3}$ 9.2 Hz), 3.27 (t, 1H, H5a, $^{3}J_{4,5a}$ 10.5 Hz, $^{2}J_{5a,5b}$ −11.3 Hz), 3.36 (t, 1H, H3, $^{3}J_{3,4}$ 9.3 Hz), 3.53–3.58 (m, 1H, H4), 3.84 (dd, 1H, H5b, $^{3}J_{4,5b}$ 5.4 Hz), 4.55 (d, 1H, H1).

^{13}C NMR (D_2O): δ [ppm] = 65.7 (C5), 70.6 (C4), 76.8 (C2), 77.1 (C3), 101.0 (C1).

molar Zn(dien):sugar ratio of 2:1

^{1}H NMR (D_2O): δ [ppm] = 2.82–2.86 (m, 1H, H2), 3.22–3.32 (m, 2H, H3, H5a, 3.43–353 (m, 1H, H4), 3.78–3.85 (m, 1H, H5b), 5.06 (d, 1H, H1, $^{3}J_{1,2}$ 6.4 Hz).

^{13}C NMR (D_2O): δ [ppm] = 66.3 (C5), 71.8 (C4), 78.7 (C3), 78.9 (C2), 103.8 (C1).

[Zn(dien)(α-D-Xyl*f*1,2H$_{-2}$-κ^2*O*^{1,2})] (24c)

molar Zn(dien):sugar ratio of 2:1

^{1}H NMR (D_2O): δ [ppm] = 3.43–3.55 (m, 3H, H2, H5a, H5b), 3.87–3.93 (m, 2H, H3, H4), 5.44–5.48 (m, 1H, H1).

^{13}C NMR (D_2O): δ [ppm] = 61.8 (C5), 78.9 (C2, C3, C4), 104.0 (C1).

5.7.27 Reaction of D-ribose with the Zn^{II}(dien) fragment

A solution of dimethyl zinc (1.0 mL, 2.0 mmol, 2M in toluene) was added slowly to a suspension of D-ribose (150 mg, 1.0 mmol / 300 mg, 2.0 mmol) and diethylenetriamine (217 µL, 2.0 mmol) in toluene (5 mL) under nitrogen atmosphere. The solvent was removed *in vacuo* after stirring at 4 °C for 1–2 hours. The precipitate obtained was dissolved in D_2O (2 mL), yielding a clear, colourless solution which was stirred for 1–2 hours under ice cooling and subsequently stored at −60 °C.

[Zn(dien)(α-D-Rib*p*1,2H$_{-2}$-κ^2*O*^{1,2})] (25a)

molar Zn(dien):sugar ratio of 1:1

^{1}H NMR (D_2O): δ [ppm] = 3.57–3.60 (m, 1H, H2), 3.60–3.63 (m, 2H, H4, H5a), 3.74–3.78 (m, 1H, H3), 3.80 (dd, 1H, H5b, $^3J_{4,5b}$ 3.4 Hz, $^2J_{5a,5b}$ −11.9 Hz), 4.83 (d, 1H, H1, $^3J_{1,2}$ 1.3 Hz).

^{13}C NMR (D_2O): δ [ppm] = 63.4 (C5), 70.8 (C4), 71.1 (C3), 75.9 (C2), 99.4 (C1).

molar Zn(dien):sugar ratio of 2:1

^{1}H NMR (D_2O): δ [ppm] = 3.54–3.57 (m, 1H, H2), 3.57–3.63 (m, 2H, H4, H5a), 3.74 (t, 1H, H3, $^3J_{2,3}$ 2.5 Hz, $^3J_{3,4}$ 2.5 Hz), 3.76 (dd, 1H, H5b, $^3J_{4,5b}$ 3.2 Hz, $^2J_{5a,5b}$ −11.7 Hz), 4.82 (d, 1H, H1, $^3J_{1,2}$ 1.3 Hz).

^{13}C NMR (D_2O): δ [ppm] = 63.3 (C5), 70.9 (C4), 71.5 (C3), 76.5 (C2), 99.8 (C1).

[Zn(dien)(β-D-Rib*p*1,2H$_{-2}$-κ^2*O*^{1,2})] (25b)

molar Zn(dien):sugar ratio of 1:1

^{1}H NMR (D_2O): δ [ppm] = 3.38–3.41 (m, 1H, H2), 3.61–3.65 (m, 1H, H5a), 3.71 (dd, 1H, H5b, $^3J_{4,5b}$ 5.3 Hz, $^2J_{5a,5b}$ −10.9 Hz), 3.81–3.84 (m, 1H, H4), 4.03–4.05 (m, 1H, H3), 4.54–4.55 (m, 1H, H1).

^{13}C NMR (D_2O): δ [ppm] = 65.0 (C5), 68.8 (C4), 69.8 (C3), 73.9 (C2), 97.6 (C1).

(molar Zn(dien):sugar ratio of 2:1)

^{1}H NMR (D_2O): δ [ppm] = 3.16–3.19 (m, 1H, H2), 3.71–3.78 (m, 3H, H4, H5a, H5b), 3.94–3.97 (m, 1H, H3), 4.91–4.94 (m, 1H, H1).

^{13}C NMR (D_2O): δ [ppm] = 65.3 (C5), 69.7 (C4), 70.8 (C3), 75.9 (C2), 99.3 (C1).

5.7.28 Reaction of D-galactose with the Zn^{II}(dien) fragment

A solution of dimethyl zinc (1.0 mL, 2.0 mmol, 2M in toluene) was added slowly to a suspension of D-galactose (180 mg, 1.0 mmol / 360 mg, 2.0 mmol) and diethylenetriamine (217 µL, 2.0 mmol) in toluene (5 mL) under nitrogen atmosphere. The solvent was removed *in vacuo* after stirring at 4 °C for 1–2 hours. The precipitate obtained was dissolved in D_2O (2 mL), yielding a clear, colourless solution which was stirred for 1–2 hours under ice cooling and subsequently stored at −60 °C.

[Zn(dien)(α-D-Gal*p*1,2H$_{-2}$-κ^2*O*^{1,2})] (26a)

molar Zn(dien):sugar ratio of 1:1

^{1}H NMR (D_2O): δ [ppm] = 3.36–3.40 (m, 1H, H2), 3.78–3.82 (m, 1H, H3), 5.07 (d, 1H, H1, $^3J_{1,2}$ 3.4 Hz).

^{13}C NMR (D_2O): δ [ppm] = 61.9 (C6), 70.2 / 70.3 / 70.5 / 71.0 (C2, C3, C4, C5), 95.5 (C1).

molar Zn(dien):sugar ratio of 2:1

^{1}H NMR (D_2O): δ [ppm] = 3.43–3.47 (m, 1H, H2), 3.81–3.85 (m, 1H, H3), 5.07 (d, 1H, H1, $^{3}J_{1,2}$ 3.6 Hz).

^{13}C NMR (D_2O): δ [ppm] = 62.1 (C6), 70.4 / 70.5 / 71.3 / 72.6 (C2, C3, C4, C5), 97.8 (C1).

[Zn(dien)(β-D-Gal*p*1,2H$_{-2}$-κ^2*O*^{1,2})] (26b)

molar Zn(dien):sugar ratio of 1:1

^{1}H NMR (D_2O): δ [ppm] = 3.34 (dd, 1H, H2, $^{3}J_{1,2}$ 7.5 Hz, $^{3}J_{2,3}$ 10.0 Hz), 3.58 (dd, 1H, H3, $^{3}J_{3,4}$ 3.5 Hz), 3.63–3.75 (m, 3H, H5, H6a, H6b), 3.85–3.87 (m, 1H, H4), 4.56 (d, 1H, H1).

^{13}C NMR (D_2O): δ [ppm] = 62.0 (C6), 70.0 (C4), 74.0 (C5), 74.4 (C3), 75.5 (C2), 100.2 (C1).

molar Zn(dien):sugar ratio of 2:1

^{1}H NMR (D_2O): δ [ppm] = 3.17 (dd, 1H, H2, $^{3}J_{1,2}$ 7.3 Hz, $^{3}J_{2,3}$ 9.8 Hz), 3.50 (dd, 1H, H3, $^{3}J_{3,4}$ 3.6 Hz), 3.55–3.67 (m, 3H, H5, H6a, H6b), 3.78–3.81 (m, 1H, H4), 4.46 (d, 1H, H1).

^{13}C NMR (D_2O): δ [ppm] = 62.3 (C6), 71.0 (C4), 74.9 (C5), 75.8 (C3), 76.1 (C2), 102.5 (C1).

[Zn(dien)(α-D-Gal*f*1,2H$_{-2}$-κ^2*O*^{1,2})] (26c)

molar Zn(dien):sugar ratio of 1:1

^{1}H NMR (D_2O): δ [ppm] = 3.62–3.68 (m, 1H, H6a), 3.68–3.79 (m, 3H, H2, H5, H6b), 3.81–3.84 (m, 1H, H3), 3.96 (t, 1H, H4, $^{3}J_{3,4}$ 3.5 Hz, $^{3}J_{4,5}$ 3.3 Hz), 5.45 (s, 1H, H1).

^{13}C NMR (D_2O): δ [ppm] = 64.0 (C6), 71.9 (C5), 78.7 (C2), 79.9 (C3), 82.4 (C4), 103.2 (C1).

molar Zn(dien):sugar ratio of 2:1

^{1}H NMR (D_2O): δ [ppm] = 3.55–3.60 (m, 1H, H6a), 3.61–3.68 (m, 3H, H2, H5, H6b), 3.78–3.83 (m, 1H, H3), 3.95 (t, 1H, H4, $^{3}J_{3,4}$ 3.2 Hz, $^{3}J_{4,5}$ 3.1 Hz), 5.46 (d, 1H, H1, $^{3}J_{1,2}$ 2.1 Hz).

^{13}C NMR (D_2O): δ [ppm] = 64.1 (C6), 72.0 (C5), 78.8 (C2), 80.1 (C3), 82.6 (C4), 103.5 (C1).

5.7.29 Reaction of D-glucose with the Zn^{II}(dien) fragment

A solution of dimethyl zinc (1.0 mL, 2.0 mmol, 2M in toluene) was added slowly to a suspension of D-glucose monohydrate (198 mg, 1.0 mmol / 296 mg, 2.0 mmol) and diethylenetriamine (217 µL, 2.0 mmol) in toluene (5 mL) under nitrogen atmosphere. The solvent was removed *in vacuo* after stirring at 4 °C for 1–2 hours. The precipitate obtained was dissolved in D_2O (2 mL), yielding a clear, colourless solution which was stirred for 1–2 hours under ice cooling and subsequently stored at −60 °C.

[Zn(dien)(α-D-Glc*p*1,2H$_{-2}$-κ^2*O*^{1,2})] (27a)

molar Zn(dien):sugar ratio of 1:1

^{1}H NMR (D_2O): δ [ppm] = 3.29–3.43 (m, 3H, H2, H3, H4), 3.67–3.92 (m, 3H, H5, H6a, H6b), 5.16 (d, 1H, H1, $^3J_{1,2}$ 3.7 Hz).

^{13}C NMR (D_2O): δ [ppm] = 61.6 (C6), 70.8 (C4), 71.6 (C5), 74.1 (C2), 75.3 (C3), 96.4 (C1).

molar Zn(dien):sugar ratio of 2:1

^{1}H NMR (D_2O): δ [ppm] = 3.27–3.41 (m, 3H, H2, H3, H4), 3.65–3.87 (m, 3H, H5, H6a, H6b), 5.16 (m, 1H, H1).

^{13}C NMR (D_2O): δ [ppm] = 62.2 (C6), 71.4 (C4), 71.9 (C5), 75.2 (C2), 76.9 (C3), 98.4 (C1).

[Zn(dien)(β-D-Glc*p*1,2H$_{-2}$-κ^2*O*^{1,2})] (27b)

molar Zn(dien):sugar ratio of 1:1

^{1}H NMR (D_2O): δ [ppm] = 2.97 (dd, 1H, H2, $^3J_{1,2}$ 7.4 Hz, $^3J_{2,3}$ 9.1 Hz), 3.31 (t, 1H, H4, $^3J_{3,4}$ 9.2 Hz, $^3J_{4,5}$ 9.3 Hz), 3.36 (t, 1H, H3), 3.37–3.43 (m, 1H, H5), 3.69 (dd,1H, H6a, $^3J_{5,6a}$ 5.9 Hz, $^2J_{6a,6b}$ −12.1 Hz), 3.87 (dd, 1H, H6b, $^3J_{5,6b}$ 2.0 Hz), 4.54 (d, 1H, H1).

^{13}C NMR (D_2O): δ [ppm] = 61.8 (C6), 71.3 (C4), 76.5 (C5), 77.6 (C2, C3), 101.1 (C1).

molar Zn(dien):sugar ratio of 2:1

^{1}H NMR (D_2O): δ [ppm] = 2.87 (dd, 1H, H2, $^3J_{1,2}$ 7.2 Hz, $^3J_{2,3}$ 9.0 Hz), 3.24 (t, 1H, H4, $^3J_{3,4}$ 9.2 Hz, $^3J_{4,5}$ 9.3 Hz), 3.29 (t, 1H, H3), 3.35–3.41 (m, 1H, H5), 3.68 (dd,1H, H6a, $^3J_{5,6a}$ 6.4 Hz, $^2J_{6a,6b}$ −12.0 Hz), 3.88 (dd, 1H, H6b, $^3J_{5,6b}$ 2.0 Hz), 4.47 (d, 1H, H1).

^{13}C NMR (D_2O): δ [ppm] = 62.2 (C6), 72.4 (C4), 77.1 (C5), 78.8 (C3), 78.9 (C2), 102.6 (C1).

[Zn(dien)(α-D-Glc*f*1,2H$_{-2}$-κ^2*O*^{1,2})] (27c)

molar Zn(dien):sugar ratio of 2:1

^{1}H NMR (D_2O): δ [ppm] = 3.08–3.21 (m, 3H, H2, H3, H4), 3.58–3.72 (m, 3H, H5, H6a, H6b), 5.47 (d, 1H, H1, $^3J_{1,2}$ 2.6 Hz).

^{13}C NMR (D_2O): δ [ppm] = 65.1 (C6), 71.0 (C5), 78.3 / 78.9 / 79.3 (C2, C3, C4), 104.2 (C1).

5.7.30 Reaction of D-mannose with the Zn^{II}(dien) fragment

A solution of dimethyl zinc (1.0 mL, 2.0 mmol, 2M in toluene) was added slowly to a suspension of D-mannose (180 mg, 1.0 mmol / 360 mg, 2.0 mmol) and diethylenetriamine (217 µL, 2.0 mmol) in toluene (5 mL) under nitrogen atmosphere. The solvent was removed *in vacuo* after stirring at 4 °C for 1–2 hours. The precipitate obtained was dissolved in D_2O (2 mL), yielding a clear, colourless solution which was stirred for 1–2 hours under ice cooling and subsequently stored at −60 °C.

[Zn(dien)(α-D-Man*p*2,3H$_{-2}$-κ^2*O*^{2,3})] (28a)

molar Zn(dien):sugar ratio of 1:1

^{1}H NMR (D_2O): δ [ppm] = 3.53–3.55 (m, 1H, H4), 3.71–3.77 (m, 3H, H2, H5, H6a), 3.82–3.85 (m, 1H, H3), 3.89 (dd, 1H, H6b, $^3J_{5,6b}$ 2.3 Hz, $^2J_{6a,6b}$ −12.1 Hz), 4.91–4.93 (m, 1H, H1)

^{13}C NMR (D_2O): δ [ppm] = 62.0 (C6), 68.8 (C4), 72.1 (C2, C3), 74.5 (C5), 98.9 (C1).

molar Zn(dien):sugar ratio of 2:1

^{1}H NMR (D_2O): δ [ppm] = 3.53–3.54 (m, 1H, H4), 3.73–3.78 (m, 3H, H2, H5, H6a), 3.82–3.85 (m, 1H, H3), 3.90 (dd, 1H, H6b, $^3J_{5,6b}$ 2.3 Hz, $^2J_{6a,6b}$ −12.0 Hz), 4.89–4.90 (m, 1H, H1)

^{13}C NMR (D_2O): δ [ppm] = 62.2 (C6), 69.1 (C4), 72.0 (C3), 72.3 (C2), 75.1 (C5), 99.7 (C1).

[Zn(dien)(β-D-Man*p*1,2H$_{-2}$-κ^2*O*^{1,2})] (28b)

molar Zn(dien):sugar ratio of 1:1

^{1}H NMR (D_2O): δ [ppm] = 3.21–3.27 (m, 1H, H5), 3.49–3.53 (m, 2H, H3, H4), 3.57–3.59 (m, 1H, H2), 3.69 (dd, 1H, H6a, $^3J_{5,6a}$ 5.8 Hz, $^2J_{6a,6b}$ −12.1 Hz), 3.82 (dd, 1H, H6b, $^3J_{5,6b}$ 2.1 Hz), 4.89 (m, 1H, H1).

^{13}C NMR (D_2O): δ [ppm] = 62.0 (C6), 68.2 (C4), 75.7 (C2, C5), 76.8 (C3), 99.6 (C1).

molar Zn(dien):sugar ratio of 2:1

^{1}H NMR (D_2O): δ [ppm] = 3.21–3.26 (m, 1H, H5), 3.49–3.52 (m, 2H, H3, H4), 3.56–3.59 (m, 1H, H2), 3.68 (dd, 1H, H6a, $^3J_{5,6a}$ 5.9 Hz, $^2J_{6a,6b}$ −12.0 Hz), 3.82 (dd, 1H, H6b, $^3J_{5,6b}$ 1.7 Hz), 4.89 (m, 1H, H1).

^{13}C NMR (D_2O): δ [ppm] = 62.0 (C6), 68.3 (C4), 75.8 (C2, C5), 76.9 (C3), 99.7 (C1).

5.7.31 Reaction of D-fructose with the Zn^{II}(dien) fragment

A solution of dimethyl zinc (1.0 mL, 2.0 mmol, 2M in toluene) was added slowly to a suspension of D-fructose (180 mg, 1.0 mmol / 360 mg, 2.0 mmol) and diethylenetriamine (217 µL, 2.0 mmol) in toluene (5 mL) under nitrogen atmosphere. The solvent was removed *in vacuo* after stirring at 4 °C for 1–2 hours. The precipitate obtained was dissolved in D_2O (2 mL), yielding a clear, colourless solution which was stirred for 1–2 hours under ice cooling and subsequently stored at −60 °C.

[Zn(dien)(β-D-Fru*p*2,3H$_{-2}$-κ^2*O*^{2,3})] (29a)

molar Zn(dien):sugar ratio of 1:1

^{1}H NMR (D_2O): δ [ppm] = 3.37–3.42 (m, 1H, H1a), 3.57–3.66 (m, 2H, H1b, H6a), 3.74 (d, 1H, H3, $^3J_{3,4}$ 9.9 Hz), 3.84 (dd, 1H, H4, $^3J_{4,5}$ 3.5 Hz), 3.92–3.94 (m, 1H, H5), 3.96–4.01 (m, 1H, H6b).

^{13}C NMR (D_2O): δ [ppm] = 63.4 (C6), 65.3 (C1), 68.9 (C3), 70.2 (C5), 70.9 (C4), 100.1 (C2).

[Zn(dien)(β-D-Fru*f*2,3H$_{-2}$-κ^2*O*^{2,3})] (29b)

molar Zn(dien):sugar ratio of 1:1

^{1}H NMR (D_2O): δ [ppm] = 3.35–3.44 (m, 2H, H1a, H1b), 3.60 (dd, 1H, H6a, $^3J_{5,6a}$ 3.5 Hz, $^2J_{6a,6b}$ −12.2 Hz), 3.72 (dd, 1H, H6b, $^3J_{5,6b}$ 2.0 Hz), 3.74–3.80 (m, 2H, H4, H5), 3.92 (d, 1H, H3, $^3J_{3,4}$ 6.9 Hz).

^{13}C NMR (D_2O): δ [ppm] = 62.2 (C6), 65.8 (C1), 77.8 (C3), 78.4 (C4), 80.7 (C5), 106.2 (C2).

molar Zn(dien):sugar ratio of 2:1

^{1}H NMR (D_2O): δ [ppm] = 3.34 (d, 1H, H1a, $^2J_{1a,1b}$ −11.5 Hz), 3.39 (d, 1H, H1b), 3.56–3.61 (m, 1H, H6a), 3.67–3.72 (m, 1H, H6b), 3.72–3.76 (m, 2H, H4, H5), 3.87 (d, 1H, H3, $^3J_{3,4}$ 6.9 Hz).

^{13}C NMR (D_2O): δ [ppm] = 62.3 (C6), 66.3 (C1), 78.5 (C3), 79.1 (C4), 80.8 (C5), 106.8 (C2).

5.7.32 Reaction of D-fructose 1-phosphate with the Zn^{II}(dien) fragment

Barium D-fructose 1-phosphate trihydrate (62 mg, 0.15 mmol), zinc(II) nitrate hexahydrate (89 mg, 0.30 mmol) and diethylenetriamine (32.6 µL, 0.30 mmol) were dissolved in 1 mL D_2O, yielding a light yellow suspension. For experiments at lower or higher pH, 0.15–0.30 mmol nitric acid (2 M) or sodium hydroxide were added, respectively. The suspensions were stirred at 4 °C for 2–3 hours. They were subsequently filtrated and stored at −60 °C.

[Zn(dien)(β-D-Fru*f*1*P*2,3H$_{-2}$-κ*O*^{2,3})]$^{2-}$ (30) (observed at pH 12–14)

^{1}H NMR (D_2O): δ [ppm] = 3.56–3.63 (m, 3H, H1a, H1b, H6a), 3.67 (t, 1H, H4, $^3J_{3,4}$ 6.9 Hz, $^3J_{4,5}$ 7.4 Hz), 3.72 (dd, 1H, H6b, $^3J_{5,6b}$ 2.3 Hz, $^2J_{6a,6b}$ −12.8 Hz), 3.74–4.77 (m, 1H, H5), 3.94 (d, 1H, H3).

^{13}C NMR (D_2O): δ [ppm] = 62.1 (C6), 69.3 (C1), 79.0 (C4), 79.4 (C3), 80.0 (C5), 105.8 (C2).

^{31}P NMR (D_2O): δ [ppm] = 5.4.

β-fructopyranose 1-phosphate species at pH 8

^{1}H NMR (D_2O): δ [ppm] = 3.69 (dd, 1H, H6a, $^3J_{5,6a}$ 1.5 Hz, $^2J_{6a,6b}$ −12.7 Hz), 3.80–3.83 (m, 1H, H3), 3.81 (d, 1H, H1a, $^2J_{1a,1b}$ −10.1 Hz), 3.89–3.92 (m, 1H, H4), 3.90 (dd, 1H, H1b, $^3J_{1b,P}$ 3.4 Hz), 4.00 (ddd, 1H, H5, $^3J_{4,5}$ 3.1 Hz, $^3J_{5,6b}$ 0.9 Hz), 4.04 (dd, 1H, H6b).

^{13}C NMR (D_2O): δ [ppm] = 64.2 (C6), 66.9 (C1), 68.3 (C3), 69.7 (C5), 69.9 (C4), 98.7 (C2).

^{31}P NMR (D_2O): δ [ppm] = 5.6.

β-fructopyranose 1-phosphate species at pH 6

^{1}H NMR (D_2O): δ [ppm] = 3.70 (dd, 1H, H6a, $^{3}J_{5,6a}$ 1.5 Hz, $^{2}J_{6a,6b}$ −12.7 Hz), 3.80–3.83 (m, 1H, H3), 3.81 (d, 1H, H1a, $^{2}J_{1a,1b}$ −10.1 Hz), 3.89–3.92 (m, 1H, H4), 3.91 (dd, 1H, H1b, $^{3}J_{1b,P}$ 3.4 Hz), 4.00 (ddd, 1H, H5, $^{3}J_{4,5}$ 3.1 Hz, $^{3}J_{5,6b}$ 0.9 Hz), 4.04 (dd, 1H, H6b).

^{13}C NMR (D_2O): δ [ppm] = 64.2 (C6), 66.9 (C1), 68.3 (C3), 69.7 (C5), 69.9 (C4), 98.6 (C2).

^{31}P NMR (D_2O): δ [ppm] = 5.4.

β-fructofuranose 1-phosphate species at pH 8

^{1}H NMR (D_2O): δ [ppm] = 3.77–3.84 (m, 3H, H5, H6a, H6b), 4.02–4.13 (m, 4H, H1a, H1b, H3, H4).

^{13}C NMR (D_2O): δ [ppm] = 63.0 (C6), 66.9 (C1), 75.0 (C4), 76.9 (C3), 81.2 (C5), 101.8 (C2).

^{31}P NMR (D_2O): δ [ppm] = 5.3.

β-fructofuranose 1-phosphate species at pH 6

^{1}H NMR (D_2O): δ [ppm] = 3.78–3.84 (m, 3H, H5, H6a, H6b), 4.02–4.12 (m, 4H, H1a, H1b, H3, H4).

^{13}C NMR (D_2O): δ [ppm] = 63.1 (C6), 66.9 (C1), 74.8 (C4), 76.8 (C3), 81.4 (C5), 101.5 (C2).

^{31}P NMR (D_2O): δ [ppm] = 5.4.

5.7.33 Reaction of D-fructose 6-phosphate with the Zn^{II}(dien) fragment

Disodium D-fructose 6-phosphate hydrate (46 mg, 0.15 mmol / 91 mg, 0.30 mmol), zinc(II) nitrate hexahydrate (89 mg, 0.30 mmol) and diethylenetriamine (32.6 µL, 0.30 mmol) were dissolved in 1 mL D_2O, yielding a colourless solution. Sodium hydroxide (24 mg, 0.60 mmol) was added and the suspension was stirred at 4 °C for 2–3 hours. It was subsequently filtrated and stored at −60 °C.

[Zn(dien)(β-D-Fru*f*6*P*2,3H$_{-2}$-κ^2*O*^{2,3})]$^{2-}$ (31)

molar Zn(dien):sugar-phosphate ratio of 1:1

^{1}H NMR (D_2O): δ [ppm] = 3.11 (d, 1H, H1a, $^{2}J_{1a,1b}$ −11.5), 3.20 (d, 1H, H1b), 3.47–3.52 (m, 2H, H4, H5), 3.59 (dt, 1H, H6a, $^{3}J_{5,6a}$ 5.7 Hz, $^{3}J_{6a,P}$ 5.5 Hz, $^{2}J_{6a,6b}$ −11.0 Hz), 3.68 (d, 1H, H3, $^{3}J_{3,4}$ 7.4 Hz), 3.68–3.73 (m, 1H, H6b).

^{13}C NMR (D_2O): δ [ppm] = 65.3 (C6), 66.5 (C1), 77.0 (C3), 78.5 (C4, C5), 106.3 (C2).

^{31}P NMR (D_2O): δ [ppm] = 5.7.

molar Zn(dien):sugar-phosphate ratio of 2:1

^{1}H NMR (D_2O): δ [ppm] = 3.10 (d, 1H, H1a, $^{2}J_{1a,1b}$ −11.5), 3.19 (d, 1H, H1b), 3.46–3.51 (m, 2H, H4, H5), 3.58 (dt, 1H, H6a, $^{3}J_{5,6a}$ 5.7 Hz, $^{3}J_{6a,P}$ 5.2 Hz, $^{2}J_{6a,6b}$ −11.5 Hz), 3.68 (d, 1H, H3, $^{3}J_{3,4}$ 6.8 Hz), 3.70 (dt, 1H, H6b, $^{3}J_{5,6b}$ 2.5 Hz, $^{3}J_{6b,P}$ 5.0 Hz).

^{13}C NMR (D_2O): δ [ppm] = 65.4 (C6), 66.7 (C1), 77.2 (C3), 78.5 (C5), 78.8 (C4), 106.6(C2).

^{31}P NMR (D_2O): δ [ppm] = 5.7.

5.7.34 Reaction of D-fructose 1,6-bisphosphate with the Zn^{II}(dien) fragment

Trisodium D-fructose 1,6-bisphosphate octahydrate (83 mg, 0.15 mmol / 165 mg, 0.30 mmol), zinc(II) nitrate hexahydrate (89 mg, 0.3 mmol) and diethylenetriamine (32.6 µL, 0.3 mmol) were dissolved in 1 mL D_2O, yielding a colourless solution. Sodium hydroxide (24 mg, 0.60 mmol) was added and the suspension was stirred at 4 °C for 2–3 hours. It was subsequently filtrated and stored at −60 °C.

[Zn(dien)(β-D-Fru*f*1,6$P_2$2,3H_{-2}-κ$^2O^{2,3}$)]$^{4-}$ (32)

molar Zn(dien):sugar-phosphate ratio of 1:1

^{1}H NMR (D_2O): δ [ppm] = 3.55–3.59 (m, 2H, H1a, H1b), 3.61–3.67 (m, 1H, H4), 3.69–3.74 (m, 1H, H5), 3.77 (ddd, 1H, H6a, $^{3}J_{5,6a}$ 1.7 Hz, $^{3}J_{6a,P}$ 5.2 Hz, $^{2}J_{6a,6b}$ −11.3 Hz), 3.87–3.92 (m, 1H, H6b, 3.89–3.95 (m, 1H, H3).

^{13}C NMR (D_2O): δ [ppm] = 65.4 (C6), 69.7 (C1), 78.0 (C5), 78.3 (C3), 78.7 (C4), 105.8 (C2).

^{31}P NMR (D_2O): δ [ppm] = 5.5 (P1), 5.7 (P6).

molar Zn(dien):sugar-phosphate ratio of 2:1

^{1}H NMR (D_2O): δ [ppm] = 3.55–3.59 (m, 2H, H1a, H1b), 3.64 (dd, 1H, H4, $^{3}J_{3,4}$ 7.4 Hz, $^{3}J_{4,5}$ 8.9 Hz), 3.68–3.73 (m, 1H, H5), 3.77 (ddd, 1H, H6a, $^{3}J_{5,6a}$ 1.2 Hz, $^{3}J_{6a,P}$ 4.8 Hz, $^{2}J_{6a,6b}$ −10.5 Hz), 3.90 (dt, 1H, H6b, $^{3}J_{5,6b}$ 4.1 Hz, $^{3}J_{6b,P}$ 4.2 Hz), 3.92 (d, 1H, H3).

^{13}C NMR (D_2O): δ [ppm] = 65.3 (C6), 69.9 (C1), 78.0 (C5), 78.5 (C3), 78.9 (C4), 105.8 (C2).

^{31}P NMR (D_2O): δ [ppm] = 5.4 (P1), 5.7 (P6).

5.7.35 Reaction of D-mannose 6-phosphate with the Zn^{II}(dien) fragment

Disodium D-mannose 6-phosphate dihydrate (51 mg, 0.15 mmol), zinc(II) nitrate hexahydrate (89 mg, 0.30 mmol) and diethylenetriamine (32.6 µL, 0.30 mmol) were dissolved in 1 mL D_2O, yielding a colourless solution. Sodium hydroxide (24 mg, 0.60 mmol) was added and the suspension was stirred at 4 °C for 2–3 hours. It was subsequently filtrated and stored at −60 °C.

[Zn(dien)(α-D-Man*p*6*P*2,3H$_{-2}$-κ^2*O*^{2,3})]$^{2-}$ (33a)

^{1}H NMR (D_2O): δ [ppm] = 3.75 (dd, 1H, H4, $^3J_{3,4}$ 7.9 Hz, $^3J_{4,5}$ 9.4 Hz), 3.83–3.90 (m, 3H, H2, H3, H5), 3.90–3.06 (m, 1H, H6a), 3.98–4.04 (m, 1H, H6b), 5.17–5.19 (m, 1H, H1).

^{13}C NMR (D_2O): δ [ppm] = 63.7 (C6), 67.4 (C4), 70.9 (C3), 72.0 (C5), 72.6 (C2), 96.8 (C1).

^{31}P NMR (D_2O): δ [ppm] = 6.0.

[Zn(dien)(β-D-Man*p*6*P*1,2H$_{-2}$-κ^2*O*^{1,2})]$^{2-}$ (33b)

^{1}H NMR (D_2O): δ [ppm] = 3.59 (dd, 1H, H3, $^3J_{2,3}$ 3.4 Hz, $^3J_{3,4}$ 10.0 Hz), 3.65–3.68 (m, 1H, H2), 3.74 (t, 1H, H4, $^3J_{4,5}$ 10.0 Hz), 3.87–3.93 (m, 1H, H6a), 3.96–4.02 (m, 1H, H6b), 4.95–4.97 (m, 1H, H1).

^{13}C NMR (D_2O): δ [ppm] = 63.6 (C6), 67.0 (C4), 74.8 (C2), 75.1 (C3), 75.1 (C5), 98.4 (C1).

^{31}P NMR (D_2O): δ [ppm] = 6.0.

5.7.36 Reaction of D-glucose 6-phosphate with the Zn^{II}(dien) fragment

Disodium D-glucose 6-phosphate hydrate (46 mg, 0.15 mmol / 91 mg, 0.30 mmol), zinc(II) nitrate hexahydrate (89 mg, 0.30 mmol) and diethylenetriamine (32.6 µL, 0.30 mmol) were dissolved in 1 mL D_2O, yielding a colourless solution. Sodium hydroxide (24 mg, 0.60 mmol) was added and the suspension was stirred at 4 °C for 2–3 hours. It was subsequently filtrated and stored at −60 °C.

[Zn(dien)(α-D-Glc*p*6*P*1,2H$_{-2}$-κ^2*O*^{1,2})]$^{2-}$ (34a)

molar Zn(dien):sugar-phosphate ratio of 1:1

^{1}H NMR (D_2O): δ [ppm] = 3.42–3.59 (m, 3H, H2, H3, H4), 3.81–3.86 (m, 1H, H5), 3.87–3.92 (m, 1H, H6a), 4.00–4.06 (m, 1H, H6b), 5.18 (d, 1H, H1, $^3J_{1,2}$ 3.5 Hz).

^{13}C NMR (D_2O): δ [ppm] = 63.5 (C6), 69.8 (C4), 71.4 (C5), 73.4 (C2), 74.2 (C3), 95.3 (C1).

^{31}P NMR (D_2O): δ [ppm] = 6.1.

molar Zn(dien):sugar-phosphate ratio of 2:1

^{1}H NMR (D_2O): δ [ppm] = 3.32–3.34 (m, 1H, H2), 3.43–3.47 (m, 2H, H3, H4), 3.73–3.77 (m, 1H, H5), 3.95–3.99 (m, 2H, H6a, H6b), 5.10 (d, 1H, H1, $^3J_{1,2}$ 3.5 Hz).

^{13}C NMR (D_2O): δ [ppm] = 63.7 (C6), 70.2 (C4), 71.1 (C5), 75.2 (C2), 76.1 (C3), 98.5 (C1).

^{31}P NMR (D_2O): δ [ppm] = 6.3.

[Zn(dien)(β-D-Glc*p*6*P*1,2H$_{-2}$-κ^2*O*^{1,2})]$^{2-}$ (34b)

molar Zn(dien):sugar-phosphate ratio of 1:1

^{1}H NMR (D_2O): δ [ppm] = 3.12 (dd, 1H, H2, $^3J_{1,2}$ 7.7 Hz, $^3J_{2,3}$ 9.2 Hz), 3.42–3.59 (m, 3H, H3, H4, H5), 3.96–4.00 (m, 2H, H6a, H6b), 4.59 (d, 1H, H1).

^{13}C NMR (D_2O): δ [ppm] = 63.6 (C6), 70.2 (C4), 76.0 (C5), 76.5 (C3), 76.5 (C2), 99.3 (C1).

^{31}P NMR (D_2O): δ [ppm] = 6.1.

molar Zn(dien):sugar-phosphate ratio of 2:1

^{1}H NMR (D_2O): δ [ppm] = 2.91 (dd, 1H, H2, $^3J_{1,2}$ 7.2 Hz, $^3J_{2,3}$ 9.0 Hz), 3.39 (dd, 1H, H3, $^3J_{3,4}$ 8.5 Hz), 3.43–3.49 (m, 2H, H4, H5), 3.95–3.99 (m, 2H, H6a, H6b), 4.48 (d, 1H, H1).

^{13}C NMR (D_2O): δ [ppm] = 64.1 (C6), 71.4 (C4), 76.1 (C5), 77.7 (C3), 78.7 (C2), 102.6 (C1).

^{31}P NMR (D_2O): δ [ppm] = 6.2.

[Zn(dien)(α-D-Glc*f*6*P*1,2H$_{-2}$-κ^2*O*^{1,2})]$^{2-}$ (34c)

molar Zn(dien):sugar-phosphate ratio of 2:1

^{1}H NMR (D_2O): δ [ppm] = 3.46–3.48 (m, 1H, H2), 3.62–3.65 (m, 1H, H3), 3.81–3.85 (m, 1H, H4), 5.46–5.50 (m, 1H, H1).

^{13}C NMR (D_2O): δ [ppm] = 67.1 (C6), 70.0 (C5), 77.5 / 77.9 / 79.0 (C2, C3, C4), 104.5 (C1).

^{31}P NMR (D_2O): δ [ppm] = 6.2.

5.7.37 Reaction of α-D-glucose 1-phosphate with the Zn^{II}(dien) fragment

A solution of dimethyl zinc (1.0 mL, 2.0 mmol, 2M in toluene) was added slowly to a suspension of disodium α-D-glucose 1-phosphate tetrahydrate (376 mg, 1.0 mmol) and diethylenetriamine (217 µL, 2.0 mmol) in toluene (5 mL) under nitrogen atmosphere. The solvent was removed *in vacuo* after stirring at 4 °C for 1–2 hours. The precipitate obtained was dissolved in D_2O (2 mL), yielding a clear, colourless solution which was stirred for 1–2 hours under ice cooling and subsequently stored at −60 °C.

[Zn(dien)(α-D-Glc*p*H$_{-2}$*P*1]$^{2-}$ (35)

^{1}H NMR (D_2O): δ [ppm] = 3.09 (t, 1H, H4, $^3J_{3,4}$ 9.2 Hz, $^3J_{4,5}$ 9.6 Hz), 3.38 (ddd, 1H, H2, $^3J_{1,2}$ 3.3 Hz, $^3J_{2,3}$ 9.7 Hz, $^4J_{2,P}$ 1.9 Hz), 3.51 (dd, 1H, H3), 3.64 (dd, 1H, H6a, $^3J_{5,6a}$ 6.5 Hz, $^2J_{6a,6b}$ −12.2 Hz), 3.85–3.93 (m, 2H, H5, H6b), 5.42 (dd, 1H, H1, $^3J_{1,P}$ 7.4 Hz).

^{13}C NMR (D_2O): δ [ppm] = 62.5 (C6), 73.2 (C4), 74.3 (C2), 74.4 (C5), 75.4 (C3), 95.1 (C1).

^{31}P NMR (D_2O): δ [ppm] = 4.4.

5.7.38 Reaction of *rac*-glycerol 1-phosphate with the Zn^{II}(dien) fragment

Disodium *rac*-glycerol 1-phosphate hydrate (32 mg, 0.15 mmol), zinc(II) nitrate hexahydrate (89 mg, 0.30 mmol) and diethylenetriamine (32.6 µL, 0.30 mmol) were dissolved in 1 mL D_2O, yielding a colourless solution. Sodium hydroxide (24 mg, 0.60 mmol) was added and the suspension was stirred at 4 °C for 2–3 hours. It was subsequently filtrated and stored at −60 °C.

[Zn(dien)(*rac*-Glyc1*P*H$_{-2}$-κ^2*O*^{2,3})]$^{2-}$ (36)

^{1}H NMR (D_2O): δ [ppm] = 3.58 (dd, 1H, H3a, $^3J_{2,3a}$ 5.9 Hz, $^2J_{3a,3b}$ −11.7), 3.67 (dd, 1H, H3b, $^3J_{2,3b}$ 4.7 Hz), 3.72–3.87 (m, 3H, H1a, H1b, H2).

^{13}C NMR (D_2O): δ [ppm] = 63.0 (C3), 65.4 (C1), 72.0 (C2).

^{31}P NMR (D_2O): δ [ppm] = 6.0.

6 Appendix

6.1 Packing diagrams of the crystal structures

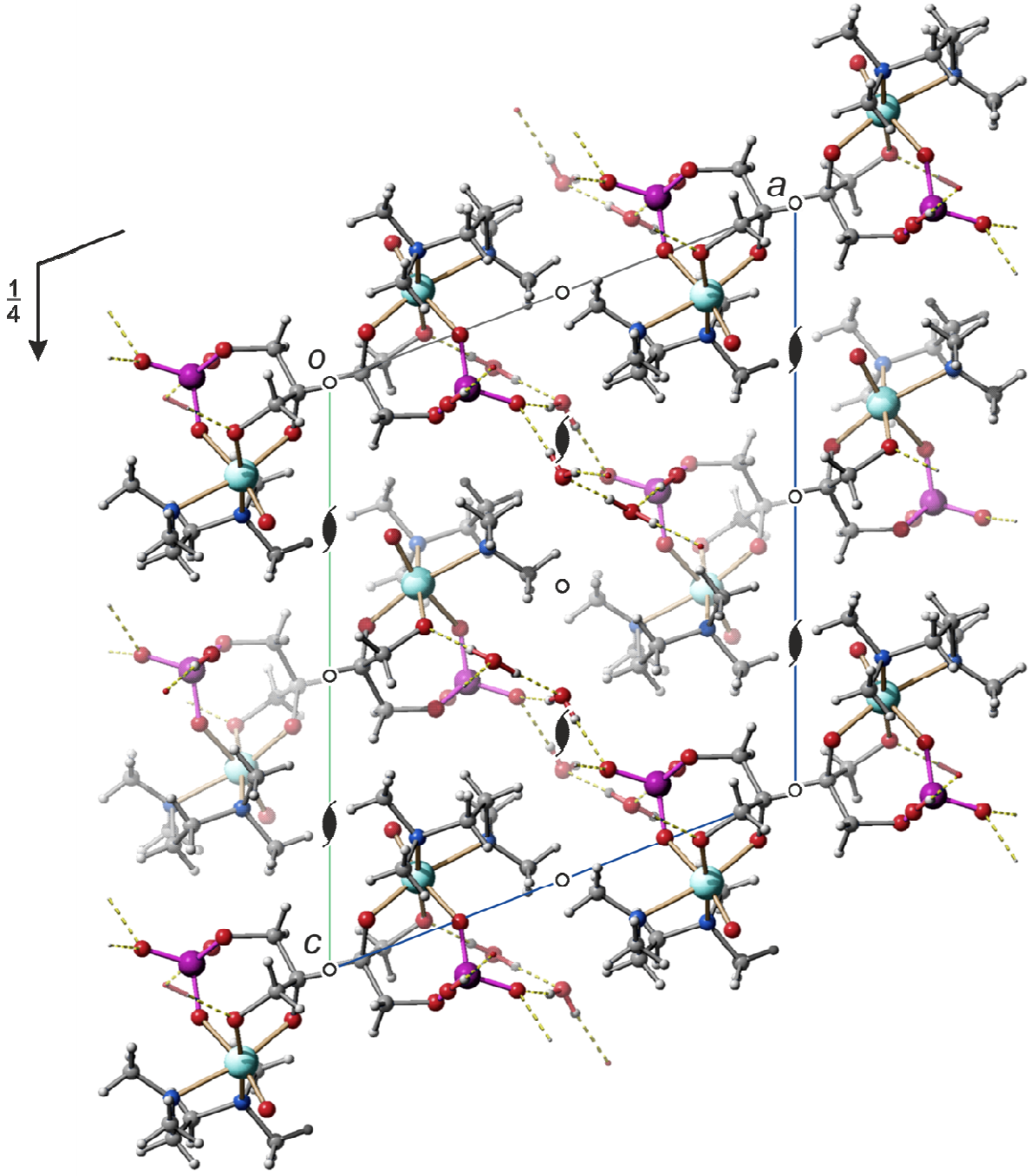

Figure 6.1 SCHAKAL packing diagram of [ReO(tmen)(*rac*-Glyc2,3H_21*P*H-κ^3*O*^{2,3,P})] (**2a**) in crystals of the dihydrate viewed along [0$\bar{1}$0]. Hydrogen bonds are indicated by yellow dashed lines. The symmetry elements of the space group $P2_1/c$ are overlaid. Atoms: carbon (grey), hydrogen (light grey, small), nitrogen (blue), oxygen (red), phosphor (magenta) and rhenium (light blue).

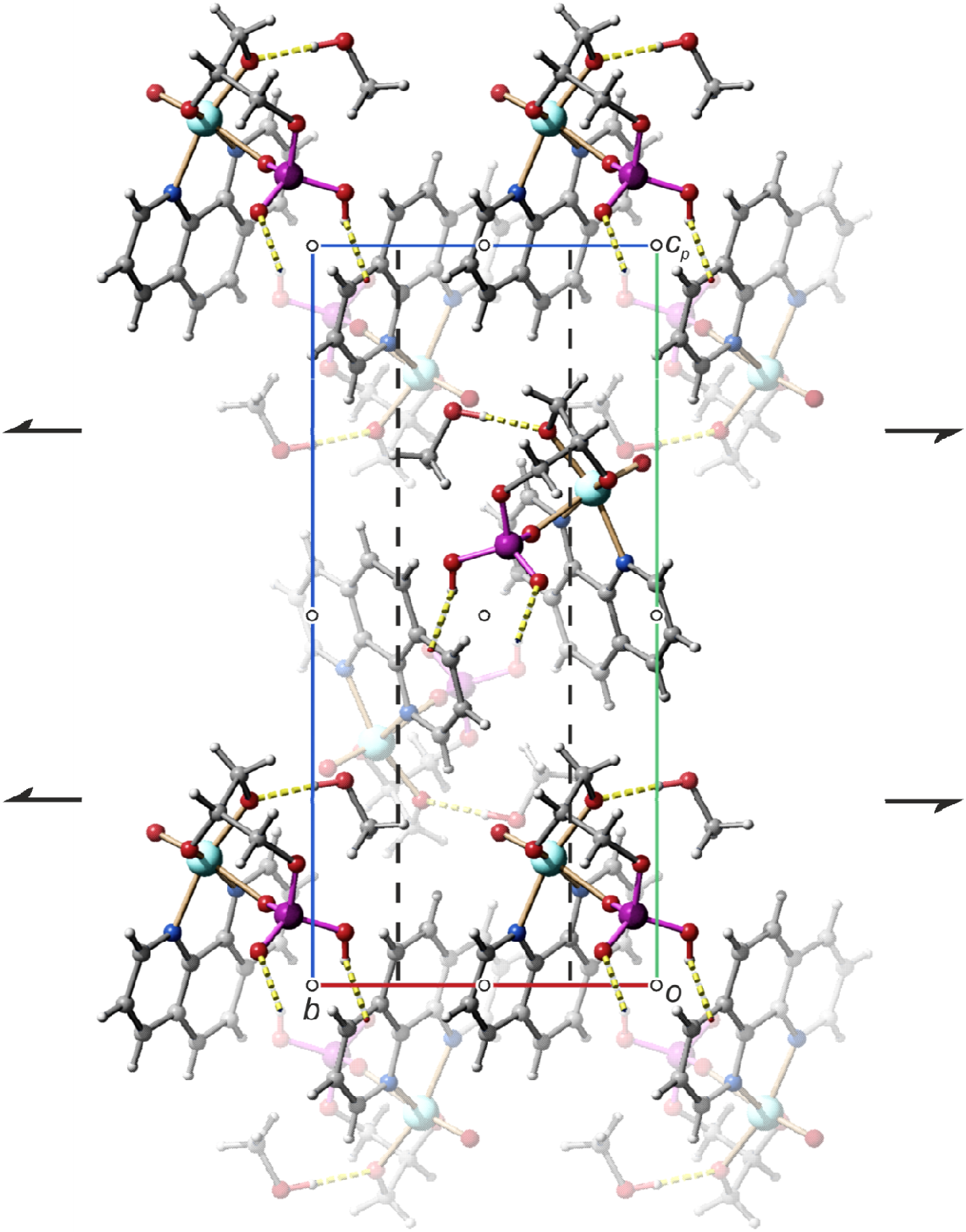

Figure 6.2 SCHAKAL packing diagram of [ReO(phen)(*rac*-Glyc2,3H$_{-2}$1*P*H-$\kappa^3O^{2,3,P}$)] (**2c**) in crystals of **2c** · MeOH viewed along [100]. Hydrogen bonds are indicated by yellow dashed lines. The symmetry elements of the space group $P2_1/c$ are overlaid. Atoms: carbon (grey), hydrogen (light grey, small), nitrogen (blue), oxygen (red), phosphor (magenta) and rhenium (light blue).

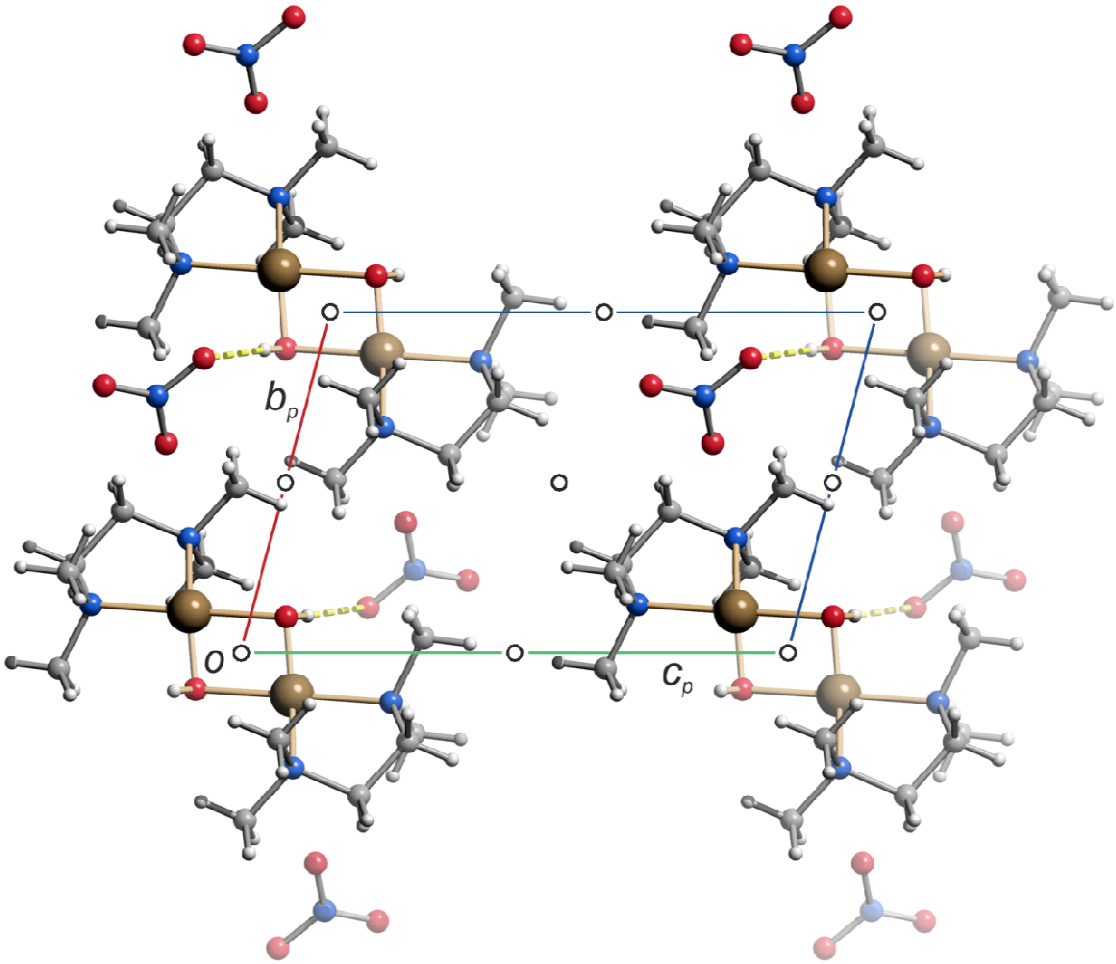

Figure 6.3 SCHAKAL packing diagram of $[\{Pd(tmen)\}_2(\mu\text{-}OH)_2](NO_3)_2$ viewed along [100]. Hydrogen bonds are indicated by yellow dashed lines. The symmetry elements of the space group $P\,\bar{1}$ are overlaid. Atoms: carbon (grey), hydrogen (light grey, small), nitrogen (blue), oxygen (red) and palladium (golden).

6.2 Crystallographic data

Table 6.1 Crystallographic data of [ReO(tmen)(*rac*-Glyc2,3H$_{-2}$1*P*H-κ^3*O*^{2,3,P})] (**2a**) · 2 H_2O, [ReO(phen)(*rac*-Glyc2,3H$_{-2}$1*P*H-κ^3*O*^{2,3,P})] (**2c**) · MeOH and [{Pd(tmen)}$_2$(μ-OH)$_2$](NO$_3$)$_2$.

Compound	**2a** · 2 H_2O	**2c** · MeOH	[{Pd(tmen)}$_2$(μ-OH)$_2$](NO$_3$)$_2$
Empirical formula	$C_9H_{26}N_2O_9PRe$	$C_{16}H_{18}N_2O_8PRe$	$C_{12}H_{34}N_6O_8Pd_2$
M_r/g mol^{-1}	523.49	583.504	603.27
Crystal size/mm	0.13 × 0.10 × 0.03	0.11 × 0.07 × 0.02	0.93 × 0.52 × 0.30
Crystal system	Monoclinic	Monoclinic	Triclinic
Space group	*P* 2$_1$/*c*	*P* 2$_1$/*c*	*P* $\bar{1}$
a/Å	14.1114(5)	10.2979(5)	6.8279(2)
b/Å	7.5592(5)	9.0749(5)	7.3255(3)
c/Å	16.5961(5)	19.4763(7)	11.4644(4)
α/°	90	90	74.7131(19)
β/°	111.0465(5)	91.399(3)	80.966(2)
γ/°	90	90	85.490(2)
V/Å^3	1652.22(13)	1819.56(14)	545.86(3)
Z	4	4	1
ρ_{calcd}/g cm^{-3}	2.10454(17)	2.13006(16)	1.83522(10)
μ/mm^{-1}	7.496	6.816	1.696
Absorption correction	multi-scan	multi-scan	None
T_{min}, T_{max}	0.411, 0.799	0.570, 0.873	–
Reflections measured	27719	6341	4499
R_{int}	0.0501	0.0837	0.0227
Mean σ(*I*)/*I*	0.0330	0.1187	0.0333
θ range/°	3.15–27.61	4.18–26.31	3.32–27.45
Refls. with $I \geq 2\sigma(I)$	3372	2717	2297
x, *y* (weighting scheme)	0.0029, 6.6091	0.0093, 0	0.0225, 0.4132
Refls. in refinement	3808	3673	2502
Parameters	220	258	130
Restraints	6	1	1
$R(F_{obs})$	0.0267	0.0474	0.0249
R_wF^2	0.0549	0.1017	0.0564
S	1.089	0.938	1.100
Shift/error$_{max}$	0.001	0.001	0.001
Max. res. density/e Å^{-3}	1.834	2.571 [a]	1.546
Min. res. density/e Å^{-3}	−1.116	−2.382	−0.710

[a] The max. residue density is found at a distance of 0.98 Å to the rhenium atom.

Bibliography

[1] T. Lundqvist, G. Schneider, *J. Biol. Chem.* **1991**, *266*, 12604–12611.

[2] Y. Nishitani, S. Yoshida, M. Fujihashi, K. Kitagawa, T. Doi, H. Atomi, T. Imanaka, K. Miki, *J. Biol. Chem.* **2010**, *285*, 39339–39347.

[3] S. D. Lahiri, G. Zhang, D. Dunaway-Mariano, K. N. Allen, *Science* **2003**, *299*, 2067–2071.

[4] N. M. Koropatkin, H. M. Holden, *J. Biol. Chem.* **2004**, *279*, 44023–44029.

[5] J. Du, R. F. Say, W. Lu, G. Fuchs, O. Einsle, *Nature* **2011**, *478*, 534–537.

[6] J. K. Hines, X. Chen, J. C. Nix, H. J. Fromm, R. B. Honzatko, *J. Biol. Chem.* **2007**, *282*, 36121–36131.

[7] J.-Y. Choe, S. W. Nelson, H. J. Fromm, R. B. Honzatko, *J. Biol. Chem.* **2003**, *278*, 16008–16014.

[8] B. W. Shen, A.-L. Perraud, A. Scharenberg, B. L. Stoddard, *J. Mol. Biol.* **2003**, *332*, 385–398.

[9] J. Jenkins, J. Janin, F. Rey, M. Chiadmi, H. van Tilbeurgh, I. Lasters, M. De Maeyer, D. Van Belle, S. J. Wodak, M. Lauwereys, P. Stanssens, N. T. Mrabet, J. Snauwaert, G. Matthyssens, A.-M. Lambeir, *Biochemistry* **1992**, *31*, 5449–5458.

[10] H. L. Carrell, H. Hoier, J. P. Glusker, *Acta Crystallogr., Sect. D* **1994**, *50*, 113–123.

[11] L. M. van Staalduinen, C.-S. Park, S.-J. Yeom, M. A. Adams-Cioaba, D.-K. Oh, Z. Jia, *J. Mol. Biol.* **2010**, *401*, 866–881.

[12] W. Liang, S. Ouyang, N. Shaw, A. Joachimiak, R. Zhang, Z.-J. Liu, *FASEB J.* **2011**, *25*, 497–504.

[13] Y. Zhang, J. Y. Liang, S. Huang, H. Ke, W. N. Lipscomb, *Biochemistry* **1993**, *32*, 1844–1857.

[14] S. Yoshiba, T. Ooga, N. Nakagawa, T. Shibata, Y. Inoue, S. Yokoyama, S. Kuramitsu, R. Masui, *J. Biol. Chem.* **2004**, *279*, 37163–37174.

[15] S. D. Pegan, K. Rukseree, S. G. Franzblau, A. D. Mesecar, *J. Mol. Biol.* **2009**, *386*, 1038–1053.

[16] A. Galkin, Z. Li, L. Li, L. Kulakova, L. R. Pal, D. Dunaway-Mariano, O. Herzberg, *Biochemistry* **2009**, *48*, 3186–3196.

[17] Y. Luo, J. Samuel, S. C. Mosimann, J. E. Lee, M. E. Tanner, N. C. J. Strynadka, *Biochemistry* **2001**, *40*, 14763–14771.

[18] J. M. Berrisford, A. M. Hounslow, J. Akerboom, W. R. Hagen, S. J. J. Bouns, J. van der Oost, I. A. Murray, G. M. Blackburn, J. P. Waltho, D. W. Rice, P. J. Baker, *J. Mol. Biol.* **2006**, *358*, 1353–1366.

[19] J. Akana, A. A. Fedorov, E. Fedorov, W. R. P. Novak, P. C. Babbitt, S. C. Almo, J. A. Gerlt, *Biochemistry* **2006**, *45*, 2493–2503.

[20] S. Steinbacher, S. Schiffmann, A. Bacher, M. Fischer, *Acta Crystallogr., Sect. D* **2004**, *60*, 1138–1140.

[21] A. Cleasby, A. Wonacott, T. Skarzynski, R. E. Hubbard, G. J. Davies, A. E. I. Proudfoot, A. R. Bernard, M. A. Payton, T. N. C. Wells, *Nature Struct. Biol.* **1996**, *3*, 470–479.

[22] H. Yoshida, M. Yamada, Y. Ohyama, G. Takada, K. Izumori, S. Kamitori, *J. Mol. Biol.* **2007**, *365*, 1505–1516.

[23] H. Yoshida, K. Takeda, K. Izumori, S. Kamitori, *Protein Eng., Des. Sel.* **2010**, *23*, 919–927.

[24] P. J. Baker, K. L. Britton, M. Fisher, J. Esclapez, C. Pire, M. J. Bonete, J. Ferrer, D. W. Rice, *Proc. Natl. Acad. Sci. U. S. A.* **2009**, *106*, 779–784.

[25] H. Linjalahti, G. Feng, J. C. Mareque-Rivas, S. Mikkola, N. H. Williams, *J. Am. Chem. Soc.* **2008**, *130*, 4232**–**4233.

[26] P. Orioli, R. Cini, W. Donati, S. Mangani, *Nature* **1980**, *283*, 691–693.

[27] G. B. van den Berg, A. Heerschap, *Arch. Biochem. Biophys.* **1982**, *219*, 268–276.

[28] P. Mayer, Dissertation **1997**, Universität Karlsruhe.

[29] S. Herdin, Dissertation **2004**, Ludwig-Maximilians-Universität München.

[30] R. Ahlrichs, M. Ballauff, K. Eichkorn, O. Hanemann, G. Kettenbach, P. Klüfers, *Chem. Eur. J.* **1998**, *4*, 835**–**844.

[31] P. Klüfers, T. Kunte, *Angew. Chem. Int. Ed.* **2001**, 40, 4210–4212.

[32] P. Klüfers, T. Kunte, *Eur. J. Inorg. Chem.* **2002**, 1285–1289.

[33] P. Klüfers, T. Kunte, *Chem. Eur. J.* **2003**, *9*, 2013–2018.

[34] T. Allscher, X. Kästele, G. Kettenbach, P. Klüfers, T. Kunte, *Chem. Asian J.* **2007**, *2*, 1037–1045.

[35] T. Allscher, Y. Arendt, P. Klüfers, *Carbohydr. Res.* **2010**, *345*, 2381–2389.

[36] T. Allscher, Dissertation **2011**, Ludwig-Maximilians-Universität München.

[37] K. Gilg, T. Mayer, N. Ghaschghaie, P. Klüfers, *Dalton Trans.* **2009**, 7934–7945.

[38] K. Gilg, Dissertation **2009**, Ludwig-Maximilians-Universität München.

[39] M. Kato, T. Tanase and M. Mikuriya, *Inorg. Chem.*, 2006, **45**, 2925–2941.

[40] M. Kato, A. K. Sah, T. Tanase and M. Mikuriya, *Inorg. Chem.*, 2006, **45**, 6646–6660.

[41] D. Champmartin, P. Rubini, A. Lakatos and T. Kiss, *J. Inorg. Biochem.*, 2001, **84**, 13–21.

[42] N. Ghaschghaie, Dissertation **2010**, Ludwig-Maximilians-Universität München.

[43] T. Mayer, Master thesis **2008**, Ludwig-Maximilians-Universität München.

[44] P. Grimminger, P. Klüfers, *Dalton Trans.* **2010**, *39*, 715–719.

[45] H. Günther, *NMR-Spektroskopie*, Georg Thieme Verlag, Stuttgart, **1992**.

[46] M. Hesse, H. Meier, B. Zeeh, *Spektroskopische Methoden in der organischen Chemie*, Georg Thieme Verlag, **1995**, 108–109.

[47] M. Karplus, *J. Am. Chem. Soc.* **1963**, *85*, 2870–2871.

[48] C. A. G. Haasnoot, F. A. A. M. de Leeuw, C. Altona, *Tetrahedron* **1980**, *36*, 2783–2792.

[49] M. Steinborn, Master thesis **2009**, Ludwig-Maximilians-Universität München.

[50] N. Ghaschghaie, T. Hoffmann, M. Steinborn, P. Klüfers, *Dalton Trans.* **2010**, *39*, 5535–5543.

[51] W. J. Stevens, M. Krauss, H. Basch, P. G. Jasien, *Can. J. Chem.* **1992**, *70*, 612–630.

[52] T. van Mourik, *J. Chem. Phys.* **2006**, *125*, 191101.

[53] M. Suhanji, Master thesis **2008**, Ludwig-Maximilians-Universität München.

[54] G. Pathuri, A. F. Hedrick, B. C. Disch, J. T. Doan, M. A. Ihnat, V. Awasthi, H. Gali, *Bioconjugate Chem.* **2012**, *23*, 115–124.

[55] M. Lipowska, L. Hansen, R. Cini, X. Xu, H. Choi, A. T. Taylor, L. G. Marzilli, *Inorg. Chim. Acta* **2002**, *339*, 327–340.

[56] M. Lipowska, L. Hansen, X. Xu, P. A. Marzilli, A. Taylor Jr., L. G. Marzilli, *Inorg. Chem.* **2002**, *41*, 3032–3041.

[57] M. F. Cerda, E. Mendez, L. Malacrida, C. F. Zinola, C. Melian, M. E. Martins, A. M. Castro Luna, C. Kremer, *J. Colloid Interface Sci.* **2002**, *249*, 366–371.

[58] F. J. Femia, X. Chen, J. W. Babich, J. Zubieta, *Inorg. Chim. Acta* **2001**, *316*, 145–148.

[59] L. Hansen, Y. D. Lampeka, S. P. Gavrish, X. Xu, A. T. Taylor, L. G. Marzilli, *Inorg. Chem.* **2000**, *39*, 5859–5866.

[60] L. Hansen, S. Hirota, X. Xu, A. T. Taylor, L. G. Marzilli, *Inorg. Chem.* **2000**, *39*, 5731–5740.

[61] C. Melian, C. Kremer, L. Suescun, A. Mombru, R. Mariezcurrena, E. Kremer, *Inorg. Chim. Acta* **2000**, *306*, 70–77.

[62] F. J. Femia, J. W. Babich, J. Zubieta, *Inorg. Chim. Acta* **2000**, *300–302*, 462–470.

[63] L. Hansen, M. Lipowska, E. Melendez, X. Xu, S. Hirota A. T. Taylor, L. G. Marzilli, *Inorg. Chem.* **1999**, *38*, 5351–5358.

[64] L. Hansen, X. Xu, M. Lipowska, A. Taylor Jr., L. G. Marzilli, *Inorg. Chem.* **1999**, *38*, 2890–2897.

[65] L. Hansen, K. T. Yue, X. Xu, M. Lipowska, A. Taylor Jr., L. G. Marzilli, *J. Am. Chem. Soc.* **1997**, *119*, 8965–8972.

[66] L. Hansen, X. Xu, K. T. Yue, Z. Kuklenyik, A. Taylor Jr., L. G. Marzilli, *Inorg. Chem.* **1996**, *35*, 1958–1966.

[67] L. G. Marzilli, M. G. Banaszczyk, L. Hansen, Z. Kuklenyik, R. Cini, A. Taylor Jr., *Inorg. Chem.* **1994**, *33*, 4850–4860.

[68] G. Ciani, A. Sironi, T. Beringhelli, G. D'Alfonso, M. Freni, *Inorg. Chim. Acta* **1986**, *113*, 61–65.

[69] C. A. Lippert, K. I. Hardcastle, J. D. Soper, *Inorg. Chem.* **2011**, *50*, 9864–9878.

[70] A. L. Moore, B. Twamley, C. L. Barnes, P. D. Benny, *Inorg. Chem.* **2011**, *50*, 4686–4688.

[71] C. A. Lippert, S. A. Arnstein, C. D. Sherrill, J. D. Soper, *J. Am. Chem. Soc.* **2010**, *132*, 3879–3892.

[72] A. Mondal, S. Sarkar, D. Chopra, T. N. G. Row, K. K. Rajak, *Dalton Trans.* **2004**, *20*, 3244–3250.

[73] J. S. Gancheff, C. Kremer, P. A. Denis, C. Giorgi, A. Bianchi, *Dalton Trans.* **2009**, *39*, 8257–8268.

[74] A. Barandov, U. Abram, *Inorg. Chem.* **2009**, *48*, 8072–8074.

[75] S. Basak, K. K. Rajak, *Inorg. Chem.* **2008**, *47*, 8813–8822.

[76] M. Li, A. Ellern, J. H. Espenson, *J. Am. Chem. Soc.* **2005**, *127*, 10436–10447.

[77] P. D. Benny, J. L. Green, H. P. Engelbrecht, C. L. Barnes, S. S. Jurisson, *Inorg. Chem.* **2005**, *44*, 2381–2390.

[78] P. Grimminger, P. Klüfers, *Dalton Trans.* **2010**, *39*, 715–719.

[79] P. Grimminger, P. Klüfers, *Acta Crystallogr., Sect. E* **2007**, *63*, m3188.

[80] O. Labisch, Dissertation **2006**, Ludwig-Maximilians-Universität München.

[81] M. Oßberger, Dissertation **2003**, Ludwig-Maximilians-Universität München.

[82] P. Grimminger, Dissertation **2009**, Ludwig-Maximilians-Universität München.

[83] D. Heß, Dissertation **2012**, Ludwig-Maximilians-Universität München.

[84] S. Illi, Dissertation **2012**, Ludwig-Maximilians-Universität München.

[85] T. Schwarz, D. Heß, P. Klüfers, *Dalton Trans.* **2010**, *39*, 5544–5555.

[86] L. D. Field, B. A. Messerle, *J. Magn. Reson.* **1985**, *62*, 453–460.

[87] Y. Zhu, J. Zajicek, A. S. Serianni, *J. Org. Chem.* **2001**, *66*, 6244–6251.

[88] R. G. S. Ritchie, N. Cyr, B. Korsch, H. J. Koch, A. S. Perlin, *Can. J. Chem.* **1975**, *53*, 1424–1433.

[89] J. Pierce, A. S. Serianni, R. Barker, *J. Am. Chem. Soc.* **1985**, *107*, 2448–2456.

[90] W.-Z. Shen, D. Gupta, B. Lippert, *Inorg. Chem.* **2005**, *44*, 8249–8258.

[91] K. Bock, H. Thøgersen, in *Annual Reports on NMR Spectroscopy, Vol. 13* (Ed.: G. A. Webb), Academic Press, **1983**, pp. 1–57.

[92] T. Tanase, H. Inukai, T. Onaka, M. Kato, S. Yano, S. J. Lippard, *Inorg. Chem.* **2001**, *40*, 3943–3953.

[93] R. Chiozzone, R. Gonzáles, C. Kremer, G. de Munno, J. Faus, *Inorg. Chim. Acta.* **2001**, *325*, 203–207.

[94] C. J. L. Lock, G. Turner, *Acta Crystallogr., Sect. B* **1978**, *34*, 923–927.

[95] S. Bélanger, A. L. Beauchamp, *Inorg. Chem.* **1997**, *36*, 3640–3647.

[96] F. W. Lichtenthaler, S. Ronninger, *J. Chem. Soc. Perkin Trans. 2* **1990**, 1489–1497.

[97] K. Peter, C. Vollhardt, N. E. Schore, *Organische Chemie*, Wiley-VCH Verlag, **2005**, 1267–1268.

[98] P. Klüfers, M. M. Reichvilser, *Eur. J. Inorg. Chem.* **2008**, 384–396.

[99] M. J. Frisch, G. W. Trucks, H. B. Schlegel, G. E. Scuseria, M. A. Robb, J. R. Cheeseman, J. A. Montgomery, Jr., T. Vreven, K. N. Kudin, J. C. Burant, J. M. Millam, S. S. Iyengar, J. Tomasi, V. Barone, B. Mennucci, M. Cossi, G. Scalmani, N. Rega, G. A. Petersson, H. Nakatsuji, M. Hada, M. Ehara, K. Toyota, R. Fukuda, J. Hasegawa, M. Ishida, T. Nakajima, Y. Honda, O. Kitao, H. Nakai, M. Klene, X. Li, J. E. Knox, H. P. Hratchian, J. B. Cross, V. Bakken, C. Adamo, J. Jaramillo, R. Gomperts, R. E. Stratmann, O. Yazyev, A. J. Austin, R. Cammi, C. Pomelli, J. W. Ochterski, P. Y. Ayala, K. Morokuma, G. A. Voth, P. Salvador, J. J. Dannenberg, V. G. Zakrzewski, S. Dapprich, A. D. Daniels, M. C. Strain, O. Farkas, D. K. Malick, A. D. Rabuck, K. Raghavachari, J. B. Foresman, J. V. Ortiz, Q. Cui, A. G. Baboul, S. Clifford, J. Cioslowski, B. B. Stefanov, G. Liu, A. Liashenko, P. Piskorz, I. Komaromi, R. L. Martin, D. J. Fox, T. Keith, M. A. Al-Laham, C. Y. Peng, A. Nanayakkara, M. Challacombe, P. M. W. Gill, B. Johnson, W. Chen, M. W. Wong, C. Gonzalez, J. A. Pople, *Gaussian 03*, *Revision D.01*, Gaussian, Inc., Wallingford CT, **2004**.

[100] A. Altomare, M. C. Burla, M. Camalli, G. L. Cascarano, C. Giacovazzo, A. Guagliardi, A. G. G. Moliterni, G. Polidori, R. Spagna, *J. Appl. Crystallogr.* **1999**, *32*, 115–119.

[101] G. M. Sheldrick, *Acta Crystallogr., Sect. A* **2008**, *64*, 112–122.

[102] A. L. Spek, *J. Appl. Crystallogr.* **2003**, *36*, 7–13.

[103] L. J. Farrugia, *J. Appl. Crystallogr.* **1997**, *30*, 565.

[104] E. Keller, *J. Appl. Crystallogr.* **1989**, *22*, 19–22.

[105] J. Chatt, G. A. Rowe, *J. Chem. Soc.* **1962**, 4019–4033.

[106] A. Gutbier, M. Woernle, *Chem. Ber.* **1906**, *39*, 2716–2717.

[107] D. R. Walt, M. A. Findeis, V. M. Rios-Mercadillo, J. Auge, G. M. Whitesides, *J. Am. Chem. Soc.* **1984**, *106*, 234–239.

Danksagung

Herrn Prof. Dr. Peter Klüfers danke ich für die interessante Themenstellung, den mir gewährten wissenschaftlichen Freiraum sowie für die wertvollen Anregungen und Unterstützungen.

Herrn Prof. Dr. Hans-Christian Böttcher möchte ich für die Übernahme der Tätigkeit als Zweitgutachter danken. Für die Mitwirkung in der Promotionskommission danke ich außerdem Herrn Prof. Dr. Konstantin Karaghiosoff, Herrn Prof. Dr. Achim Hartschuh, Herrn Prof. Dr. Wolfgang Beck sowie Frau Prof. Dr. Sonja Herres-Pawlis.

Lida Holowatyi-den Toom danke ich sowohl für ihre Hilfe in organisatorischen Angelegenheiten aller Art als auch für das Korrekturlesen von Abstracts, Publikationen und anderer wissenschaftlicher Texte.

Meinen Laborkollegen Dr. Thorsten Allscher, Dr. David Heß, Christine Neumann und Xaver Wurzenberger danke ich für das stets angenehme Arbeitsklima und die entspannte Atmosphäre.

Christine Neumann danke ich außerdem für ihre sehr guten Ratschläge und ihre stetige Hilfe im Laboralltag sowie das immer schnelle Bereitstellen neuer Laborgeräte und -utensilien.

Für ihre Geduld und Anstrengungen beim Aufsetzen meiner Kristalle danke ich Sandra Albrecht, Anna Gallien, Dr. Helene Giglmeier, Dr. Tobias Kerscher, Leonie Lindner, Dr. Peter Mayer, Dr. Moritz Reichvilser, Johanna Schulten und Xaver Wurzenberger.

Sandra Albrecht danke ich außerdem für das teilweise nicht ganz unkomplizierte Organisieren der von mir benötigten Chemikalien.

Xaver Kästele möchte ich danken für seine wertvollen Ratschläge zum sicheren Arbeiten und seinen nimmermüden Einsatz für die Sicherheit im Laboralltag.

Für die sehr gute Zusammenarbeit als Administratoren danke ich Dr. Thorsten Allscher, Markus Wolf und Xaver Wurzenberger.

Ferner danke ich Dr. Thorsten Allscher für die gute Zusammenarbeit auf dem Gebiet der Palladium-Komplexchemie sowie für die ausführliche Einführung in das Lösen von Kristallstrukturen.

Den Mitarbeitern der Analytik-Abteilungen der Häuser C, D und F danke ich für das Messen etlicher Proben, die für den Erfolg dieser Arbeit von großer Bedeutung waren. Diesbezüglich danke ich Prof. Dr. Konstantin Karaghiosoff sehr für die Messungen der ^{31}P–^{1}H-HETCOR-Spektren, für die er so manches Wochenende opferte. Ein großes Dankeschön gilt hierbei aber vor allem Peter Mayer und Christine Neumann, ohne deren großartigen Einsatz in der NMR-Abteilung das Fertigstellen dieser Arbeit undenkbar gewesen wäre.

Ein besonderer Dank gilt außerdem meinen Forschungs-Praktikanten Erik Bader, Corinna Jansen, Julia Janik, Jan Geldsetzer, Jeffrey Hammann und Shanshan He, die durch ihre engagierte Arbeitsweise immens zum Erfolg dieser Arbeit beigetragen haben.

Für die aufmerksame Durchsicht dieser Arbeit danke ich sehr Christina Daschkin, Dr. Hannelore Meyer, Johanna Schulten und Lida Holowatyi-den Toom.

Ein großer Dank gilt allen aktuellen und ehemaligen Mitarbeitern unseres Arbeitskreises für die jederzeit freundschaftliche Atmosphäre während aber auch außerhalb der Arbeit. Die stimmungsvollen Runden in der Kaffeeküche werde ich immer in guter Erinnerung behalten.

Unvergessen bleiben in jedem Fall auch die gemeinsamen Besuche der Konferenzen in Dortmund und Prag. Für die großartigen Erlebnisse dort möchte ich mich sehr bedanken bei Christina Daschkin, Anna Gallien, Karola Gasteiger, Dr. Sarah Illi, Leonie Lindner, Stefan Schießer und Markus Wolf.

• ~ •

Ein ganz besonderes Dankeschön gilt meiner Freundin Christina Daschkin sowie meinen Eltern und meiner Schwester für ihre Unterstützung, ihre Geduld und ihr Vertrauen in der Welt außerhalb der Chemie.